ANL-21/68
ISSN 1931-5007
March 2022

APS SCIENCE 2021

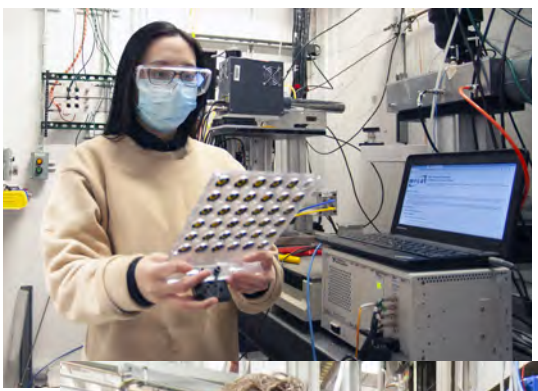

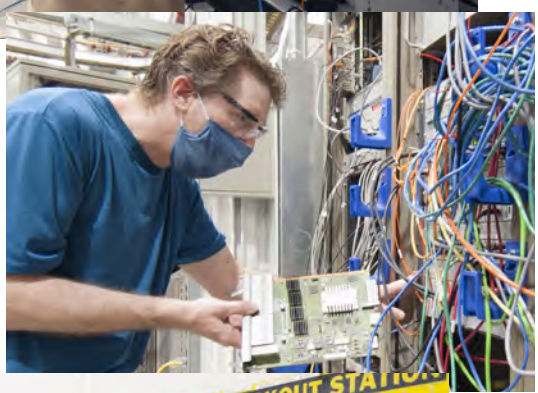

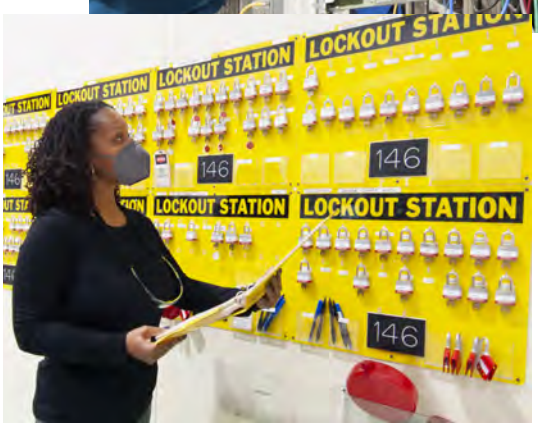

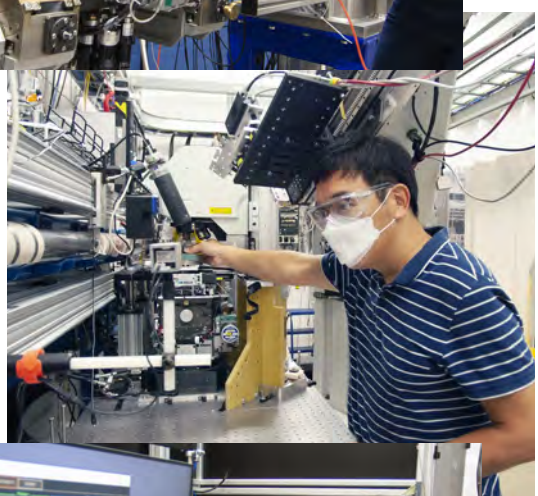

Research and engineering highlights from the Advanced Photon Source at Argonne National Laboratory

Includes APS research into the SARS-CoV-2 virus

Argonne NATIONAL LABORATORY

ANL-21/68 • SSN 1931-5007 • March 2022

About Argonne National Laboratory

Argonne is a U.S. Department of Energy laboratory managed by UChicago Argonne, LLC under contract DE-AC02-06CH11357. The Laboratory's main facility is outside Chicago, at 9700 South Cass Avenue, Lemont, Illinois 60439. For information about Argonne and its pioneering science and technology programs, see www.anl.gov.

DOCUMENT AVAILABILITY

Online Access: U.S. Department of Energy (DOE) reports produced after 1991 and a growing number of pre-1991 documents are available free at OSTI.GOV (http://www.osti.gov/), a service of the US Dept. of Energy's Office of Scientific and Technical Information.

Reports not in digital format may be purchased by the public from the National Technical Information Service (NTIS):U.S. Department of Commerce National Technical Information Service
5301 Shawnee Rd
Alexandria, VA 22312
www.ntis.gov
Phone: (800) 553-NTIS (6847) or (703) 605-6000
Fax: (703) 605-6900
Email: orders@ntis.gov

Reports not in digital format are available to DOE and DOE contractors from the Office of Scientific and Technical Information (OSTI):
U.S. Department of Energy
Office of Scientific and Technical Information
P.O. Box 62
Oak Ridge, TN 37831-0062
www.osti.gov
Phone: (865) 576-8401
Fax: (865) 576-5728
Email: reports@osti.gov

On the cover, clockwise from top left:

Yujia Ding, sector scientist with the Materials Research Collaborative Access Team (CAT), in the 10-BM research station.

Mary Upton, physicist with the X-ray Science Division (XSD) Inelastic X-ray & Nuclear Resonant Scattering Group, in the 27-ID research station.

Wonsuk Cha, assistant physicist with the XSD Microscopy Group, in the 34-ID-C research station.

Stella Chariton, beamline scientist with GeoSoilEnviroCARS, in the 13-ID-D research station.

Debbie Curry, technician senior with the APS Engineering Support (AES) Division, in the APS experiment hall mezzanine.

Cassandra Hayden, ESH Coordinator with Argonne Environment, Safety, Health & Quality, in the APS Experiment Assembly Area.

Brian Pruitt, Senior Computer Specialist with the AES Division Information Technology Group, in the APS experiment hall.

ANL-21/68
ISSN 1931-5007
March 2022

APS SCIENCE 2021

RESEARCH AND ENGINEERING HIGHLIGHTS FROM THE ADVANCED PHOTON SOURCE AT ARGONNE NATIONAL LABORATORY

Argonne is a U.S. Department of Energy (DOE) laboratory managed by UChicago Argonne, LLC.
The Advanced Photon Source is a DOE Office of Science user facility
operated for the DOE Office of Science by Argonne National Laboratory under Contract No. DE-AC02-06CH11357.

Table of Contents

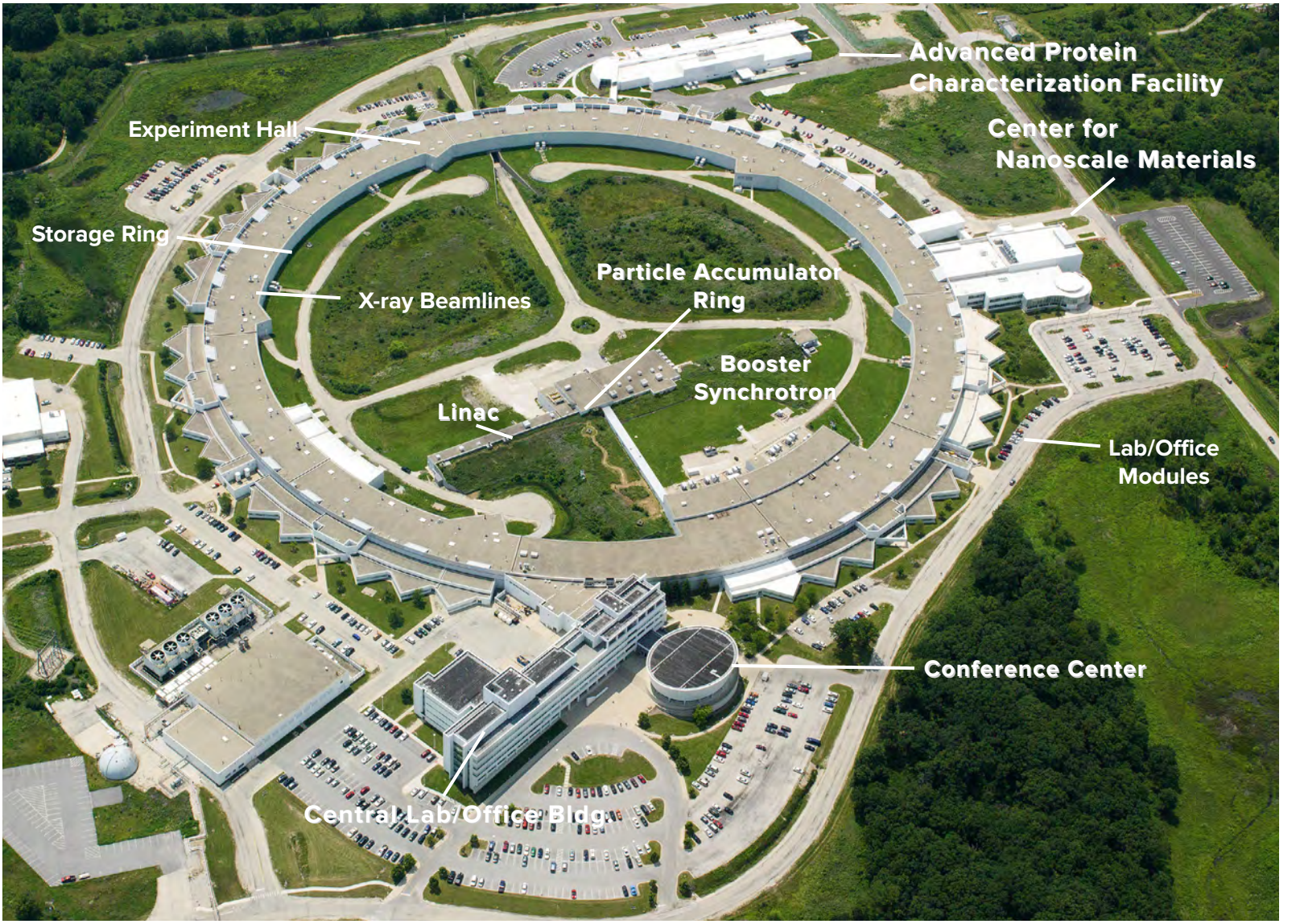

The Advanced Photon Source Facility at Argonne National Laboratory

The U.S. Department of Energy's Advanced Photn Source (APS) is one of the world's most productive x-ray light source facilities. Each year, the APS provides high-brightness x-ray beams to a diverse community of more than 5,000 researchers in materials science, chemistry, condensed matter physics, the life and environmental sciences, and applied research. Researchers using the APS produce over 2,000 publications each year detailing impactful discoveries, and solve more vital biological protein structures than users of any other x-ray light source research facility. APS x-rays are ideally suited for explorations of materials and biological structures; elemental distribution; chemical, magnetic, electronic states; and a wide range of technologically important engineering systems from batteries to fuel injector sprays, all of which are the foundations of our nation's economic, technological, and physical well-being.

The APS occupies an 80-acre site on the Argonne campus, about 25 miles from downtown Chicago, Illinois. It shares a site with the Center for Nanoscale Materials and the Advanced Protein Characterization Facility.

For directions to Argonne, see https://www.anl.gov/visiting-argonne.

Contact us

For more information about the APS send an email to apsinfo@aps.anl.gov or write to APS Info, Bldg. 401, Rm. A4113, Argonne National Laboratory, 9700 S. Cass Ave., Lemont, IL 60439.

To order additional copies of this, or previous, issues of *APS Science* send email to apsinfo@aps.anl.gov.

To download PDF versions of *APS Science* back issues go to www.aps.anl.gov/Science/APS-Science

Visit the APS on the Web at www.aps.anl.gov

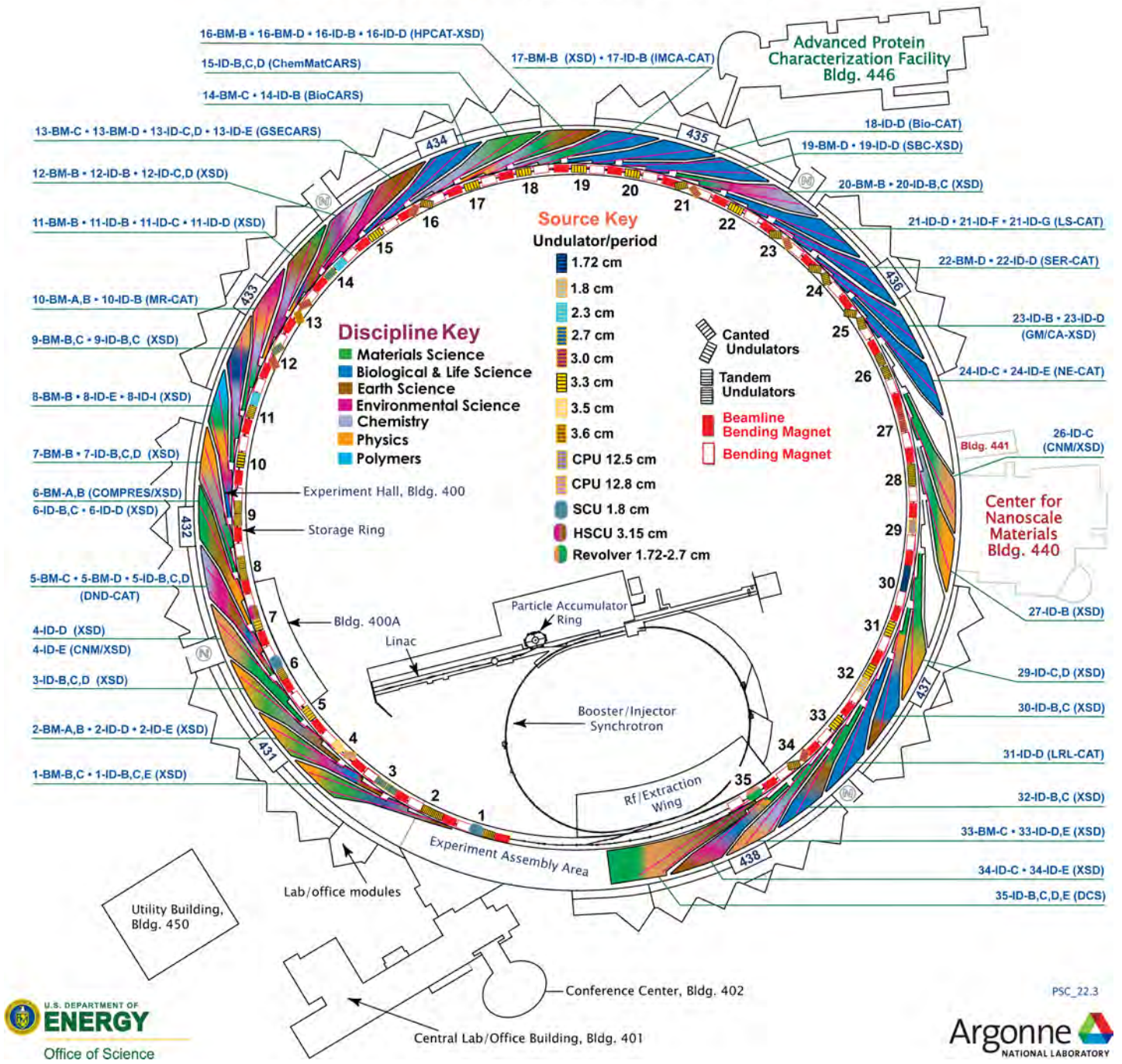

APS sectors: At the APS, a "sector" comprises the radiation sources (one bending magnet and nominally one insertion device, although the number of insertion devices in the straight sections of the storage ring can vary) and the beamlines, enclosures, and instrumentation that are associated with a particular storage ring sector. The APS has 35 sectors dedicated to user science and experimental apparatus. X-ray Science Division (XSD) sectors comprise those beamlines operated by the APS. Collaborative access team (CAT) sectors comprise beamlines operated by independent groups made up of scientists from universities, industry, and/or research laboratories both federal and private.

APS Beamlines (as of 3.22)

Key: Beamline designation • Sector operator • Disciplines • Techniques • Radiation source energy • User access mode(s) • General-user status

1-BM-B,C • **X-ray Science Division (XSD)** • Materials science, physics • Optics testing, detector testing, topography, white Laue single-crystal diffraction • 6-30 keV, 50-120 keV • On-site • Accepting general users

1-ID-B,C,E • XSD • Materials science, physics, chemistry, life science • High-energy x-ray diffraction, tomography, small-angle x-ray scattering, fluorescence spectroscopy, pair distribution function, phase contrast imaging • 41-136 keV, 45-116 keV • On-site • Accepting general users

2-BM-A,B • XSD • Physics, life sciences, geoscience, materials science • Tomography, phase contrast imaging • 10-170 keV, 11-35 keV • On-site • Accepting general users

2-ID-D • XSD • Life sciences, materials science, environmental science • Microfluorescence, micro x-ray absorption fine structure, nanoimaging, ptychography • 5-30 keV • On-site, remote, mail-in, beamline staff • Accepting general users

2-ID-E • XSD • Life sciences, environmental science, materials science • Microfluorescence, tomography • 5-20 keV • On-site, remote, mail-in, beamline staff • Accepting general users

3-ID-B,C,D • XSD • Physics, geoscience, life sciences, chemistry, materials science • Nuclear resonant scattering, high-pressure diamond anvil cell • 7-27 keV, 14.41-14.42 keV • On-site • Accepting general users

4-ID-D • XSD • Physics, materials science • Anomalous and resonant scattering, magnetic x-ray scattering, magnetic circular dichroism, high-pressure diamond anvil cell • 2.7-40 keV • Remote • Accepting general users

4-ID-E • CNM/XSD • Materials science, physics • Synchrotron x-ray scanning tunneling microscopy (SX-STM), magnetic circular dichroism, x-ray photoemission spectroscopy • 400-1900 eV • On-site • Accepting general users

5-BM-C • **DuPont-Northwestern-Dow Collaborative Access Team (DND-CAT)** • Materials science, polymer science • Powder diffraction, tomography, wide-angle x-ray scattering • 10-42 keV • On-site, mail-in • Accepting general users

5-BM-D • DND-CAT • Materials science, polymer science, chemistry, environmental science • X-ray absorption fine structure, high-energy x-ray diffraction, general diffraction • 4.5-25 keV, 4.5-80 keV • On-site, mail-in • Accepting general users

5-ID-B,C,D • DND-CAT • Materials science, polymer science, chemistry, life science • Powder diffraction, x-ray standing waves, x-ray optics development/techniques, small-angle x-ray scattering, surface diffraction, x-ray reflectivity, wide-angle x-ray scattering • 6-17.5 keV • On-site, mail-in • Accepting general users

6-BM-A,B • **COMPRES/XSD** • Materials science, geoscience • Energy dispersive x-ray diffraction, high-pressure multi-anvil press, radiography, tomography • 20-200 keV • On-site • Accepting general users

6-ID-B,C • XSD • Physics, materials science • Magnetic x-ray scattering, anomalous and resonant scattering, general diffraction, grazing incidence diffraction • 4-38 keV • Remote • Accepting general users

6-ID-D • XSD • Physics, materials science • High-energy x-ray diffraction, powder diffraction, pair distribution function • 50-100 keV, 70-130 keV • Remote • Accepting general users

7-BM-B • XSD • Physics • Radiography, tomography, microfluorescence • 5-150 keV, 6-15 keV, 15-60 keV • On-site • Accepting general users

7-ID-B,C,D • XSD • Materials science, atomic physics, chemistry • Time-resolved x-ray scattering, time-resolved x-ray absorption fine structure, phase contrast imaging • 6-18 keV, 12-26 keV • On-site, remote • Accepting general users

8-BM-B • XSD • Chemistry, life sciences, environmental science, materials science • Fluorescence spectroscopy • 9-18 keV • On-site, mail-in, beamline staff • Accepting general users

8-ID-E • XSD • Materials science, polymer science, physics • Grazing incidence small-angle scattering, x-ray photon correlation spectroscopy • 7.35-7.35 keV, 10.9-10.9 keV • On-site, remote • Accepting general users

8-ID-I • XSD • Polymer science, materials science, physics • X-ray photon correlation spectroscopy, small-angle x-ray scattering • 7.35-7.35 keV, 10.9-10.9 keV • On-site, remote • Accepting general users

9-BM-B,C • XSD • Materials science, chemistry, environmental science • X-ray absorption fine structure, x-ray absorption near-edge structure • 2.1-22.5 keV • On-site, remote, mail-in • Accepting general users

9-ID-B,C • XSD • Chemistry, materials science, life sciences • Nano-imaging, microfluorescence, ultra-small-angle x-ray scattering, tomography, ptychography, x-ray absorption near-edge structure • 4.5-30 keV • On-site • Accepting general users

10-BM-A,B • **Materials Research (MR)-CAT** • Materials science, chemistry, environmental science, physics • X-ray absorption fine structure, time-resolved x-ray absorption fine structure, microfluorescence • 4-32 keV • On-site, remote, mail-in, observer, beamline staff • Accepting general users

10-ID-B • MR-CAT • Materials science, environmental science, chemistry, physics • X-ray absorption fine structure, time-resolved x-ray absorption fine structure, microfluorescence, x-ray photoemission spectroscopy, x-ray emission spectroscopy • 4.8-32 keV, 15-65 keV • On-site, remote, mail-in, observer, beamline staff • Accepting general users

11-BM-B • XSD • Chemistry, materials science, physics • Powder diffraction • 15-33 keV • On-site, remote, mail-in • Accepting general users

11-ID-B • XSD • Chemistry, environmental science, materials science • Pair distribution function, high-energy x-ray diffraction, grazing incidence diffraction • 58.66 keV, 86.7 keV • On-site, remote, mail-in • Accepting general users

11-ID-C • XSD • Materials science, chemistry, physics • High-energy x-ray diffraction, diffuse x-ray scattering, pair distribution function • 105.7 keV • On-site, remote • Accepting general users

11-ID-D • XSD • Chemistry, environmental science, materials science • Time-resolved x-ray absorption fine structure, time-resolved x-ray scattering • 6-25 keV • On-site, remote • Accepting general users

12-BM-B • XSD • Materials science, polymer science, chemistry, physics, environmental science • X-ray absorption fine structure, small-angle x-ray scattering, wide-angle x-ray scattering • 4.5-30 keV, 10-40 keV • On-site, remote, mail-in • Accepting general users

12-ID-B • XSD • Chemistry, materials science, life sciences, polymer science, physics • Small-angle x-ray scattering, grazing incidence small-angle scattering, wide-angle x-ray scattering, grazing incidence diffraction • 7.9-14 keV • On-site, remote • Accepting general users

12-ID-C,D • XSD • Chemistry, physics, materials science • Small-angle x-ray scattering, grazing incidence small-angle scattering, wide-angle x-ray scattering, surface diffraction • 4.5-40 keV • On-site • Accepting general users

13-BM-C • **GeoSoilEnviro Center for Advanced Radiation Sources (GSECARS)** • Geoscience, environmental science • Surface diffraction, high-pressure diamond anvil cell, single-crystal diffraction • 15-15 keV, 28.6-28.6 keV • On-site • Accepting general users

13-BM-D • GSECARS • Geoscience, environmental science • Tomography, high-pressure diamond anvil cell, high-pressure multi-anvil press • 4.5-100 keV • On-site • Accepting general users

13-ID-C,D • GSECARS • Geoscience, environmental science • Surface diffraction, microdiffraction, x-ray standing waves, x-ray absorption fine structure, resonant inelastic x-ray scattering, x-ray emission spectroscopy, high-pressure diamond anvil cell, high-pressure multi-anvil press • 4.9-45 keV, 10-75 keV • On-site • Accepting general users

13-ID-E • GSECARS • Geoscience, environmental science • Microfluorescence, micro x-ray absorption fine structure, microdiffraction, fluorescence spectroscopy • 2.4-28 keV, 5.4-28 keV • On-site • Accepting general users

14-BM-C • **BioCARS** • Life sciences • Macromolecular crystallography, fiber diffraction, biohazards at the BSL2/3 level • 8-14.9 keV • On-site, remote, beamline staff • Accepting general users

14-ID-B • BioCARS • Life sciences • Time-resolved crystallography, time-resolved x-ray scattering, Laue crystallography, wide-angle x-ray scattering, biohazards at the BSL2/3 level, macromolecular crystallography, serial crystallography • 7-19 keV • On site, remote, beamline staff • Accepting general users

15-ID-B,C,D • **ChemMatCARS** • Materials science, chemistry • Resonant diffraction — single-crystal, high-pressure diamond anvil cell-single crystal, photo-crystallography, single-crystal diffraction, liquid interface scattering, liquid interface spectroscopy, anomalous small-angle x-ray scattering • 5.5-32 keV, 10-70 keV • On-site, remote, mail-in • Accepting general users

16-BM-B • **HPCAT-XSD** • Materials science, geoscience, chemistry, physics • White Laue single-crystal diffraction, energy dispersive x-ray diffraction, phase contrast imaging, radiography, pair distribution function • 10-120 keV • Remote • Accepting general users

16-BM-D • HPCAT-XSD • Materials science, geoscience, chemistry, physics • Powder angular dispersive x-ray diffraction, single-crystal diffraction, x-ray absorption near-edge structure, x-ray absorption fine structure, tomography • 6-45 keV • Remote • Accepting general users

16-ID-B • HPCAT-XSD • Materials science, geoscience, chemistry, physics • Microdiffraction, single-crystal diffraction • 18-50 keV • Remote • Accepting general users

16-ID-D • HPCAT-XSD • Materials science, geoscience, chemistry, physics • Nuclear resonant scattering, inelastic x-ray scattering (1-eV resolution), x-ray emission spectroscopy • 5-37 keV, 14.41-14.42 keV • Remote • Accepting general users

17-BM-B • XSD • Chemistry, materials science • Powder diffraction, pair distribution function • 27-51 keV • On-site, remote, mail-in • Accepting general users

17-ID-B • **Industrial Macromolecular Crystallography Association (IMCA)-CAT** • Life sciences • Macromolecular crystallography, multi-wavelength anomalous dispersion, microbeam, single-wavelength anomalous dispersion, large unit cell crystallography • Subatomic (<0.85 Å) resolution • 6-20 keV • On-site, remote, mail-in • Accepting general users

18-ID-D • **Biophysics (Bio)-CAT** • Life sciences • Fiber diffraction, micro-diffraction, small-angle x-ray scattering, time-resolved x-ray scattering • 3.5-35 keV • On-site, remote, mail-in • Accepting general users

19-BM-D • **Structural Biology Center (SBC)-XSD** • Life sciences • Multi-wavelength anomalous dispersion, macromolecular crystallography, single-wavelength anomalous dispersion • 6-18.5 keV • Remote, on-site, mail-in • Accepting general users

19-ID-D • SBC-XSD • Life sciences • Macromolecular crystallography, multi-wavelength anomalous dispersion, subatomic (<0.85 Å) resolution, large unit cell crystallography, single-wavelength anomalous dispersion, serial crystallography • 6-19 keV • On-site, remote, mail-in • Accepting general users

20-BM-B • XSD • Materials science, environmental science, chemistry • X-ray absorption fine structure, microfluorescence • 2.7-32 keV, 2.7-35 keV • On-site, remote, mail-in • Accepting general users

20-ID-B,C • XSD • Materials science, environmental science, chemistry • X-ray absorption fine structure, x-ray Raman scattering, micro x-ray absorption fine structure, microfluorescence, x-ray emission spectroscopy • 4.3-27 keV, 7-52 keV • On-site, remote, mail-in • Accepting general users

21-ID-D • **Life Sciences (LS)-CAT** • Life sciences • Macromolecular crystallography • 6.5-20 keV • On-site, remote, mail-in • Accepting general users

21-ID-F • LS-CAT • Life sciences • Macromolecular crystallography • 12.7 keV • Remote, on-site, mail-in • Accepting general users

21-ID-G • LS-CAT • Life sciences • Macromolecular crystallography • 12.7 keV • On-site, remote, mail-in • Accepting general users

22-BM-D • **Southeast Regional (SER)-CAT** • Life sciences • Macromolecular crystallography, single-wavelength anomalous dispersion, multi-wavelength anomalous dispersion • 8-16 keV • On-site, remote • Accepting general users

22-ID-D • SER-CAT • Life sciences • Macromolecular crystallography, multi-wavelength anomalous dispersion, single-wavelength anomalous dispersion, microbeam • 6-16 keV • On-site, remote • Accepting general users

23-ID-B • **National Institute of General Medical Sciences and National Cancer Institute (GM/CA)-XSD** • Life sciences • Macromolecular crystallography, microbeam, large unit cell crystallography, subatomic (<0.85 Å) resolution, multi-wavelength anomalous dispersion, single-wavelength anomalous dispersion • 6-20 keV • On-site, remote • Accepting general users

23-ID-D • GM/CA-XSD • Life sciences • Macromolecular crystallography, microbeam, large unit cell crystallography, subatomic (<0.85 Å) resolution, multi-wavelength anomalous dispersion, single-wavelength anomalous dispersion, serial crystallography • 6.3-20 keV • On-site, remote • Accepting general users

24-ID-C • **Northeastern (NE)-CAT** • Life sciences • Macromolecular crystallography, microdiffraction, single-wavelength anomalous dispersion, single-crystal diffraction, microbeam, multi-wavelength anomalous dispersion, subatomic (<0.85 Å) resolution • 6.5-20 keV • On-site, remote • Accepting general users

24-ID-E • NE-CAT • Life sciences • Macromolecular crystallography, microbeam, microdiffraction, single-wavelength anomalous dispersion, single-crystal diffraction • 12.68 keV • On-site, remote • Accepting general users

26-ID-C • **Center for Nanoscale Materials (CNM)/XSD** • Physics, materials science • Nanodiffraction, nano-imaging, coherent x-ray scattering • 7-12 keV • On-site, remote, mail-in, observer, beamline staff • Accepting general users

27-ID-B • XSD • Physics, materials science, chemistry • Resonant inelastic x-ray scattering • 5-14 keV • On-site • Accepting general users

29-ID-C,D • XSD • Physics, materials science • Resonant soft x-ray scattering, angle-resolved photoemission spectroscopy • 250-2200 eV, 2200-3000 eV • Remote, mail-in • Accepting general users

30-ID-B,C • XSD • Physics, materials science, geoscience, life sciences • Inelastic x-ray scattering (1-meV resolution), nuclear resonant scattering • 23.7-23.9 keV • On-site • Accepting general users

31-ID-D • **Lily Research Laboratories (LRL)-CAT** • Life sciences • Macromolecular crystallography, single-wavelength anomalous dispersion • 5-22 keV • Mail-in • Accepting general users

32-ID-B,C • XSD • Materials science, life sciences, geoscience • Phase contrast imaging, radiography, transmission x-ray microscopy, tomography • 7-40 keV • On-site • Accepting general users

33-BM-C • XSD • Materials science, physics, chemistry • Diffuse x-ray scattering, general diffraction, powder diffraction, x-ray reflectivity, grazing incidence diffraction, anomalous and resonant scattering • 5-35 keV • On-site • Accepting general users

33-ID-D,E • XSD • Materials science, physics, chemistry, environmental science • Anomalous and resonant scattering, diffuse x-ray scattering, general diffraction, surface diffraction, surface diffraction (UHV), x-ray reflectivity • 5-30 keV • On-site • Accepting general users

34-ID-C • XSD • Materials science, physics • Coherent x-ray scattering • 5-15 keV • On-site, remote • Accepting general users

34-ID-E • XSD • Materials science, physics, environmental science, geoscience • Microdiffraction, Laue crystallography, microbeam, microfluorescence • 7-30 keV • On-site • Accepting general users

35-ID-B,C,D,E • **Dynamic Compression Sector (DCS)** • Physics, materials science, geoscience • Time-resolved x-ray scattering, phase contrast imaging, radiography • 7-35 keV, 7-100 keV, 24-24 keV • On-site, remote • Accepting general users

Welcome

Laurent Chapon

March 2022

For years I had the pleasure of watching the APS and its user community grow and evolve, first close-up when I was a postdoc at the Argonne Materials Science Division, and then throughout my career. Now my first months as APS director have given me an even greater appreciation for this superb facility, the people who operate it and use it, and the science they produce.

By their nature, collections of research highlights such as this one present just a sample of the year-after-year scientific discoveries and feats of engineering that advance our leadership in science and technology and justify the faith of our sponsors in the Department of Energy Office of Science, and the Basic Energy Sciences (BES) Program Scientific User Facilities Division. After all, in 2021, our users and staff produced more than 2200 publications (and counting), including over 2090 peer-reviewed journal articles (40% of them in journals with an Impact Factor Above 7, which is the new threshold for impactful results set by BES).

Beginning in March 2020, APS staff and remote (and later some on-site) users produced extensive and important science that examined the SARS-CoV-2 virus, including critical contributions to development of Paxlovid, the new antiviral Pfizer treatment for COVID-19 (see page 104). For a complete listing of that research, see "Publications, Preprints, Highlights, and Features about SARS-CoV-2 Research at the Advanced Photon Source" on our web site. This is all thanks to the dedication, skill, and efforts of the X-ray Science Division beamline staff under division director Jonathan Lang; the beamline staff that keep our collaborative access team facilities up and running; the APS accelerator, technical, and support personnel; and the APS and Argonne support staff. A great deal of the skill mentioned above rests in the hands and minds of the physicists, engineers, and technicians in our Accelerator Systems Division under John Byrd, and APS Engineering Support Division under new division director Mike Edelen. Without them, there would be no electrons in the storage ring, and so no results published in this book. Every day I find new reasons to applaud these dedicated people; the list of their achievements is too long for this space, but we will bring more of them to the fore in next year's volume in this series.

The APS Upgrade (APS-U) Project is well under way, with a start of the installation shutdown planned for April 2023. The project will culminate in a new electron storage ring that will provide x-ray beams up to 500 times brighter than now available, nine completely new beamlines, and enhancements to several of our current beamlines. We owe a great deal to the BES Scientific User Facilities Division for their unwavering support; to Argonne Director Paul Kearns for his steadfast encouragement at every turn; and to Bob Hettel and Jim Kerby and their APS-U team for the splendid work they have done thus far and the successful outcome they will achieve in the near future. I look forward to leaning on Jim and Elmie Peoples-Evans for their leadership in their positions with the APS-U, and on Bob for his counsel as Advisor.

Coming to the APS at Argonne impresses upon me the value of interacting with the Argonne directorates and their varied scientific programs. The APS draws users from Argonne scientists pursuing topics in materials, biological, energy, chemistry, environment, climate, and more. Access to the enormous computing power of the Polaris supercomputer and upcoming Aurora, operated by the Argonne Leadership Computing Facility, will provide our staff and users with real-time, post-experiment data processing and analysis, and new ways to integrate experimental science and artificial intelligence. This synergy will become even more important when the APS-U is complete.

This is an exciting time and future for the APS, its staff and users, and for me. None of us would be at this point without Stephen Streiffer, my predecessor in this job. His steady, imaginative leadership of the Photon Sciences Directorate has us all firmly on the road to a bright future.

Laurent Chapon
Associate Laboratory Director for Photon Sciences
Director, Advanced Photon Source

APS Upgrade Update

Jim Kerby

January 2022

This past year has been a lesson in perspective. Like everyone, those of us working on the Advanced Photon Source Upgrade Project (APS-U) at Argonne National Laboratory have been met with challenges. The COVID-19 pandemic and the attendant supply chain issues have affected the APS-U Project, as they have affected all of our lives.

And like everyone, the APS-U team has been called upon to meet those challenges. In spite of innumerable impacts to the cost, schedule, and contingency of the project, the past year has seen significant progress. This is thanks to the diligence, creativity, and boundless energy exhibited by the best team with whom anyone could hope to work.

As of this date, the APS-U Project is 64% complete, and the total project scope, cost, and completion schedule remain unchanged since the Critical Decision 2 (CD-2) agreement with the Department of Energy (DOE) that began our work in earnest. Our effort has shifted from design to full receipt and assembly of technical components–essentially, we're now bringing the upgraded APS to life, building and testing important pieces of the new electron storage ring, and the new and enhanced beamlines.

The new multi-bend achromat storage ring at the heart of the upgraded APS will take a year to install, during which time the APS will shut down, its x-ray beams inaccessible to the user community. The start of that shutdown period is driven by the accelerator and front-end assembly work; completion of the project is driven by beamline completion.

Last year, in consultation with DOE's Basic Energy Sciences program, we set a new start date of April 17, 2023, for the storage ring installation period. This new date means that users will get a full year of APS operations in 2022 and at least an abbreviated run at the start of 2023. While COVID-19-related delays continue to affect the project, it is our top priority to hold to that start date, and to deliver the upgraded APS on time and on budget.

A critical component of the APS-U is construction of nine feature beamlines and the enhancement of several existing beamlines. Some of those beamlines will need to shut down in advance of the year-long installation period to facilitate construction work. The project team is in the process of communicating the timing and scope of that work to users of each of the affected scientific programs. The latest information will be posted on the APS Upgrade Project website.

The PAR shielding installation team, left to right: Randy Brown, Rob Lange, Vic Guarino, Valerie Rivas, Jessie Morales, Ryan Roberts, Stan Wiedmeyer, Frank Skrzecz, and Kathy Harkay. Not pictured: Jeremy Carvelli, Greg Fystro, and Bradley Micklich. Photo: Elroy Chang/Argonne

In preparation for the upgrade, modifications were needed for the radiation shielding in the particle accumulator ring (PAR). This was a large undertaking by the team entrusted with this task (photo above), considering the tight working conditions, and that each steel panel of shielding was 4 inches thick, 2 feet wide, 76 inches tall, and weighed approximately 2,100 lbs. The modifications required a double layer of steel panels on the PAR concrete walls, totaling 8-inch thickness. The job involved installing a total of over 50 tons of steel. A custom installation cart was designed to fit the PAR's limited work space. The team expertly completed the job ahead of the estimated time needed.

Construction of the Long Beamline Building (LBB), the most visible sign of APS-U progress, has moved forward ahead of schedule since its groundbreaking ceremony on July 22, 2020, and is on track for completion in June

"APS Upgrade" cont'd. on next page

The Long Beamline Building, March 22, 2022.

"APS Upgrade" cont'd. from previous page

2022. The team was granted beneficial occupancy of the new building in February 2022, and work is now under way on the two beamlines it will house.

2021 saw a major milestone: the arrival of the 1,000th APS-U magnet, one of the 1,321 electromagnets that comprise the lattice for the new storage ring. This magnet was an eight-pole fast corrector magnet, which is used to alter the trajectory of the electron beam as it circulates around the storage ring.

The magnets that have been received and tested are currently being assembled into 200 modules, which will be transported to the APS and installed during the shutdown period. About 50 of those modules have been partially completed, and the team recently moved one of the heavy concrete plinths that will support these modules into the current APS storage ring area, to help prepare for any challenges that might arise when moving the completed components.

Most recently, the first new instrument created as part of the APS-U is now available for users. The resonant inelastic x-ray spectroscopy (RIXS) instrument at beamline 27-ID replaces an earlier model and includes improvements that make it easier to use and more adaptable to thin-film samples.

And through all of this, Argonne's Photon Sciences directorate (PSC) and APS-U management have never lost sight of the first-order imperative: assuring the health and safety of everyone is the most important thing we do.

The successes above can be attributed to the APS-U team. The scientists, engineers, and technicians working on the upgrade bring with them a variety of backgrounds and areas of expertise, and we're spotlighting members of the team in a regular series called "People of the APS Upgrade." Taken together, these profiles start to tell the story of this massive project through the people making it happen. You can find them on the APS-U website.

The APS-U Project is committed to answering user questions and keeping open communication flowing. To that end, we're organizing twice-yearly Q&A sessions with users, in May (as part of the APS/CNM Users Meeting) and in November of each year. The questions and answers are captured in an evolving document on the APS-U website.

On behalf of everyone working on the APS-U and in PSC, I offer profound thanks to Bob Hettel, who has transitioned to a new role as advisor to Laurent Chapon, the new PSC associate laboratory director and APS director. The APS-U is on firm ground and headed toward a bright future thanks to the work Bob has done as project director.

Elmie Peoples-Evans has stepped into the role of project manager, continuing to guide the ship with the help of the tireless efforts of associate project managers Glenn Decker (accelerators) and Mohan Ramanathan (experimental systems and insertion devices). They are proof, as is everyone working on the APS-U, that the heart and soul of this project is its people.

Remember this: All parties–our sponsors in the DOE Office of Science and Basic Energy Sciences, Argonne, and PSC–are committed to the success of the APS-U and PSC and to assuring that the APS will emerge from the upgrade on schedule and continue to be a world-leading hard x-ray facility for our user community. We're grateful for the efforts of so many to make this project a reality.

Jim Kerby

APS Upgrade Project Director

Engineering Materials and Applications

Twisting, Flexible Crystals are Key to Solar Energy Production

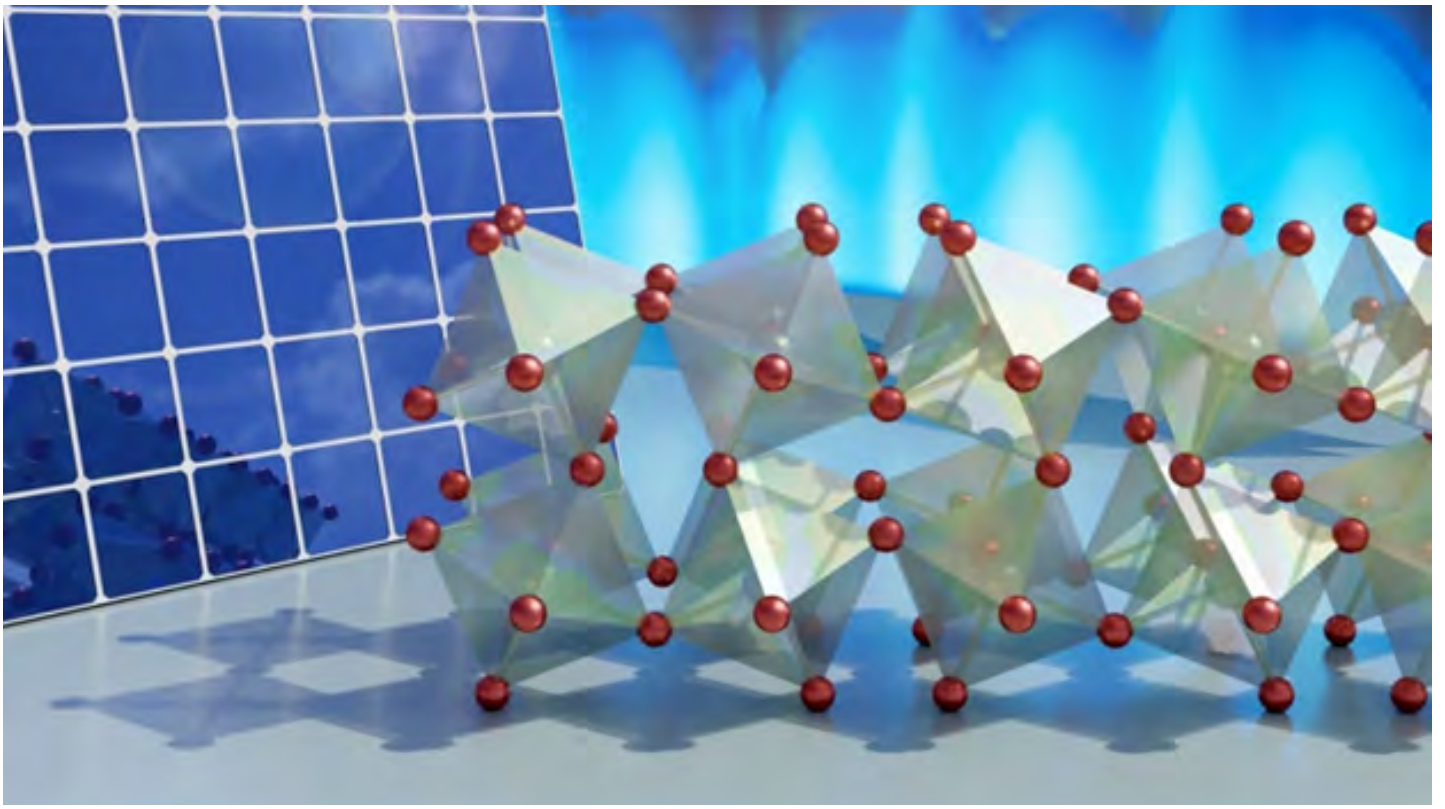

Researchers have discovered that the way eight-sided molecules move around hinge-like bromine atoms (red) gives them their unique energy properties. Image: ORNL/Jill Hemman.

The Duke University press release by Ken Kingery can be read here.

Long-hidden molecular dynamics that provide desirable properties for solar energy and heat energy applications to an exciting class of materials called halide perovskites have been revealed by researchers using two U.S. Department of Energy (DOE) facilties including the APS. Details of the discovery were published in the journal *Nature Materials*.

A key contributor to how these materials create and transport electricity hinges on the way their atomic lattice twists and turns in a hinge-like fashion. The results will help materials scientists in their quest to tailor the chemical recipes of these materials for a wide range of applications in an environmentally friendly way.

"There is a broad interest in halide perovskites for energy applications like photovoltaics, thermoelectrics, optoelectronic radiation detection and emission—the entire field is incredibly active," said Olivier Delaire, associate professor of mechanical engineering and materials science at Duke. "While we understand that the softness of these materials is important to their electronic properties, nobody really knew how the atomic motions we've uncovered underpin these features."

Perovskites are a class of materials that—with the right combination of elements—are grown into a crystalline structure that makes them particularly well-suited for energy applications. Their ability to absorb light and transfer its energy efficiently makes them a common target for researchers developing new types of solar cells, for example. They're also soft, sort of like how solid gold can be easily dented, which gives them the ability to tolerate defects and avoid cracking when made into a thin film.

One size, however, does not fit all, as there is a wide range of potential recipes that can form a perovskite. Many of the simplest and most studied recipes include a halogen—such as chlorine, fluorine or bromine—giving them the name halide perovskites. In the crystalline struc-

ture of perovskites, these halides are the joints that tether adjoining octahedral crystal motifs together.

While researchers have known these pivot points are essential to creating a perovskite's properties, nobody has been able to look at the way they allow the structures around them to dynamically twist, turn and bend without breaking, like a Jell-O mold being vigorously shaken.

"These structural motions are notoriously difficult to pin down experimentally. The technique of choice is neutron scattering, which comes with immense instrument and data analysis effort, and very few groups have the command over the technique that Olivier and his colleagues do," said Volker Blum, professor of mechanical engineering and material science at Duke who does theoretical modeling of perovskites, but was not involved with this study. "This means that they are in a position to reveal the underpinnings of the materials properties in basic perovskites that are otherwise unreachable."

In the study, Delaire and Duke University co-authors working with colleagues from Argonne, Oak Ridge National Laboratory, the University of Maryland, Northwestern University, and the National Institute of Science and Technology reveal important molecular dynamics of the structurally simple, commonly researched halide perovskite ($CsPbBr_3$) for the first time.

The researchers started with diffuse scattering measurements performed at the XSD Magnetic Materials Group's 6-ID-D x-ray beamline at the APS on small, millimeter-scale single crystals of the halide perovskite. These results suggested that further experiments to investigate the atomic dynamics using neutrons would be important. Fortunately, Argonne's Materials Science Division (MSD) and Northwestern had the expertise to grow the large, centimeter-scale, single crystals required for the neutron measurements. The team then barraged the crystal with neutrons from the Spallation Neutron Source at the DOE's Oak Ridge National Laboratory. By measuring how the neutrons and x-rays bounced off the crystals over many angles and at different time intervals, the researchers teased out how its constituent atoms moved over time. "This work is a beautiful example of the complementarity of neutrons and x-rays in revealing both the structure and dynamics of complex materials," said Ray Osborn, a scientist in MSD, who was involved in both sets of measurements.

After confirming their interpretation of the measurements with computer simulations, the researchers discovered just how active the crystalline network actually is. Eight-sided octahedral motifs attached to one another through bromine atoms were caught twisting collectively in plate-like domains and constantly bending back and forth in a very fluid-like manner.

"Because of the way the atoms are arranged with octahedral motifs sharing bromine atoms as joints, they're free to have these rotations and bends," said Delaire. "But we discovered that these halide perovskites in particular are much more 'floppy' than some other recipes. Rather than immediately springing back into shape, they return very slowly, almost more like Jell-O or a liquid than a conventional solid crystal."

Delaire explained that this free-spirited molecular dancing is important to understand many of the desirable properties of halide perovskites. Their "floppiness" stops electrons from recombining into the holes the incoming photons knocked them out of, which helps them make a lot of electricity from sunlight. It likely also makes it difficult for heat energy to travel across the crystalline structure, which allows them to create electricity from heat by having one side of the material be much hotter than the other.

Because the perovskite used in the study has one of the simplest recipes, yet already contains the structural features common to the broad family of these compounds, Delaire believes that these findings likely apply to a large range of halide perovskites. For example, he cites hybrid organic-inorganic perovskites (HOIPs), which have much more complicated recipes, as well as lead-free double-perovskite variants that are more environmentally friendly.

"This study shows why this perovskite framework is special even in the simplest of cases," said Delaire. "These findings very likely extend to much more complicated recipes, which many scientists throughout the world are currently researching. As they screen enormous computational databases, the dynamics we've uncovered could help decide which perovskites to pursue."

"Twisting" cont'd. on page 5

Going with the Flow: Studying Microjets from Liquid and Solid Tin

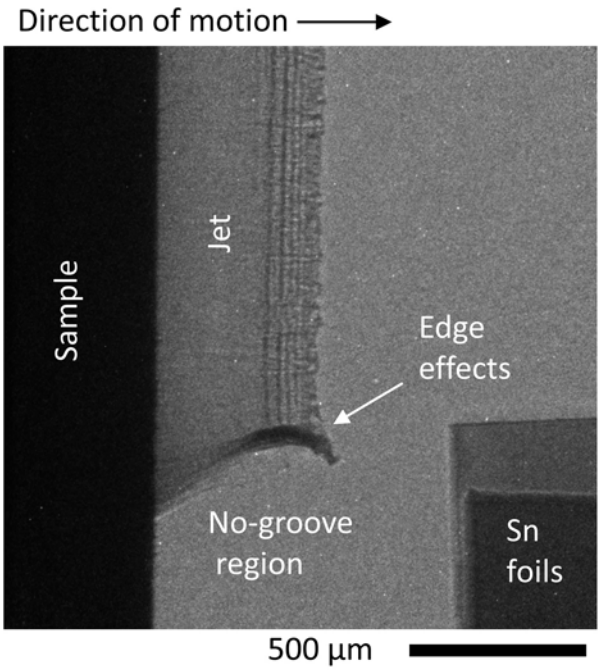

Fig. 1. A Sn jet can be seen traveling from left to right. The sample base and no-groove control region are also visible on the left, along with thickness calibration foils in the lower right

When a material receives a strong impact, the resulting shock wave propagates until it reaches a free surface. There, expelled microjets of the material can launch from defect sites. The characteristics of these microjets depend on a number of factors, including the initial surface profile of the impacted material, the strength and profile of the shock, the materials' density, and its resistance to shear and cavitation. But how crossing the material's melt boundary might affect them is less clear. Theoretical and experimental studies have suggested a sudden increase in the mass of ejected material as the base material is driven above the melt boundary, which makes intuitive sense given the shift from strong solid to easily deformed liquid; however, recent computational studies suggest that melting plays a more nuanced role. To examine this question, a team of researchers from Lawrence Livermore National Laboratory used the APS to examine microjets in tin (Sn) above and below impacts that result in melting, showing some trends for microjets from solid and liquid base materials that vary significantly with the surface defect size. These findings, published in the *Journal of Applied Physics*, add some insight about differences between solid and liquid microjets, findings that could be directly applicable to fields like planetary impact and indirectly to other shock-related work such as industry, in which these phenomena could disrupt measurements, damage equipment, or even present safety hazards.

The researchers compared the behavior of Sn with that of copper (Cu), which melts at a significantly higher impact pressure. In polished samples of both of these metals, they cut V-shaped grooves to serve as surface defects. They then subjected these samples to strikes at different impact velocities, measuring the microjets' morphology, velocity, and mass of ejected materials with high-speed synchrotron phase contrast imaging (PCI) carried out at the DCS 35-ID x-ray beamline at the APS.

When shock-compressed to ~23 GPa, Sn melts upon release. Impact velocities were chosen to achieve two pressures below this value (Sn1 and Sn2) and two above it (Sn3 and Sn4). The Cu samples received impacts that produced pressures between the two highest values of Sn (Cu1) and slightly above them (Cu2). Because the Cu melt line is significantly higher than that of Sn, the researchers were able to compare the resulting Cu solid microjets at pressures similar or higher than the Sn liquid ones.

PCI results for Sn1, Sn2, and Cu1 showed the solid microjets forming wavy bands that break up into a net-like field. In contrast, the melted microjets of Sn3 and Sn4 showed a different pattern, with striations perpendicular to the leading edge of the jet with no evidence of breakup. The solid Sn2 microjet showed neither striations nor breakup, instead appearing as a nearly smooth sheet with each observation (Fig. 1).

The researchers note that while it's tempting to credit melting for the lack of breakup in Sn3 and Sn4, solid Cu2 microjets also show the same prolonged intact elongation, suggesting that this effect may be due to increasing jet velocity causing an increase in stable elongation independent of material property changes.

"Going"cont'd. on next page

"Going" cont'd. from previous page

Both molten Sn3 and Sn4 microjets showed longitudinal striations along the direction of shock propagation, which aren't observed in any of the solid jets; they also showed lateral striations in the leading part of the jet parallel to the shock front. In addition, Sn3 and Sn4 both showed spike-like ejected material from smaller surface defects in the no-groove regions of the material. Each of these features appear to be directly related to these samples' melted nature.

Interestingly, the researchers found that the mass of ejected material in Sn was nearly identical for the two conditions that straddled the point of melt on release (~23 GPa), Sn2 and Sn3, with significantly larger jumps between the mass of ejecta between Sn1 and Sn2, and between Sn3 and Sn4. Thus, increasing the shock pressure led to increasing jet mass accumulation rates both above and below this critical pressure, but not in its immediate vicinity. However, this effect seems to apply only to the grooves cut into the material and not to ejecta from the small surface defects in the no-groove regions, which produced larger masses of ejecta with increased pressures.

– Christen Brownlee

See: David B. Bober* Kyle K. Mackay, Minta C. Akin, and Fady M. Najjar, "Understanding the evolution of liquid and solid microjets from grooved Sn and Cu samples using radiography," J. Appl. Phys. **130**, 045901 (2021).
DOI: 10.1063/5.0056245
Author affiliation: Lawrence Livermore National Laboratory
Correspondence: * bober1@llnl.gov

This work was performed under the auspices of the U.S. Department of Energy (DOE) by Lawrence Livermore National Laboratory under Contract No. DE-AC52-07NA27344. The Dynamic Compression Sector is operated by Washington State University under the U.S. DOE/National Nuclear Security Administration award no. DE-NA0003957. This research used resources of the Advanced Photon Source, a U.S. DOE Office of Science user facility, operated for the DOE Office of Science by Argonne National Laboratory under Contract No. DE-AC02-06CH11357.

"Twisting" cont'd. from page 3

See: T. Lanigan-Atkins[1], X. He[1], M. J. Krogstad[2], D. M. Pajerowski[3], D. L. Abernathy[3], Guangyong N. M. N. Xu[4], Zhijun Xu[4,5], D.-Y. Chung[2], M. G. Kanatzidis[2,6], S. Rosenkranz[2], R. Osborn[2]*, and O. Delaire[1]**, "Two-Dimensional Overdamped Fluctuations of Soft Perovskite Lattice in $CsPbBr_3$," Nat. Mater. **20**, 977 (2021).
DOI: 10.1038/s41563-021-00947-y
Author affiliations: [1]Duke University, [2]Argonne National Laboratory, [3]Oak Ridge National Laboratory, [4]National Institute of Standards and Technology, [5]University of Maryland, [6]Northwestern University,
Correspondence: * rosborn@anl.gov,
** olivier.delaire@duke.edu

T.L.-A. was supported by the U.S. Department of Energy (DOE) Office of Science-Basic Energy Sciences, Materials Sciences and Engineering Division, under Award No. DE-SC0019299. X.H. and O.D. were supported by the U.S. DOE Office of Science-Basic Energy Sciences, Materials Sciences and Engineering Division, under Award No. DE-SC0019978. Initial support of T.L.-A. by Duke Energy Initiative seed funds is acknowledged. Work at Argonne (synthesis, characterization and X-ray and neutron scattering measurements) is supported by the U.S. DOE Office of Science-Basic Energy Sciences, Materials Science and Engineering Division. The use of Oak Ridge National Laboratory's Spallation Neutron Source was sponsored by the Scientific User Facilities Division, Basic Energy Sciences, U.S. DOE. We acknowledge the support of the National Institute of Standards and Technology, U.S. Department of Commerce, in providing the neutron research facilities used in this work. Theoretical calculations were performed using resources of the National Energy Research Scientific Computing Center, a U.S. DOE Office of Science user facility supported by the Office of Science of the U.S. DOE under Contract No. DE-AC02-05CH11231. This research used resources of the Advanced Photon Source, a U.S. DOE Office of Science user facility operated for the DOE Office of Science by Argonne National Laboratory under Contract No. DE-AC02-06CH11357.

Unveiling what Governs Crystal Growth

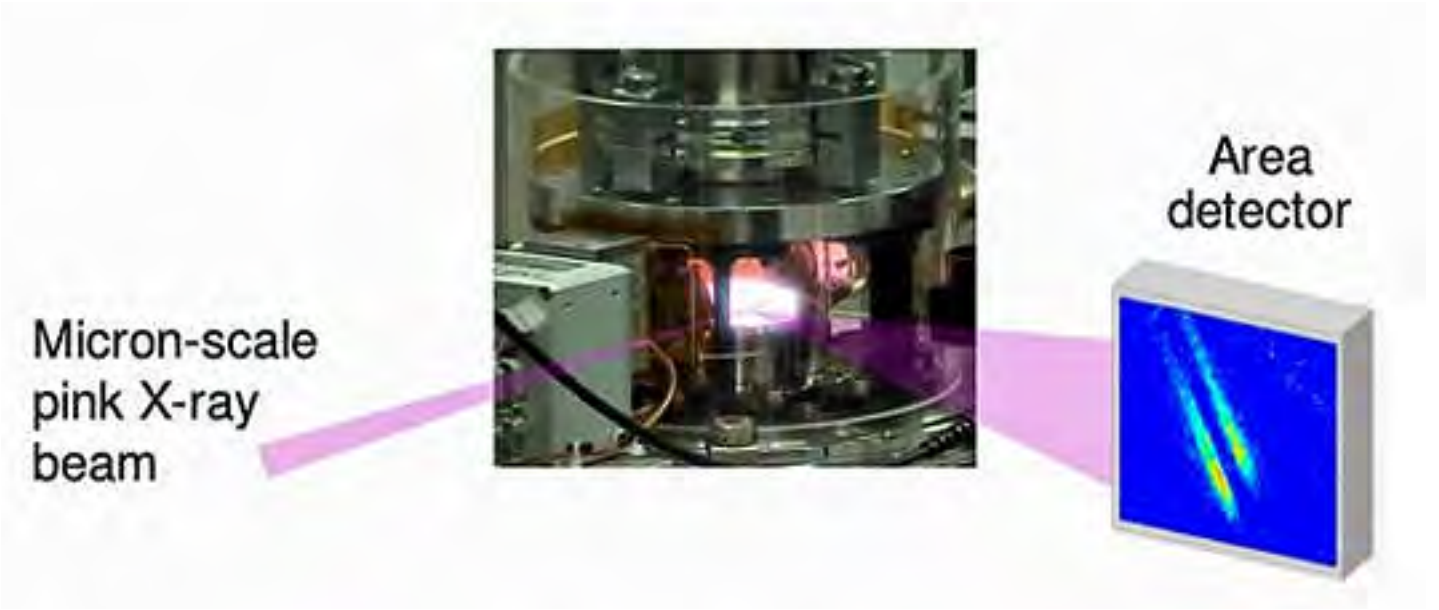

Schematic of microbeam surface x-ray scattering during growth of gallium nitride crystal at high temperature. Image: Argonne National Laboratory.

The original Argonne press release by Joseph E. Harmon can be read here.

With brilliant colors and picturesque shapes, many crystals are wonders of nature. Some crystals are also wonders of science, with transformative applications in electronics and optics. Understanding how best to grow such crystals is key to further advances.

Scientists from Argonne and three universities have revealed new insights into the mechanism behind how gallium nitride crystals grow at the atomic scale and published their results in *Nature Communications*.

Gallium nitride crystals are already in wide use in light-emitting diodes, better known as LEDs. They might also be applied to form transistors for high-power switching electronics to make electric grids more energy efficient and smarter. The use of such "smart grids," which could better balance high power within the overall system, might prevent people from losing power in severe storms.

The same technology could also make individual homes more energy efficient. And it could find use in optical communications, where lasers transmit information. Such information transfer can be more precise, faster and more secure than current capabilities.

Because of these diverse applications, scientists worldwide have been working to improve the process for growing gallium nitride crystals.

"Gallium nitride has a more complicated crystal structure than silicon, the typical crystalline material in electronics," said co-author G. Brian Stephenson, an Argonne Distinguished Fellow in the Materials Science Division. "When you grow this crystal, you get more fascinating behavior at the surface."

At the atomic scale, a growing gallium nitride crystal surface typically looks like a staircase of steps, where every stair is a layer of the crystal structure. Atoms are added to a growing crystal surface by attachment at the edges of the steps. Because of the gallium nitride crystal structure, the steps have alternating edge structures, labeled A and B. The different atomic structures lead to different growth behaviors of the A and B steps. Most theoretical models indicate that atoms accumulate faster on a B-type step, but experimental confirmation has been lacking.

"Because of the high temperatures and chemical atmosphere involved, it is not possible to examine the growth of gallium nitride with a standard electron microscope and test the model prediction," Stephenson said. For that, the team called upon the APS.

The very high energy of the x-rays available at the APS, with a beam only a few micrometers , the XSD Chemical & Materials Science Group's beamline 12-ID-D allowed the team to monitor the rate of gallium nitride growth on

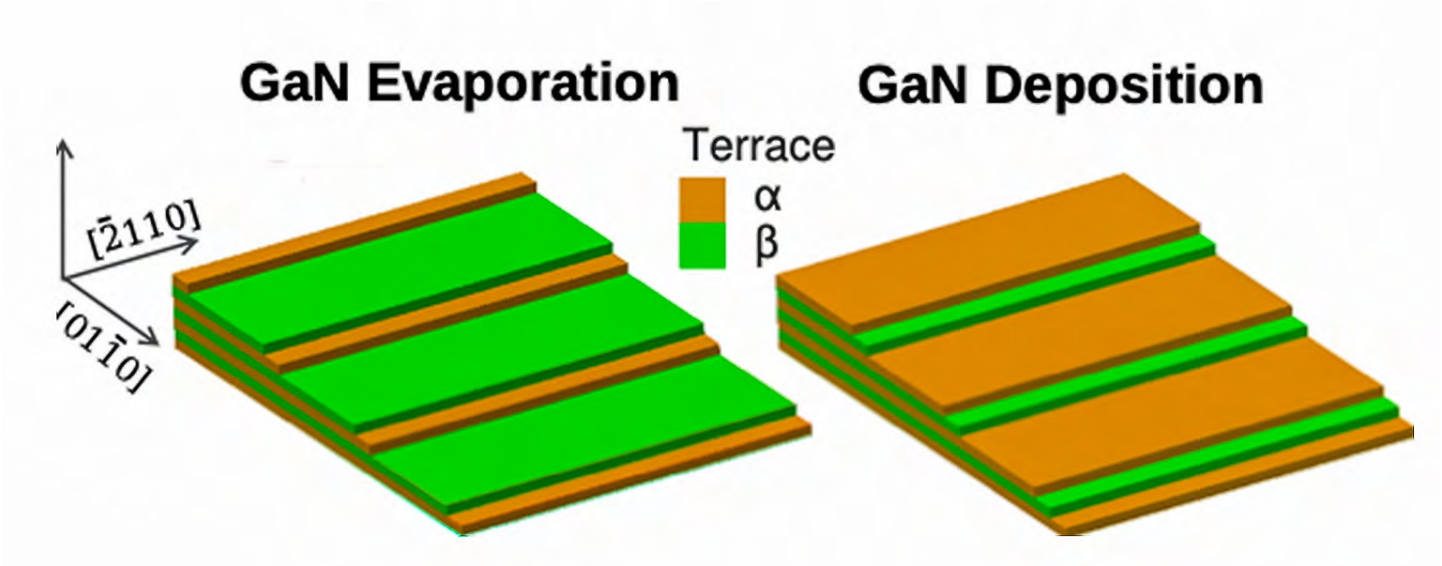

Schematic of surface structures that form during gallium nitride growth processes (evaporation and deposition). The steps at the edges of each atomic layer have alternating structures (α or β). (Image: Argonne National Laboratory.)

the crystal surface steps. These x-rays are an ideal probe since they are sensitive to atomic-scale structure and can penetrate the environment of the crystal at the high temperatures involved, over 1400° F, while it is growing.

"Based on modeling, many had assumed that atoms probably build up faster on the type-B step," Stephenson said. "Imagine our surprise when it turned out to be step A. This suggests the chemistry of the growth process may be more complicated than previously thought."

"This work is a great example of the importance and power of probing a material while a process is underway," added co-author Matt Highland, a physicist in XSD. "Quite often when we use such probes to study processes like synthesis, we find the story to be more complex than we originally thought and counter to conventional wisdom."

The results have obvious implications for refining the current understanding of the atomic-scale mechanisms of gallium nitride growth. This understanding has important practical implications for design of advanced gallium nitride devices by allowing better control of growth and incorporation of additional elements for improved performance. The findings can also be applied to growth of related crystals, including host semiconductor materials for quantum information science.

See: Guangxu Ju[1‡*], Dongwei Xu[1,2], Carol Thompson[3], Matthew J. Highland[1], Jeffrey A. Eastman[1], Weronika Walkosz[4], Peter Zapol[1], and G. Brian Stephenson[1**], "In situ microbeam surface X-ray scattering reveals alternating step kinetics during crystal growth," Nat Commun. **12**, 1721 (2021) 10.1038/s41467-021-21927-5

Author affiliations: [1]Argonne National Laboratory, [2]Huazhong University of Science and Technology, [3]Northern Illinois University, [4]Lake Forest College [‡]Present address: Lumileds Lighting Co.

Correspondence: * juguangxu@gmail.com,
** stephenson@anl.gov

This work was supported by the U.S. Department of Energy (DOE) Office of Science-Basic Energy Sciences, Materials Science and Engineering Division. This research used resources of the Advanced Photon Source, a U.S. DOE Office of Science user facility, operated for the DOE Office of Science by Argonne National Laboratory under contract no. DE-AC02-06CH11357.

Taking Lessons from a Sea Slug Points to Better Hardware for Artificial Intelligence

Fig. 1. By stimulating this quantum material (tiny gray-and-black striped rectangle, arrow, center) with gases, researchers discovered that the material could mimic basic forms of learning found in the sea slug. Purdue University photo/Kayla Wiles.

The original Purdue University press release by Kayla Wiles can be read here (© 2015-20 Purdue University).

For artificial intelligence (AI) to get any smarter, it needs first to be as intelligent as one of the simplest creatures in the animal kingdom: the sea slug. A new study by researchers who carried out experiments at the APS has found that a material can mimic the sea slug's most essential intelligence features. The discovery is a step toward building hardware that could help make AI more efficient and reliable for technology ranging from self-driving cars and surgical robots to social media algorithms.

The study, published in the *Proceedings of the National Academy of Sciences of the United States of America*, was conducted by a team of researchers from Purdue University, Rutgers University, the University of Georgia, and Argonne.

"Through studying sea slugs, neuroscientists discovered the hallmarks of intelligence that are fundamental to any organism's survival," said Shriram Ramanathan, a Purdue professor of materials engineering. "We want to take advantage of that mature intelligence in animals to accelerate the development of AI."

Two main signs of intelligence that neuroscientists have learned from sea slugs are habituation and sensitization. Habituation is getting used to a stimulus over time, such as tuning out noises when driving the same route to work every day. Sensitization is the opposite–it's reacting strongly to a new stimulus, like avoiding bad food from a restaurant. AI has a really hard time learning and storing new information without overwriting information it has already learned and stored, a problem that researchers studying brain-inspired computing call the "stability-plasticity dilemma." Habituation would allow AI to "forget" unneeded information (achieving more stability) while sensitization could help with retaining new and important information (enabling plasticity).

In this study, the researchers found a way to demonstrate both habituation and sensitization in nickel oxide, a quantum material. The material is called "quantum" because its properties can't be explained by classical physics.

If a quantum material could reliably mimic these forms of learning, then it may be possible to build AI directly into hardware. And if AI could operate both through hardware and software, it might be able to perform more-complex tasks using less energy.

"We basically emulated experiments done on sea slugs in quantum materials toward understanding how these materials can be of interest for AI," Ramanathan said.

Neuroscience studies have shown that the sea slug demonstrates habituation when it stops withdrawing its gill as much in response to being tapped on the siphon. But an electric shock to its tail causes its gill to withdraw much more dramatically, showing sensitization.

For nickel oxide, the equivalent of a "gill withdrawal" is an increased change in electrical resistance. The researchers found that repeatedly exposing the material to hydrogen gas causes nickel oxide's change in electrical resistance to decrease over time but introducing a new stimulus like ozone greatly increases the change in electrical resistance (Fig. 1).

Inspired by these findings, a research group under Kaushik Roy, Purdue's Edward G. Tiedemann Jr. Distinguished Professor of Electrical and Computer Engineering, modeled nickel oxide's behavior and built an algorithm that successfully used these habituation and sensitization strategies to categorize data points into clusters.

"The stability-plasticity dilemma is not solved. But we've shown a way to address it based on behavior we've observed in a quantum material," Roy said. "If we could turn a material that learns like this into hardware in the future, then AI could perform tasks much more efficiently."

For practical use of quantum materials as AI hardware, researchers will need to figure out how to apply habituation and sensitization in large-scale systems. They also would have to determine how a material could respond to stimuli while integrated into a computer chip.

This study is a starting place for guiding those next steps, the researchers said. In addition to the experiments performed at Purdue, a team at Rutgers University performed detailed theory calculations to understand what was happening within nickel oxide at a microscopic level to mimic the sea slug's intelligence features. The nickel oxide sample's properties were characterized using three synchrotron x-ray light source techniques at two APS beamlines. Synchrotron x-ray diffraction and x-ray absorption near-edge structure measurements were carried out at the XSD Surface Scattering & Microdiffraction x-ray beamline 33-ID. X-ray absorption spectroscopy studies were performed at the XSD Magnetic Materials Group 29-ID x-ray beamline. The University of Georgia researchers measured conductivity to further analyze the material's behavior.

See: Zhen Zhang[1]*, Sandip Mondal[1], Subhasish Mandal[2], Jason M. Allred[1], Neda Alsadat Aghamiri[3], Alireza Fali[3], Zhan Zhang[4], Hua Zhou[4], Hui Cao[4], Fanny Rodolakis[4], Jessica L. McChesney[4], Qi Wang[1], Yifei Sun[1], Yohannes Abate[3], Kaushik Roy[1], Karin M. Rabe[2]**, and Shriram Ramanathan1***, "Neuromorphic learning with Mott insulator NiO," Proc. Natl. Acad. Sci. USA **118**(39) e2017239118 (September 28, 2021). DOI: 10.1073/pnas.2017239118.
Author affiliations: [1]Purdue University, [2]Rutgers University, [3]University of Georgia, [4]Argonne National Laboratory
Correspondence: * zhennzhang@outlook.com,
** rabe@physics.rutgers.edu, ***shriram@purdue.edu

This work was supported in part by C-BRIC, a JUMP center sponsored by the Semiconductor Research Corporation and DARPA, and by the National Science Foundation (NSF), Intel Corporation, Sandia National Labs, and the Vannevar Bush Fellowship. We acknowledge AFOSR Grant FA9559-16-1-0172, AFOSR Grant FA9550-18-1-0250, ARO Grant W911NF1920237, ONR N00014-17-1-2770 and NSF Grant 1904097 for support. Additional support by NSF under Grant no. DMR-0703406. This research used resources of the Advanced Photon Source, a U.S. Department of Energy (DOE) Office of Science user facility operated for the DOE Office of Science by Argonne National Laboratory under Contract No. DE-AC02-06CH11357.

Thermoelectrics Heat Up with Promising New Magnesium-Based Materials

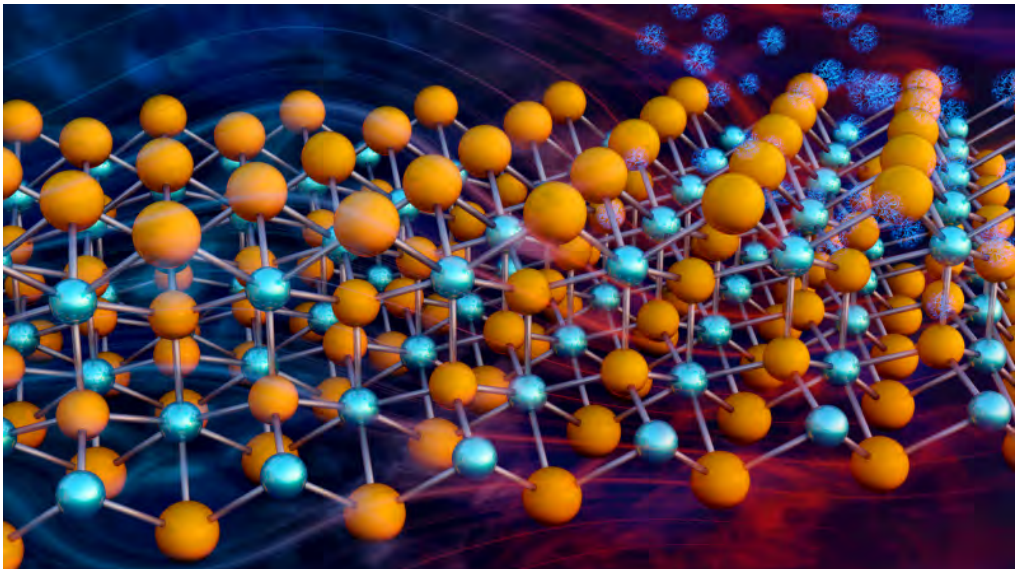

A representation of the crystal lattice of the thermoelectric compound Mg_3Sb_2 (magnesium atoms in orange, antimony in blue). An electric current is generated as heat traverses the material, propelled by phonon waves. Image: ORNL/Jill Hemman

The original Oak Ridge National Laboratory press release by Jeremy Rumsey can be read here.

The landing of NASA's Perseverance rover was another leap forward not only for space exploration but also for the technology that's powering the craft on its years-long mission on Mars—a thermoelectric generator that turns heat into electricity. Looking for the next leap in thermoelectric technologies, researchers at Duke University and Michigan State University using three U.S. DOE research facilities gained new fundamental insights into two magnesium-based materials (Mg_3Sb_2 and Mg_3Bi_2) that have the potential to significantly outperform traditional thermoelectric designs and would also be more environmentally friendly and less expensive to manufacture. Contrary to prevailing scientific wisdom regarding the use of heavy elements, the researchers showed that replacing atoms of heavier elements such as calcium and ytterbium with lighter magnesium atoms actually led to a threefold increase in the magnesium-based materials' performance.

In their research, published in the journal *Science Advances*, the team used neutron and x-ray scattering experiments at the DOE's Oak Ridge (ORNL) and Argonne national laboratories, respectively, as well as supercomputer simulations at the National Energy Research Scientific Computing Center (NERSC). Investigations at the atomic scale revealed the origin and mechanism behind the materials' ability to convert thermal energy at room temperature into electricity. The findings indicate possible new pathways for improving thermoelectric applications such as those in the Perseverance rover and myriad other devices and energy-generation technologies.

Thermoelectric materials essentially create a voltage from a temperature difference between the hot and cold sides of the material. By converting thermal energy into electricity, or vice-versa, thermoelectric devices can be used for refrigeration or electric power generation from heat exhaust.

"Traditional thermoelectric materials rely on heavy elements such as lead, bismuth, and tellurium—elements that aren't very environmentally friendly, and they're also not very abundant, so they tend to be expensive," said Olivier Delaire, associate professor at Duke. "Magnesium on the other hand is lighter and more abundant, which makes it an ideal material for transportation and spaceflight applications, for example."

Typically, Delaire explained, lighter materials are not well suited for thermoelectric designs because their thermal conductivities are too high, meaning they transfer too much heat to maintain the temperature differential needed to produce the voltage. Heavier materials are generally more desirable because they conduct less heat, allowing them to preserve and convert thermal energy more effi-

ciently. “These magnesium materials, however, have remarkably low thermoelectric conductivity despite having a low mass density. Those properties could potentially open the door to designing new types of thermoelectrics that don’t rely on heavy materials with toxic elements,” Delaire explained.

The magnesium materials the team studied belong to a larger class of metal compounds called Zintls. The atomic structure, or arrangement of atoms, in Zintl compounds is such that it’s relatively easy to experiment with and substitute different elements in the material—for example, replacing a heavy element with a light element to achieve optimal performance and functionality.

“In chemical studies, exploring possibilities for new materials often involves substituting one element for another just to see what happens. Usually, we replace them with chemically similar elements in the periodic table, and one of the big advantages to using Zintls is that we can experiment with a lot of different elements and different combinations,” said first author Jingxuan Ding, a graduate student researcher in Delaire’s group. “No one expected magnesium to be the better compound, but when our collaborators at Michigan State substituted it into the materials’ ingredients, we were surprised to find that was in fact the case, so the next step was to find out why.”

The atoms in a material are not static; they vibrate with amplitudes that increase with higher temperatures. The collective vibrations create a ripple effect, called a phonon, that looks like sets of waves on the surface of a pond. Those waves are what transport heat through a material, which is why measuring phonon vibrations is important for determining a material’s thermal conductivity.

Neutrons are uniquely suited for studying quantum phenomena such as phonons because neutrons have no charge and can interact with nuclei. Delaire likened neutron interactions to plucking a guitar string in that they can transfer energy to the atoms to excite the vibrations and elicit hidden information about the atoms inside a material.

The team used the Wide Angular-Range Chopper Spectrometer (ARCS) at the ORNL Spallation Neutron Source (SNS) to measure the phonon vibrations. The data they acquired enabled them to trace the materials’ favorable low thermal conductivity to a special magnesium bond that disrupts the travel of phonon waves through the material by causing them to interfere with each other.

“Neutrons are one of the best ways to measure atomic vibrations like the ones we’re studying in these materials,” said Ding. “ARCS can detect a wide range of frequencies and wavelengths that helps us measure the phonon waves found in the material, which is exactly what we need to better understand how these low thermal conductivity materials operate.”

The neutron scattering measurements provided the research team with a broad survey of the internal dynamics of the magnesium Zintl materials that helped guide and refine computer simulations and x-ray experiments led by Ding, which were used to build a complete understanding of the origins of the materials’ thermal conductivity.

Complementary x-ray experiments employing inelastic x-ray scattering (IXS) were carried out by the team members and colleagues from Argonne using the high-resolution IXS beamline HERIX at the XSD Inelastic X-ray & Nuclear Resonant Scattering Group’s 30-ID beamline at the APS. They zoomed in on specific phonon modes in crystal samples too small for neutron measurements. Both the neutron and x-ray measurements agreed with the supercomputer simulations performed at NERSC.

“Thermoelectrics are essential in applications like the Mars Perseverance rover that require simpler, more lightweight and reliable designs instead of the bulky engines with moving parts that are traditionally used to generate electricity from heat,” said Delaire. “These magnesium-based materials are a big advance in the field that could offer significantly more power efficiency and a lot of potential for more advanced thermoelectric applications.”

See: Jingxuan Ding[1], Tyson Lanigan-Atkins[1], Mario Calderón-Cueva[2], Arnab Banerjee[3,4], Douglas L. Abernathy[3], Ayman Said[5], Alexandra Zevalkink[2], and Olivier Delaire[1]*, “Soft anharmonic phonons and ultralow thermal conductivity in $Mg_3(Sb, Bi)_2$ thermoelectrics,” Sci. Adv. **7**, eabg1449 (21 May 2021). DOI: 10.1126/sciadv.abg1449
Author affiliations: [1]Duke University, [2]Michigan State University, [3]Oak Ridge National Laboratory, [4]Purdue University, [5]Argonne National Laboratory
Corresponding author: * olivier.delaire@duke.edu

X-ray and neutron scattering data collection and analysis by J.D. and T.L.-A. and first-principles simulations by J.D. were supported by the U.S. Department of Energy (DOE) Office of Science-Basic Energy Sciences (BES), Materials Sciences and Engineering Division, under award no. DE-SC0019299. Sample synthesis by M.C.-C. was supported by the U.S. DOE Office of Science-BES, Materials Sciences and Engineering Division under award no. DE-SC0019252. The use of Oak Ridge National Laboratory’s Spallation Neutron Source was sponsored by the Scientific User Facilities Division, BES, U.S. DOE. Theoretical calculations were performed using the National Energy Research Scientific Computing Center, a U.S. DOE Office of Science user facility supported by the Office of Science of the U.S. DOE under contract no. DE-AC02-05CH11231. This research used resources of the Advanced Photon Source, a U.S. DOE Office of Science user facility operated for the DOE Office of Science by Argonne National Laboratory under Contract No. DE-AC02-06CH11357.

The Ceramic that Breathes Oxygen to Make Hydrogen

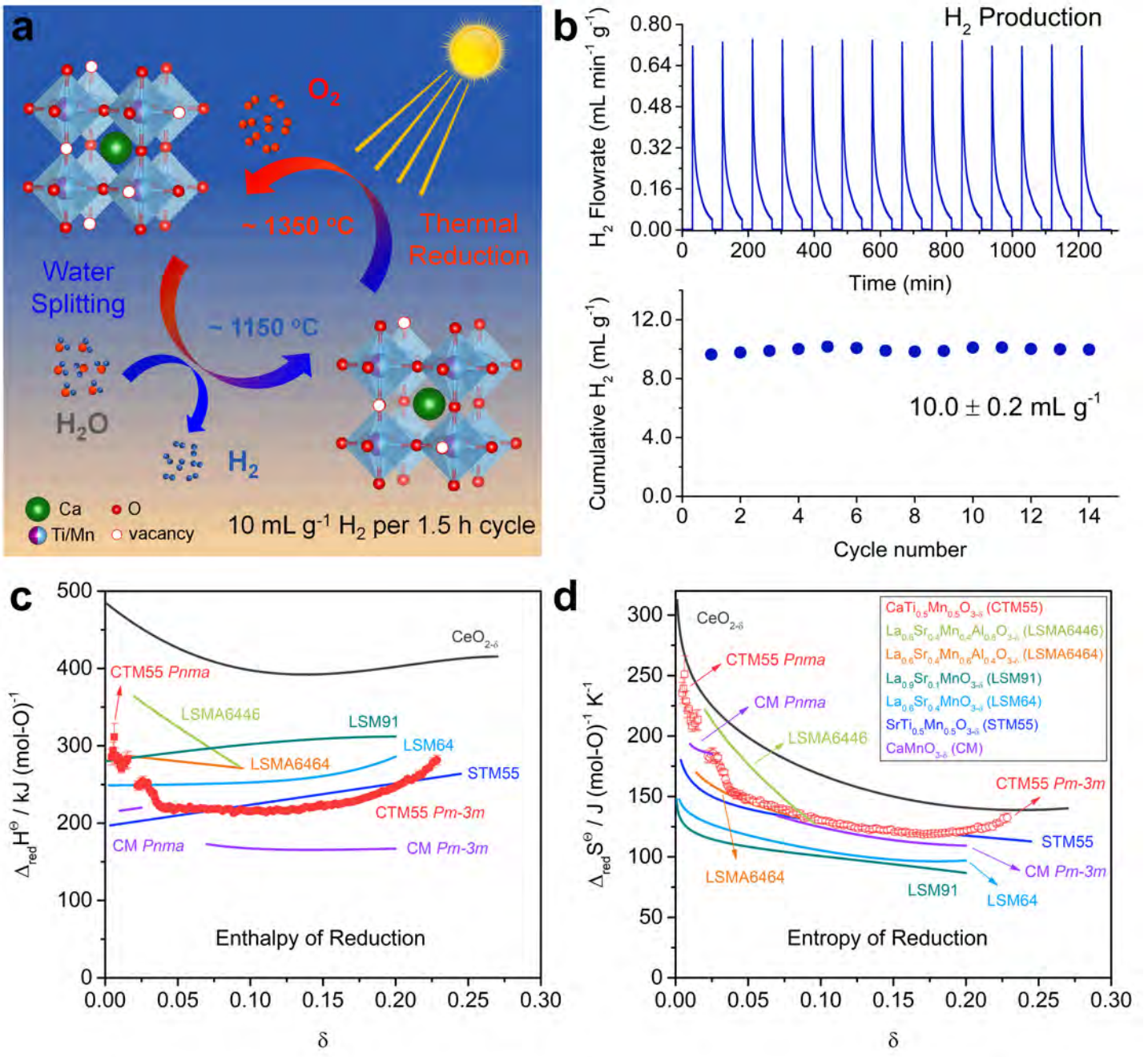

Fig. 1. Concentrated sunlight provides heat to cause oxygen release from the crystal, which then splits water by taking back oxygen from steam at a lower temperature (a). The reaction achieves high rates of hydrogen production during each cycle (b). The material shows moderate enthalpy of reduction and (c) large entropy of reduction (d) compared to other perovskite materials

As the world tries to reduce its dependence on fossil fuels and shift to renewable energy sources, such as solar power, one challenge is finding a way to store the energy produced. A possible solution is two-step solar thermochemical hydrogen production, in which energy from the Sun is used to drive a reduction-oxidation reaction to split water into oxygen and hydrogen. The hydrogen can then be stored for later use. The reaction requires efficient, low-cost materials. Researchers using the APS have examined one such material and found it to have exceptionally efficiency. Their results were published in the journal *Matter*.

The material in question is calcium titanium manganese oxide, in a crystal structure known as a perovskite, a promising form for solar energy applications. Tests showed that during the water-splitting phase, the reaction yielded 10 ± 0.2 mL g^{-1} of hydrogen, in a cycle that took an hour and a half. That's higher than any previous reports of fuel production without having to use an excessively long cycle time. The cycle consisted of a high-temperature step at 1350° C, during which the oxide released some of its oxygen into a flow of argon gas. The temperature was then quickly lowered to 1150° C and steam was introduced. The material removed some of the oxygen from the steam, restoring the oxide and releasing hydrogen. The researchers found that the material had a large entropy of reduction and intermediate enthalpy of reduction, the combination of which creates favorable conditions for water splitting (Fig. 1).

The researchers took care to report not only the hydrogen output but also other details of the procedure, including oxidation and reduction temperatures, gas flow rates, and cycling time. Those are all important for determining the usefulness of a given material and knowing them all allows scientists to accurately compare one candidate with another in their search for the best material. For instance, the mixed poly-cation system $(FeMgCoNi)O_x$ has a very high H_2 yield, similar to calcium titanium manganese oxide, but this is only achieved with a much longer cycle time. A perovskite has a chemical formula of ABO_3. In the material studied here, the A-site atom is calcium, and the B site is an equally split mix of titanium and manganese atoms. These researchers wanted to understand which of the elements was driving the reaction by changing its oxidation state. They were sure the calcium did not change state, but they wanted to characterize the role of the titanium and manganese.

To do that, they performed x-ray absorption near-edge spectroscopy (XANES) at DND-CAT beamline 5-BM-D at the APS. They first grew a thin film of the $Ca(Ti_{0.5}Mn_{0.5})O_3$ perovskite oxide on a sapphire substrate. They heated the film to different temperatures, from 800° C to 1000° C, and collected x-ray spectra from the material. While the spectra from the titanium remained stable with changing temperatures, the researchers observed a shift in the manganese spectra as the temperature increased, indicating that its oxidation state was changing. The titanium, however, is beneficial for the process because it produces a more stable crystal structure than a material made out of only calcium and manganese. It also increases the enthalpy of reduction, improving fuel output.

Further studies, looking at different ratios of titanium to manganese, may help researchers to tune the enthalpy for even higher fuel productivity. – Neil Savage

See: Xin Qian[1*], Jiangang He[1], Emanuela Mastronardo[1,2], Bianca Baldassarri[1], Weizi Yuan[1], Christopher Wolverton[1], and Sossina M. Haile[1**], "Outstanding Properties and Performance of $CaTi_{0.5}Mn_{0.5}O_{3-\delta}$ for Solar-Driven Thermochemical Hydrogen Production," Matter **4**, 688 (February 3, 2021). DOI: 10.1016/j.matt.2020.11.016
Author affiliations: [1]Northwestern University, [2]Spanish National Research Council
Correspondence: * xinqian2021@u.northwestern.edu, ** sossina.haile@northwestern.edu

This research is funded by the U.S. Department of Energy (DOE) through the office of Energy Efficiency and Renewable Energy (EERE) contract DE-EE0008089. The support from the European Union's Horizon 2020 Research and Innovation Programme under the Marie Sklodowska-Curie grant agreement no. 746167 is also acknowledged. This work made use of the Jerome B. Cohen X-Ray Diffraction Facility and the Pulsed Laser Deposition Shared Facility at the Materials Research Center at Northwestern University supported by the National Science Foundation MRSEC program (DMR- 1720139) and the Soft and Hybrid Nanotechnology Experimental (SHyNE) Resource (NSF ECCS-1542205). DND-CAT is supported by Northwestern University, The Dow Chemical Company, and DuPont de Nemours, Inc. This research used resources of the Advanced Photon Source, a U.S. DOE Office of Science user facility operated for the DOE Office of Science by Argonne National Laboratory under Contract No. DE-AC02-06CH11357.

A Peculiar State of Matter in Layers of Semiconductors

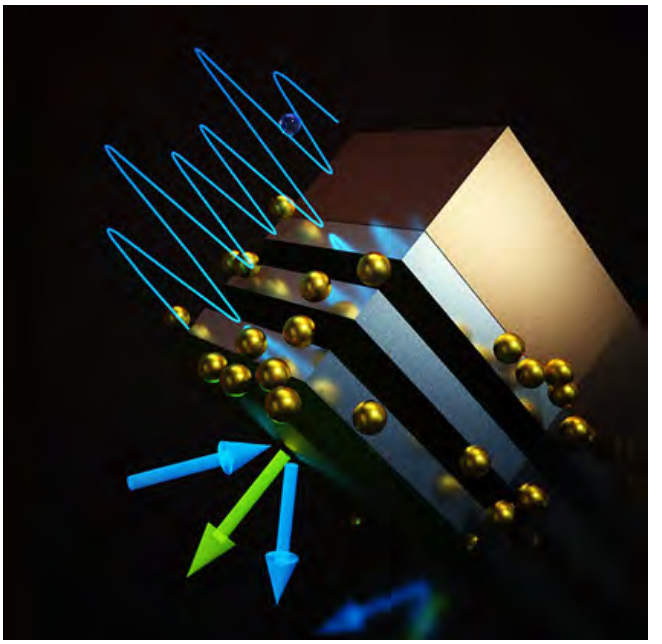

Rendering courtesy of the researchers.

The original MIT Nuclear Science & Engineering press release by Matthew Hutson can be read here.

Scientists around the world are developing new hardware for quantum computers, a new type of device that could accelerate drug design, financial modeling, and weather prediction. These computers rely on qubits, bits of matter that can represent some combination of 1 and 0 simultaneously. The problem is that qubits are fickle, degrading into regular bits when interactions with surrounding matter interfere. But new research at MIT, aided by experiments at the APS and published in the journal *Nano Letters*, suggests a way to protect their states, using a phenomenon called many-body localization (MBL).

MBL is a peculiar phase of matter, proposed decades ago, unlike solid or liquid. Typically, matter comes to thermal equilibrium with its environment. That's why soup cools and ice cubes melt. But in MBL, an object consisting of many strongly interacting bodies, such as atoms, never reaches equilibrium. Heat, like sound, consists of collective atomic vibrations and can travel in waves; an object always has such heat waves internally. But when there's enough disorder and enough interaction in the way its atoms are arranged, the waves can become trapped, thus preventing the object from reaching equilibrium.

MBL had been demonstrated in "optical lattices," arrangements of atoms at very cold temperatures held in place using lasers. But such setups are impractical. MBL had also arguably been shown in solid systems, but only with very slow temporal dynamics, in which the phase's existence is hard to prove because equilibrium might be reached if researchers could wait long enough. The MIT research found a signature of MBL in a "solid-state" system—one made of semiconductors—that would otherwise have reached equilibrium in the time it was watched.

"It could open a new chapter in the study of quantum dynamics," said Rahul Nandkishore, a physicist at the University of Colorado at Boulder, who was not involved in the work.

Mingda Li, the Norman C. Rasmussen Assistant Professor of Nuclear Science and Engineering at MIT, led the new study. The researchers built a system containing alternating semiconductor layers, creating a microscopic lasagna—aluminum arsenide, followed by gallium arsenide, and so on, for 600 layers, each 3 nanometers (millionths of a millimeter) thick. Between the layers they dispersed "nanodots," 2-nanometer particles of erbium arsenide, to create disorder. The lasagna, or "superlattice," came in three recipes: one with no nanodots, one in which nanodots covered 8 percent of each layer's area, and one in which they covered 25 percent.

According to Li, the team used layers of material, instead of a bulk material, to simplify the system so dissipation of heat across the planes was essentially one-dimensional. And they used nanodots, instead of mere chemical impurities, to crank up the disorder.

To measure whether these disordered systems are still staying in equilibrium, the researchers measured them using the XSD Inelastic & X-ray Scattering Group's 3-ID-C x-ray beamline at the APS to carry out grazing incidence inelastic x-ray scattering experiments. They shot beams of x-ray radiation at an energy around 21,600 electron volts, and resolved the energy difference between the incoming x-ray and the energy after its reflection off the sample's surface, with an energy resolution less than one-thousandth of an electron volt. To avoid penetrating the superlattice and hitting the underlying substrate, they shot it at an angle of just half a degree from parallel.

Just as light can be measured as waves or particles, so too can heat. The collective atomic vibration for heat in the form of a heat-carrying unit is called a phonon. X-rays interact with these phonons, and by measuring how x-rays reflect off the sample, the experimenters can determine if it is in equilibrium.

The researchers found that when the superlattice was cold—30 K, about -400 ° F—and it contained nanodots, its phonons at certain frequencies were not in equilibrium.

More work remains to prove conclusively that MBL has been achieved, but "this new quantum phase can open up a whole new platform to explore quantum phenomena," Li said, "with many potential applications, from thermal storage to quantum computing." To create qubits, some quantum computers employ specks of matter called quantum dots. Li says quantum dots similar to Li's nanodots could act as qubits. Magnets could read or write their quantum states, while the many-body localization would keep them insulated from heat and other environmental factors.

In terms of thermal storage, such a superlattice might switch in and out of an MBL phase by magnetically controlling the nanodots. It could insulate computer parts from heat at one moment, then allow parts to disperse heat when it won't cause damage. Or it could allow heat to build up and be harnessed later for generating electricity.

Conveniently, superlattices with nanodots can be constructed using traditional techniques for fabricating semiconductors, alongside other elements of computer chips. According to Li, "It's a much larger design space than with chemical doping, and there are numerous applications."

"I am excited to see that signatures of MBL can now also be found in real material systems," said Immanuel Bloch, scientific director at the Max-Planck-Institute of Quantum Optics, of the new work. "I believe this will help us to better understand the conditions under which MBL can be observed in different quantum many-body systems and how possible coupling to the environment affects the stability of the system. These are fundamental and important questions, and the MIT experiment, are an important step helping us to answer them."

See: Thanh Nguyen[1], Nina Andrejevic[1], Hoi Chun Po[1], Qichen Song[1], Yoichiro Tsurimaki[1], Nathan C. Drucker[3], Ahmet Alatas[4], Esen E. Alp[4], Bogdan M. Leu[4], Alessandro Cunsolo[5], Yong Q. Cai[6], Lijun Wu[6], Joseph A. Garlow[6], Yimei Zhu[6], Hong Lu[7], Arthur C. Gossard[8], Alexander A. Puretzky[9], David B. Geohegan[9], Shengxi Huang[2**], and Mingda Li[1*], "Signature of Many-Body Localization of Phonons in Strongly Disordered Superlattices," Nano Lett. **21**(17), 7419 (July 27, 2021).
DOI: 10.1021/acs.nanolett.1c01905
Author affiliations: [1]Massachusetts Institute of Technology, [2]The Pennsylvania State University, [3]Harvard University, [4]Argonne National Laboratory, [5]University of Wisconsin-Madison, [6]Brookhaven National Laboratory, [7]Nanjing University, [8]University of California, Santa Barbara, [9]Oak Ridge National Laboratory
Correspondence: * mingda@mit.edu, * sjh5899@psu.edu

T.N., N.A., N.C.D., and M.L. acknowledge support from the U.S. Department of Energy (DOE), Office of Science-Basic Energy Sciences (BES) award DE-SC0020148. N.A. acknowledges the support of the National Science Foundation (NSF) Graduate Research Fellowship Program under Grant 1122374. M.L. acknowledges support from Norman C. Rasmussen Career Development Chair. S.H. acknowledges the support from the NSF under grant number ECCS-1943895. H.C.P. is supported by a Pappalardo Fellowship at MIT and a Croucher Foundation Fellowship. Work of Q.S. and Y.T. was supported by Solid State Solar-Thermal Energy Conversion Center (S3TEC), an Energy Frontier Research Center funded by the U.S. DOE Office of Science-BES, award DESC0001299 (prior to January 2019). Y.Q.C., L.W., J.G., and Y.Z. acknowledge the support from DOE-BES Materials Science and Engineering Division, under Contract DESC0012704. Raman measurements were conducted at the Center for Nanophase Materials Sciences, which is a DOE Office of Science user facility. This research used resources of the Advanced Photon Source, a U.S. DOE Office of Science user facility operated for the DOE Office of Science by Argonne National Laboratory under Contract No. DE-AC02-06CH11357.

Correlated Electrons "Tango" in a Perovskite Oxide at the Extreme Quantum Limit

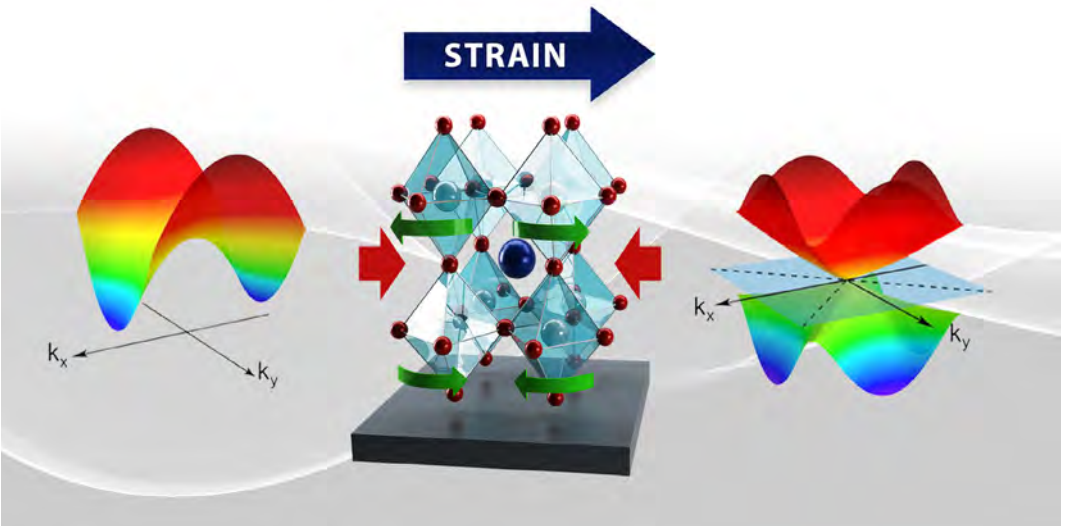

Compression (red arrows) alters crystal symmetry (green arrows), which changes band dispersion (left and right), leading to highly mobile electrons. Image: Jaimee Janiga, Andrew Sproles, Satoshi Okamoto/ORNL, U.S. DOE

The original Oak Ridge National Laboratory press release by Dawn M. Levy can be read here.

A team led by the U.S. Department of Energy's (DOE's) Oak Ridge National Laboratory (ORNL) has found a rare quantum material in which electrons move in coordinated ways, essentially "dancing." Straining the material creates an electronic band structure that sets the stage for exotic, more tightly correlated behavior – akin to tangoing – among Dirac electrons, which are especially mobile electric charge carriers that may someday enable faster transistors. The results, which include studies carried out at the APS, were published in the journal *Science Advances*.

"We combined correlation and topology in one system," said co-principal investigator Jong Mok Ok, who conceived the study with principal investigator Ho Nyung Lee of ORNL. Topology probes properties that are preserved even when a geometric object undergoes deformation, such as when it is stretched or squeezed. "The research could prove indispensable for future information and computing technologies," added Ok, a former ORNL postdoctoral fellow.

In conventional materials, electrons move predictably (for example, lethargically in insulators or energetically in metals). In quantum materials in which electrons strongly interact with each other, physical forces cause the electrons to behave in unexpected but correlated ways; one electron's movement forces nearby electrons to respond.

To study this tight tango in topological quantum materials, Ok led synthesis of an extremely stable crystalline thin film of a transition metal oxide. He and colleagues made the film using pulsed-laser epitaxy and strained it to compress the layers and stabilize a phase that does not exist in the bulk crystal. They were the first to stabilize this phase.

Using theory-based simulations, co-principal investigator Narayan Mohanta, a former ORNL postdoctoral fellow, predicted the band structure of the strained material. "In the strained environment, the compound that we investigated, strontium niobate, a perovskite oxide, changes its structure, creating a special symmetry with a new electron band structure," Mohanta said.

Different states of a quantum mechanical system are called "degenerate" if they have the same energy value upon measurement. Electrons are equally likely to fill each degenerate state. In this case, the special symmetry results in four states occurring in a single energy level.

"Because of the special symmetry, the degeneracy is protected," Mohanta said. "The Dirac electron dispersion that we found here is new in a material." He performed calculations with Satoshi Okamoto, who developed a model for discovering how crystal symmetry influences band structure.

"Think of a quantum material under a magnetic field as a 10-story building with residents on each floor," Ok said. "Each floor is a defined, quantized energy level. Increasing the field strength is akin to pulling a fire alarm that drives all the residents down to the ground floor to meet at a safe place. In reality, it drives all the Dirac electrons to a ground energy level called the extreme quantum limit."

Lee added, “Confined here, the electrons crowd together. Their interactions increase dramatically, and their behavior becomes interconnected and complicated.” This correlated electron behavior, a departure from a single-particle picture, sets the stage for unexpected behavior, such as electron entanglement. In entanglement, a state Einstein called “spooky action at a distance,” multiple objects behave as one: key to realizing quantum computing.

“Our goal is to understand what will happen when electrons enter the extreme quantum limit, where we find phenomena we still don’t understand,” Lee said. “This is a mysterious area.”

Speedy Dirac electrons hold promise in materials including graphene, topological insulators and certain unconventional superconductors. ORNL’s unique material is a Dirac semimetal, in which electron valence and conduction bands cross and this topology yields surprising behavior. Ok led measurements of the Dirac semimetal’s strong electron correlations. “We found the highest electron mobility in oxide-based systems,” Ok said. “This is the first oxide-based Dirac material reaching the extreme quantum limit.”

That bodes well for advanced electronics. Theory predicts that it should take about 100,000 tesla (a unit of magnetic measurement) for electrons in conventional semiconductors to reach the extreme quantum limit. The researchers took their strain-engineered topological quantum material to Eun Sang Choi of the National High Magnetic Field Laboratory at the University of Florida to see what it would take to drive electrons to the extreme quantum limit. There, he measured quantum oscillations showing the material would require only 3 tesla to achieve that.

Other specialized facilities allowed the scientists to experimentally confirm the behavior Mohanta predicted. The experiments occurred at low temperatures so that electrons could move around without getting bumped by atomic-lattice vibrations.

Jeremy Levy’s group at the University of Pittsburgh and the Pittsburgh Quantum Institute confirmed quantum transport properties. With synchrotron x-ray diffraction carried out at the XSD Surface Scattering & Microdiffraction (SSM) Group’s 33-ID-D x-ray beamline at the APS, Hua Zhou of the SSM Group confirmed that the material’s crystallographic structure stabilized in the thin film phase yielded the unique Dirac band structure.

Sangmoon Yoon and Andrew Lupini, both ORNL, conducted scanning transmission electron microscopy experiments at ORNL that showed the epitaxially grown thin films had sharp interfaces between layers and the transport behaviors were intrinsic to strained strontium niobate.

“Until now, we could not fully explore the physics of the extreme quantum limit due to the difficulties in pushing all electrons to one energy level to see what would happen,” Lee said. “Now, we can push all the electrons to this extreme quantum limit by applying only a few tesla of magnetic field in a lab, accelerating our understanding of quantum entanglement.”

See: Jong Mok Ok[1‡], Narayan Mohanta[1], Jie Zhang[1], Sangmoon Yoon[1], Satoshi Okamoto[1], Eun Sang Choi[2], Hua Zhou[3], Megan Briggeman[4,5], Patrick Irvin[4,5], Andrew R. Lupini[1], Yun-Yi Pai[1], Elizabeth Skoropata[1], Changhee Sohn[1], Haoxiang Li[1], Hu Miao[1], Benjamin Lawrie[1], Woo Seok Choi[6], Gyula Eres[1], Jeremy Levy[4,5], and Ho Nyung Lee[1*], “Correlated oxide Dirac semimetal in the extreme quantum limit,” Sci. Adv. **7**, eabf9631 (15 September 2021).
DOI: 10.1126/sciadv.abf9631
Author affiliations: [1]Oak Ridge National Laboratory, [2]National High Magnetic Field Laboratory, [3]Argonne National Laboratory, [4]University of Pittsburgh, [5]Pittsburgh Quantum Institute, [6]Sungkyunkwan University ‡Present address: Pusan National University
Correspondence: * hnlee@ornl.gov

This work was supported by the U.S. Department orf Energy (DOE) Office of Science-Basic Energy Sciences, Materials Sciences and Engineering Division, and in part by the Computational Materials Sciences Program. The high-magnetic field measurements were performed at the National High Magnetic Field Laboratory, which is supported by National Science Foundation (NSF) cooperative agreement no. DMR-1644779 and the state of Florida. Extraordinary facility operations were supported, in part, by the DOE Office of Science through the National Virtual Biotechnology Laboratory, a consortium of DOE national laboratories focused on the response to COVID-19, with funding provided by the Coronavirus CARES Act. W.S.C. was supported by Basic Science Research Programs through the National Research Foundation of Korea (NRF) (NRF-2021R1A2C2011340). J.L. acknowledges support from NSF (PHY-1913034) and Vannevar Bush Faculty Fellowship (N00014-15-1-2847). This research used resources of the Advanced Photon Source, a DOE Office of Science user facility, operated for the DOE Office of Science by Argonne National Laboratory under contract no. DE-AC02-06CH11357.

A New Cathode Coating Significantly Improves High-Temperature Performance of Li-ion Batteries

The exponential growth in the use of lithium-ion batteries (LIBs) for electric vehicle and stationary power applications is challenging researchers to design LIBs that are better able to operate stably across regional and seasonable temperature fluctuations, particularly at high temperatures. Current high-capacity layered oxide cathodes such as $LiNi_{0.8}Co_{0.1}Mn_{0.1}O_2$ (NCM811) are susceptible to deleterious changes while charging and discharging at elevated temperatures. Calendar aging is another issue made worse by elevated temperatures, as LIBs in electric vehicles typically see intermittent use, having long idle hours under high states of charge. The susceptibility of LIBs to thermal runaway remains a serious safety concern, as well. An international team of researchers used the APS to test coating-layered NCM811 cathodes with ultra-conformal poly (3, 4-ethylenedioxythiophene) (PEDOT) as a way of suppressing performance degradations during high-temperature (HT) LIB operation. Their results, published in the journal Advanced Materials, suggest that the PEDOT coating can significantly improve the thermal stability of lay-

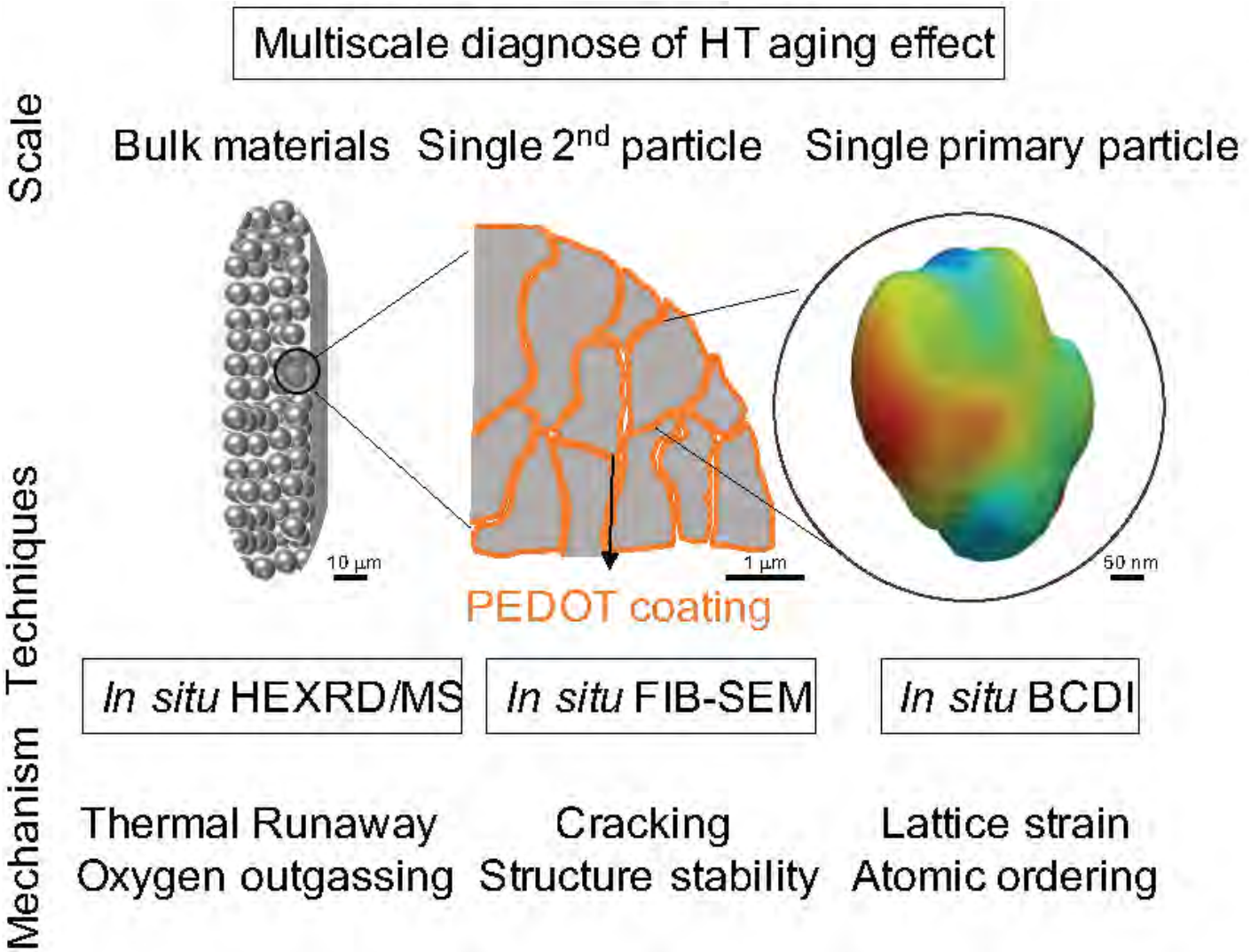

Fig. 1. Use of a combination of various *in situ* synchrotron x-ray and electron microscopy techniques led to a multiscale understanding of surface structure effects in regulating the high-temperature operational resilience of polycrystalline Ni-rich layered cathodes.

ered NCM811 cathodes at the bulk level, which can thus increase safety performance and high-temperature operational resiliency.

Through a series of advanced characterization techniques including *in/ex situ* Bragg coherent diffractive imaging (BCDI), *in situ* focused-ion-beam scanning electron microscopy (FIB-SEM) and transmission electron microscopy (TEM), and *in situ* high-energy x-ray diffraction coupled with mass spectrometry (HEXRD-MS), they systematically investigated the structural transformations NCM811 cathodes undergo with and without PEDOT coatings during cycling aging, calendar aging, and thermal runaway (Fig. 1). They then sought the reasons for the differences they saw at the atomic scale and at the primary particle, secondary particle, and bulk powder levels. The BCDI experiment was conducted at the XSD Microscopy Group's 34-ID-C x-ray beamline at the APS, while the HEXRD-MS experiment took place at the XSD Structural Science Group's 17-BM beamline also at the APS.

The cycle aging tests found that the coated NCM811 cathode showed higher capacity retention than the bare cathode after 100 cycles at 55° C and maintained a much higher average discharge voltage, indicating that structural transformations had been reduced. When the cut-off voltage was increased to 4.5 V, the coated cathode had a much higher capacity (197.3 mAh/g) than the bare cathode (159.3 mAh/g) after charge/discharge at C/3 and 55° C for 50 cycles, leading to a higher capacity retention of 86.3% than the bare NCM811 cathode (74.2%). In general, abusive calendar aging resulted in compromised electrochemical performance for both cathodes. Nevertheless, the PEDOT coating was able to mitigate this problem, with a reversible capacity of 159.8 mAh/g and capacity retention of 72.5%, in comparison with only 121.4 mAh/g and 56.3%, respectively, for the bare NCM811 cathode. When heated to 500° C in the thermal runaway test, the layered NCM811 cathode with the PEDOT coating showed significantly improved thermal stability, which could improve the safety performance and high-temperature operational resiliency of a LIB having such a cathode.

In seeking the origins of the electrochemical performance difference between the bare and coated cathodes during abusive calendar aging, the researchers found that electrolyte had penetrated the surface of the bare NCM811 cathode to a depth of ~15 nanometers, leading to transition metal dissolution and severe surface reconstruction. In contrast, the 10-nanometers-thick PEDOT coating prevented direct contact between the electrolyte and the coated NCM811 cathode during high state-of-charge and HT calendar aging, thereby stabilizing the cathode-electrolyte interface.

The *in situ* BCDI and FIB-SEM tests of single primary and secondary particle behavior collectively revealed that the PEDOT coating can alleviate the mechanical stress inside and between the primary particles after HT and high state-of-charge aging, again showing the PEDOT coating's ability to provide a well-maintained crystallographic structure and hence better battery performance. Upon heating the 4.5-V-charged NCM811 cathodes from room temperature to 500° C, the researchers found that both cathodes underwent structural transformations and oxygen outgassing, but that the PEDOT coating postponed the conversion to the rock salt phase to a higher temperature and reduced oxygen outgassing by 50%. – Vic Comello

See: Xiang Liu[1], Xinwei Zhou[1], Qiang Liu[2], Jiecheng Diao[3], Chen Zhao[1], Luxi Li[1]*, Yuzi Liu[1]**, Wenqian Xu[1], Amine Daali[1], Ross Harder[1], Ian K. Robinson[3], Mouad Dahbi[4], Jones Alami[4], Guohua Chen[2], Gui-Liang Xu[1]***, and Khalil Amine[1]****, "Multiscale understanding of surface structural effects on high-temperature operational resiliency of layered oxide cathodes," Adv. Mater. **34**(4), 2107326 (26 October 2021). DOI: 10.1002/adma.202107326
Correspondence: * luxili@anl.gov, ** yuziliu@anl.gov, *** xug@anl.gov, **** amine@anl.gov
Affiliations: [1]Argonne National Laboratory, [2]The Hong Kong Polytechnic University, [3]University College London, [4]Mohammed VI Polytechnic University

Research at Argonne National Laboratory was funded by the U.S. Department of Energy (DOE) Vehicle Technologies Office. The Advanced Photon Source and Center for Nanoscale Materials are DOE Office of Science User Facilities operated for the DOE Office of Science by Argonne National Laboratory; research there was supported by the DOE under Contract No. DE-AC02-06CH11357. X.L., G.X., and K.A. acknowledge the support of the U.S. China Clean Energy Research Center (CERC-CVC2). Q.L. and G.C. acknowledge funding support from the Hong Kong Research Grants Council (GRF 15221719), Otto Poon Charitable Foundation (No. 847W), and The Hong Kong Polytechnic University (P0034050).

In Search of Fast-Charging Lithium-ion Batteries

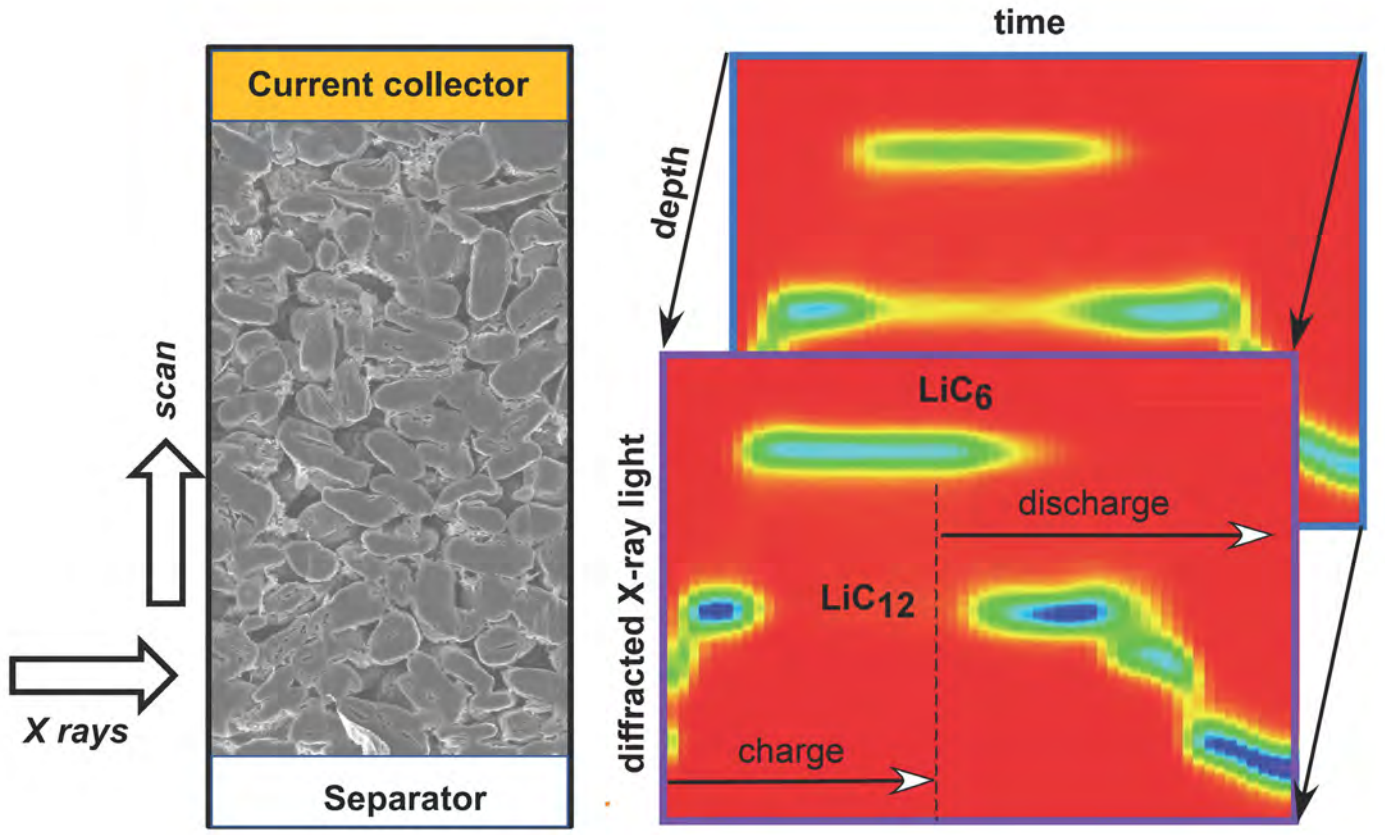

Fig. 1. A schematic showing the x-ray beam slicing the graphite anode during electrochemical cycling of the lithium-ion battery (left image). On the right are false color representations of phase distributions, in areas near the polymer separator (lower image) and those near the copper current collector (upper image), as a function of cycling time. The electrode goes through a succession of dilute phases until the LiC_{12} phase, and finally the LiC_6 phase, are formed. During charging, lithium leaves the electrode, and the LiC_6 reverts to LiC_{12} and then to multiple phases that contain a dilute distribution of lithium among the graphite planes.

It takes about an hour to charge an electric car's battery, but only 10 minutes to fill up a gas tank. Electric car drivers would love to have a battery that charged in 10 minutes, but the lithium-ion batteries in cars degrade if you charge them too fast. Examining processes that lead to battery failure as they occur could help engineers develop better ones. Researchers used high-brightness x-rays from the APS to register changes in battery materials layer by layer and in real time as they pushed the batteries closer to the limits of fast charging. Insights gained from these results, published in the *Journal of Power Sources*, could lead to electric cars that can keep up with gas powered cars—even at the filling station.

A typical lithium-ion (Li-ion) battery has a positively charged cathode made of a layered material such as a nickel-manganese-cobalt oxide, and a negatively charged anode made of layered graphite. When the two are connected in a circuit, lithium ions flow between the two electrodes.

The rapid movement of lithium ions through the battery stresses the electrode materials. As lithium ions fill the spaces between sheets of graphite in the anode, the sheets move apart. The whole anode swells, and the extra space allows more lithium ions to flow inside. Something similar happens at the cathode when the battery is charged.

At normal charging and discharging rates, the Li ions move smoothly. But when the rate increases, traffic jams can occur. Instead of sliding into open slots in the electrode materials, the lithium ions bunch up, sticking to sur-

faces and forming metallic lithium on the anode. That blocks the smooth transit of lithium ions into the electrode bulk, eventually degrading the cell performance.

To see exactly how this happens in real time, a team of researchers from Argonne and Princeton University used the XSD Materials, Physics & Engineering Group's 6-BM beamline at the APS to view lithium-ion cells (a cell is a section of a battery) as they charged and discharged at various rates. The 6-BM beamline was chosen for its extremely bright, polychromatic light, which allows the scientists to use energy dispersive x-ray diffraction. The crystal lattices of different materials diffract the x-rays differently, so changes in the diffraction patterns reveal chemical composition changes in the lattices. With the bright x-ray beam illuminating the electrode layer-by-layer, the researchers could take frequent, multiple images of the materials as they changed across the battery.

As lithium ions insert into the anode, several phases form—ordered regions with the same chemical composition. These phases depend on the concentration of lithium in graphite. The maximum amount of lithium that can be stored in graphite is 1 lithium ion for every 6 carbon atoms. That's one phase. Another phase would be 1 lithium ion for every 12 carbon atoms in the graphite. Each phase has its own crystal lattice that diffracts x-rays differently from other phases. Measuring the intensity of the diffracted beam in these phases across the anode allows the mapping of the chemical composition in great detail.

When the researchers ran the experiment at various charge rates, they observed that the faster the cell charged, the greater was the rate of phase change (or gradient) across the electrode thickness. Portions of the anode—the layered graphite structure that holds lithium ions—adjacent to the cathode had phases with a higher concentration of lithium ions than those deeper in the electrode (Fig. 1). Moreover, the lithium gradient persisted over time. Even after the battery's circuit was opened so that it was no longer actively charging, the lithium-ion gradients in different phases remained, meaning that different areas of the anode with different compositions and concentrations of lithium stayed distinct. The lithium concentration did not "even out".

This phase gradient poses one of the fundamental challenges of fast charging: How do materials scientists make it easier for lithium ions to hustle through the graphite anode, filling it up to the maximum extent, as uniformly as possible? If ions don't do this, the electric car will have less juice when it's fast-charged than when it's slow-charged. It is as if a gas tank shrank when the pump filled it with gasoline too quickly.

The top speed at which the researchers charged the lithium cell was equivalent to fully charging the battery in 12 minutes. Their next step will be to look at what happens inside the cathode (positively charged) end of the battery at these speeds. Eventually, the researchers will look at the battery as a whole. Their goal is to gain insights that will lead to the ideal battery, one in which every part responds as quickly as possible, allowing ion flow with minimal disruptions and roadblocks. Which is what every driver wants, whether they're in an electric- or gas-powered vehicle. – Judy Meyers

See: Abhi Raj[1, 2], Ilya A. Shkrob[1], John S. Okasinski[2], Marco-Tulio Fonseca Rodrigues[1], Andrew C. Chuang[2], Xiang Huang[2], and Daniel P. Abraham[1]*, "Spatially-resolved lithiation dynamics from *operando* X-ray diffraction and electrochemical modeling of lithium-ion cells," J. Power Sources **484**, 229247 (2021).
DOI: 10.1016/j.jpowsour.2020.229247
Author affiliations: [1]Argonne National Laboratory, [2]Princeton University
Correspondence: * abraham@anl.gov

I.A.S., X.H., and D.P.A. are grateful for support from the Argonne Laboratory Directed Research & Development (LDRD) program. A.R. acknowledges support from the U. S. Department of Energy (DOE) Graduate Student Research (SCGSR) program. The SCGSR program is administered by the Oak Ridge Institute for Science and Education for the U. S. DOE under contract number DE-SC0014664. M.T.F.R. acknowledges support from the U. S. DOE Vehicle Technologies Office. The electrodes examined in this study were produced at the U.S. DOE CAMP (Cell Analysis, Modeling and Prototyping) Facility at Argonne. The CAMP Facility is fully supported by the U.S. DOE Vehicle Technologies Office. This research used resources of the Advanced Photon Source, a U.S. DOE Office of Science user facility operated for the DOE Office of Science by Argonne National Laboratory under Contract No. DE-AC02-06CH11357.

Gaining Critical Insights into Fast Charging of Lithium-Ion Batteries

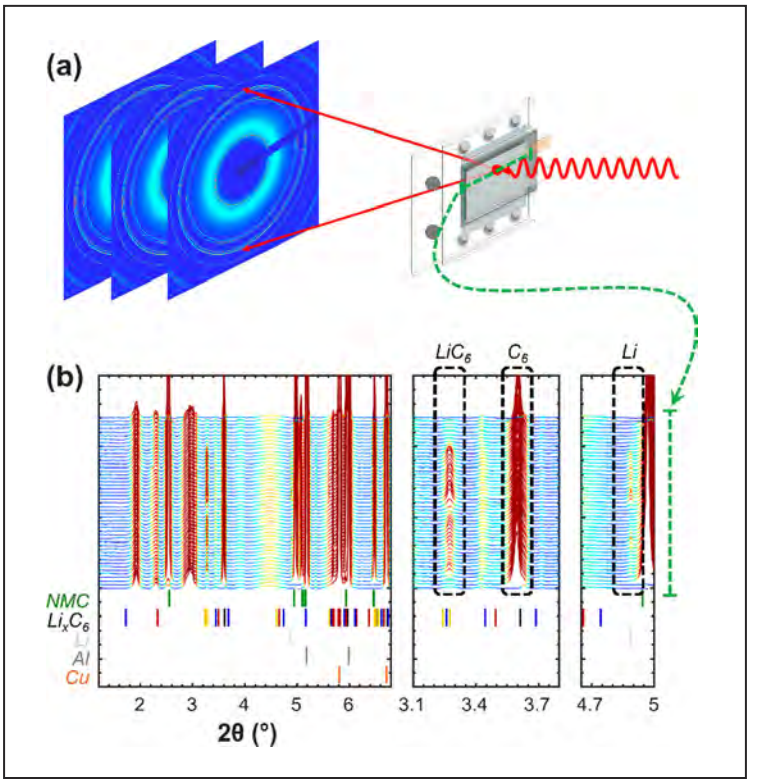

Fig. 1. (a) Schematic of the experimental setup and (b) representative set of x-ray diffraction patterns collected along the green dashed line as indicated. The diffraction patterns contain contributions from the $LiNi_{0.5}Mn_{0.3}Co_{0.2}O_2$ (NMC532) cathode, Li_xC_6 anode, metallic lithium plating, and aluminum and copper current collectors (left panel). LiC_6(001) and C_6(002) peaks (center panel) and Li(110) peak (right panel) are plotted and highlighted.

A team of scientists utilized the high-energy x-rays available at the APS to understand the process of lithium plating under rapid charging conditions. The high-energy x-rays allowed the team to non-destructively follow and quantify the changes in relative amounts of well characterized phases, including the deposition of metallic lithium over the entire area of a working lithium-ion battery throughout extended cycle life. Their results were published in the journal *ACS Energy Letters*.

Recent years have seen a steady rise in the number of electric vehicles (EV) utilizing lithium-ion batteries for energy storage and according to Bloomberg New Energy Finance, the market is expected to grow to as much as 40 million EV sales per year by 2030. While the replacement of the combustion engine is essential for the transition to a green economy, more widespread adoption of electric vehicles is hampered by limited driving range and lengthy charging time. Fast charging is being researched to solve the second problem. In conventional lithium-ion batteries however, long-term stability is a major issue. Specifically, rapid charging results in several detrimental effects including limited transport kinetics, excessive heating, heterogenous performance, and the deposition of lithium metal (lithium plating). Lithium plating, which occurs on top of the graphite anode, is a major concern because it causes the battery to consume some of the available lithium ions, resulting in shortened driving range. The graphite anode tends to more commonly experience irreversible lithium

metal deposition in fast-charge conditions. Lithium plating is believed to be a precursor for dendrite formation which can cause catastrophic failure of batteries. In order to solve the plating issue, we must first provide an accurate characterization of lithium metal in conventional full-cell batteries: the amount of lithium consumed during plating, the growth of plating regions and overall concentration of lithium metal, the level of heterogeneity of the plating across the anode, and its reversibility during discharge (lithium stripping). However, many characterization techniques are destructive and preclude this kind of deeper, time resolved understanding of the nature of plating or stripping.

In a study carried out at the XSD Structural Science Group's beamline 11-ID-B at the APS, a lithium-ion battery containing an $LiNi_{0.5}Mn0.3Co_{0.2}O_2$ (NMC532) cathode and a graphite anode was subjected to fast charging conditions of 6C (10-minute charge time) and periodically mapped using x-ray diffraction in the charged and discharged states over 1200 cycles. Data showed evolution of anode electrode composition over time and reviled the nucleation and autocatalytic growth mechanism of metallic lithium plating (Fig. 1). Overall concentration of metallic lithium growed along an "S-shaped" curve, which indicated a two-step nucleation and growth mechanism.

Additionally, by comparing the amount of metallic lithium at charge and discharge for the same cycles an exponential decay of the stripping efficiency was observed. At first metallic lithium began to nucleate at isolated sites, initially stripping off efficiently during discharge. Over hundreds of cycles further plating spread out from those initial nucleation sites. As the lithium sites densify the stripping efficiency decays exponentially, resulting in a rapid build-up of metallic lithium. Later in the cycle life, the plating became slower and the amount of plating reduced in each cycle. It was noted that residual lithiated graphite regions at the end of discharge, resulting from heterogeneous graphite delithiation, served as a dangerous precursor to initiate lithium plating and cells should either be designed to avoid overcharging the anode during fast charging or to minimize spatial heterogeneities in lithiation. As lithiated graphite has a higher x-ray scattering cross section compared to lithium metal and is easier to observe using XRD it can provide a more sensitive, indirect signature of plating for industrial applications.

These findings provide crucial insights for future accurate modeling and serve as a baseline for mitigation strategies to prevent or slow metallic lithium deposition for safe and long-lasting batteries. Therefore, this comprehensive study of lithium plating in batteries under fast-charging conditions provides the groundwork for future studies aimed to develop battery systems that exhibit little to no plating and reliable performance regardless of the charging time or operating temperature. Ultimately, future advances are required to design better battery systems to meet consumer expectations for electric vehicles.

– Stephen Taylor

See: Harry Charalambous[1], Olaf J. Borkiewicz[1], Andrew M. Colclasure[2] , Zhenzhen Yang[1], Alison R. Dunlop[1], Stephen E. Trask[1], Andrew N. Jansen[1], Ira D. Bloom[1], Uta Ruett[1], Kamila M. Wiaderek[1]*, and Yang Ren[1]**, "Comprehensive Insights into Nucleation, Autocatalytic Growth, and Stripping Efficiency for Lithium Plating in Full Cells," ACS Energy Lett. **6**, 3725 (2021).
DOI: 10.1021/acsenergylett.1c01640
Author affiliations: [1]Argonne National Laboratory, [2]National Renewable Energy Laboratory
Correspondence: * kwiaderek@anl.gov, ** yren@anl.gov

The electrodes and pouch cells in this study were produced at the U.S. Department of Energy's (DOE's) CAMP (Cell Analysis, Modeling and Prototyping) Facility, Argonne National Laboratory. The CAMP Facility is fully supported by the DOE Vehicle Technologies Office (VTO). Funding was provided by the U.S. DOE Office of Vehicle Technology Extreme Fast Charge Cell Evaluation of Lithium-Ion Batteries (XCEL) Program managed by Samuel Gillard. This research used resources of the Advanced Photon Source, a U.S. DOE Office of Science user facility operated for the DOE Office of Science by Argonne National Laboratory under Contract No. DE-AC02-06CH11357.

X-ray Mapping Reveals Non-Uniformity in Pouch Cell Lithium-Ion Batteries

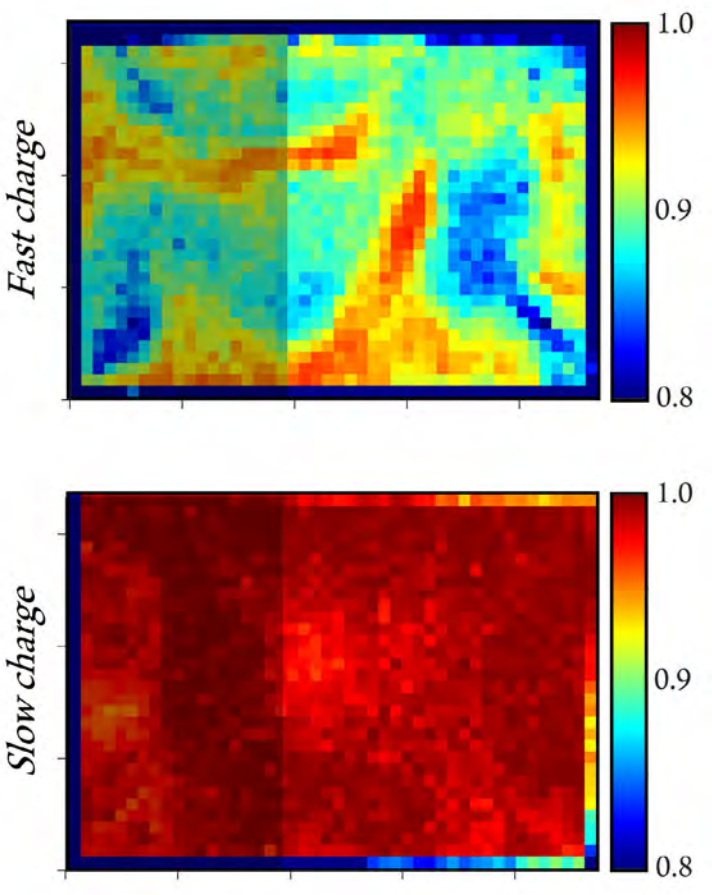

Fig. 1. X-ray diffraction mapping of the concentration and distribution of lithium ions in the graphite anodes of two pouch cells. Lithium concentration varies from a maximum of 100% (red) down to 80% (blue). In the top image lithium concentrations are seen to vary wildly throughout a cell's anode following a quick charge. By contrast, the bottom map reveals that lithium-ion concentration in the anode of a slowly charged cell is on average much higher and distributed much more evenly. In both images the shaded area on the left indicates an area of applied pressure. Both images reveal that lithium-ion distribution was largely unaffected by uneven pressure.

Pouch cell-type lithium-ion (Li-ion) batteries are widely used in applications ranging from power tools to electric vehicles. Compared to traditional cylindrical cells, pouch cells possess superior energy density, increased battery life, and faster charge/discharge rate capabilities. Due to their ever-increasing utilization, researchers are keen to further improve the reliability, safety, and performance of pouch cells. Recently, scientists from three U.S. Department of Energy (DOE) national laboratories collaborated to explore large-scale (macroscopic) heterogeneity and degradation in lithium-ion pouch cells. By performing x-ray diffraction (XRD) mapping at the APS, they were able to characterize lithium concentrations and structural changes across the area of the anodes and cathodes in single-layer pouch cells following repeated charge/discharge cycling. The experiments revealed that high charging rates, along with other factors, can produce significant non-uniformities in a cell's lithium concentration. Such distortions inhibit the transport of lithium ions in pouch cells, reducing performance. The experimental results, published in the *Journal of Power Sources*, will guide scientists in developing improved materials and charge/discharge protocols that preserve the uniformity of pouch cell anodes and cathodes, thereby increasing battery performance and lifespan. Improvements in lithium-ion battery performance and durability are urgently needed to promote the widespread use of environmentally friendly electric vehicles.

The standard architecture of Li-ion batteries is the cylindrical design, shaped like a soda can. By contrast, pouch cells are composed of numerous flat layers stacked like the pages in a book. The entire stack is encased within a plastic cover, or pouch. Regardless of type, the internal components of a Li-ion battery are initially rather homogeneous (uniform). However, after repeated charging and discharging, areas of heterogeneity (non-uniformity) can arise, lowering battery performance.

Considerable research has been devoted to understanding and improving the microscale performance of Li-ion batteries through advances in chemistries and microstructures. Less understood are structural and chemical concentration issues at the millimeter-to-centimeter scale. The researchers in this study set out to characterize large-scale heterogeneity by applying XRD to single-layer pouch cells possessing a graphite anode and metallic cathode ($LiNi_{0.5}Mn_{0.3}Co_{0.2}O_2$; commonly denoted as NMC). The XRD measurements were carried out at the XSD Structural Science Group's 11-ID-B and 17-BM-B x-ray beamlines. According to these researchers, XRD mapping is a "universal area-imaging tool" applicable to a wide variety of battery chemistries, active material loadings, operating temperatures, and charge/discharge cycling rates.

The experimental pouch cells were cycled according to different protocols. For instance, two of the cells were charged at high (10-minute fast charging) and low (2-hour slow charging), over 25 cycles. The XRD then mapped lithium concentrations at full charge.

Some mapping results are illustrated in Fig. 1, which contrasts lithium concentrations in the anodes of a fast-charged cell and a slow-charged cell. For the fast-charge cell, the high degree of heterogeneity in lithium distribution is an indication of highly variable charge efficiency. Compared to slowly charged cells, the fast-charged cells exhibited four times greater deviation in lithium distribution within their graphite anodes. The researchers further demonstrated that lithium heterogeneity in a pouch cell was reversed by resting it over extended time periods. However, the heterogeneity reappeared after the resumption of fast charging.

Deviations in stack pressure can also degrade cell performance, such as when the anodes and/or cathodes are not compressed evenly. To gauge this effect, glass slides were used to apply an uneven pressure. However, the applied pressure had no noticeable effect after 25 cycles (Fig. 1).

The impact of gas accumulation was examined as well. Solid electrolyte interphase (SEI) formation and other side reactions can produce gas byproducts in lithium-ion batteries. An SEI is an extremely thin solid layer that forms a buffer between a lithium-ion battery's graphite anode and its electrolyte. To investigate this effect, a virgin pouch cell was charged and discharged at a slow (10 hour) rate and then mapped following the initial charge/discharge cycle, which is when most SEI is formed. The data revealed that gas generated by SEI formation consolidated into bubbles which impeded lithium transport.

These experimental findings reveal important facets of large-scale heterogeneities in lithium-ion pouch cells. However, the researchers caution that the pouch cells examined in this study experienced a very limited number of charge/discharge cycles. For instance, the mappings in Fig. 1 resulted from 25 charge/discharge cycles. By contrast, commercial pouch cell batteries typically experience 600 charge/discharge cycles before approaching 80% of their original storage capacity. Additional XRD studies examining highly cycled pouch cells will clarify the full, long-term impact of high charge-rate, pressure, and gas formation on pouch cell performance. – Philip Koth

See: Harry Charalambous[1], Daniel P. Abraham[1], Alison R. Dunlop[1], Stephen E. Trask[1], Andrew N. Jansen[1], Tanvir R. Tanim[2], Parameshwara R. Chinnam[2], Andrew M. Colclasure[3], Wenqian Xu[1], Andrey A. Yakovenko[1], Olaf J. Borkiewicz[1], Leighanne C. Gallington[1], Uta Ruett[1], Kamila M. Wiaderek[1]*, Yang Ren[1‡]**, "Revealing causes of macroscale heterogeneity in lithium ion pouch cells via synchrotron X-ray diffraction," J. Power Sources **507**, 230253 (30 September 2021).
DOI: 10.1016/j.jpowsour.2021.230253
Author affiliations: [1]Argonne National Laboratory, [2]Idaho National Laboratory, [3]National Renewable Energy Laboratory
Correspondence: * kwiaderek@anl.gov,
** yangren@cityu.edu.hk
‡Present address: City University of Hong Kong

Idaho National Laboratory is operated by the Battelle Energy Alliance, LLC, under Contract No.AC07-05ID14517. The National Renewable Energy Laboratory is operated by Alliance for Sustainable Energy, LLC, for the U.S. Department of Energy (DOE) under Contract No. DE-AC36-08GO28308. The electrodes and pouch cells in this study were produced at the U.S. DOE Cell Analysis, Modeling and Prototyping (CAMP) Facility at Argonne National Laboratory. The CAMP Facility is fully supported by the DOE Vehicle Technologies Office (VTO). Funding was provided by the U.S. DOE Office of Vehicle Technology Extreme Fast Charge Cell Evaluation of Lithium-Ion Batteries (XCEL) Program managed by Samuel Gillard. This research used resources of the Advanced Photon Source, a U.S. DOE Office of Science user facility operated for the DOE Office of Science, Office of Basic Energy Sciences, by Argonne National Laboratory under Contract No. DE-AC02-06CH11357.

Electron Transfer Discovery is a Step Toward Viable Grid-Scale Batteries

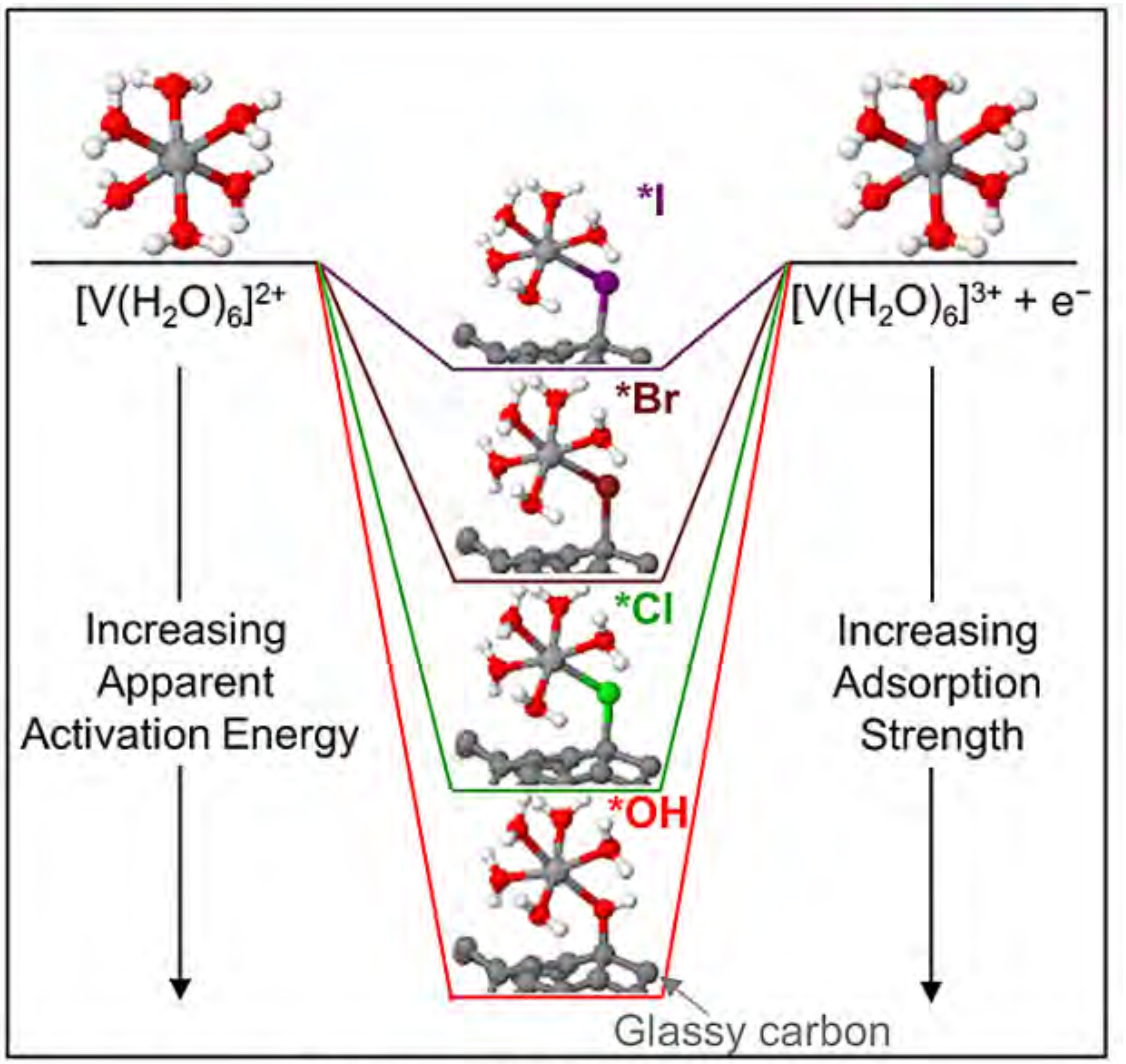

A U-M team found that, contrary to what researchers had believed, the negatively-charged molecular groups from five different acidic electrolytes didn't provide more spots for electron transfer to take place on the battery's negative electrode. Instead, they lowered the energy barrier of that transfer by serving as a sort of bridge between the active metal in the fluid—vanadium in this case—and the electrode. This helps the vanadium give up its electron. Image: Harsh Agarwal, Singh Group; and Jacob Florian, Goldsmith Group; University of Michigan.

The University of Michigan College of Engineering press release by Heather Guenther can be read here.

The way to boost electron transfer in grid-scale batteries is different than researchers had believed, a new study from the University of Michigan (U-M) has shown. The findings, using data obtained at the APS, are a step toward being able to store renewable energy more efficiently.

As governments and utilities around the world roll out intermittent renewable energy sources such as wind and solar, we remain reliant on coal, natural gas, and nuclear power plants to provide energy when the wind isn't blowing and the sun isn't shining. Grid-scale "flow" batteries are one proposed solution, storing energy for later use. But because they aren't very efficient, they need to be large and expensive.

In a flow battery, the energy is stored in a pair of "electrolyte" fluids which are kept in tanks and flow through the working part of the battery to store or release energy. An active metal gains or loses electrons from the electrode on either side, depending on whether the battery is charging or discharging. One efficiency bottleneck is how quickly electrons move between the electrodes and the active metal.

"By maximizing the charge transfer, we can reduce the overall cost of flow batteries," said Harsh Agarwal, a chemical engineering Ph.D. student and the study's first author. He works in the lab of Nirala Singh, an assistant professor of chemical engineering.

Researchers have been trying different chemical combinations to improve it, but they don't know what's going on at the molecular level. This study, published in *Cell Reports Physical Science*, is one of the first to explore it.

What Singh's team found is that, contrary to what researchers had believed, the negatively-charged molecular groups from the acids didn't provide more spots for electron transfer to take place on the battery's negative electrode. Instead, they lowered the energy barrier of that transfer by serving as a sort of bridge between the active metal in the fluid—vanadium in this case—and the electrode. This helps the vanadium give up its electron.

"Our findings suggest that bridging may play a critical yet underexplored role in other flow battery chemistries employing transition metals," said Nirala Singh. "This discovery is not only relevant to energy storage but also fields of corrosion and electrodeposition."

The study shows that the reaction rate in flow batteries can be tuned by controlling how well the acid in the liquid electrolyte binds with the active metal.

"Researchers can apply this knowledge to electrolyte engineering or electrocatalyst development, both of which are important disciplines in sustainable energy," said Agarwal.

Agarwal and Singh measured the reaction rate between the vanadium and electrode for five different acidic electrolytes. To get a clearer picture of the details at the atomic level, the team used a form of quantum mechanical modeling, known as Density Functional Theory, to calculate how well the vanadium-acid combinations bind to the electrode. This part of the study was undertaken by Bryan Goldsmith, the Dow Corning Assistant Professor of Chemical Engineering and co-senior author on the paper, and Jacob Florian, a chemical engineering senior undergraduate student working in the Goldsmith lab.

At the XSD Spectroscopy Group's 20-BM x-ray beamline at the APS, Agarwal and Singh used x-ray spectroscopy to discover details about how the vanadium ions configured themselves when in contact with different acids. Density functional theory calculations helped interpret the x-ray spectroscopy measurements. The study also provides the first direct experimental verification of how water attaches to vanadium ions.

See: Harsh Agarwal, Jacob Florian, Bryan R. Goldsmith, and Nirala Singh*, "The Effect of Anion Bridging on Heterogeneous Charge Transfer for V^{2+}/ V^{3+}," Cell Rep. Phys. Sci. **2**, 100307 (January 20, 2021).
DOI: 10.1016/j.xcrp.2020.100307
Author affiliation: University of Michigan
Correspondence: * snirala@umich.edu

This research is funded by University of Michigan Office of Research grant no. UMOR-29814. This research used the resources of the National Energy Research Scientific Computing Center (NERSC), a U.S. Department of Energy (DOE) Office of Science user facility operated under contract no. DE-AC02-05CH11231. This research used resources of the Advanced Photon Source Sector 20, a U.S. DOE Office of Science user facility operated for the DOE Office of Science by Argonne National Laboratory under contract no. DE-AC02-06CH11357, and the Canadian Light Source and its funding partners.

Nanoscale Defects Could Boost Energy Storage Materials

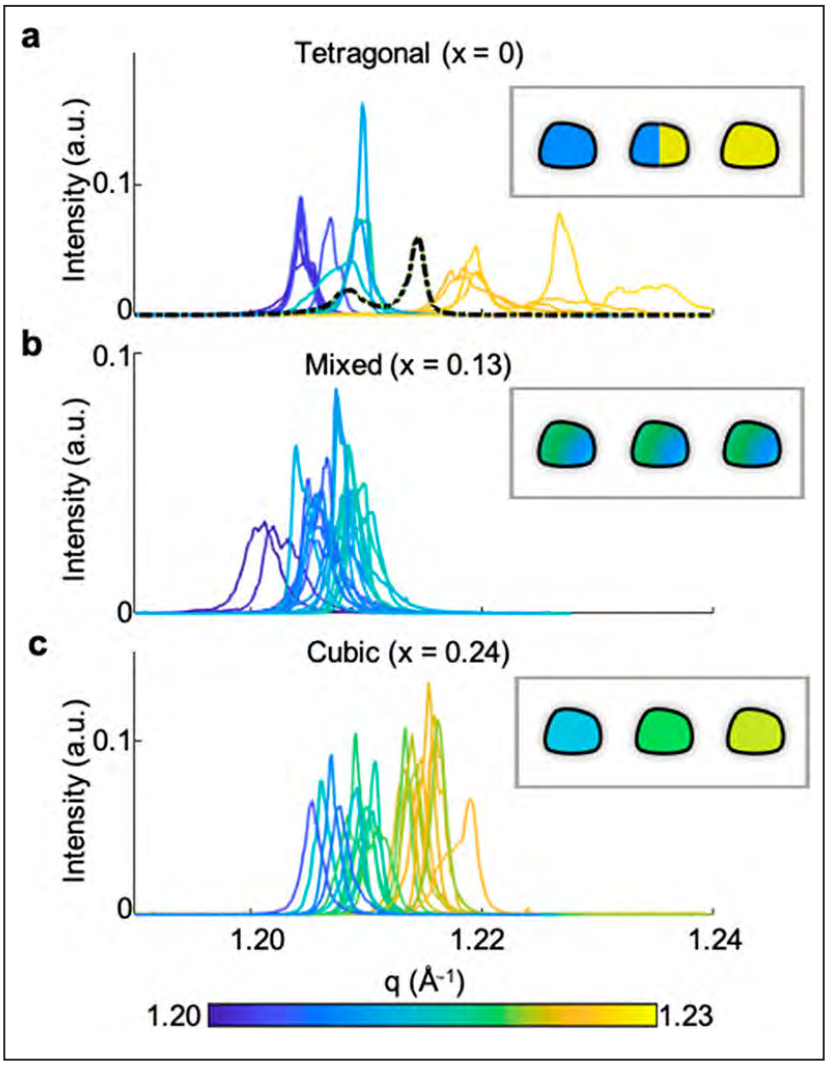

X-ray diffraction intensity for individual LLZO grains in the (a) tetragonal, (b) mixed, and (c) cubic structure as a function of momentum transfer q. The colors of the peak indicate the peak position in q, and every peak curve has one fixed color. The intensity is normalized by the integrated intensity of the peak (note the maximum intensity is higher in the cubic phase due to the sharper diffraction peaks in (c)). In (a), two types of tetragonal peaks are visible: split peaks (one example is shown in a dashed black line for clarity) and single peaks at either low q (blue) or high q (yellow). The insets illustrate the possible constitution of crystal domains for each type of grain. Tetragonal grains can either be in the two uniform crystal orientations, (211) as blue and (112) as yellow rotated by 90° from the other, or contain two coexisting domains. The mixed-phase grains all display a similar lattice constant, but the peak broadening indicates a strain gradient. The cubic structure has a uniform domain, but the lattice constant varies between different grains. From S. Sun et al., Nano Lett. **21**(11), 4570 (2021).

The original Cornell [University] Chronicle story by David Nutt can be read here. © Cornell University, Ithaca, New York

Some imperfections pay big dividends. A Cornell University-led collaboration used x-ray nanoimaging at the APS to gain an unprecedented view into solid-state electrolytes, revealing previously undetected crystal defects and dislocations that may now be leveraged to create superior energy storage materials. The group's paper was published in the journal *Nano Letters*.

For a half-century, materials scientists have been investigating the effects of tiny defects in metals. The evolution of imaging tools has now created opportunities for exploring similar phenomena in other materials, most notably those used for energy storage.

A group led by Andrej Singer, assistant professor and David Croll Sesquicentennial Faculty Fellow in the Department of Materials Science and Engineering at Cornell, uses synchrotron radiation to uncover atomic-scale defects in battery materials that conventional approaches, such as electron microscopy, have failed to find.

The Singer Group is particularly interested in solid-state electrolytes because they could potentially be used to replace the liquid and polymer electrolytes in lithium-ion batteries. One of the major drawbacks of liquid electrolytes is they are susceptible to the formation of spiky dendrites between the anode and cathode, which short out the battery or, even worse, cause it to explode.

Solid-state electrolytes have the virtue of not being flammable, but they present challenges of their own. They don't conduct lithium ions as strongly or quickly as fluids and maintaining contact between the anode and cathode can be difficult. Solid-state electrolytes also need to be extremely thin; otherwise, the battery would be too bulky and any gain in capacity would be negated.

What is the one thing that could make solid-state electrolytes viable? Tiny defects, Singer said.

"These defects might facilitate ionic diffusion, so they might allow the ions to go faster. That's something that's known to happen in metals," he said. "Also like in metals, having defects is better in terms of preventing fracture. So, they might make the material less prone to breaking."

Singer's group collaborated with Nikolaos Bouklas, assistant professor in the Cornell Sibley School of Mechanical and Aerospace Engineering and a co-author of the paper, who helped them understand how defects and dislocations might impact the mechanical properties of solid-state electrolytes.

The Cornell team then partnered with researchers at Virginia Tech–led by Feng Lin, the paper's co-senior author–who synthesized the sample: a garnet crystal structure, lithium lanthanum zirconium oxide (LLZO), with various concentrations of aluminum added in a process called doping.

Using the XSD Microscopy Group's 34-ID-C x-ray beamline at the APS they and a colleague from the APS employed the Bragg coherent diffractive imaging technique in which a pure, collimated x-ray beam is focused on a single micron-sized grain of LLZO. Electrolytes consist of millions of these grains. The beam created a three-dimensional (3-D) image that ultimately revealed the material's morphology and atomic displacements.

"These electrolytes were assumed to be perfect crystals," Sun said. "But what we find are defects such as dislocations and grain boundaries that haven't been reported before. Without our 3-D imaging, which is extremely sensitive to defects, it would be likely impossible to see those dislocations because the dislocation density is so low."

The researchers now plan to conduct a study that measures how the defects impact the performance of solid-state electrolytes in an actual battery.

"Now that we know exactly what we're looking for, we want to find these defects and look at them as we operate the battery," Singer said. "We are still far away from it, but we may be at the beginning of a new development where we can design these defects on purpose to make better energy storage materials."

See: Yifei Sun[1], Oleg Gorobstov[1], Linqin Mu[2], Daniel Weinstock[1], Ryan Bouck[1], Wonsuk Cha[3], Nikolaos Bouklas[1], Feng Lin[2]*, and Andrej Singer[1]**, "X-ray Nanoimaging of Crystal Defects in Single Grains of Solid-State Electrolyte $Li_{7-3x}Al_xLa_3Zr_2O_{12}$," Nano Lett. **21**(11), 4570 (2021).
DOI: 10.1021/acs.nanolett.1c00315
Author affiliations: [1]Cornell University, [2]Virginia Tech, [3]Argonne National Laboratory
Correspondence: * fenglin@vt.edu, ** asinger@cornell.edu

The work at Cornell was supported by the National Science Foundation (NSF) under Grand No. (CAREER DMR 1944907). The work at Virginia Tech was supported by the NSF (Grant no. DMR 1832613). This research used resources of the Advanced Photon Source, a U.S. Department of Energy (DOE) Office of Science user facility, operated for the DOE Office of Science by Argonne National Laboratory under Contract No. DE-AC02- 06CH11357.

Making the Most of Metal

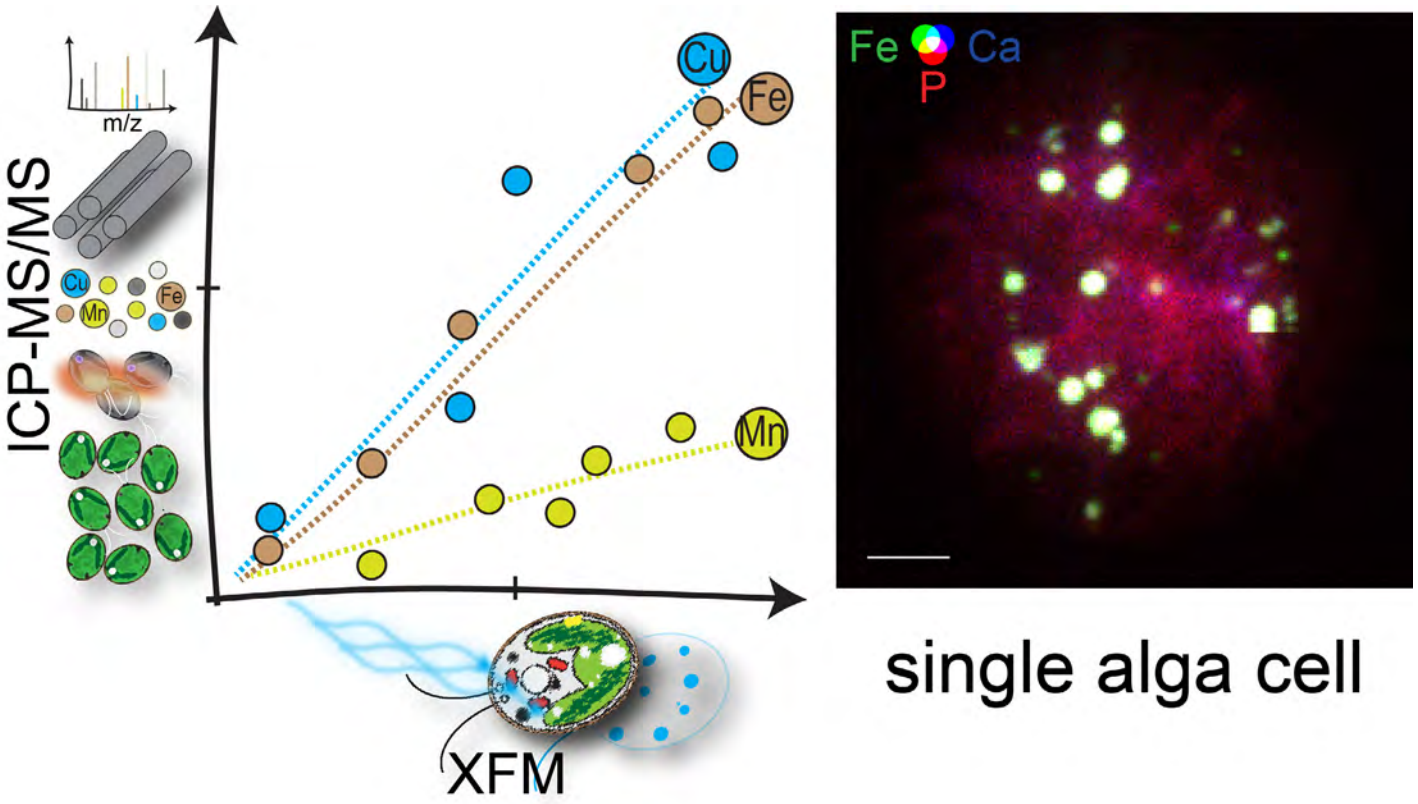

Fig. 1. Single-cell concentrations of trace metal content (XFM) compare well across a gradient of nutritional states with bulk cell measurements (ICP-MS). XFM imaging demonstrates the role of acidocalcisomes in Fe sequestration.

Earth's inhabitants are described as carbon-based life forms, yet we wouldn't amount to much without metal. Trace metals in particular play critical roles in the all-important redox chemistry that enables Earth dwellers to turn solar rays and food into energy. The importance of metals in biology is made obvious by the elaborate mechanisms organisms use to regulate metal acquisition, storage, and usage. In a recent study, researchers took a close look at how a photosynthetic microbe—the eukaryotic green alga *Chlamydomonas reinhardtii*—manages its metal resources. Using the APS they unraveled the complex strategy the organism employs to deal with times of metal feast and metal famine. Their results were published in the *Proceedings of the National Academy of Sciences of the United States of America*.

Trace metals such as iron, copper, manganese, and zinc have multiple jobs in life processes. For example, they provide structural support to biomolecules and facilitate catalysis in around 40% of enzymes. But not just any metal will do. Enzymes typically require specific metal cofactors to function properly. Mismetalation (incorrect metallation of enzymes) can harm the cell; therefore, the cell is heavily invested in avoiding that outcome.

One strategy cells use to get the right metal for the job is to compartmentalize trace metals, which locally adjusts the concentration of metals in the cell to influence the biomolecule to which a particular metal will bind. Storage sites that sequester particular trace metals include organelles called acidocalcisomes, which, as their name suggests, are acidic and high in calcium. These organelles, found in the cytoplasm of most eukaryotes, are easy to see in whole cells by x-ray fluorescence microscopy (XFM) thanks to their unique elemental signature. In this technique, x-rays are directed at a cell to stimulate the release of photons with energies that reveal the identities of elements within the cell, creating a map of

cellular contents. High-energy x-rays, like those produced at the APS penetrate deep within cells, allowing researchers to image whole cells without destroying them (Fig. 1).

In Chlamydomonas, which is a common reference organism, deficiency of a particular trace metal reduces growth rate, and encourages the cells to uptake alternate metals, often more than the cell can handle safely. These excess micronutrients can be stored for later, when perhaps the metal is suddenly in short supply. A previous study demonstrated that when Chlamydomonas is deprived of zinc, its acidocalcisomes begin to store excess amounts of other trace metals.

In situations where Chlamydomonas encounters excess iron or manganese in its environment, the researchers in this study suspected that the role of the acidocalcisome may be to sequester this bounty to prevent the cytoplasm from being overloaded with the metal, a situation that can lead to cell damage or mismetalation. To test this hypothesis, they subjected Chlamydomonas cells to excess iron, then measured how much of the iron ended up in acidocalcisomes using XFM at the Bionanoprobe in four sessions over a two-year period, first at the LS-CAT 21-ID-D x-ray beamline; and then, after the Bionanoprobe was relocated, at the XSD Microscopy Group's 9-ID beamline, both at the APS. They found that 80% of the total cellular iron ended up in acidocalcisomes under these conditions. They found similar results in zinc-deficient scenarios, when the cells took up extra iron in an attempt to gather the missing zinc. Again, 60% of the total iron ended up in the acidocalcisomes, keeping the concentration in the cytoplasm at levels similar to environments with just the right amount of trace metal supply.

Interestingly, the cell's response to copper turned out to be different than that for iron. Under conditions with limited zinc and iron, total copper in the cells was elevated, as if the cells tried to amass whatever metals were around in an effort to compensate for those missing metals. But in this case, the researchers found that the acidocalcisome was only taking up a portion of the excess copper, while a substantial portion of the copper was still found outside of the storage sites.

The findings are interesting in and of themselves, but the study also establishes a framework for future research. The researchers compared results in single cells to data from whole cultures and found excellent correlation. This suggests that bulk data accurately reflects the status of metal nutrition in single cells, and vice versa, offering a powerful tool for the study of the remarkable metals of biology. – Erika Gebel Berg

See: Stefan Schmollinger[1,2], Si Chen[3], Daniela Strenkert[1,2], Colleen Hui[1,2,4], Martina Ralle[5], and Sabeeha S. Merchant[1,2]*, "Single-cell visualization and quantification of trace metals in Chlamydomonas lysosome-related organelles," Proc. Natl. Acad. Sci. U.S.A. **118**(16), e2026811118 (2021). DOI: 10.1073/pnas.2026811118
Author affiliations: [1]University of California, Berkeley, [2]University of California, Los Angeles, [3]Argonne National Laboratory, [4]Lawrence Livermore National Laboratory, [5]Health and Sciences University
Correspondence: * sabeeha@berkeley.edu

This work was supported by a grant from the National Institutes of Health (GM42143) to S.S.M. for the work on copper, and by a grant from the U.S. Department of Energy (DOE, DE-SC0020627) to S.S.M. and S.S. for the work on iron. Use of the LS-CAT was supported by the Michigan Economic Development Corporation and the Michigan Technology Tri-Corridor (Grant 085P1000817). The authors appreciate the support of Keith Brister and Michael Bolbat at LS-CAT and the support of Evan Maxey at beamline 9-ID-B. This research used resources of the Advanced Photon Source, a U.S. DOE Office of Science user facility, operated for the DOE Office of Science by Argonne National Laboratory under Contract No. DE-AC02-06CH11357.

A Rare Mineral from Rocks Found in Mollusk Teeth

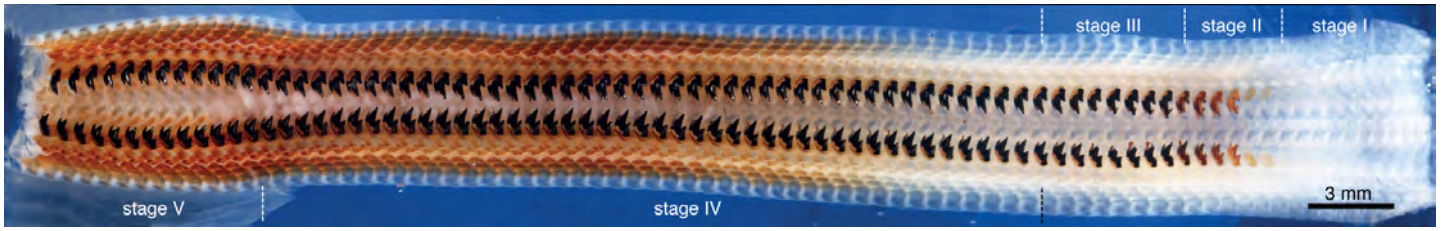

Fig. 1. Mosaic image of the entire chiton radula showing all stages of development, including deposition of the organic scaffold (stage I), infiltration of the cusp with ferrihydrite (stage II), conversion to magnetite (stage III), mineralization of the core (stage IV), and mature teeth (stage V). Figures from L. Stegbauer et al., Proc. Natl. Acad. Sci. USA **118**(23), e202016011 (June 8 2021). ©Copyright 2021 National Academy of Sciences

The original Northwestern University press release by Amanda Morris can be read here. 2021 Northwestern University

Northwestern University researchers have, for the first time, discovered a rare mineral hidden inside the teeth of a chiton, a large mollusk found along rocky coastlines. Before this strange surprise, the iron mineral, called santabarbaraite, only had been documented in rocks. The new finding, using data obtained at the APS helps us understand how the whole chiton tooth, not just the ultra-hard, durable cusp, is designed to allow them to chew on rocks to feed. Based on minerals found in chiton teeth, the researchers developed inks for three-dimensional (3-D) printing of bioinspired composites. The study was published in the *Proceedings of the National Academy of Sciences of the United States of America*.

“This mineral has only been observed in geological specimens in very tiny amounts and has never before been seen in a biological context,” said Northwestern’s Derk Joester, the study’s senior author. “It has high water content, gives it low density at relatively high strength. We think this might toughen the teeth without adding a lot of weight.”

One of the hardest known materials in nature, chiton teeth are attached to a soft, flexible, tongue-like radula (Fig. 1), which scrapes over rocks to collect algae and other food. Having long studied chiton teeth, Joester and his team most recently turned to *Cryptochiton stelleri*, a giant, reddish-brown chiton that is sometimes affectionately referred to as the “wandering meatloaf.”

To examine a tooth from *Cryptochiton stelleri*, Joester’s team collaborated with several x-ray beamline personnel at the APS to use the facility’s high-brightness x-rays to carry out a variety of experiments. X-ray absorption spectro-microscopy at the iron K-edge was performed at the GSECARS x-ray microprobe beamline 13-ID-E where x-ray fluorescence maps were recorded to determine regions of interest for subsequent micro-x-ray near edge structure (μXANES) collection of XANES spectra. Synchrotron x-ray computed microtomography was performed on the DND-CAT beamline 5-BM-C at the APS. Synchrotron x-ray computed microtomography was performed on the DND-CAT beamline 5-BM-C at the APS. and synchrotron Mössbauer spectroscopy (Fig. 2) was performed at the XSD Inelastic X-ray and Nuclear Scattering Group's beamline 3-ID-B. “

This kind of mineralogical mapping using the newly developed Mössbauer microscopy for the first time has allowed us to follow a biomineralization process," said co-author and APS senior scientist Ercan Alp, “producing interesting results. I expect more applications will follow.”

In addition, co-author Paul Smeets of Northwestern used transmission electron microscopy at the Northwestern University Atomic and Nanoscale Characterization and Experiment (NUANCE) Center.

The results showed that the rare santabarbaraite dispersed throughout the chiton’s upper stylus, a long, hollow structure that connects the head of the tooth to the flexible radula membrane.

“The stylus is like the root of a human tooth, which connects the cusp of our tooth to our jaw,” Joester said. “it is a tough material composed of extremely small santabarbaraite nanoparticles in a fibrous matrix made of biomacromolecules, similar to bones in our body.”

Joester’s group challenged itself to recreate this material in an ink designed for 3-D printing. Stegbauer devel-

oped a reactive ink comprising iron and phosphate ions mixed into a biopolymer derived from chitin. Along with Shay Wallace, a Northwestern graduate student in Mark Hersam's laboratory, Stegbauer found that the ink printed well when mixed immediately before printing.

"As the nanoparticles form in the biopolymer, it gets stronger and more viscous. This mixture can then be easily used for printing. Subsequent drying in air leads to the hard and stiff final material," Joester said. Joester believes we can continue to learn from and develop materials inspired by the chiton's stylus, which connects ultra-hard teeth to a soft radula. "We've been fascinated by the chiton for a long time," he said. "Mechanical structures are only as good as their weakest link, so it's interesting to learn how the chiton solves the engineering problem of how to connect its ultrahard tooth to a soft underlying structure. This remains a significant challenge in modern manufacturing, so we look to organisms like the chiton to understand how this is done in nature, which has had a couple hundred million years of lead time to develop."

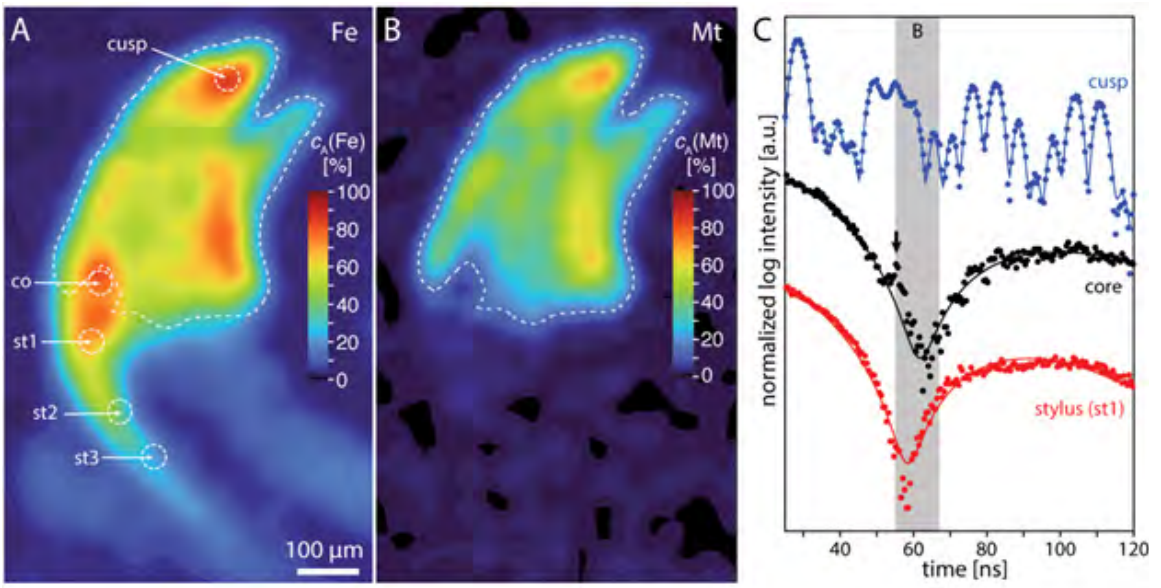

Fig. 2. (A) SMS image of iron distribution, (B) Mineral selective SMS image, showing the magnetite concentration, and (C) SMS spectra od magnetite in the cusp, as well as non-magnetic iron in the core and stylus.

See: Linus Stegbauer[1], E. Ercan Alp[2], Paul J. M. Smeets[1], Robert Free[1], Shay G. Wallace[1], Mark C. Hersam[1], and Derk Joester[1]*, "Persistent Polyamorphism in the Chiton Tooth: From a New Biomineral to Inks for Additive Manufacturing," Proc. Natl. Acad. Sci. USA **118**(23), e202016011 (June 8 2021). DOI: 10.1073/pnas.2020160118
Author affiliations: [1]Northwestern University, [2]Argonne National Laboratory
Correspondence: * d-joester@northwestern.edu

L.S. was supported by a research fellowship of the Deutsche Forschungsgemeinschaft (STE2689/1-1). This work was in part supported by the National Science Foundation (DMR-1508399 and DMR-1905982). R.F. was supported by an F31 fellowship from the National Institutes of Health (NIH-DE026952). S.G.W. and M.C.H. acknowledge support from the Air Force Research Laboratory under agreement FA8650-15-2-5518. This work made use of the following core facilities operated by Northwestern University: MatCI; BioCryo, SPID, NUANCE and EPIC, which received support from the International Institute for Nanotechnology (IIN), the Keck Foundation, and the State of Illinois, through the IIN; IMSERC, QBIC, which received support NASA Ames Research Center NNA06CB93G. MatCI, BioCryo, SPID, NUANCE, and EPIC were further supported by the MRSEC program (NSF DMR-1720139) at the Materials Research Center; BioCryo, SPID, NUANCE, EPIC, and IMSERC were also supported by the Soft and Hybrid Nanotechnology Experimental (SHyNE) Resource (NSF ECCS-1542205). It also made use of the CryoCluster equipment of BioCryo, which has received support from the MRI program (NSF DMR-1229693). The DuPont-Northwestern-Dow Collaborative Access Team is supported by Northwestern University, The Dow Chemical Company, and DuPont de Nemours, Inc. Data was collected using an instrument funded by the National Science Foundation under Award Number 0960140. GeoSoilEnviroCARS is supported by the National Science Foundation–Earth Sciences (EAR–1634415) and U.S. Department of Energy (DOE)-GeoSciences (DE-FG02-94ER14466). The authors thank Tony Lanzirotti, Matt Newville, Thomas Toellner, and Jiyong Zhao for technical support. This research used resources of the APS, a U.S. DOE Office of Science user facility operated for the DOE Office of Science by Argonne National Laboratory under Contract No. DE-AC02-06CH11357.

Multi-Scale Experiments Inform Modeling of Titanium Alloy Durability

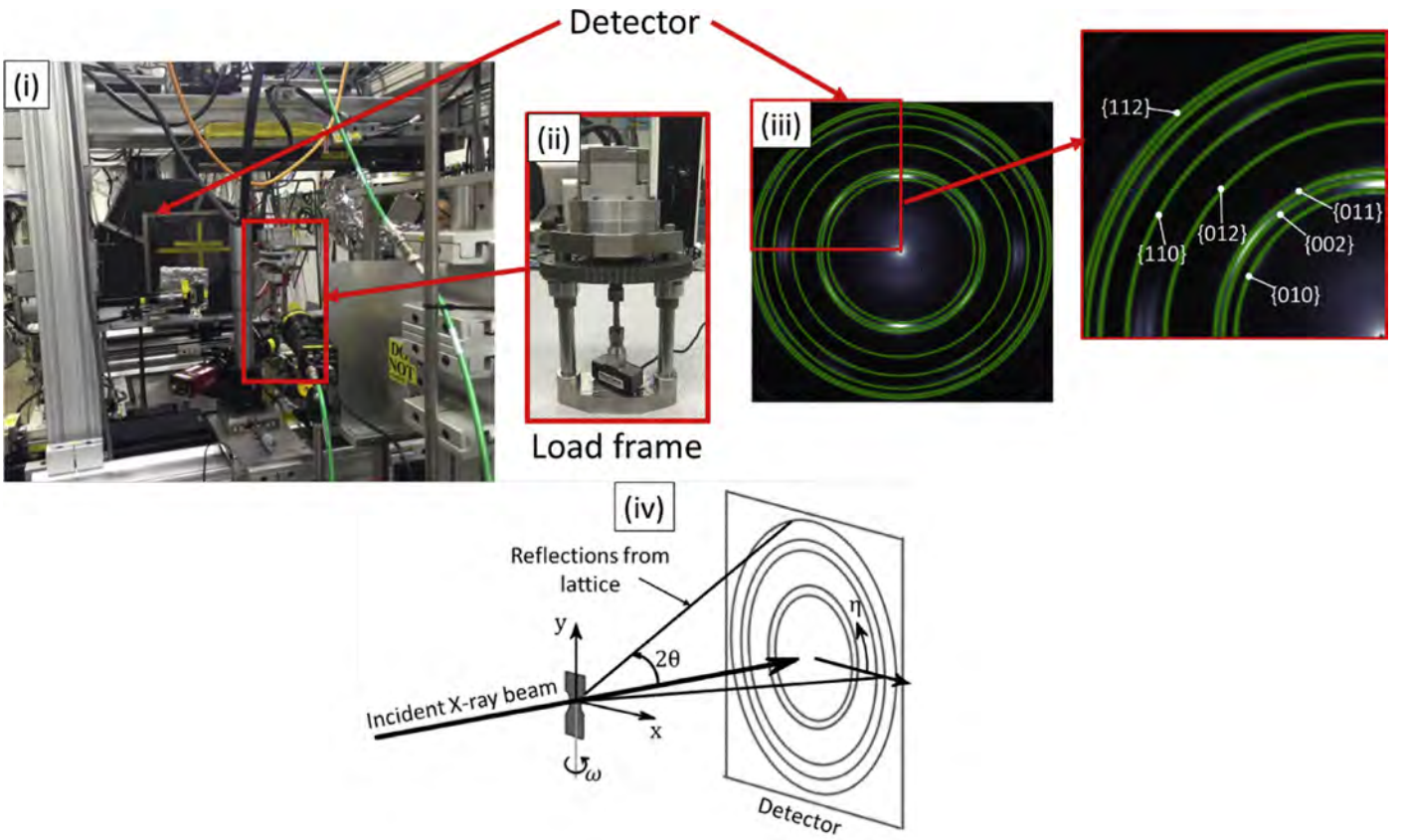

Fig. 1. HEXD experiment: (i) Experimental setup at Sector 1 of the APS, showing the detector and the load frame; (ii) zoomed in view of the load frame; (iii) observed diffraction rings on the detector, with a zoomed view showing the α phase {hkl} planes corresponding to the rings; (iv) schematic of the HEXD experiment, showing the geometry of the specimen and the associated nomenclature.

Titanium alloys are widely used in the biomedical and aerospace industries. Even though these alloys have been in use for decades, the mechanisms associated with their deformation and the ensuing mechanical properties are still not well understood. A computational technique called crystal plasticity modeling can effectively describe the stress-strain response of these alloys at the single-crystal level. The technique relies on a range of constitutive equations, in which the incorporation of additional physics-based relationships typically results in additional model parameters. These additional parameters need to be calibrated, which often requires the use of experimental data acquired at multiple length scales. Researchers recently developed a crystal plasticity based finite element (CPFE) model for a dual-phase titanium alloy, Ti–6Al–4V, with explicit modeling of the orientation and morphology of the alloy's α and β phases. The model was then calibrated with experimental data consisting of macroscopic stress-strain curves coupled with lattice strains on different crystallographic planes for the two phases obtained at the APS. The fully calibrated CPFE model was then used to examine deformation within Ti–6Al–4V. Their results, published in the *Journal of the Mechanics and Physics of Solids* show that compared to dual-phase microstructures, single-phase α and β alloys are not suitable due to homogeneity in the deformation behavior leading to reductions in the fatigue lifetimes. Comparing the dual-phase microstructures used in this study, the results also show bi-modal microstructures, in which α and β phases are oriented in a way that aligns their slip systems, are more likely to minimize stress relax-

ation over time leading to improvements in the time-dependent fatigue behavior of alloy components.

The atoms of pure titanium (Ti) align in either a hexagonal close-packed crystalline structure, called the alpha (α) phase, or a body-centered cubic structure, called the beta (β) phase. In the pure metal, transformation from the α to the β phase occurs upon heating above 883° C, but most alloying elements either stabilize the α phase to higher temperatures (aluminum) or stabilize the β phase to lower temperatures (vanadium). In dual-phase titanium alloys, the phases exist alongside each other.

The titanium alloy Ti-6Al-4V is known for its high strength-to-weight ratio and resistance to corrosion. Accounting for half of all titanium alloy manufactured, Ti-6Al-4V is commonly used in aerospace, biomedical, and high-performance sports applications. A wide range of physical and mechanical properties of Ti-6Al-4V can be achieved by varying the microstructure of the alloy via deformation and recrystallization processes. The mechanisms associated with deformation, however, have not been well characterized.

In dual-phase titanium alloys with bi-modal microstructure, the α and β phases can be oriented in a manner that makes their slip systems aligned or not aligned. This orientation can be controlled by varying the thermomechanical-processing route and the heat treatment used to manufacture the alloy. Understanding the effect of crystallographic orientation of the phases on specific material properties like time-dependent cyclic loading can inform the design of dual-phase alloys for specific applications.

Traditional macroscopic models of Ti-6Al-4V's plasticity are unable to capture the local details of the deformation mechanisms at the microstructural level. While deformation in titanium alloys can be studied at different length scales, examining the material at the meso-scale (crystal scale) is necessary to understand strain localization associated with various phenomena including fatigue crack initiation as the local microstructure significantly influences the crack initiation and small crack propagation behaviors

Crystal plasticity modeling is a computational technique used to obtain the relationship between stress and strain and which also captures the underlying physics of materials at the crystal level.

Crystal plasticity-based finite element (CPFE) modeling is a powerful tool for understanding deformation at the crystal scale. In an effort to reduce model complexity and computation time, many CPFE models for dual-phase titanium alloys neglect the β phase due to its relatively low volume fraction. In addition, several other parameters that have an inherent physical basis also pose challenges in being measured directly at the grain scale that best illustrates deformation. Therefore, the calibration of accurate and precise crystal plasticity modeling requires the use of a larger dataset derived from experiments performed across multiple length scales.

To calibrate CPFE model parameters, the researchers in this study coupled stress-strain curve data from specimen-level tension tests with lattice strain data from the individual α and β phases of Ti–6Al–4V, the latter of which were obtained from high-energy x-ray diffraction (HEXD) experiments (Fig. 1) conducted at the XSD Materials Physics & Engineering Group's beamline 1-ID at the APS.

They found that not including the β phase in the simulations results in under-predicting the localized heterogeneity in deformation. They also showed that single-phase α and β alloys are not suitable due to homogeneous slip resulting in relatively higher amount of plasticity in the microstructure, compared to dual-phase microstructures. In addition, the results demonstrated Ti-6Al-4V with higher concentration of the β phase will result in higher accumulation of plasticity, which would have detrimental effects on the time-dependent fatigue behavior. The research further suggests that introducing mechanisms to promote the alignment of α and β phases slip systems limits the redistribution of stresses within the alloy and hence may improve time-dependent cyclic loading performance. – Chris Palmer

See: Kartik Kapoor[1], Priya Ravi[1], Ryan Noraas[2], Jun-Sang Park[3], Vasisht Venkatesh[2], and Michael D. Sangid[1]*, "Modeling Ti–6Al–4V using crystal plasticity, calibrated with multiscale experiments, to understand the effect of the orientation and morphology of the α and β phases on time dependent cyclic loading," J. Mech. Phys. Solids **146**, 104192 (2021). DOI: 10.1016/j.jmps.2020.104192
Author affiliations: [1]Purdue University, [2]Pratt & Whitney, [3]Argonne National Laboratory
Correspondence: * msangid@purdue.edu

This work was financially supported by Pratt and Whitney. This research used resources of the Advanced Photon Source, a U.S. DOE Office of Science user facility operated for the DOE Office of Science by Argonne National Laboratory under Contract DE-AC02-06CH11357.

Probing the Structure of a Promising NASICON Material

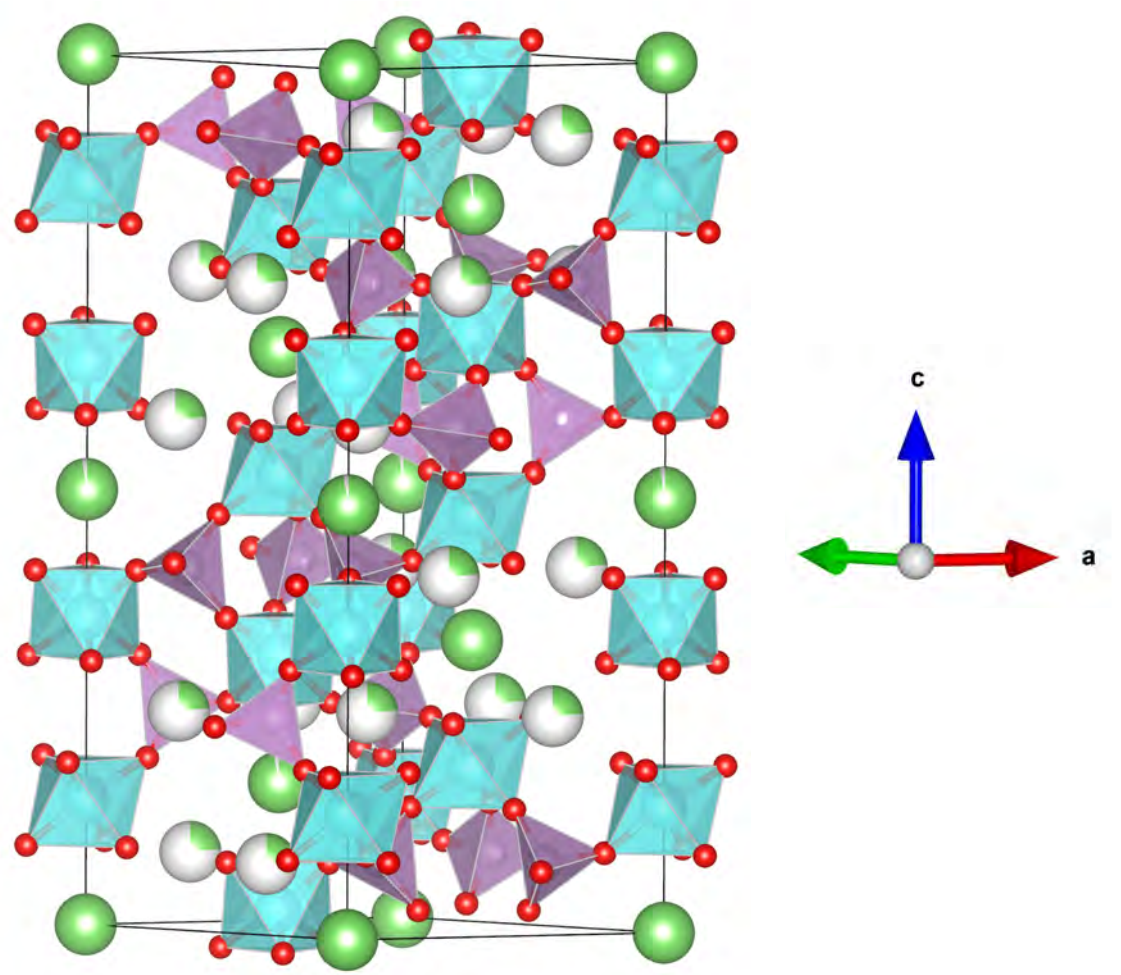

Fig. 1. NASICON crystal structure showing the tetrahedral $P^{(4)}$ phosphate motifs (purple), octahedral GeO_6 motifs (cyan) and Na^+ ions (green). Oxygen atoms are depicted in red.

As physicists, materials scientists, and engineers continue striving to enhance and improve batteries and other energy storage technologies, a key focus is on finding or designing new ways to make electrodes and electrolytes. One promising avenue of research involves solid-state materials, making possible batteries free of liquid electrolytes, which can pose fire and corrosion hazards. An international group of researchers joined with scientists at Argonne National Laboratory to investigate the structure of crystalline and amorphous compounds based on the NASICON system, or sodium super-ion conductors. The work (using research carried out at the APS and published in the *Journal of Chemical Physics*) reveals some substantial differences between the crystalline and glass phases of the NAGP system, which affect the ionic conductivity of the various materials. The investigators note that the fraction of non-bridging oxygen (NBO) atoms appears to play a significant role, possibly altering the Na^+ ion mobility, and suggest this as an area of further study. The work provides fresh insights into the process of homogeneous nucleation and identifying superstructural units in glass – a necessary step in engineering effective solid-state electrolytes with enhanced ionic conductivity.

Because of their high ionic conductivity, materials with a NASICON structure are prime candidates for a solid electrolyte in sodium-ion batteries. They can be prepared by a glass-ceramic route, which involves the crystallization of a precursor glass, giving them the usefulness of moldable bulk materials. In this work, the research team specifically studied the NAGP system [$Na_{1+x}Al_xGe_{2-x}(PO_4)_3$] with $x = 0$, 0.4 and 0.8 in both crystalline and glassy forms. Working at several different facilities, they used a combination of techniques, including neutron and x-ray diffraction, along with ^{27}Al and ^{31}P magic angle spinning and $^{31}P/^{23}Na$ double-resonance nuclear magnetic resonance spectroscopy. The glassy form of NAGP materials was examined both in its as-prepared state and after thermal annealing, so that the changes on crystal nucleation could be studied.

Neutron powder diffraction measurements were performed at the BER II reactor source, Helmholtz-Zentrum Berlin, using the fine resolution powder diffractometer E9 (FIREPOD), followed by Rietveld analysis. Further neutron diffraction observations were conducted at the Institut Laue-Langevin using the D4c diffractometer and at the ISIS pulsed neutron source using the GEM diffractometer. X-ray diffraction studies were performed at XSD Magnetic Materials Group's beamline 6-ID-D of the APS.

The studies reveal the structural changes that accompany the increase with x in the ionic conductivity of the crystalline material (Fig. 1). The NAGP $x = 0$ and $x = 0.4$ compounds are classified as space group R3 while the $x = 0.8$ compound is space group R3c. The $x = 0$ phase shows tetrahedral PO_4 motifs linked by bridging oxygen (BO) atoms to four octahedral GeO_6 motifs. This permits Na^+ ions to reside at the interstices, allowing ionic conductivity. In the glassy NAGP phases, the formation of sub-octahedral Ge and Al-centered units leads to NBO atoms. Upon annealing, the fraction of NBO atoms decreases as the Ge and Al coordination numbers increase. Again, the ionic conductivity increases with the concentration of Na+ ions in the glassy NAGP material.

Based on the Ren and Eckert model for vitreous sodium phosphosilicates, the researchers propose a model for the $x = 0$ glass in which superstructural units are formed. In these units, $P^{(3)}$ phosphate motifs with three BO and one NBO atoms are converted to $P^{(4)}$ phosphate motifs with four BO atoms, thereby converting GeO_4 to GeO_6 motifs and increasing the size of the superstructural units. Annealing the as-prepared glass leads to increases in both the Ge coordination number and the fraction of $P^{(4)}$ motifs, which provide the nucleation sites for crystal growth. – Mark Wolverton

See: Lawrence V. D. Gammond[1], Henry[2], Rita Mendes Da Silva[1], Anita Zeidler[1], Jairo F. Ortiz-Mosquera[3], Adriana M. Nieto-Muñoz[3], Ana Candida M. Rodrigues[3], Igor d'Anciães Almeida Silva[4], Hellmut Eckert[4,5], Chris J. Benmore[6], and Philip S. Salmon[1]*, "Structure of crystalline and amorphous materials in the NASICON system $Na_{1+x}Al_xGe_{2-x}(PO_4)_3$," J. Chem. Phys. **155**, 074501 (2021).
DOI: 10.1063/5.0049399
Author affiliations: [1]University of Bath, [2]Fraunhofer Institute for Ceramic Technologies and Systems IKTS, [3]Universidade Federal de São Carlos, [4]Universidade de São Paulo, [5]Institut für Physikalische Chemie, [6]Argonne National Laboratory
Correspondence: * p.s.salmon@bath.ac.uk

L.V.D.G. acknowledges funding and support from the EPSRC Centre for Doctoral Training in Condensed Matter Physics (CDT-CMP), Grant No. EP/L015544/1, the Science and Technology Facilities Council (STFC) and Diamond Light Source Ltd (Reference No. STU0173). R.M.D.S. acknowledges funding and support from the Royal Society. PSS received support from the University of Bath's International Funding Scheme. A.Z. was supported by a Royal Society-EPSRC Dorothy Hodgkin Research Fellowship. I.D.A.S. and H.E. appreciate funding by FAPESP, Center of Research, Technology and Education, process number 2013/07793-6. I.D.A.S. also acknowledges FAPESP funding for a postdoctoral fellowship, process number 2017/17800-0. J.F.O.M. and A.M.N.M. were supported by CNPq (Conselho Nacional de Desenvolvimento Científico e Tecnológico), Process Nos. 168682/2017-6 and 141220/2016-3, respectively. This study was financed in part by the Coordenação de Aperfeiçoamento de Pessoal de Nível Superior - Brasil (CAPES) - Finance Code 001. This research used resources of the Advanced Photon Source, a U.S. Department of Energy (DOE) Office of Science user facility operated for the DOE Office of Science by Argonne National Laboratory under Contract No. DE-AC02-06CH11357.

Building a Better Simulation for a Better Refractory Oxide

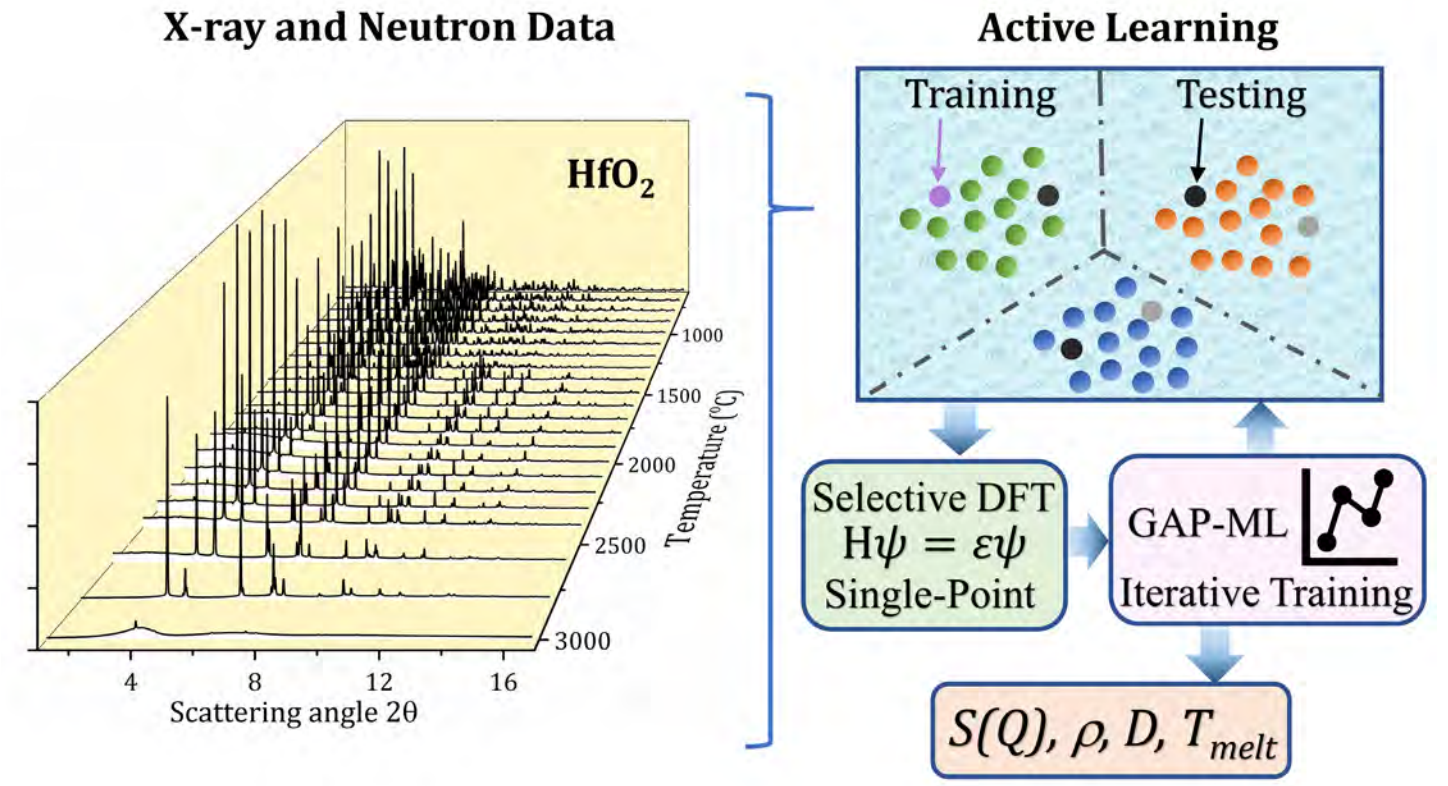

Fig. 1. Multiphase, high-energy x-ray and spallation neutron data, measured over a wide range of temperatures, are used to drive an active learning algorithm that tests many density functional theory simulations on a supercomputer. A machine-learned Gaussian approximation potential is trained from those simulations that agree best with the experimental data. The resulting model is used to reproduce the structures as well as predict the thermodynamic and thermophysical properties of the system.

Refractory materials, defined as nonmetallic substances with very high melting points that allow them to withstand extremely high temperatures above 1500° C, are essential for industrial applications and processes that occur in such extreme conditions. Refractory materials are used to coat the interiors of furnaces, incinerators, reactors, and wherever it's necessary to withstand great pressures and temperatures. Properly testing such materials in such extreme environments is obviously challenging, so materials scientists greatly depend upon computational modeling techniques to accurately characterize the behavior of refractory materials. Methods such as ab initio molecular dynamics simulations (AIMD) have their limitations, however. Some modeling techniques can only handle relatively small systems and short time scales, or do not always agree with experimental data. Recent attempts to address these issues have focused on incorporating machine learning methods with quantum-mechanical calculations to achieve models of larger systems and time scales. A group of researchers demonstrated this approach by creating a scheme to generate multiphase machine learning inter-atomic potentials (ML-IP) for the common refractory oxide material hafnium dioxide (HfO_2) and testing it at the APS and Spallation Neutron Source. Their results were published as an Editor's Suggestion in *Physical Review Letters*.

The investigators from the from University of Cambridge (UK), Helmholtz-Institute Munster (Germany), and Argonne devised an automated scheme of three parts, beginning with experimental measurements of sample material to obtain phase information up to the melting point. In this work, x-ray diffraction data was collected on high-purity samples of HfO_2 up to about 3000° C in reducing and oxygen atmospheres at the XSD Magnetic Materi-

als Group's 6-ID-D x-ray beamline of the APS, followed by complementary neutron diffraction measurements at the Spallation Neutron Source of Oak Ridge National Laboratory (Fig. 1).

In the second step of the researchers' automated scheme, the dataset of x-ray and neutron diffraction measurements is used to initialize active learning to create approximate ML-IP models of the interaction potentials between atoms, and then in the final step, using these to perform ab initio calculations which are used to retrain the ML-IP model to its final form. The process continues in a closed loop until an interatomic potential is found that can reproduce the measured structures over the experimentally determined phase space.

The active learning in this demonstration uses the Gaussian approximation potential (GAP) framework to generate and train the ML-IP model. ML-IP based on GAPs have been previously shown to be applicable to a broad range of models including liquids, crystal defects, and amorphous, multicomponent, and molecular systems. Here, the resulting model spans the HfO_2 phase space from the liquid to amorphous to crystalline over 2053 configurations.

As it is heated, HfO_2 passes from monoclinic to tetragonal to cubic phases and melts at about 2800° C. Production simulations were conducted with the ML-IP model, using a 6144-atom cell for monoclinic and cubic HfO_2 and a 6912-atom cell for the tetragonal phase. The decrease in long-range ordering with higher temperatures seen by neutron diffraction patterns in the tetragonal and cubic forms in the liquid and amorphous phases was accurately shown in the ML model. Multiphase potential of HfO2 was also theoretically evaluated by comparing cohesive energy and diffusion coefficients using several methods. The GAP technique was most accurate in predicting cohesive energies. Diffusion calculations based on the MD simulations show little diffusion of either Hf or O at simulation temperatures but indicate greater diffusion of Hf in liquid HfO_2 at higher temperatures.

This work provides a proof of concept demonstrating how a three-step automated scheme can be used to generate a multiphase ML-IP for a refractory oxide material. The scheme can initialize ab initio calculations directly from experimental models or measurements and thus effectively validate the models with ab initio accuracy.

The scheme presented here can also be used with ML-IP techniques other than the GAP framework employed in this demonstration and can be adapted to characterize a wide range of refractory oxides and similar materials. It offers a new tool for computational modeling and simulation to supplement and enhance the development of unique materials for difficult applications.

– Mark Wolverton

See: Ganesh Sivaraman[1], Leighanne Gallington[1], Anand Narayanan Krishnamoorthy[2], Marius Stan[1], Gábor Csányi[3], Álvaro Vázquez-Mayagoitia[1], and Chris J. Benmore[1]*, "Experimentally Driven Automated Machine-Learned Interatomic Potential for a Refractory Oxide," Phys. Rev. Lett. **126**, 156002 (2021). DOI: 10.1103/PhysRevLett.126.156002
Author affiliations: [1]Argonne National Laboratory, [2]Helmholtz-Institute Munster, [3]University of Cambridge
Correspondence: * benmore@anl.gov

This material is based upon work supported by Laboratory Directed Research and Development (LDRD) funding from Argonne National Laboratory, provided by the Director, Office of Science, of the U.S. Department of Energy (DOE) under Contract No. DE-AC02-06CH11357. This research used resources of the Argonne Leadership Computing Facility, which is a DOE Office of Science user facility supported under Contract No. DE-AC02- 06CH11357. Argonne National Laboratory's work was supported by the U.S. DOE Office of Science, under Contract No. DE-AC02-06CH11357. We gratefully acknowledge the computing resources provided on Bebop; a high-performance computing cluster operated by the Laboratory Computing Resource Center at Argonne National Laboratory. This research used resources of the Advanced Photon Source, a U.S. DOE Office of Science user facility operated for the DOE Office of Science by Argonne National Laboratory under Contract No. DE-AC02-06CH11357 and the Spallation Neutron Source operated by Oak Ridge National Laboratory. Use of the Center for Nanoscale Materials, an Office of Science user facility, was supported by the U.S. DOE Office of Science-Basic Energy Sciences, under Contract No. DEAC02-06CH11357. A.N.K gratefully acknowledges financial support from the German Funding Agency (Deutsche Forschungsgemeinschaft-DFG) under Germany's Excellence Strategy—EXC 2075—390740016.

Enhanced Electrical Transport in Two-Dimensional Perovskite Solar Cells

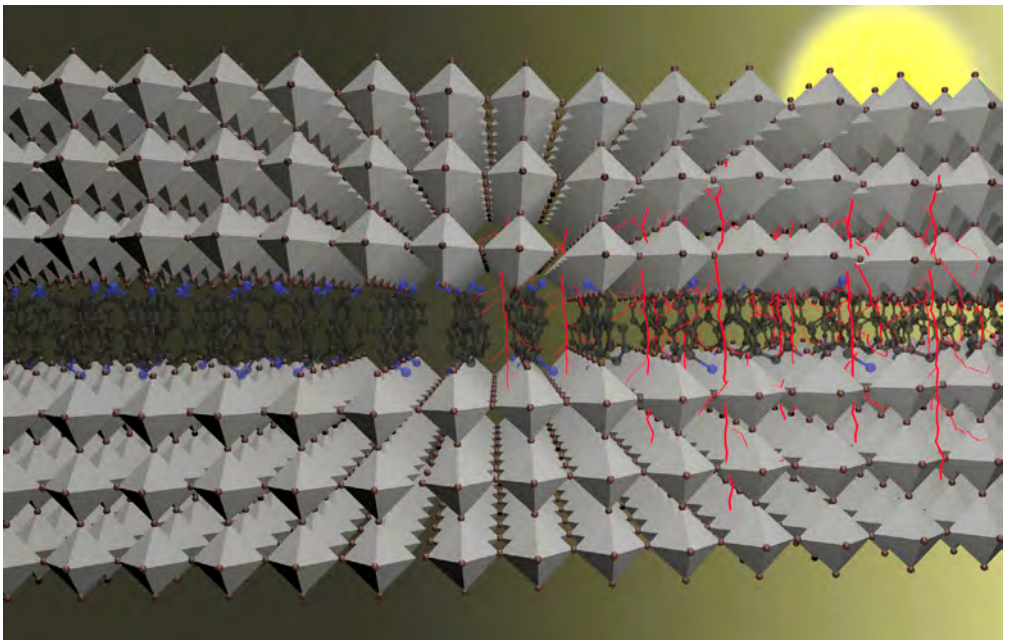

Visualization of a 2-D perovskite lattice in the dark (left) and illuminated (right). In the region under light, the structure has contracted, bringing the layers closer to together; electrons are flowing between the layers (as represented by the red lightning bolts), which was not possible prior to illumination.

Scientists using the APS and the National Synchrotron Light Source II (NSLS-II) have captured details of the atomic level interactions in a novel type of two-dimensional (2-D) solar cell. The international team of researchers from universities and U.S. national laboratories say that these findings could help us develop more efficient and stable perovskite solar cells, which have the potential to be cheaper, lighter and more flexible than their silicon counterparts. The results were published in *Nature Nanotechnology*.

Most solar cells are made from crystalline silicon. But in the last decade, there has been increasing interest in solar cells made from perovskites. These materials have a similar crystal structure to calcium titanium oxide, a mineral also known as perovskite.

In recent years, the performance of perovskite solar cells has started to match that of silicon solar cells, with reported laboratory efficiencies of around 25%. Researchers have also developed dual silicon–perovskite solar cells with even higher efficiencies. But perovskite solar cells have issues with chemical stability and can degrade rapidly outdoors. This is a challenge to their wider adoption.

Perovskites in solar cells typically have a three-dimensional (3-D) crystal structure. In 2016, researchers developed solar cells made of layered 2-D perovskites. These showed lower efficiencies than their 3-D cousins but much more stability to light exposure, humidity, and heat stress.

Since then, the team, led by engineers at Rice University, have been trying to increase the efficiency of 2-D perovskite solar cells, while maintaining their stability. These 2-D perovskites consist of atomically thin layers of inorganic material separated by insulating organic spacers, which act as springs. In such 2-D materials, electrical charges can typically travel within the layers – in two directions, or dimensions – but there is little interaction between the layers.

Now the researchers have shown that under continuous light illumination in some 2-D perovskites, the interaction between the layers is enhanced, allowing charge to flow across the layers. This in turn increases the efficiency of the solar cells. They have reported a 2-D perovskite solar cell with an efficiency of 18.3%, pushing it much closer to that of 3-D perovskite and silicon solar cells.

There are three known types of 2-D perovskites,

which each have slightly different crystal structures. The researchers noticed that when they shone light on one type, known as Dion–Jacobson perovskite, where the gap between the atomically thin layers is smaller than the others, they kept getting spikes in the voltage produced by the material.

To find out what was going on, the researchers teamed up with XSD at the APS, and the Center for Functional Nanomaterials at the NSLS-II, at Argonne National Laboratory and Brookhaven National Laboratory, respectively. They used the XSD Dynamics & Structure Group's beamline 8-ID-E at the APS and beamline 11-BM at the NSLS-II to perform grazing-incidence wide-angle x-ray scattering to measure changes in the structure of the perovskites when illuminated by a solar simulator, with simultaneous measurement of electrical transport properties.

The team found that under continuous illumination, iodine atoms in the 2-D perovskite become electron poor and more positively charged. This increases the interaction between these atoms in the different 2-D layers, changing the interlayer electrical transport and resulting in a 3-fold increase in charge carrier mobility. These changes start to occur after around 10 minutes of illumination.

X-rays showed that the abrupt change in charge transport occurs at the same time as a contraction of the structure of the perovskite; the layers move slightly closer to each other. According to the researchers, this is caused by the enhanced bonding of the iodine atoms. Due to the improved charged transport, the efficiency of a Dion–Jacobson-based photovoltaic device increases from 15.6% to 18.3%, they calculate.

The researchers say their results show that by focusing on atomic structure, interactions between positively charged atoms and the sensitivity of 2-D perovskites to external stimuli (like sunlight), interactions between the layers can be enhanced leading to performances closer to those of 3-D perovskites.

Using these techniques to probe structural changes in the materials could also give clues to their long-term stability; for example, do they degrade or undergo changes in the crystal structure over time. The team add that their results and techniques could also improve our understanding of the physics of other 2-D materials.

– Michael Allen

See: Wenbin Li[1,2], Siraj Sidhik[1,2], Boubacar Traore[2], Reza Asadpour[3], Jin Hou[1], Hao Zhang[1], Austin Fehr[1], Joseph Essman[1], Yafei Wang[1], Justin M. Hoffman[7], Ioannis Spanopoulos[4], Jared J. Crochet[5], Esther Tsai[6], Joseph Strzalka[7], Claudine Katan[2], Muhammad A. Alam[3], Mercouri G. Kanatzidis[4], Jacky Even[3], Jean-Christophe Blancon[1]* and Aditya D. Mohite[1]**, "Light-activated interlayer con-traction in two-dimensional perovskites for high-efficiency solar cells," Nat. Nanotechnol. **17**, 45 (22 November 2021).
DOI: 10.1038/s41565-021-01010-2

Author affiliations: [1]Rice University, [2]University Rennes, [3]Purdue University, [4]Northwestern University, [5]Los Alamos National Laboratory, [6]Brookhaven National Laboratory, [7]Argonne National Laboratory
Correspondence: * blanconjc@gmail.com,
** adm4@rice.edu

The work at Rice University was supported by the U.S. Department of Defense Short-Term Innovative Research (STIR) programe funded by the Army Research Office. J. Even acknowledges the financial support from the Institut Universitaire de France. W.L. acknowledges the National Science Foundation (NSF) Graduate Research Fellowship Program. This material is based upon work supported by the NSF Graduate Research Fellowship Program under grant no. NSF 20-587. Work at Northwestern on the stability of perovskite solar cells was supported by the Office of Naval Research (N00014-20-1-2725). DFT calculations were performed at Institut FOTON as well as Institut des Sciences Chimiques de Rennes, and the work was granted access to the HPC resources of Très Grand Centre de Calcul du CEA (TGCC), the Centre Informatique National de l'Enseignement Supérieur (CINES) and Institut du développement et des ressources en informa-tique scientifique (IDRIS) under allocations 2019-A0060906724 and 2019-A0070907682 made by Grand Équipement National de Calcul Intensif (GENCI). This research used beamline 11-BM (CMS) of the NSLS-II and the Center for Functional Nanomaterials, both of which are U.S. Department of Energy (DOE) Office of Science User Facilities operated for the Department of Energy Office of Science by Brookhaven National Laboratory under contract no. DE-SC0012704. The work at Purdue University was supported by the NSF under grant no. 1724728, CIF21 DIBBs: "EI: Creating a Digital Environment for Enabling Data-Driven Science (DEEDS)," awarded by the Office of Advanced Cyberinfrastructure. This research used resources of the Advanced Photon Source, a U.S. DOE Office of Science user facility operated for the DOE Office of Science by Argonne National Laboratory under contract no. DE-AC02-06CH11357.

A Sharper Picture of Conductive 2-D Metal-Organic Frameworks

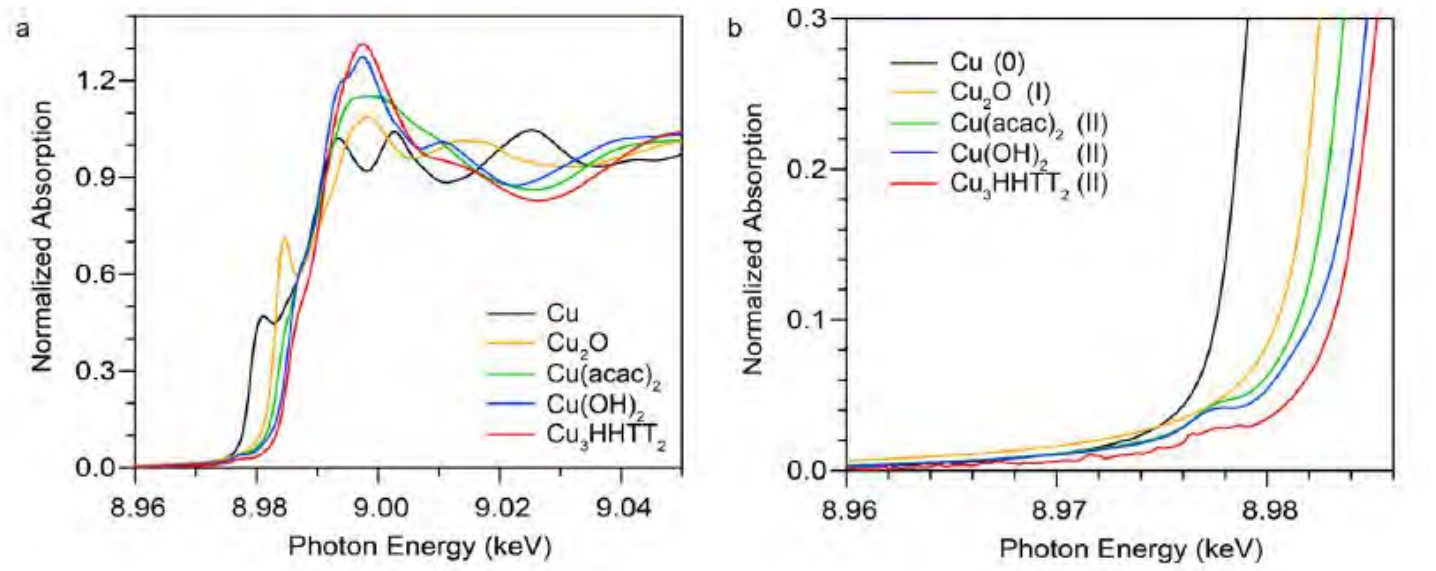

Fig. 1. (a) The x-ray absorption spectra for Cu (black), Cu_2O (orange), $Cu(acac)_2$ (green), $Cu(OH)_2$ (blue), and Cu_3HHTT_2 (red) at the Cu K edge (8.979 keV), with enlarged pre-edge region depicted in (b).

One of the most exciting recent developments in materials science is the discovery that some two-dimensional (2-D) metal-organic framework (MOF) materials, generally considered to be strong electrical insulators, can actually be conducting in certain forms. This opens a whole range of possible applications for MOF materials: for batteries, for fuel cells, for supercapacitors, and for sensors. Such applications would require precise structural information of the materials to allow tailoring of the desired properties but obtaining single crystals of these MOFs for detailed analysis has been a problem. An international team of researchers, with an assist from the high-brightness x-rays produced by the APS, has succeeded in precisely defining single crystals of a group of 2-D π-coordinated MOFs with atomic resolution, also demonstrating a strong correlation between their structure and conductivity. The close correlation between conductivity and sheet packing in MOFs revealed by the precise structural picture made possible in this work raises a host of interesting prospects for the development of new metal-organic framework materials and applications. Armed with a far more detailed understanding of the properties and specific structure of these conductive MOFs, scientists will eventually be able to tailor them for specific purposes, choosing different metal ions, organic ligands, and packing arrangements. The work appeared in Nature Materials.

Getting a clear understanding of the fundamental structure of a material generally means examining its crystalline arrangement through x-ray diffraction and various other means, but the very nature of MOF structure, consisting of cores of metal ions connected to organic ligands to form a hexagonal one, two, or three-dimensional structure, makes growing a single crystal an elusive proposition. Electrically conductive 2-D MOFs form very strong metal-ligand bonds in the a-b or horizontal plane but far weaker π-stacking bonds in the c or vertical direction, with the result that these materials tend to grow in long needle or thread-like formations and single crystals too small to adequately characterize with x-ray diffraction. The research team set out to control this growth behavior to make it easier to grow larger sheets of the material and thereby isolate single crystals.

Realizing that the typical strategies for controlling crystal growth, such as adjusting temperature or reactant concentration and timing, would be ineffective, the experimenters instead chose to alter an organic ligand in the MOFs in a way that would allow larger crystal structures to grow by modifying the nature of the metal-ligand bond to alter in-plane growth while also modifying the π-stacking between the 2-D sheets. They identified a particular ligand, hexahydroxytetraazanaphthotetraphene (HHTT), that features reduced electron density at its metal-binding site, enabling it to form weaker in-plane bonds so that the MOF crystal grows faster and more readily in the *a-b* direction. To alter out-of-plane π-stacking growth and arrangement, the experimenters also combined several different metal molecules with the HHTT ligand including cobalt, nickel, copper, and magnesium.

Using these methods, the investigators were able to grow single crystal MOFs in large enough sizes so that their structure could be studied at the atomic level with various techniques including x-ray absorption spectroscopy (Fig. 1) at the MR-CAT 10-BM beamline and synchrotron powder x-ray diffraction at the XSD Structural Science Group's 11-BM beamline, both at the APS. Further studies, including atomic force microscopy, high-resolution transmission electron microscopy at the Center for Functional Nanomaterials at Brookhaven National Laboratory, x-ray photoelectron spectroscopy and scanning electron microscopy at the Harvard Center for Nanoscale Systems, and single-crystal x-ray diffraction at beamlines BL17B1, BL19U1 of the Shanghai Synchrotron Radiation Facility.

To study the electrical conductivity of the different MOF structures, the research team fabricated a series of samples using the HHTT ligand and each of the four metals. The samples used both "eclipsed" stacking, in which the layers of metal-ligand units are precisely aligned with those above and below to create a highly porous structure, and "staggered" packing, in which the MOF layers out of alignment vertically and eliminating porosity. As expected, the experimenters found that conductivity in-plane tended to be higher than out-of-plane in all the various HHTT-metal forms, but conductivity was much greater both horizontally and vertically in the eclipsed configurations. In particular, the CuHHTT displayed conductivity comparable to the highest yet reported in MOFs, while the eclipsed form of NiHHTT was ten times more conductive than the staggered form. Vertical conductivity in all the samples increased with closer stacking of the layers, whether eclipsed or staggered. – Mark Wolverton

See: Jin-Hu Dou[1], Maxx Q. Arguilla[1], Yi Luo[2,3], Jian Li[2,3], Weizhe Zhang[4], Lei Sun[1], Jenna L. Mancuso[5], Luming Yang[1], Tianyang Chen[1], Lucas R. Parent[6], Grigorii Skorupskii[1], Nicole J. Libretto[7], Chenyue Sun[1], Min Chieh Yang[5], Phat Vinh Dip[8], Edward J. Brignole[8], Jeffrey T. Miller[7], Jing Kong[8], Christopher H. Hendon[5], Junliang Sun[2,3]*, and Mircea Dincă[1]**, "Atomically precise single-crystal structures of electrically conducting 2D metal–organic frameworks," Nat. Mater. **20**, 222 (February 2021). DOI: 10.1038/s41563-020-00847-7

Author affiliations: [1]Massachusetts Institute of Technology, [2]Beijing National Laboratory for Molecular Sciences, [3]Stockholm University, [4]Shanghai Advanced Research Institute, [5]University of Oregon, [6]University of Connecticut, [7]Purdue University, [8]Massachusetts Institute of Technology
Correspondence: * junliang.sun@pku.edu.cn,
** dinca@mit.ed

This work was supported by the Army Research Office (grant number W911NF-17-1-0174). J.S. thanks the National Natural Science Foundation of China (grant number 21527803,21621061) and Ministry of Science and Technology of China (grant number 2016YFA0301004). The Center for Functional Nanomaterials, Brookhaven National Laboratory, is supported by the U.S. Department of Energy (DOE). MR-CAT operations are supported by the U.S. DOE and the MR-CAT member institutions. Part of the characterization and device fabrication was performed at the Harvard Center for Nanoscale Systems, a member of the National Nanotechnology Infrastructure Network, which is supported by the National Science Foundation (NSF) under NSF award no. ECS-0335765. Y.L. thanks the Swedish Research Council and the Knut and Alice Wallenberg Foundation (KAW). This research used resources of the Advanced Photon Source, a U.S. Department of Energy (DOE) Office of Science user facility operated for the DOE Office of Science by Argonne National Laboratory under Contract No. DE-AC02-06CH11357.

Rodolakis of the APS Conveys Excitement of Science Via Argonne STEM Chat

Fanny Rodolakis was a big hit with the Lowell Elementary fifth graders when she spoke to them virtually about science under the auspices of the Argonne National Laboratory STEM Chat program sponsored by Argonne Education and Outreach. Rodolakis, who is a physicist with the Argonne X-ray Science Division Magnetic Materials Group at the U.S. Department of Energy's APS, held a Google Meet with 15 students from the District 200 Wheaton-Warrenville (IL) school. Her chat subjects ranged from the personal to the professional to the scientific as she described herself, her work, how she became a physicist, what light is, what physics is, what kinds of experiments she does, and why that type of research is important.

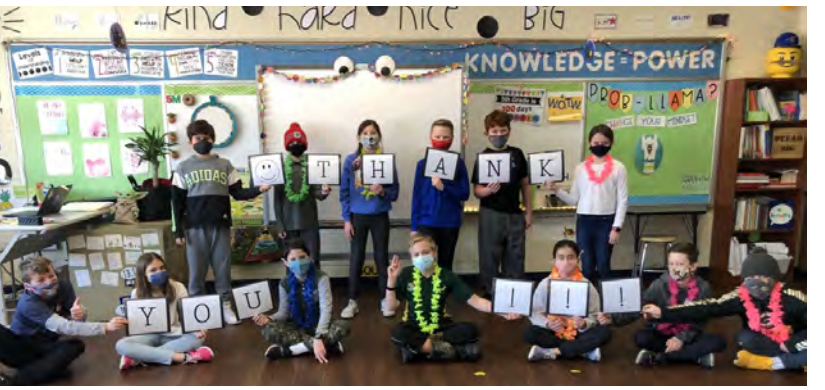

Image: AnneMarie McDonald, District 200 Wheaton-Warrenville (IL)

"The kids were very engaged," Rodolakis said. "They asked a lot of excellent questions." These included:

How small are the samples you measure? ("From a few millimeters [mm]–roughly the size of a sharp pencil point–down to 1/10 of a mm, about the size of a human hair.")

How do you find them if they are so small? ("Good question. I use cameras to locate the sample and sometimes, if they are too small to be seen with a camera, I have to move them around in the x-ray beam; when the x-ray beam touches the sample, a lot of electrons come out, which tells me I am on the sample.")

Do the samples burn when you put the x-ray on them? ("It depends what type of sample; the ones I measure are like rocks, so they are not destroyed by the x-ray beam, but if you were to put some plastics, for example, in the x-ray path, then yes, they will burn.")

What is the coolest thing you have measured? ("Some scientists have measured mummies! I did not participate in this one but I think that is definitely the coolest experiment that was done at the APS!")

"I absolutely love the STEM chats," said Rodolakis, who is co-chair of the APS Diversity, Equity & Inclusion (DEI) Council. "I believe outreach is an essential part of the Argonne DEI effort. Representation is key; the more children get exposed to this kind of thing, the better we can increase diversity in science. Every little girl I can inspire to become a scientist is a step toward improving that diversity. It is going to be a long haul, but definitely worth it. A parent contacted me on LinkedIn to thank me for inspiring his little girl to become a scientist!

"I focus on the youngest grades [K-5] because I believe that if you don't like science by the time you reach middle school, it is often too late; there is no coming back from it. Talking science to a 6-year-old is definitely a challenge, but it is also more impactful. Kids that age are so genuinely curious!

"I literally spent an entire day on my first presentation, trying to find ways to make it accessible and interesting, following the guidance of [Argonne Outreach Coordinator] Brandon Pope who gave us some tips during the STEM Chat training session. I ended up giving my presentation to both of my kids' classes, after which my son Owen told me two of his female friends said they wanted to become a scientist like me (my youngest son Micah was more interested in the presentation from a University of Chicago student who talked about black holes!)"

These STEM chats are free, 30-minute, live virtual Q&A sessions with a STEM professional (either an Argonne staff member or a University of Chicago student). Teachers are instructed to select up to a maximum of two chats/slots from the session list. After selection and confirmation, the Argonne Education office sends a bio of the elected STEM professional(s), so that students can prepare questions ahead of the chat day and time. The STEM professional gives a brief 10-minute presentation, then the remaining 20 minutes are open for Q & A by the students.

"One of the best things STEM chat volunteers say to the students are comments like 'I had no idea this is what I would end up being while I was in high school!,'" said Brandon Pope. "Those statements tell students that it is ok to not have your life figured out while in your teens. Furthermore, as long as they are open to new opportunities, they will have many professional options to choose from."

– Fanny Rodolakis & Richard Fenner

Electronic and Magnetic Materials

Probing Exotic Excitations in a Kitaev Magnet Using RIXS

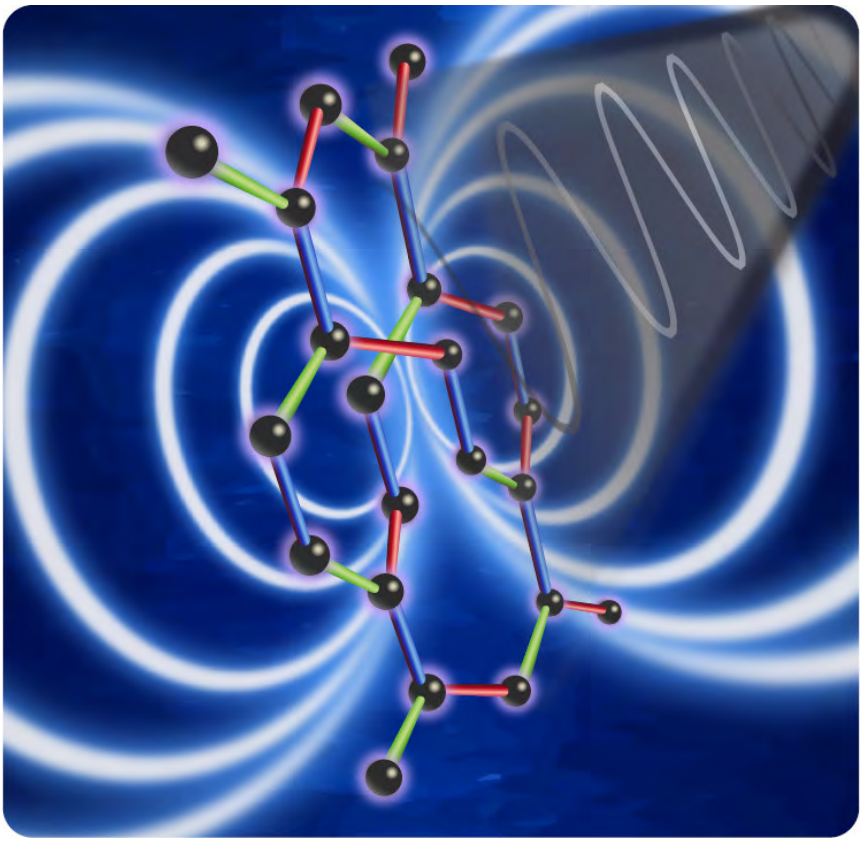

Fig. 1. Illustration of the basic experimental setup. The honeycomb-like structure of the Kitaev magnetic material β-Li_2IrO_3 is depicted, with small black spheres, representing atoms and molecules, joined together via distinct chemical bonds (the red, green, and blue rods). The β-Li_2IrO_3 crystal was irradiated with high-energy x-rays during RIXS experiments at the APS, as indicated by the sinusoidal wave coming from the upper right of the figure. The RIXS experiments detected numerous exotic excitations, most notably magnons and spinons.

The elusive state of matter known as a quantum spin liquid (QSL) is currently the subject of intense research. This special magnetic state arises in materials when the spins of strongly interacting electrons refuse to arrange in orderly patterns, even at very low temperatures, and instead exhibit a variety of ever-shifting, liquid-like arrangements of spins. In this work, scientists looked for the telltale signs of a QSL within crystals of lithium iridate (Li_2IrO_3) by studying the low-energy magnetic excitations emerging from the electron spin interactions. To measure these excitations, the researchers utilized the APS. Their experiments, detailed in the journal *Physical Review B*, revealed two distinct types of excitations. The first were conventional magnons arising from a low-temperature, antiferromagnetic ordering of electron spins. The magnons existed from near-absolute zero up to 38 K. The second type consisted of spinon-like excitations that coexisted with the low-temperature magnons, but then continued to persist up to room temperature. These exotic spinons are expected to show up in the fluctuating quantum-spin state and have been proposed as the basis of quantum computing; they may also shed light into the physics of high-temperature superconductors.

Quantum spin liquids can only form by the frustrated interaction of electron spins in certain magnetic materials. A Kitaev quantum spin liquid is a special subtype of QSL

that arises in a honeycomb-like lattice with a frustrated magnetic exchange between spins. Li_2IrO_3 crystals come in three distinct structures, or polymorphs, identified by the Greek letters a, b, and g (alpha, beta, and gamma). The researchers investigated the beta structure, denoted as β-Li_2IrO_3.

Although β-Li_2IrO_3 can theoretically support a Kitaev quantum spin state, other quantum interactions tend to stabilize antiferromagnetic order at low temperature, obscuring the QSL formation. Nevertheless, clear fingerprints of Kitaev physics have been found in the magnetic excitations of β-Li_2IrO_3 and a few other compounds. Several research teams have probed these compounds using techniques such as highly precise thermal Hall measurements, neutron scattering, and x-ray measurements like resonant inelastic x-ray scattering (RIXS).

Likewise, a quasiparticle can move within a crystal even though it's not a real particle. Whereas magnons are collective excitations of the electrons' spins that show up in most magnetic materials, spinons are very exotic excitations which can be found in a QSL when the spin moves independently from other degrees of freedom of electrons such as charge and orbital.

The researchers in this study performed RIXS experiments at the XSD Inelastic X-ray & Nuclear Resonant Scattering Group's 27-ID x-ray beamline at the APS. They searched for quasiparticles within a highly-pure crystal of β-Li_2IrO_3 (see Fig. 1). Finding the right sorts of quasiparticles might indicate the presence of Kitaev-type processes.

The x-ray data revealed a dichotomy between two types of quasiparticles, namely conventional magnons detected at low temperatures, and spinon-like excitations detected at both low and high temperatures. Additionally, during the x-ray experiments, the β-Li_2IrO_3 sample was subjected to both 0 and large (2 tesla) magnetic fields. The same quasiparticles were detected regardless of magnetic field strength.

The magnons observed in β-Li_2IrO_3 disappeared with the antiferromagnetic order at 38 K. In contrast the spinon-like excitations remained constant up to 100 K before gradually declining with increasing temperature, in agreement with theoretical calculations involving the Kitaev model. In this model the spinons are expected as pairwise excitations of Majorana fermions, which are fermions that act as their own antiparticle. Unequivocal experimental observation of Majorana fermions remains elusive, but recent experiments carried out on various Kitaev QSL candidate materials show promising results.

While stopping well short of declaring detection of the long-sought-after Majorana fermions, the researchers nonetheless contend that their findings provide additional evidence toward confirming their existence. What the researchers did firmly establish is that a "proximate" Kitaev spin state exists in β-Li_2IrO_3, with exotic spinons being present even when the material's electron spins arranged into ordered states at low temperatures. – Philip Koth

See: Alejandro Ruiz[1,2*], Nicholas P. Breznay[3], Mengqun Li[4], Ioannis Rousochatzakis[5], Anthony Allen[1], Isaac Zinda[3], Vikram Nagarajan[6,7], Gilbert Lopez[6,7], Zahirul Islam[8], Mary H. Upton[8], Jungho Kim[8], Ayman H. Said[8], Xian-Rong Huang[8], Thomas Gog[8], Diego Casa[8], Robert J. Birgeneau[6,7], Jake D. Koralek[9], James G. Analytis[6,7], Natalia B. Perkins[4], and Alex Frano[1**], "Magnon-spinon dichotomy in the Kitaev hyperhoneycomb β-Li_2IrO_3," Phys. Rev. B **103**, 184404 (2021). DOI: 10.1103/PhysRevB.103.184404
Author affiliations: [1]University of California, San Diego, [2]Massachusetts Institute of Technology, [3]Harvey Mudd College, [4]University of Minnesota, [5]Loughborough University, [6]University of California, Berkeley, [7]Lawrence Berkeley National Laboratory, [8]Argonne National Laboratory, [9]SLAC National Accelerator Laboratory
Correspondence: * alejandro@ucsd.edu,
** afrano@ucsd.edu

Synthesis was supported by the U.S. Department of Energy (DOE) Early Career program, Office of Science-Basic Energy Sciences (BES), Materials Sciences and Engineering Division, under Contract No. DE-AC02-05CH11231. The work at LBNL is funded by the U.S. DOE Office of Science-BES, Materials Sciences and Engineering Division under Contract No. DEAC02- 05-CH11231 within the Quantum Materials Program (KC2202). Jake Koralek is supported by the U.S. DOE Office of Sciences-BES under Contract No. DE-AC02-76SF00515. Alejandro Ruiz acknowledges support from the University of California President's Postdoctoral Fellowship Program. Natalia B. Perkins and Mengqun Li were supported by the U.S. DOE Office of Science-BES under Award No. DE-SC0018056. N.P.B. and I.Z. acknowledge the support of Harvey Mudd College. A.F. acknowledges support from the Alfred P. Sloan Fellowship in Physics. This research used resources of the Advanced Photon Source, a U.S. DOE Office of Science user facility operated for the DOE Office of Science by Argonne National Laboratory under Contract No. DE-AC02-06CH11357.

Direct Observation of Piezomagnetic Domains in Uranium Dioxide using X-ray Diffraction in a Pulsed Magnetic Field

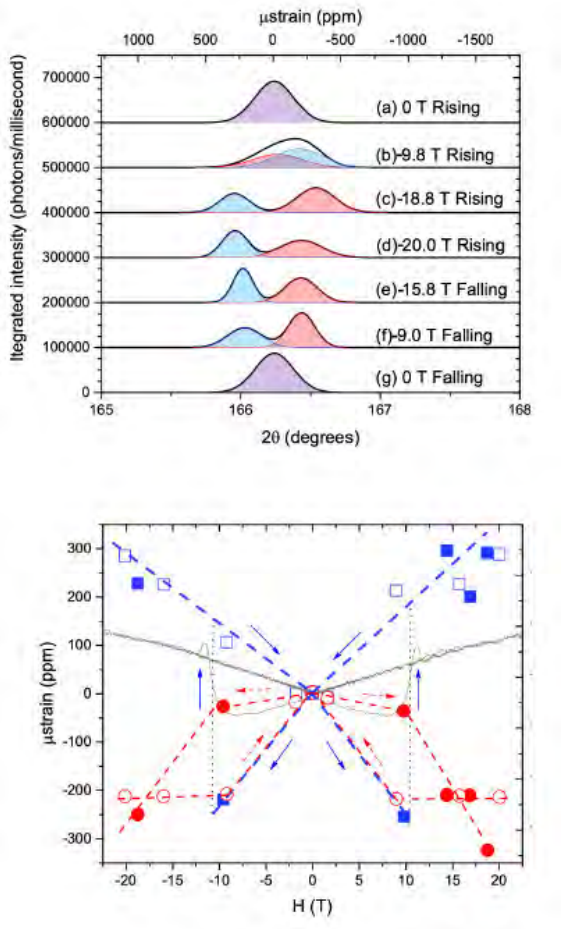

Fig. 1. Top: The integrated intensity vs scattering angle for selected fields and at temperature, T = 25 K. The higher angle peak is initially larger, but then a change in relative intensities and peak position can be seen. Bottom: A plot of the relative strain calculated from the peak positions in the reversed field state at 25 K. The peak corresponding to the dominant strain behavior as determined by the bulk magnetostriction is the blue squares and the secondary peak corresponding to negative strain is the red circles. Open symbols are used for rising fields and closed for falling fields. The blue solid line is guide to the eye. The solid black line is the reversed field measurements using the FBG technique taken in positive and negative fields at 25 K. From D. Antonio et al., "Piezomagnetic switching and complex phase equilibria in uranium dioxide" Commun. Mater. **2**, 17 (2021). DOI: 10.1038/s43246-021-00121-6. ©2020 Springer Nature Limited

Only a few crystalline compounds are known to exhibit the rare phenomenon of piezomagnetism. Squeezing or stretching a piezomagnetic material alters its internal magnetic ordering and creates a magnetic moment. Conversely, exposing the material to a magnetic field causes it to expand or contract. Although previous studies had examined piezomagnetism in uranium dioxide (UO_2) and a few other crystalline materials, none had observed the detailed crystallographic changes that occur during the transition to piezomagnetic behavior. In a first-of-its-kind experiment, scientists have now used x-ray diffraction to directly measure the microscopic distortions in crystalline UO_2 associated with piezomagnetism induced by pulsed magnetic fields. The x-ray diffraction measurements were gathered at the APS. The experimental results provide new information on the complex relationship between piezomagnetism and crystallographic structure, which will aid in clarifying the origins of this obscure phenomenon. It is hoped that these insights will eventually allow scientists to control piezomagnetism in new ways, for instance by applying an electric field to materials with strong piezomagnetic properties. Such control could lead to new types of sensors and other electronic devices. The study was published in *Communications Materials*.

Piezomagnetism is analogous to the better-known phenomenon of piezoelectricity. A piezoelectric material produces electricity when deformed; applying electricity to the material causes it to change shape. Piezoelectric behavior was fully confirmed in the 1880s via experimental and theoretical studies. A broad range of compounds are known piezoelectrics, including quartz, topaz, compounds called ferroelectrics, and even cane sugar. Piezoelectrics are used in a myriad of industrial and consumer applications, from ultrasound machines to solid-state lighters.

Piezomagnetism, in contrast, was only fully confirmed in the 1960s and its widespread application awaits development. The biggest obstacle lies in the uncertainty surrounding its origins. While experiments have shed light on piezomagnetic behavior, no firm theoretical framework explaining its underlying mechanism has been established.

All known piezomagnetic compounds are antiferromagnetic. In an antiferromagnetic material, its molecular-scale magnetic moments, akin to tiny bar magnets, are aligned opposite one another. Uranium dioxide, which is best known as one of the main nuclear fuels in fission reactors, transitions from a paramagnetic to antiferromagnetic state at very low cryogenic temperatures, whereupon it exhibits one of the strongest known magnitudes of piezomagnetism.

To obtain new information about the factors responsible for piezomagnetism in uranium dioxide, the multinational, multi-institution team of researchers employed synchrotron x-rays at the XSD Magnetic Materials Group's 6-ID-C x-ray beamline at the APS to view changes at the unit-cell level of a high quality UO_2 crystal. The powerful x-rays from the APS were complimented by an advanced prototype x-ray detector–a compound-type mixed-mode pixel array detector with a silicon sensor–which together provided a series of highly precise images of the crystal's diffraction peaks, each recorded within a millisecond time frame. Additional structural characterization in zero-field using XRD was carried out on an HPCAT-XSD 16-BM-D beamline.

During x-ray diffraction measurements, the UO_2 crystal was subjected to a pulsed magnetic field. The strength and direction of the field could be altered with half-sine pulses with a rise time of as little as ~3.5 milliseconds. The crystal reacted differently depending on whether the magnetic field direction remained constant or was switched. X-ray diffraction revealed that two magnetic domains coexisted within the UO_2 crystal during exposure to an alternating magnetic field direction. This behavior was not seen when the magnetic field's direction remained fixed.

As the magnetic field grew from zero to maximum strength, the crystalline lattice containing one domain expanded while the other domain's lattice shrank. When the field was suddenly reversed, the domain that had previously expanded began to contract, while the other domain shifted from shrinking to expanding. Plotting the expansion and contraction of the domains in relation to a back-and-forth reversal of magnetic field direction yields a so-called butterfly pattern (see bottom illustration of Fig. 1). The x-ray diffraction setup utilizing back-reflection geometry designed for this study was essential in providing the researchers the first molecular-scale data of dynamic piezomagnetic behavior. Although any observations of magnetic domains were beyond the reach of this scattering study due to pulsed nature of magnetic fields, future availability of high-field DC magnets at user facilities will usher in direct investigations of such domains.

The two observed piezomagnetic domains persisted throughout the experiment. This seems somewhat puzzling as one might suspect that the two domains would irreversibly merge together. The researchers have proposed several mechanisms to explain the observed behavior. For instance, sensitivity of the phenomena to small stresses induced within the crystal, such as from gluing the UO_2 crystal to its substrate, might support the creation and maintenance of the domains. Also, electric multipoles that can arise in uranium dioxide may also have contributed to the observed complex piezomagnetic behavior. This later possibility suggests that piezomagnetism in some materials might be controlled through applied electric fields. – Philip Koth

See: Daniel J. Antonio[1], Joel T. Weiss[2], Katherine S. Shanks[2], Jacob P. C. Ruff[2], Marcelo Jaime[3‡‡], Andres Saul[4], Thomas Swinburne[4], Myron Salamon[3], Keshav Shrestha[1‡], Barbara Lavina[5], Daniel Koury[5], Sol M. Gruner[2], David A. Andersson[6], Christopher R. Stanek[6], Tomaz Durakiewicz[1], James L. Smith[6], Zahir Islam[7]*, and Krzysztof Gofryk[1]**, "Piezomagnetic switching and complex phase equilibria in uranium dioxide" Commun. Mater. **2**, 17 (2021). DOI: 10.1038/s43246-021-00121-6

Author affiliations: [1]Idaho National Laboratory, [2]Cornell University, [3]National High Magnetic Field Laboratory, [4]Aix-Marseille University, [5]University of Nevada, [6]Los Alamos National Laboratory, [7]Argonne National Laboratory Present address: ‡West Texas A&M University, ‡‡National Metrology Institute

Correspondence: ** gofryk@inl.gov, * zahir@anl.gov

Work by D.A., K.S., and K.G. was supported by the U.S. Department of Energy (DOE) Early Career Research Program under the project "Actinide materials under extreme conditions." The high-field pulsed magnet and a choke coil were installed at the APS through a partnership with the International Collaboration Center at the Institute for Materials Research (ICC-IMR) and Global Institute for Materials Research Tohoku (GIMRT) at Tohoku University. Detector research in S.G's laboratory is supported by DOE grant DE-SC0017631. J.P.C.R.'s research at CHESS/CHEXS was supported by the National Science Foundation under awards DMR-1332208 and DMR-1829070. This research used resources of the Advanced Photon Source, a U.S. DOE Office of Science user facility operated for the DOE Office of Science by Argonne National Laboratory under Contract No. DE-AC02-06CH11357.

Dynamic Ferroelectric Domain Tilting Opens a New Window to Domain Wall Charging

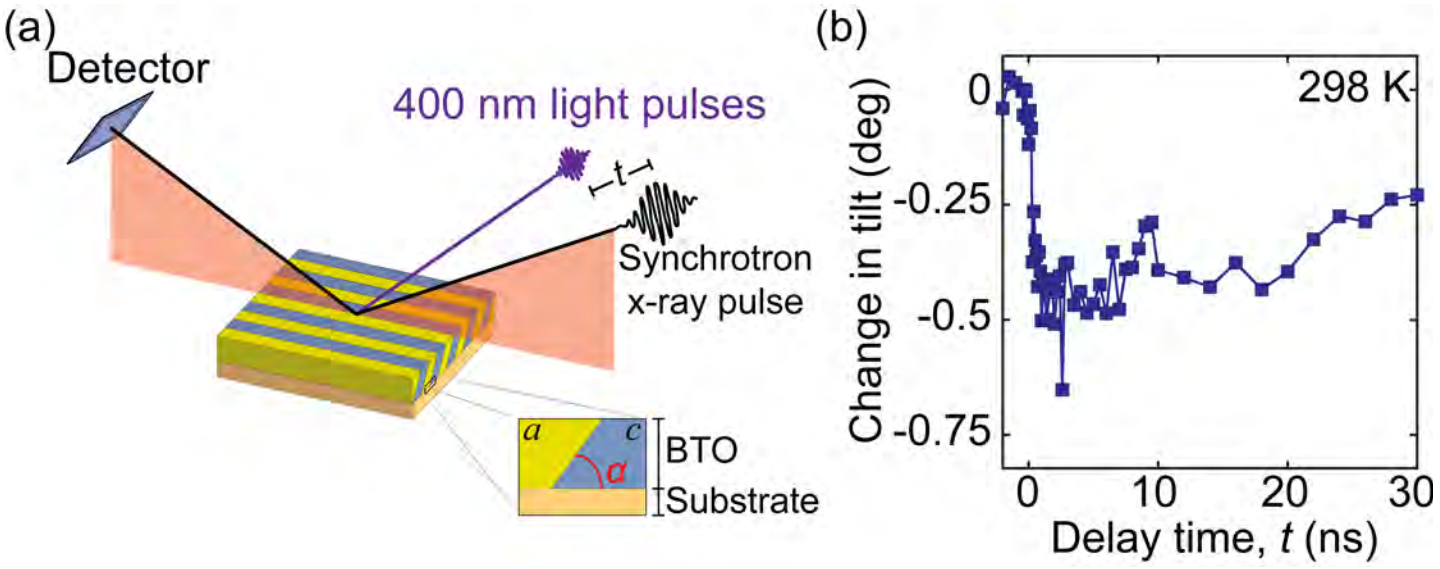

Fig. 1 (a) Time-resolved synchrotron x-ray diffraction experiments on a BTO thin film with the *a/c* domain pattern. Femtosecond 400-nanometer light pulses were used to excite the BTO film probed by synchrotron x-ray pulses. Delay times, *t*, between pump and probe pulses were electronically shifted. Domain wall tilt orientation, *α*, is the angle between the plane of domain walls and the film/substrate interface. (b) Change in tilt orientation of the a/c domain wall as a function of delay time, *t*, at 298 K. Negative changes indicate that the domain walls tilt toward the film/substrate interface.

Ferroelectric domains were considered well understood until about 10 years ago when new analytical capabilities began revealing their true complexity. There is now evidence that nanoscale-thickness regions near ferroelectric domain walls possess dramatically different properties than the domains themselves in both bulk and thin-film ferroelectrics. These discoveries have demonstrated the importance of probing the physical properties of nanoscale volumes near domain walls to learn how they evolve with domain configuration and in response to external stimuli. Recently an international team of researchers used the APS to investigate both areas. They showed that the coexistence of two different types of domain patterns in a barium titanate ($BaTiO_3$) (BTO) thin film can create a delicate balance of elastic forces. Their results were published in *Physical Review Letters*.

The balance is easily perturbed, making it possible to produce large effects with relatively modest excitations. The team found that instantaneous changes in domain wall tilt orientation occur in a BTO film that is optically excited by 50-femtosecond-duration, 400-nanometers light pulses generated by an ultrafast laser source. Time-resolved synchrotron x-ray diffraction experiments at the XSD Time Resolved Research Group's 7-ID beamline of the APS used the configuration shown in Fig. 1(a). The experiment showed that the resultant changes in tilt orientation emerged over a period of about a nanosecond and then relaxed over several more nanoseconds, an interval similar to the time constant for the recombination of photoexcited charge carriers. The tilting and recovery are shown in Fig. 1(b). The effect clearly depended on the balance of two competing domain configurations. The tilt

variations did not change when the relative abundance of the two domain patterns was varied by adjusting the temperature and ceased when only one of the patterns remained in the film.

In the lower end of the temperature range probed in these experiments, the BTO layer essentially consisted of: (i) a domain configuration with alternating orthogonal domains of in-plane and out-of-plane polarization (the *a/c* pattern, as in Fig. 1(a)) and (ii) stripes of orthogonal in-plane polarization (*a/b* pattern). Temperature-dependent x-ray diffraction measurements conducted at the European Synchrotron Radiation Facility indicated that the *a/c* and *a/b* phases coexisted at 298 K, with the majority of the volume of the BTO film being in the *a/b* phase. The configuration was quite different at higher temperatures. At 343 K, all of the domains were in the better ordered a/c phase.

In modeling the optically induced tilting phenomenon, the researchers determined that the orientation of domain walls depends on multiple contributions to the free energy, including the contribution from the density of bound charges. Changes in the electrostatic contribution to the free energy can occur through screening of the bound charges by mobile charges, such as photoexcited electron-hole pairs that had come under the influence of the large electrical potential step at the domain walls. This change in the screening ultimately led to the variation of the domain wall orientation.

When no other phases are present, the head-to-tail orientation of the polarization in the *a/c* pattern ensures that there is no net bound charge at the domain walls. Bound charges are possible only when multiple domain configurations coexist. Phase coexistence at 298 K leads to an increased domain-wall charge density, and thus to a larger screening effect by optically excited charge carriers than in the single-phase regime.

The domain-wall tilting uniquely occurs in domain configurations in which there is elastic heterogeneity near domain walls due to a coexistence of different domain patterns. The mechanism relating domain tilting changes to domain-wall charging allows the tilting and other domain distortion effects to be used to probe the existence of domain-wall charge. The structural heterogeneity in complex domain patterns is, further, a route toward the discovery of unusual responses to external perturbations.

– Vic Comello

See: Youngjun Ahn[1], Arnoud S. Everhardt[2], Hyeon Jun Lee[1], Joonkyu Park[1], Anastasios Pateras[1], Silvia Damerio[2], Tao Zhou[3], Anthony D. DiChiara[4], Haidan Wen[4], Beatriz Noheda[2], and Paul G. Evans[1]*, "Dynamic Tilting of Ferroelectric Domain Walls Caused by Optically Induced Electronic Screening," Phys. Rev. Lett. **127**, 097402 (2021). DOI: 10.1103/PhysRevLett.127.097402
Author affiliations: [1]University of Wisconsin-Madison, [2]University of Groningen, [3]European Synchrotron Radiation Facility, [4]Argonne National Laboratory
Correspondence: * pgevans@wisc.edu

This work was supported by the U.S. National Science Foundation (NSF) through Grant No. DMR-1609545. A.S.E., S.D., and B.N. acknowledge financial support from the alumni organization of the University of Groningen, De Aduarderking (Ubbo Emmius Fonds). H.W. acknowledges the support of U.S. Department of Energy (DOE) Office of Science-Basic Energy Sciences, Materials Sciences and Engineering Division, for instrumentation development of time-resolved x-ray microdiffraction. The researchers gratefully acknowledge use of facilities and instrumentation supported by the NSF through the University of Wisconsin Materials Research Science and Engineering Center, Grant No. DMR-1720415. This research used resources of the Advanced Photon Source, a DOE Office of Science user facility operated for the DOE Office of Science by Argonne National Laboratory under Contract No. DE-AC02-06CH11357.

Under Pressure, Quantum Secrets Emerge

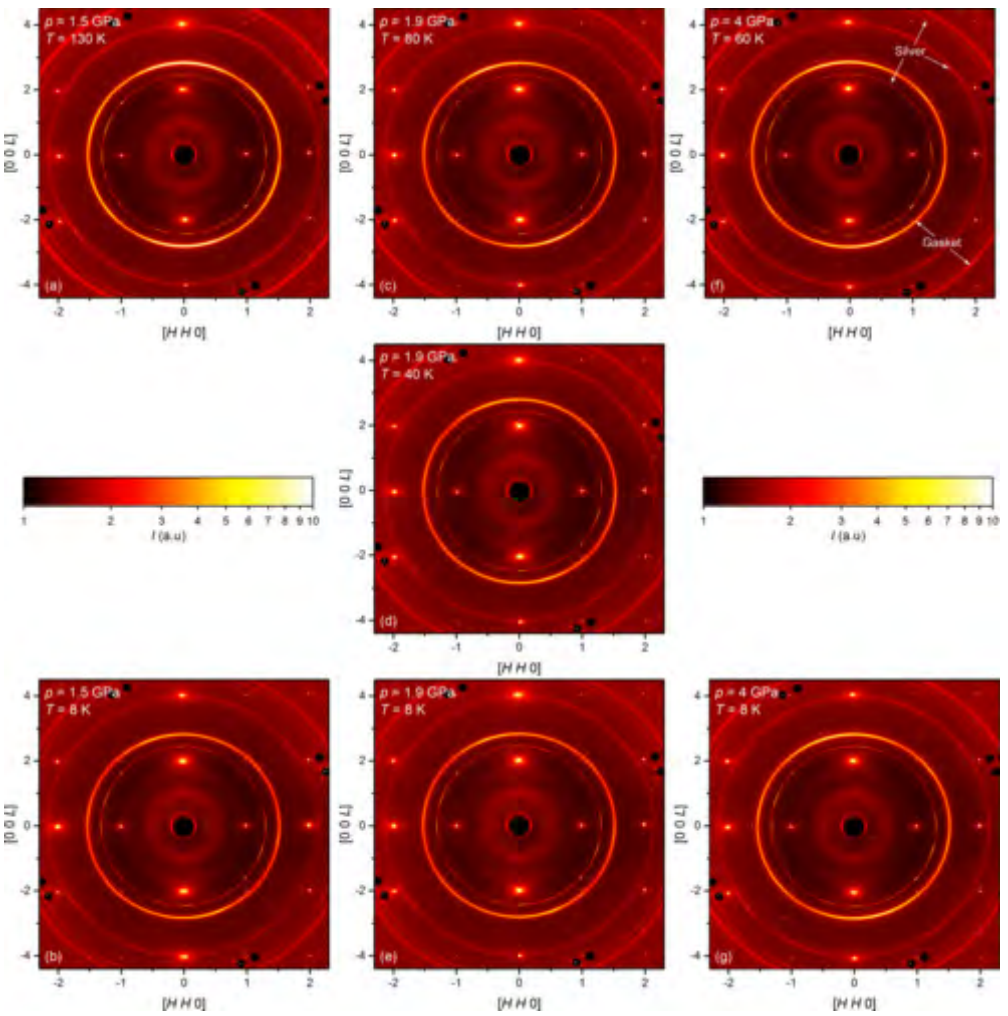

Fig. 1. High-energy x-ray diffraction data on a $LaCrGe_3$ single crystal measured at different temperatures and pressures. Image plots of the (H H L) plane are shown in each panel with intensities color coded to a log plot as indicated in the color bars. The large, noncentral, black circles are from masking the Bragg peaks from the diamond anvils in the DAC, whereas the polycrystalline rings are from the silver foil and the stainless-steel gasket, as exemplarily indicated by the white arrows in the top right panel. From E. Gati et al., Phys. Rev. B **103**, 075111 (2021). ©2021 American Physical Society

Some materials can show interesting new properties under the right conditions, such as at high pressures and ultracold temperatures when the effects of quantum mechanics start to take over from classical physics. For instance, near absolute zero, many metals become superconducting, allowing current to flow unimpeded. If scientists can understand the quantum behavior, they might be able to harness its power, for instance by creating superconductors that operate closer to room temperature and could provide lossless electrical transmission. Researchers are using the APS to help them identify exotic behavior resulting from quantum effects. Their latest results were published in *Physical Review B*.

The researchers in this study, from the U.S. Department of Energy's Ames Laboratory and Oak Ridge National Laboratory, from Iowa State University, and from the Paul Scherrer Institute (Switzerland) studied the ferromagnetic metal lanthanum chromium germanium ($LaCrGe_3$) at

low temperatures and high pressures. Based on their thermodynamic data, they created a temperature-pressure phase diagram delineating the stability region of various phases, such as ferromagnetism and paramagnetism. As they increased pressure, they found that the ferromagnetic-paramagnetic transition temperature was suppressed to lower temperatures. As quantum effects started to take over, $LaCrGe_3$ did not show a direct transition from ferromagnetism to paramagnetism. Instead, a new state of quantum matter appeared.

The main result of the research was that this new quantum state consists of clusters of short-range ferromagnetic order at high pressures in the phase diagram. Short-range order refers to clusters of a few nanometers in size in which the magnetic spins are aligned, but different clusters are not aligned with each other.

Existing theory and earlier experiments on the same compound suggested that the material would have long-range antiferromagnetic order at high pressures. However, the formation of ferromagnetic clusters suggests this is not the case.

To understand the structure of their material, the researchers performed x-ray diffraction measurements under pressure on single crystals at the XSD Magnetic Materials Group's beamline 6-ID-D at the APS, and on powder at the HPCAT-XSD beamline 16-BM-D at the APS. They used diamond anvil cells (DACs) to pressurize the samples, with steel gaskets and helium gas as a pressure-transmitting medium. The single-crystal and powder measurements provided complementary data that allowed the researchers to check whether changes in pressure and temperature led to any modification in the material's crystalline structure that could cause changes in its magnetic properties (Fig. 1). Ruling that out reassured them that it was indeed quantum effects that were behind the phase transitions.

They also performed neutron diffraction measurements on the single crystals using the HB1 diffractometer at the High Flux Isotope Reactor at Oak Ridge National Laboratory and muon-spin resonance (μSR) measurements at the Paul Scherrer Institute. Whereas the APS was used to study crystallographic structure, the μSR and neutron diffraction data provided information about the magnetic structure of the material. As a result, the μSR and neutron studies provided the researchers with an estimation of the size of the short-range clusters.

This is just one of several materials systems that the researchers are examining to understand phase transitions and how quantum effects give rise to various phenomena, beyond just superconductivity. The measurements help condensed matter physicists to refine their theoretical models, which in turn points experimentalists to new areas to explore. The hope is to gather enough data to determine which key features are needed in a model to explain observed quantum behavior in materials and to eventually predict novel, unconventional quantum phenomena. – Neil Savage

See: Elena Gati[1,2]*, John M. Wilde[1,2], Rustem Khasanov[3], Li Xiang[1,2], Sachith Dissanayake[4], Ritu Gupta[3], Masaaki Matsuda[4], Feng Ye[4], Bianca Haberl[4], Udhara Kaluarachchi[1,2], Robert J. McQueeney[1,2], Andreas Kreyssig[1,2], Sergey L. Bud'ko[1,2], and Paul C. Canfield[1,2], "Formation of short-range magnetic order and avoided ferromagnetic quantum criticality in pressurized $LaCrGe_3$," Phys. Rev. B **103**, 075111 (2021). DOI: 10.1103/PhysRevB.103.075111
Author affiliations: [1]Ames Laboratory, [2]Iowa State University, [3]Paul Scherrer Institute, [4]Oak Ridge National Laboratory
Correspondence: * egati@iastate.edu

Work at the Ames Laboratory was supported by the U.S. Department of Energy (DOE) Office of Science-Basic Energy Sciences, Materials Sciences and Engineering Division. The Ames Laboratory is operated for the U.S. DOE by Iowa State University under Contract No. DEAC02-07CH11358. E.G. and L.X. were funded, in part, by the Gordon and Betty Moore Foundation's EPiQS Initiative through Grant No. GBMF4411. In addition, L.X. was funded, in part, by the W. M. Keck Foundation. A portion of this research used resources at the High Flux Isotope Reactor and the Spallation Neutron Source, U.S. DOE Office of Science User Facilities, operated by the Oak Ridge National Laboratory. HPCAT-XSD operations are supported by DOE-National Nuclear Security Administration under Grant No. DE-NA0001974, with partial instrumentation funding by the National Science Foundation (NSF). Use of the COMPRES-GSECARS gas loading system was supported by COMPRES under NSF Cooperative Agreement Grant No. EAR-11-57758 and by GeoSoilEnviroCARS through NSF Grant No. EAR-1128799 and DOE Grant No. DE-FG02-94ER14466. Research of R.G. is supported by the Swiss National Science Foundation (SNF-Grant No. 200021-175935). This research used resources of the Advanced Photon Source, a U.S. DOE Office of Science user facility operated for the U.S. DOE Office of Science by Argonne National Laboratory under Contract No. DE-ac02-06CH11357.

Induced Flaws in Quantum Materials Could Enhance Superconducting Properties

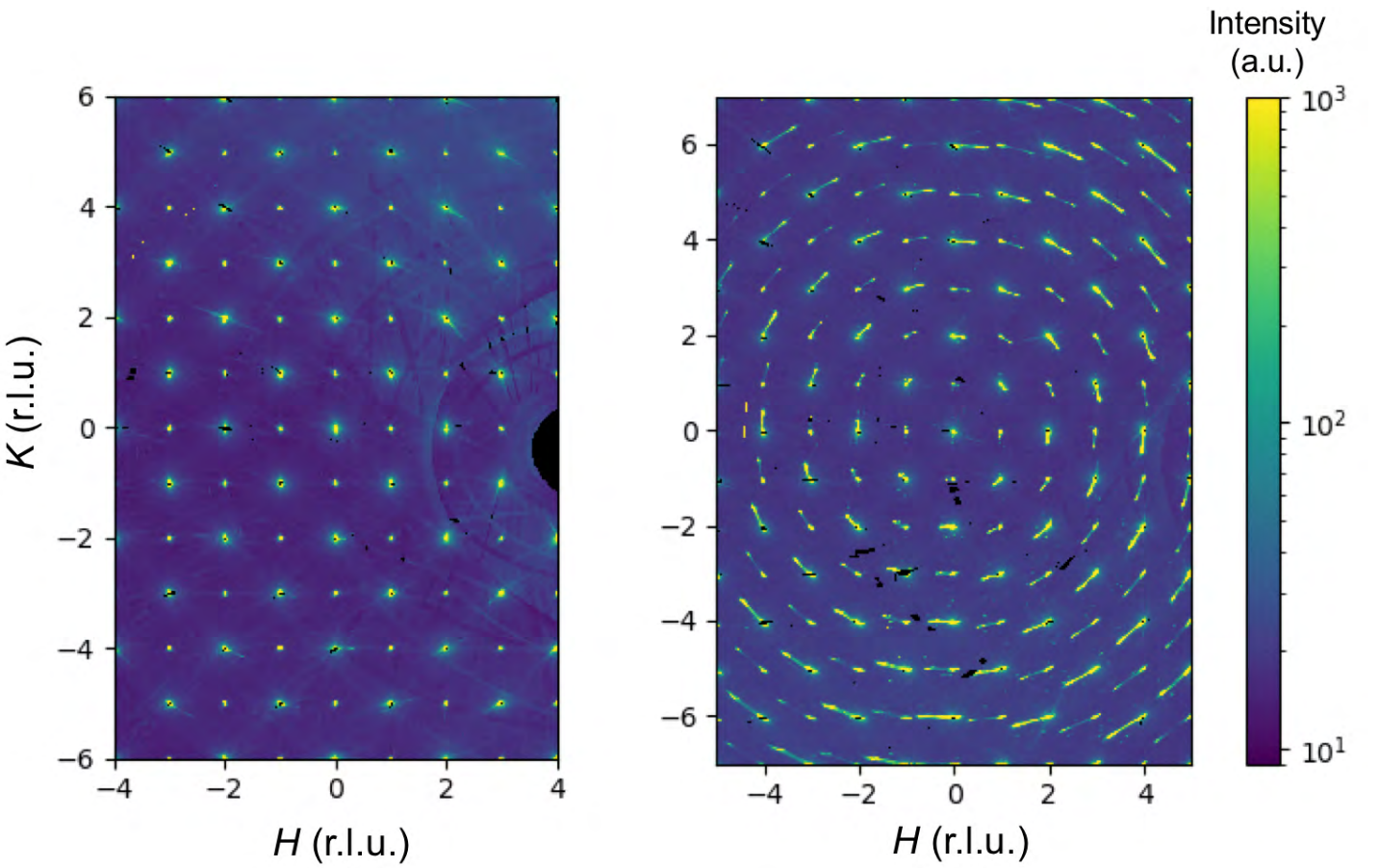

Fig. 1. Diffuse x-ray scattering in deformed strontium titanate.

The original University of Minnesota news brief can be read here.

In a surprising discovery, an international team of researchers, led by scientists in the University of Minnesota Center for Quantum Materials using two U.S. Department of Energy (DOE) national user facilities including the APS, found that deformations in quantum materials that cause imperfections in the crystal structure can actually improve the material's superconducting and electrical properties. The groundbreaking findings could provide new insight for developing the next generation of quantum-based computing and electronic devices. The research was published in *Nature Materials*.

"Quantum materials have unusual magnetic and electrical properties that, if understood and controlled, could revolutionize virtually every aspect of society and enable highly energy-efficient electrical systems and faster, more accurate electronic devices," said study co-author Martin Greven, a Distinguished McKnight Professor in the University of Minnesota's School of Physics and Astronomy and the Director of the Center for Quantum Materials. "The ability to tune and modify the properties of quantum materials is pivotal to advances in both fundamental research and modern technology."

Elastic deformation of materials occurs when the material is subjected to stress but returns to its original shape once the stress is removed. In contrast, plastic deforma-

tion is the non-reversible change of a material's shape in response to an applied stress—or, more simply, the act of squeezing or stretching it until it loses its shape. Plastic deformation has been used by blacksmiths and engineers for thousands of years. An example of a material with a large plastic deformation range is wet chewing gum, which can be stretched to dozens of times its original length.

While elastic deformation has been extensively used to study and manipulate quantum materials, the effects of plastic deformation have not yet been explored. In fact, conventional wisdom would lead scientists to believe that "squeezing" or "stretching" quantum materials may remove their most intriguing properties.

In this pioneering new study, the researchers used plastic deformation to create extended periodic defect structures in a prominent quantum material known as strontium titanate ($SrTiO_3$). The defect structures induced changes in the electrical properties and boosted superconductivity.

"We were quite surprised with the results" Greven said. "We went into this thinking that our techniques would really mess up the material. We would have never guessed that these imperfections would actually improve the materials' superconducting properties, which means that, at low enough temperatures, it could carry electricity without any energy waste."

Greven said this study demonstrates the great promise of plastic deformation as a tool to manipulate and create new quantum materials. It can lead to novel electronic properties, including materials with high potential for applications in technology, he said.

Greven also said the new study highlights the power of state-of-the-art neutron and x-ray scattering probes in deciphering the complex structures of quantum materials and of a scientific approach that combines experiment and theory. Diffuse neutron scattering experiments were performed on the CORELLI spectrometer of the DOE's Spallation Neutron Source at Oak Ridge National Laboratory. Diffuse x-ray scattering experiments (Fig. 1) were carried out on the XSD Magnetic Materials Group's beamline 6-ID-D at the APS.

"Scientists can now use these techniques and tools to study thousands of other materials," Greven said. "I expect that we will discover all kinds of new phenomena along the way."

See: S. Hameed[1], D. Pelc[1,2*], Z. W. Anderson[1], A. Klein[3], R. J. Spieker[1], L. Yue[4], B. Das[1], J. Ramberger[1], M. Lukas[2], Y. Liu[5], M. J. Krogstad[6], R. Osborn[6], Y. Li[4], C. Leighton[1], R. M. Fernandes[1] , and M. Greven[1**], "Enhanced superconductivity and ferroelectric quantum criticality in plastically deformed strontium titanate," Nat. Mater. **21**, 54 (04 October 2021). DOI: 10.1038/s41563-021-01102-3
Author affiliations: [1]University of Minnesota, [2]University of Zagreb, [3]Ariel University, [4]Peking University, [5]Oak Ridge National Laboratory, [6]Argonne National Laboratory
Correspondence: * dpelc@phy.hr, ** greven@umn.edu

We thank D. Robinson and S. Rosenkranz for assistance with x-ray scattering experiments at the APS. The work at the University of Minnesota was funded by the U.S. Department of Energy (DOE) through the University of Minnesota Center for Quantum Materials, under grant number DE-SC-0016371. The work at Argonne was supported by the U.S. DOE Office of Science-Basic Energy Sciences, Materials Sciences and Engineering Division. A portion of this research used resources at the Spallation Neutron Source, a U.S. DOE Office of Science user facility operated by the Oak Ridge National Laboratory. D.P. acknowledges support from the Croatian Science Foundation through grant number UIP-2020-02-9494. The work at Peking University was funded by the National Natural Science Foundation of China, under grant number 11874069. Sputtering and contacting of samples was conducted in the Minnesota Nano Center, which is supported by the National Science Foundation through the National Nano Coordinated Infrastructure Network, award number NNCI-1542202. This research used resources of the Advanced Photon Source, a U.S. DOE Office of Science user facility operated for the DOE Office of Science by Argonne National Laboratory under Contract No. DE-AC02-06CH11357.

APS Research on COVID-19 Drug and Superionic Ice are Spotlighted by DOE

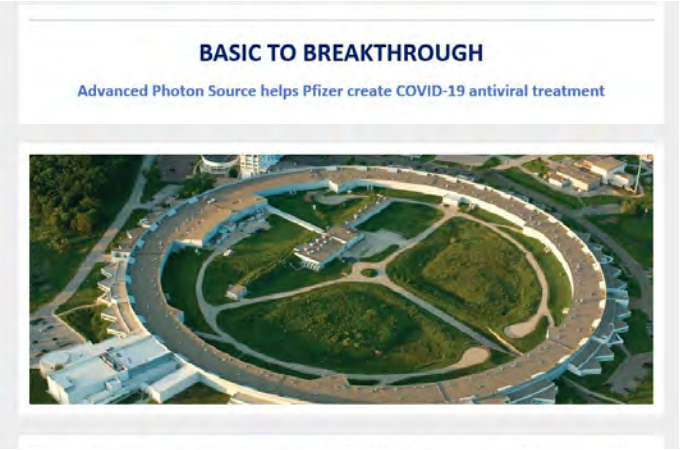

A new drug candidate, Paxlovid, which has proven to be effective against the SARS-CoV-2 virus, and a superionic ice that is neither liquid nor solid, both based on research at the APS, are featured in the November 15, 2021 issue of the U. S. Department of Energy (DOE) "Communique" e-newsletter.

Stephen Streiffer, then Argonne Deputy Laboratory Director for Science & Technology and Interim Associate Laboratory Director for Photon Sciences, called this "great recognition for our users and for the APS!"

The "Communique" Basic Breakthrough section reports that the "Advanced Photon Source helps Pfizer create COVID-19 antiviral treatment. Pharmaceutical company Pfizer has announced the results of clinical trials of its new oral antiviral treatment against COVID-19. The new drug candidate, Paxlovid, proved to be effective against the SARS-CoV-2 virus, which causes COVID-19, according to results released by Pfizer on November 5. The antiviral drug has the potential to eliminate up to nine out of ten hospitalizations caused by the virus. Scientists at Pfizer created Paxlovid with the help of the ultrabright x-rays of the APS. The National Virtual Biotechnology Consortium helped make the APS available for COVID-19 research. The scientists used the facility to determine the atomic structure of the antiviral candidate." This breakthrough research was carried out at the Industrial Macromolecular Crystallography Association Collaborative Access Team (IMCA-CAT) beamline at the APS, operated by the Hauptman-Woodward Medical Research Institute on behalf of a collaboration of pharmaceutical companies, of which Pfizer is a member.

Under the heading "In the News," Strange, dark, and hot ice could explain Uranus and Neptune's wonky magnetic fields links to the Popular Science article about a layer of "hot," electrically conductive ice that could be responsible for generating the magnetic fields of ice giant planets like Uranus and Neptune. This work from the Carnegie Institute for Science and the University of Chicago Center for Advanced Radiation Sources researchers was carried out at the GSECARS 13-ID x-ray beamline at the APS. The study, published in *Nature Physics*, reveals the conditions under which two such superionic ices form. More on this subject can be found on the APS web site, the Carnegie Institute for Science web site, and the University of Chicago web site.

A Mummy's Secrets

In an interview by Karen Thomas with the International Society for Optics and Photonics (SPIE), APS user Stuart Stock (above) from Northwestern University (NU) discussed how x-ray diffraction reveals details of mummified remains.

In 2018, NU's Block Museum of Art held an exhibit titled "Paint the Eyes Softer: Mummy Portraits from Roman Egypt." The centerpiece of the exhibit was the "Hawara Portrait Mummy Four"—a mummified child buried with a luminous painted portrait. Stock used position-resolved x-ray diffraction at the APS with "a very narrow beam of x-rays, smaller than the diameter of a hair-one scans the beam across the sample and observes the resulting diffraction patterns" to characterize an object superimposed on the mummy's abdomen as possibly a scarab, a sacred symbol of rebirth in the ancient Egyptian, made of culture calcite. Read the entire interview here. Excerpt © 2021 SPIE

Soft Materials and Liquids

Kitaev Quantum Spin Liquid Revealed by Phonons

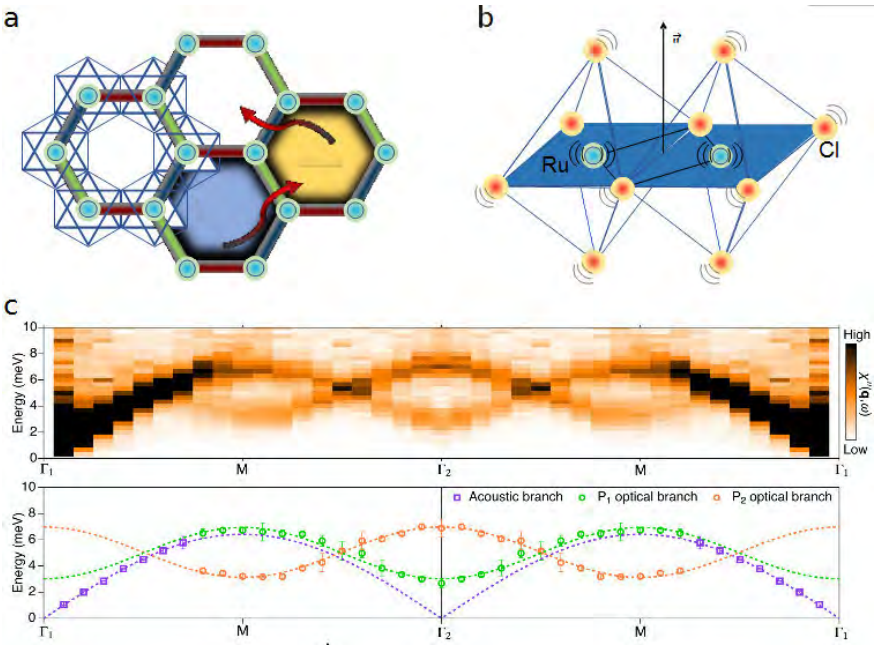

Fig. 1. Panel (a) depicts the honeycomb-like lattice of crystalline $RuCl_3$. The chemical bonds highlighted in red, green, and blue represent three perpendicular interactions that occur in a Kitaev quantum spin liquid. In the Kitaev QSL, quantum excitations are quasiparticles composed of Majorana fermions (red arrows) and magnetic flux modes (blue and yellow hexagons). Schematic in (b) shows the nearly 90° bonds between the ruthenium atoms (blue) and chlorine atoms (yellow), which supports a magnetic interaction perpendicular to the blue-green plane. Lattice vibrations (indicated by circular arcs near each atom) modify the magnetic interactions, inducing a coupling between phonons and quasiparticles. Top of panel (c) shows phonon excitations derived by x-ray measurements. The extracted phonon peak positions appear at bottom, revealing both optical and acoustic phonons. From H. Li et al., Nat. Commun. **12**, 3513 (2021). © 2021 Springer Nature Limited

An international research team has demonstrated a new technique for detecting exotic quantum states in crystalline materials. The researchers used the quantum-mechanical equivalent of sound waves to confirm that a phase of matter known as a quantum spin liquid was present in a crystal of ruthenium trichloride ($RuCl_3$) chilled to cryogenic temperatures. A quantum spin liquid, or QSL, is a special kind of magnetic state that can only occur in particular types of materials. By observing changes in the quantum sound waves (phonons) traveling within a tiny sample of $RuCl_3$, the scientists were able to identify two distinct quantum excitations characteristic of a QSL. The phonons were detected and measured during inelastic x-ray scattering (IXS) experiments carried out using the APS. The experimental results, published in the journal *Nature Communications*, confirm that $RuCl_3$ can host a QSL, which was suspected based on previous investigations and theoretical considerations. More importantly, demonstrating that phonons can be used to identify quantum spin liquids and other quantum states provides scientists a powerful new tool for probing a wide variety of promising materials for these exotic phenomena. Future research into QSLs may lead to advances in quantum materials and quantum computing.

A quantum spin liquid arises when the spins of the electrons in certain compounds enter a fluctuating magnetic arrangement. This arrangement is quite different than those of typical magnetic systems. For example, in a ferromagnetic material such as iron the spins of its electrons tend to align in the same direction within a magnetic field. By contrast, a QSL exhibits a frustrated spin state. This state consists of continuous fluctuations of the material's electron spins. This absence of ordinary spin/magnetic order is reminiscent of the molecules in liquid, hence the reference to “liquid” in “quantum spin liquid.”

Although scientists are confident that quantum spin

liquids can exist in a variety of compounds, confirming their presence has proven rather difficult. In previous scientific studies, magnetic measurements and neutron diffraction experiments have met with limited success in confirming the QSL state. In this study a new approach using phonons was used for the first time to spot a QSL.

Theoretical models indicate that certain quantum quasiparticles and excitations will arise within a QSL. Although not actual particles, quasiparticles sometimes behave like particles. For instance, a semiconductor "doped" with an impurity can produce an electron hole, which is a region lacking one or more electrons. Like an electron, the positively-charged hole can move around and form an electrical current. Though not a real particle, the hole behaves like one. Because of this particle-like behavior, the electron hole is considered a quasiparticle.

Majorana fermions are quasiparticles that appear in quantum spin liquids. Majorana fermions follow the same quantum rules that govern the ubiquitous fermions that compose ordinary matter, such as protons and electrons. In addition to Majorana fermions, so-called gauge flux modes can also arise in a QSL. A gauge flux mode is a kind of magnetic quasiparticle. Theorists have proposed that both types of quasiparticles can couple (interact) with phonons. This interaction can significantly alter the phonons, and these changes can be measured to confirm the presence and strength of the quasiparticles.

The researchers looked for the fingerprints of the quantum spin liquid state in ruthenium trichloride by looking for changes in its phonons. These phonons were detected and their intensity measured via inelastic x-ray scattering (IXS) performed on single crystals of $RuCl_3$ using the HERIX spectrometer at the XSD Inelastic X-ray & Nuclear Scattering Group's 30-ID x-ray beamline. The lattice of the $RuCl_3$ crystals formed a honeycomb-like structure, as depicted in Fig. 1(a). This honeycomb structure is very important because it supports a special type of QSL, called a Kitaev quantum spin liquid.

The $RuCl_3$ crystals were subjected to a range of cryogenic temperatures during the x-ray scattering experiments. The x-rays detected distinct phonons within the crystals (Fig. 1c). At certain temperatures abrupt changes in the phonon spectral intensity and phonon energy were observed, indicating the presence of Majorana fermions and gauge flux modes. The detection of these quasiparticles in the $RuCl_3$ samples unequivocally demonstrated the presence of a Kitaev quantum spin liquid.

The experimental results show that phonons can be used to detect and characterize quantum spin liquids, including Kitaev QSLs. The researchers note that the phonon coupling method might prove especially helpful for detecting QSLs in iridium-based compounds, which are resistant to neutron diffraction. – Philip Koth

See: Haoxiang Li[1], T. T. Zhang[2], A. Said[3], G. Fabbris[3], D.G. Mazzone[4,5], J.Q. Yan[1], D. Mandrus[1,6], Gábor B. Halász[1], S. Okamoto1, S. Murakami[2], M.P.M. Dean[4], H.N. Lee[1], and H. Miao[1*], "Giant phonon anomalies in the proximate Kitaev quantum spin liquid α-RuCl3," Nat. Commun. **2**, 3513 (2021). DOI: 10.1038/s41467-021-23826-1
Author affiliations: [1]Oak Ridge National Laboratory, [2]Tokyo Institute of Technology, [3]Argonne National Laboratory, [4]Brookhaven National Laboratory, [5]Paul Scherrer Institut, [6]University of Tennessee at Knoxville
Correspondence: * miaoh@ornl.gov

This research at Oak Ridge National Laboratory (ORNL) was sponsored by the U.S. Department of Energy (DOE) Office of Science-Basic Energy Sciences, Materials Sciences and Engineering Division (IXS data analysis, material synthesis, and data interpretation) and by the Laboratory Directed Research and Development Program of ORNL, managed by UT-Battelle, LLC, for the U.S. DOE (IXS experiment). Part of IXS data interpretation work at Brookhaven National Laboratory was supported by the U.S. DOE Office of Science-Basic Energy Sciences, Materials Sciences, and Engineering Division under Contract No. DE-SC0012704. Extraordinary facility operations were supported, in part, by the DOE Office of Science through the National Virtual Biotechnology Laboratory, a consortium of DOE national laboratories focused on the response to COVID-19, with funding provided by the Coronavirus CARES Act. T.T.Z. and S.M. acknowledge support from the Tokodai Institute for Element Strategy (TIES) funded by MEXT Elements Strategy Initiative to Form Core Research Center. T.T.Z. also acknowledge the support by Japan Society for the Promotion of Science (JSPS), KAKENHI Grant No. 21K13865. S.M. also acknowledges support by JSPS KAKENHI Grant No. JP18H03678. G.B.H. and S.O. were supported by the U.S. DOE Office of Science, National Quantum Information Science Research Centers, Quantum Science Center. D.G.M. acknowledges support from the Gordon and Betty Moore Foundation's EPiQS Initiative, Grant GBMF9069. This research used resources of the Advanced Photon Source, a U.S. DOE Office of Science user facility operated for the DOE Office of Science by Argonne National Laboratory under Contract No. DE-AC02-06CH11357.

Researchers Discover Foam "Fizzics"

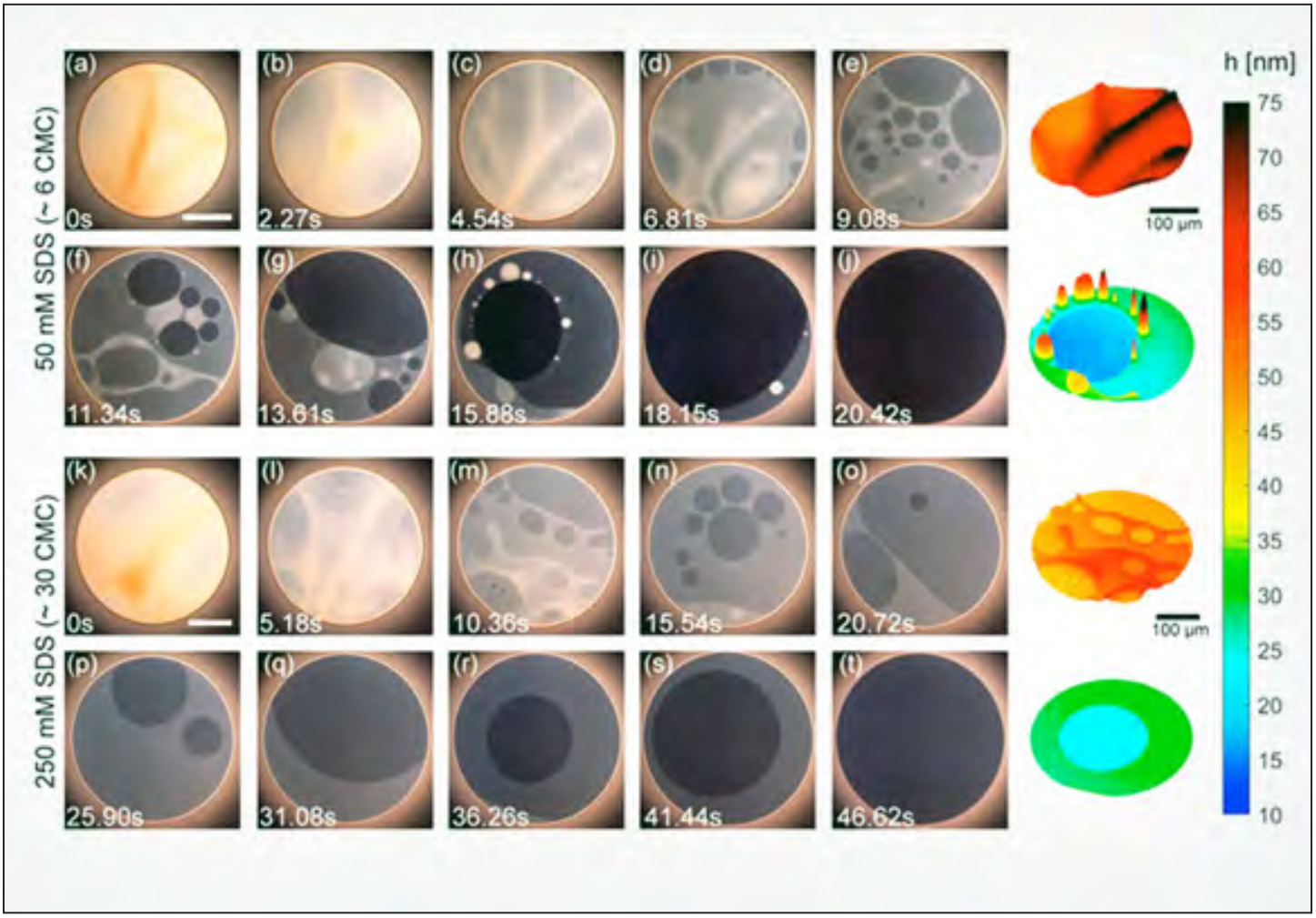

Micellar foam films show grayscale intensity variations that correspond to rich nanoscopic topography mapped using IDIOM protocols. Image: Chrystian Ochoa and Vivek Sharma/UIC

The original UCLA Samueli School of Engineering article can be read here. © Copyright 2022 UCLA Samueli School Of Engineering

Chemical engineers at the University of Illinois Chicago and UCLA used the APS in answering longstanding questions about the underlying processes that determine the life cycle of liquid foams. The breakthrough in understanding how liquid foams dissipate could help improve the commercial production and application of foams in a broad range of industries and could lead to improved products. Findings of the research were featured in the *Proceedings of the National Academy of Sciences of the United States of America*.

Foams are a familiar phenomenon in everyday lives — mixing soaps and detergents into water when doing dishes, blowing bubbles out of soapy water toys, sipping the foam off a cup of lattes or milk shake. Liquid foams can occur in a variety of natural and artificial settings. While some foams are produced naturally, as in bodies of water creating large ocean blooms on the beaches, others arise in industrial processes. In oil recovery and fermentation, for example, foams are a byproduct.

Whenever soapy water is agitated, foams are formed. They are mostly gas pockets separated by thin liquid films that often contain tiny molecular aggregates called micelles. Oily dirt, for example, is washed away by hiding in the water-phobic cores of micelles. In addition, fat digestion in our bodies relies on the role of micelles formed by bile salts.

Over time, foams dissipate as liquid within the thin films is squeezed out. Soap and detergent molecules that are by very nature amphiphilic (hydrophilic and hydrophobic) aggregate within water to form spherical micelles, with their outward-facing heads being hydrophilic and water-phobic tails forming the core.

Micelles are tiny, but influential, not just in cleaning and solubilizing oil-loving molecules but also in affecting flows within foam films," said co-principal investigator Vivek Sharma, an associate professor of chemical engineering at the UIC College of Engineering. For nearly a decade, he has pursued the question of how and why the presence of micelles leads to stepwise thinning, or stratification, within ultrathin foam films and soap bubbles.

To solve the puzzle, Sharma and his collaborators developed advanced imaging methods they call IDIOM (interferometry digital imaging optical microscopy) protocols that are implemented with high speed and digital single-lens reflex cameras. They found that foam films have a rich, ever-changing topography, and the thickness differences between different strata are much greater than the size of micelles.

"We used the precision technique called small-angle x-ray scattering [SAXS] to resolve the micelles' shape, sizes, and densities," said co-principal investigator Samanvaya Srivastava, an assistant professor of chemical and biomolecular engineering at the UCLA Samueli School of Engineering. "We found that the foam film thickness decreases in discrete jumps, with each jump corresponding to the exact distance between the micelles in the liquid film." The SAXS studies were performed on the XSD Chemical & Materials Science's 12-ID-B x-ray beamline at the APS.

The team also discovered that the arrangement of micelles in foam films is governed primarily by the ionic interactions between micelles. The electrostatic attraction and repulsion between ions influences how long foams remain stable and how their structure decays. With these findings, the researchers determined that by simply measuring the foam film thickness, which can be accomplished with a DSLR camera using the IDIOM protocols, they could characterize both the nanoscale interactions of micelles in liquids and the stability of the foams.

Compared to previous techniques that are more time-consuming and require expensive, customized equipment, the new method is not only less expensive but is also more comprehensive and efficient.

"The knowledge and understanding could aid in the development of new products — from food and personal care to pharmaceuticals," said the study's co-lead authors, graduate students Shang Gao of UCLA Samueli and Chrystian Ochoa of UIC. "It could also help engineers improve the control of foams in industrial processes."

See: Chrystian Ochoa[1], Shang Gao[2], Samanvaya Srivastava[2]*, and Vivek Sharma[1]**, "Foam film stratification studies probe intermicellar interactions," Proc. Natl. Acad. Sci. U.S.A. **118**(25), e2024805118 (2021).
DOI: 10.1073/pnas.2024805118
Author affiliations: [1]University of Illinois at Chicago, [2]University of California, Los Angeles
Correspondence: * samsri@ucla.edu, ** viveks@uic.edu

V.S. acknowledges funding support from NSF-CBET 1806011 (National Science Foundation–Chemical, Bioengineering, Environmental and Transport Systems) and the UIC College of Engineering. S.G. and S.S. acknowledge funding support from the UCLA Samueli School of Engineering and the Department of Chemical and Biomolecular Engineering. We acknowledge the support provided by Dr. Xiaobing Zuo. This research used resources of the Advanced Photon Source, a U.S. Department of Energy (DOE) Office of Science user facility operated for the DOE Office of Science by Argonne National Laboratory under Contract DE-AC02-06CH11357.

Strong, Resilient Synthetic Tendons from Hydrogels

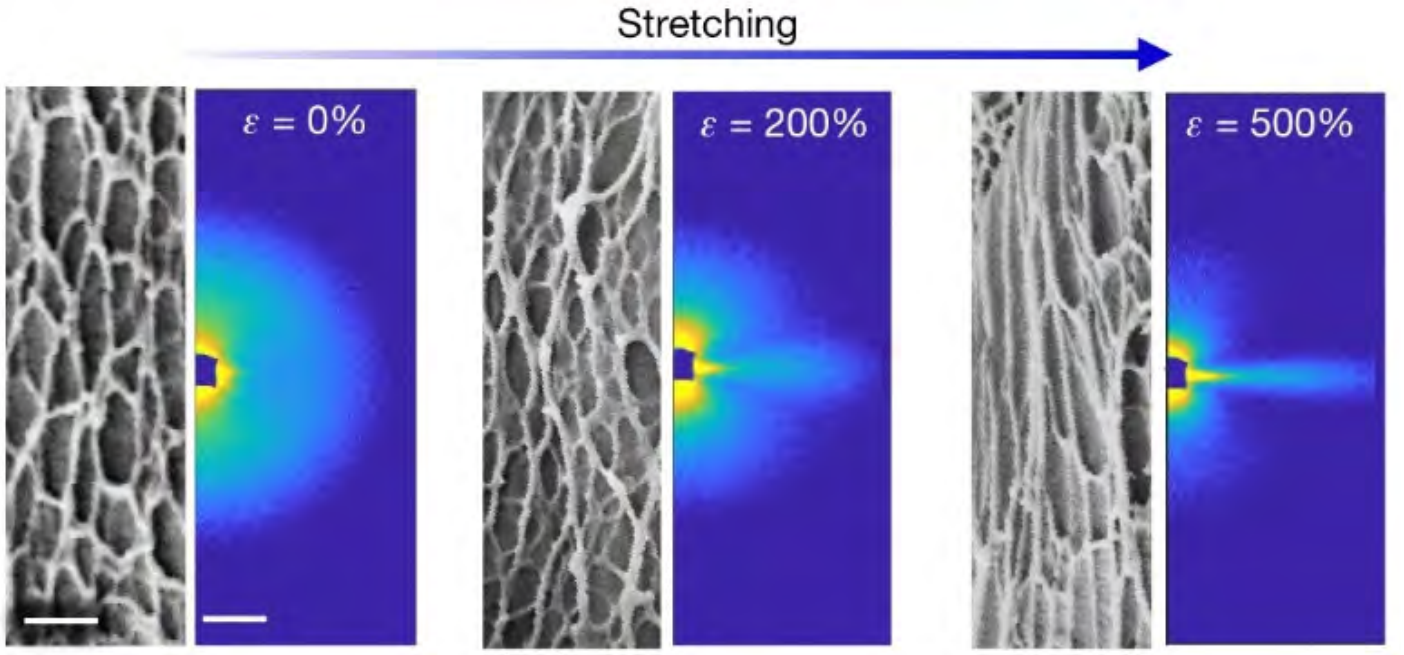

Fig. 1. SEM images (left) showing the deformation of the mesh-like nanofibril network during stretching and corresponding *in situ* SAXS patterns (right). Scale bars, 1 μm (SEM images); 0.025 Å−1 (SAXS images). From M. Hua et al., Nature **590**, 594 (25 February 2021). © 2021 Springer Nature Limited

Human tissues exhibit a remarkable range of properties. A human heart consists mostly of muscle that cyclically expands and contracts over a lifetime. Skin is soft and pliable while also being resilient and tough. And our tendons are highly elastic and strong and capable of repeatedly stretching thousands of times per day. While limited success has been achieved in producing man-made materials that can mimic some of the properties of natural tissues (for instance polymers used as synthetic skin for wound repair) scientists have failed to create artificial materials that can match all the outstanding features of tendons and many other natural tissues. An international team of researchers has transformed a standard hydrogel into an artificial tendon with properties that meet and even surpass those of natural tendons. This new material was examined via electron microscopy and x-ray scattering to reveal the microscopic structures responsible for its outstanding features. The x-ray measurements were gathered at the APS. The researchers have shown that their new hydrogel-based material can be modified to mimic a variety of human tissues and could also potentially be adapted to non-biological roles. Their results were published in the journal *Nature*.

Connective tissues are present throughout the body. Skin is connective tissue, as are tendons and ligaments. Tendons anchor muscles to bone, while ligaments bind bones together. The two primary constituents of connective tissues are water and the protein collagen. The resilience, flexibility, and toughness of connective tissues are in large part due to the way they are structured. Distinct structural arrangements at each length scale, from nanoscale features up to the millimeter scale, work synergistically to achieve optimum performance.

In order to produce artificial tissues, scientists start with materials that share key traits with living tissues. Natural tendons, for instance, are composed of 70% water. Hydrogels are a class of soft materials with an inherently high water content, making them a good starting point for constructing tendons and other synthetic tissues. Considerable effort has been devoted to transforming weak hydrogels into robust artificial tissues by using a variety of processing techniques, such as extruding the hydrogel, stretching it, or inserting microscopic synthetic fibers.

However, these efforts have failed to create materials that can simultaneously match all the outstanding properties of most natural tissues. For example, hydrogels processed to increase their toughness and strength typi-

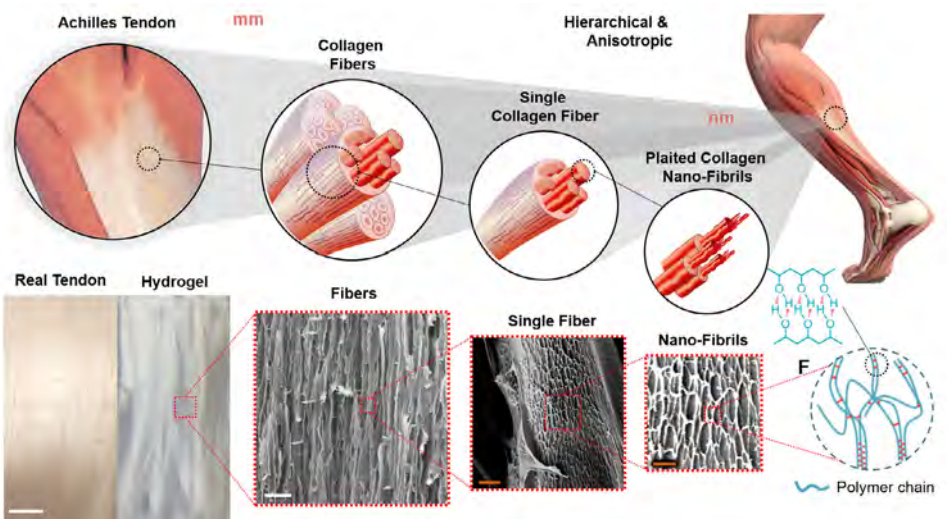

Fig. 2. Comparison of real-versus-synthetic tendon structure. Upper half shows the hierarchical structures present in human tendons. Note that collagen fibers form highly ordered structures from the millimeter scale to the nanoscale. Similarly, the hydrogel-based polymer material is also highly ordered over a range of dimensions. In the four images at the bottom of the illustration, successively smaller structures of the synthetic tendon are shown. Scale bars (tiny line segments) appear at lower left in each image. From left to right the scale bar indicates 5 millimeters, 50 micrometers (50 µm), 1 µm, and 0.5 µm.

cally show poor stretchability. The researchers in this study have demonstrated hydrogel-based artificial tendons with performance parameters that rival or even exceed those of their natural counterparts. The synthetically derived tendons exhibited very high stress resistance coupled with a toughness 10 times greater than natural tendon. Furthermore, the simulated tendons readily endured 30,000 stretch-and-release cycles without failure.

The new synthetic materials were created by applying the processes of freeze-casting and salting-out to a hydrogel consisting of polyvinyl alcohol (PVA) polymers disbursed in an aqueous solution. Freeze-casting was first applied to directionally freeze the polymer solution, meaning that the solution initially froze at one end and then continued freezing to the other end. After the water was extracted, a highly porous, sponge-like solid remained. The salting-out process was then applied. The porous solid was immersed in a concentrated salt solution, which caused the microscopic polymers to clump together to form tiny fibrous bundles. The end result was a highly anisotropic (directionally oriented) material with outstanding properties.

The highly modified hydrogel was examined using scanning electron microscopy (SEM) along with two complimentary x-ray techniques, small angle x-ray scattering (SAXS) and wide angle x-ray scattering (WAXS), both performed at the XSD Dynamics & Structure Group's 8-ID-E x-ray beamline of the APS (Fig. 1). Together these imaging techniques revealed that the modified hydrogel formed distinct structures over multiple length scales, from the nanoscale to the millimeter level (Fig. 2). Such multiscale structures are reminiscent of those seen in natural tendons, and were responsible for the modified hydrogel's exceptional strength, toughness, stretchability, and fatigue resistance.

The researchers demonstrated the adaptability of their new hydrogel-based material by varying its stiffness and other properties, including making it electrically conducting by infusing it with conductive polymers, all without reducing strength and toughness.

The researchers further note that the processes they developed for PVA-based hydrogel can be applied to other types of polymers and compounds, which they also demonstrated by greatly increasing the strength and toughness of alginate and gelatin hydrogels, both notoriously weak materials. — Philip Koth

See: Mutian Hua[1], Shuwang Wu[1,2], Yanfei Ma[1], Yusen Zhao[1], Zilin Chen[1], Imri Frenkel[1], Joseph Strzalka[3], Hua Zhou[3], Xinyuan Zhu[2], and Ximin He[1]*, "Strong tough hydrogels via the synergy of freeze-casting and salting out," Nature **590**, 594 (25 February 2021). DOI: 10.1038/s41586-021-03212-z
Author affiliations: [1]University of California, Los Angeles, [2]Shanghai Jiao Tong University, [3]Argonne National Laboratory
Correspondence: * ximinhe@ucla.edu

This research was supported by National Science Foundation CAREER award 1724526, Air Force Office of Scientific Research awards FA9550-17-1-0311, FA9550-18-1-0449, and FA9550-20-1-0344, and Office of Naval Research awards N000141712117 and N00014-18-1-2314. X.Z. acknowledges the Shanghai Municipal Government 18JC1410800 and National Natural Science Foundation of China 51690151. This research used resources of the Advanced Photon Source, a U.S. Department of Energy (DOE) Office of Science user facility, operated for the DOE Office of Science by Argonne National Laboratory under contract number DE-AC02-06CH11357.

A Better Look at Ultrafast Plasmas in Water

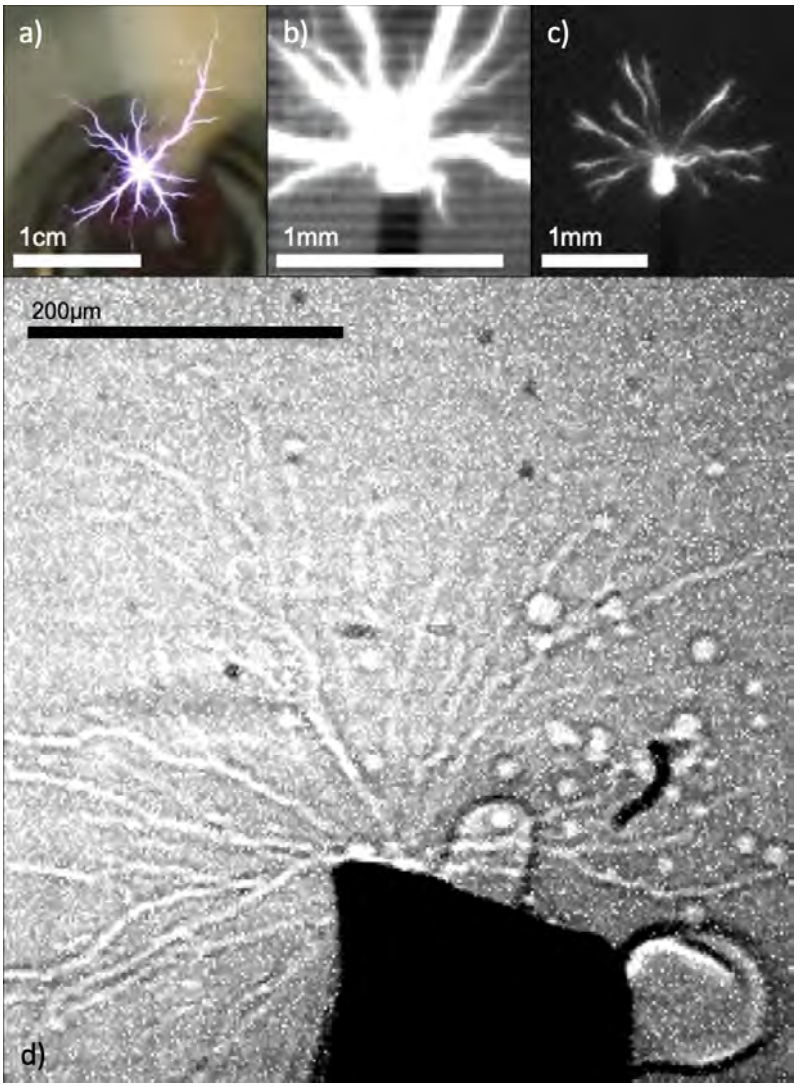

Fig. 1. Nanosecond-pulsed plasmas in water imaged with four different methods, in order of decreasing exposure time: (a) 67 milliseconds, (b) 2.38 microseconds, (c) 10 nanoseconds and (d) 50 picoseconds. Figures from C. Campbell et al., Phys. Rev. Res. **3**, L022021 (2021).

Plasmas travel through water at extreme hypersonic speeds. Using the APS ultrabright x-ray beams, scientists have captured images of these electrical discharges for the first time. Their results provide insight into the way plasmas propagate in liquids and could help realize the potential of nanosecond-pulsed plasmas, which have attracted interest in fields from medicine to three-dimensional printing. The results were published in *Physical Review Research*.

Plasma is a state of matter in which many of the atoms and molecules have been ionized, creating an electrically conducting medium with a similar number of positive and negative charged particles. Plasmas have long been used in scientific fields ranging from nuclear fusion to ion thrusters on spacecraft. In recent years, there has been significant interest in nanosecond-pulsed plasmas. These have been shown to improve the deposition of particles in nanochemistry and the strength of bonds in three-dimensional printing. They also have potential medical uses, particularly in wound healing, tissue regeneration and the treatment of skin diseases.

To help realize their potential, a thorough understanding of how these electrical discharges propagate is needed. This process is well understood in gases, but is less clear in liquids, with scientists proposing a few hypotheses. Keen to explore some of these theories, researchers at Texas A&M University and the Los Alamos National Laboratory turned to high-speed imaging.

The team submerged a tungsten electrode in filtered and distilled water. When they applied a positive high-voltage, a branched-structure plasma formed around the tip of the electrode. To produce pulsed plasmas, the researchers used a nanosecond-pulsed laser to trigger repeated electrical pulses in the circuit connected to the electrode.

The first frame captured by a high-speed video camera–with an exposure time of 2.38 microseconds–showed the propagation of light-emitting plasmas across the full field (Fig. 1). By the next frame this had stopped, and spherical bubbles had begun to form. Analysis of these images found that the plasmas propagated out from the electrode for about 100 nanoseconds before extinguishing, with the longest branches extending around 4 millimeters. The researchers estimated that the plasmas were travelling through the water at speeds of 29.1 kilometers per second, almost 20 times the speed of sound.

These hypersonic speeds make some of the proposed theories for how plasmas propagate in water unlikely. But the bright light emitted by the plasmas made

further analysis of the processes using high-speed video captures challenging. To address this, the researchers teamed up with the XSD Imaging (IMG) Group at the APS. They used the extremely bright (and thus fast) high-powered x-rays at the IMG-operated beamline 32-ID-B to image pulsed plasmas.

The x-rays showed that the plasmas propagated along narrow (around 10 micrometers) channels and then either expanded to form a single large bubble or collapsed and produced a train of small spherical bubbles (Fig. 2). The bubbles lasted for almost 50 microseconds. This shows that there is significant electrical charge near the bubble surface for tens of microseconds after they start, producing an electrostatic force, the scientists conclude. The researchers caution, however, that these process that dominate at the longer timescales are not necessarily involved in the initial plasma propagation.

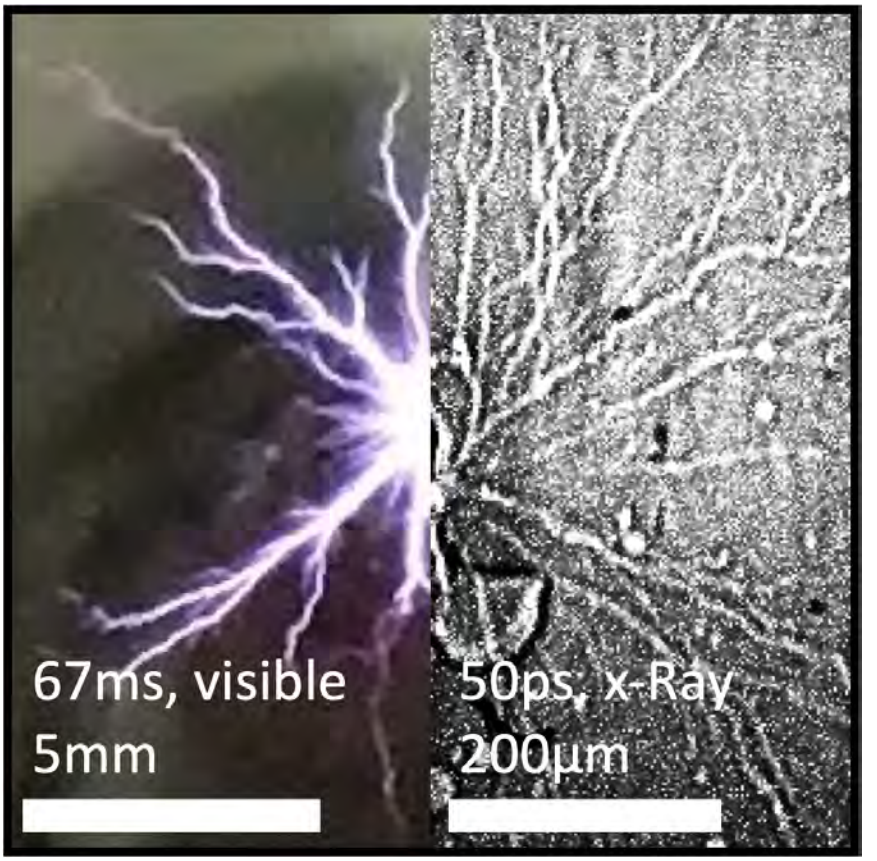

Fig. 2. Nanosecond-pulsed plasmas in water imaged with optical (left) and x-ray (right) methods, with exposure times of 67 milliseconds and 50 picoseconds, respectively.

Following further radiographic analysis of the images and computational modelling, the team ruled out some of the proposed hypotheses. Their results were inconsistent with the idea that electrostriction–mechanical deformation in response to a nonuniform electrical field–opens nanopores in the water along which the plasma can propagate. And because pre-existing bubbles were generally unaffected by the plasmas, they refute the idea that these electrical discharges take advantage of dissolved gases in water.

This suggests, but not conclusively, that field emission could explain the propagation of the plasmas. In this scenario, the emission of electrons from the electrode tip rapidly heats the surrounding water, leading to rapid expansion and a low-density region through which electrons can avalanche.

The researchers say that although the x-rays they used at the APS were extremely fast they still did not capture the dynamics of single plasma events. They now plan to return to the APS to use x-rays coupled to even faster imaging frame rates in hopes of capturing single events.

– Michael Allen

See: Christopher Campbell[1], Xin Tang[1], Yancey Sechrest[2], Kamel Fezzaa[3], Zhehui Wang[2*], and David Staack[1**], "Ultrafast x-ray imaging of pulsed plasmas in water," Phys. Rev. Res. **3**, L022021 (2021).
DOI: 10.1103/PhysRevResearch.3.L022021
Author affiliations: [1]Texas A&M University, [2]Los Alamos National Laboratory, [3]Argonne National Laboratory
Correspondence: * zwang@lanl.gov,
** dstaack@tamu.edu

Special thanks to the High-Speed Imaging Team at the Los Alamos National Laboratory (LANL) for their collaborative efforts and financial support during these experiments and to the staff at APS 32-ID-B for their time and expertise. LANL work is supported through Triad National Security, (LLC "Triad") by the U.S. Department of Energy (DOE)/National Nuclear Security Administration, by the MaRIE Technology Maturation fund, and the C2 program. This research used resources of the Advanced Photon Source, a U.S. DOE Office of Science user facility operated for the DOE Office of Science by Argonne National Laboratory under Contract No. DE-AC02-06CH11357.

Examining the Dual Personality of Weak Colloidal Gels

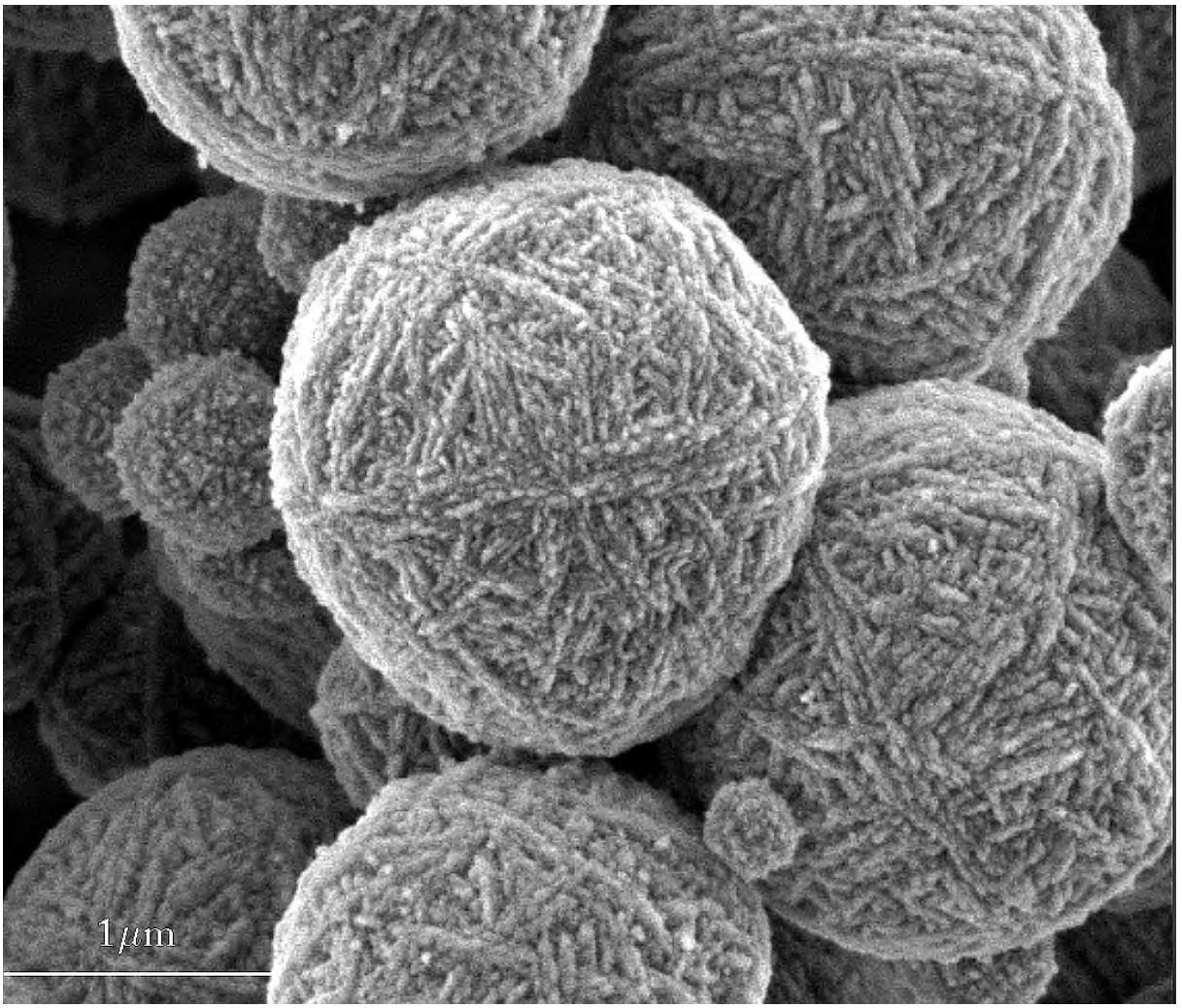

Fig. 1. The pictured microscale knitting balls are inorganic zeolite particles. These microporous crystalline minerals are formed via precipitation as the end result of an aging process in aluminosilicate colloidal hydrogels. The authors study their journey from aqueous solutions through a viscoelastic gels to a soft glassy solid. Time-resolved scattering and mechanical rheometry reveals the dichotomous nature of the intermediate gels which exhibit features of both glasses and gels, depending on (internally evolving) length and time scales. This gel/glass duality provides insight into the formation of zeolites as they progress through a soft amorphous stage before crystallization.

We probably encounter colloidal gels several times today. It may have been in the detergent used to do the laundry, the kitty litter poured out for the cat, or even the makeup put on your face or something for breakfast. Used in everything from paints to cosmetics to drugs to food products and more, colloidal gels are ubiquitous in modern life, yet their specific nature is a challenge to pin down. Their microstructural properties change over time between gel-like and glassy during the gelation process, and their mechanical characteristics, including elasticity, also change steadily as they age, making a complete picture hard to capture. Now, a team of researchers from Massachusetts Institute of Technology and the French Alternative Energies and Atomic Energy Commission (CEA)

has used the APS and a variety of research techniques to provide a much fuller understanding of the structure and behavior of colloidal gels. The work appeared in Proceedings of the *National Academy of Sciences of the United States of America*.

Past work on these materials generally concentrated on studying them in their fully mature state, thus missing the changes in their properties as they went through the full process of formation and aging. In this study, the team studied aluminosilcate gels (Fig. 1), adopting an approach called the time-connectivity superposition principle in which a series of repeated chirp signals are applied to the gel sample at regular intervals to achieve snapshots of the gelation process covering eight orders of magnitude. Combining mechanical spectroscopy, time-resolved small-angle x-ray scattering carried out at the SWING beamline of the SOLEIL Synchrotron (France) and ultra-small-angle x-ray scattering/small-angle x-ray scattering studies conducted at the XSD Chemical & Materials Science Group's 9-ID x-ray beamline at the APS provided a virtually complete picture of the viscoelastic response of these gels.

The experiments demonstrate that one reason these weak colloidal gels have been difficult to adequately characterize is that they have a distinctly dual nature, sometimes behaving as a glassy material and other times as a gel. They begin as an unremarkable collection of random Brownian nanoparticles in a solvent. As the time-resolved and ultra-small-angle x-ray scattering studies reveal across length scales from 0.1 nanometer to around 1 µm, over time these particles begin to aggregate into larger and larger clusters. At smaller time and length scales, the material is soft and glassy in nature; but at longer time scales and lengths, as clusters come together to form larger structures, the material assumes a more gel-like appearance and a defined fractal structure that persists even as the material grows and ages.

At a critical point, the relaxation time spectrum is set for the material, characterized by a power-law exponent that is positive for short relaxation times and negative for longer times. In this study, the time-connectivity superposition principle allows the various moments of this structural evolution to be placed on a universal master curve so that the material's viscoelastic properties can be determined over a broad range of deformation time scales that spans eight orders of magnitude.

To confirm the results seen in the aluminosilicate material, the team applied the same techniques to study the gelation of a silica-based colloidal gel system. With some small differences in numerical parameters, the shape of the relaxation spectrum curve was the same, demonstrating that all of these weak colloidal gels share the dual viscoelastic behavior of gel-like characteristics at long time scales, but glass-like nature at shorter timescales.

As this work demonstrates quite well, sometimes a dual nature is simply a matter of scale. The picture presented in these studies shows that the rheological behavior of weak colloidal gels at the macroscale is dependent upon what happens at the microstructural scale, as clustering nanoparticles form larger and larger repeated structural networks preserved in a fractal manner across length scales. In a way, the material can be two things at once, appearing glassy to a researcher performing one type of tests and gel-like to another investigator performing a different set of measurements.

Whichever perspective one chooses, the current work offers perhaps the best and broadest portrait yet of the dual personality of these important materials, giving a better understanding that could open the way to their more precise application and design. – Mark Wolverton

See: Bavand Keshavarz[1]*, Donatien Gomes Rodrigues[2], Jean-Baptiste Champenois[2], Matthew G. Frith[3] , Jan Ilavsky[3], Michela Geri[1] , Thibaut Divoux[4,5], Gareth H. McKinley[2], and Arnaud Poulesquen[1,4], "Time–connectivity superposition and the gel/glass duality of weak colloidal gels," Proc. Natl. Acad. Sci. U.S.A. **118**(15), e2022339118 (April 13, 2021). DOI: 10.1073/pnas.2022339118
Author affiliations: [1]Massachusetts Institute of Technology, [2]Université Montpellier, [3]Argonne National Laboratory, [4]CNRS–Massachusetts Institute of Technology, [5]Université de Lyon
Correspondence: * bavand@mit.edu

The authors acknowledge the French National Research Agency (ANR) for financial support of the DYNAMISTE project (ANR-15- CE07-0013). This research used resources of the Advanced Photon Source, a U.S. DOE Office of Science user facility operated for the DOE Office of Science by Argonne National Laboratory under Contract No. DE-AC02-06CH11357.

A Crystal-Clear Way to Save Time

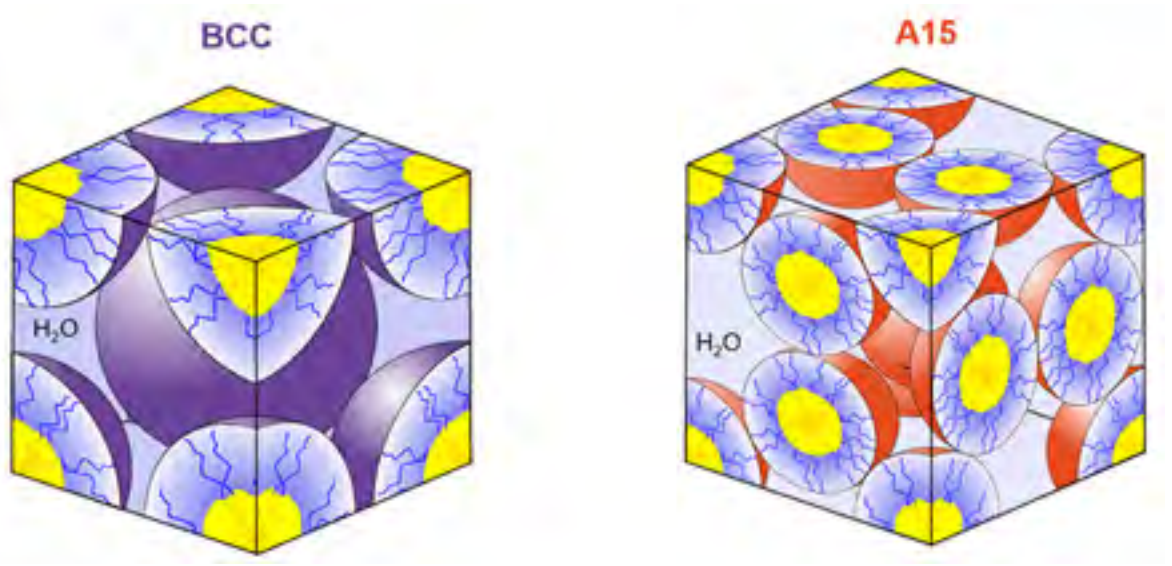

Two crystalline phases found in the diblock polymer materials used in this work. With the proper thermal and shear processing, these "unit cells" can repeat hundreds of thousands of times in every direction in perfect symmetry. Source: Connor Valentine

The original Carnegie Mellon University College of Engineering article by Tara Moore can be read here.

Carnegie Mellon University (CMU) Chemical Engineering and University of Minnesota Chemical Engineering & Materials Science (CEMS) researchers collaboratively used the APS in their discovery of a better way to make a new class of soft materials—reducing a process that used to take five months down to three minutes. Their results were published in the journal *ACS Macro Letters*.

Working with Lynn Walker (CMU) and Mahesh Mahanthappa (UMN), Connor Valentine, a CMU chemical engineering Ph.D. student, and recent UMN CEMS graduate Dr. Ashish Jayaraman study diblock polymers. Diblock polymers are chain-like molecules where one end of the chain is hydrophobic, and the other is hydrophilic. Molecules like this are used in soap because the hydrophobic side grabs onto dirt and oil, but the hydrophilic side keeps the molecules dissolved into the water.

When these molecules are placed in water at high enough concentrations, they begin to form clusters: the hydrophobic parts clump together in the center of the ball in order to avoid water. The hydrophilic sides arrange into a brush-like layer on the outside of the ball, protecting the hydrophobic center.

As you add more polymers into the water, however, they begin to run out of room and pack themselves intelligently and spontaneously. It would be as if you were trying to fit the maximum number of tennis balls in a box—you would carefully stack each layer.

When these stacks form, they are called crystals, because the organizational patterns will repeat over and over in every direction. Crystalline structures like this are found throughout nature, including in gemstones, metals, and polymeric materials. People have taken advantage of the repeating and consistent spacing to create polymeric membranes for filtering water and gases. There are also exciting potential uses in new soft materials, with applications that include medical implants, adhesives, sustainable food packaging, liquid beauty products, and condiments.

However, the problem comes in when researchers are trying to make specific crystalline structures. Engineers need to be able to consistently produce crystals with specific arrangements and sizes so that they can achieve the desired material performance at market scale. However, processing issues can arise when they don't fully understand the forces driving crystal formation. The wrong temperature change, mixing speed, or formulation can cause crystals to suddenly form, degrade, or transition to another crystalline organization. The accompanying change in material properties can jam mixers, ruin equipment, and result in a worthless final product.

In the case of this work, the desired crystalline state can take months to form at room temperature. This can cause huge issues, with companies discovering they have a product with completely different properties after three months—maybe it's chunky, or it's become stiff—or perhaps the company just has to wait three months to sell their product because it takes that long to get the gel consistency they desire.

"It's important for people to understand how these polymer molecules will turn into crystals," said Valentine. "And that's not just if they turn into the crystal they want, it's the rate of it, the speed. Also, are there going to be other crystal phases present? Is every piece of that crystalline material going to be oriented consistently?"

Valentine and Walker worked with collaborators from the University of Minnesota, who discovered that the rate of heating and cooling can produce intermediate crystal structures that last for several months. Valentine's team built on the initial work of their University of Minnesota collaborators, Ashish Jayaraman and Mahesh K. Mahanthappa, and investigated the impact of shear processing on these crystal structures. Shear processing is a broad term that includes steps like mixing, painting, coating, and shaking—the material is moving. The speed, duration, and direction of shear can really matter for materials like those used in this work.

"Ketchup is a great example about why shear processing affects soft materials because ketchup has a yield stress and thins when you mix or process it," said Valentine. "If you're trying to get ketchup out of a glass bottle and it is gel or solid-like, it will not flow. But small taps (on the correct part of the bottle) will get the ketchup to flow very nicely. The shear is changing the microstructure of the ketchup, which then changes the flow properties. It's important we understand how shear impacts any material we work with in the same way."

The authors used an oscillatory shear flow, which involves placing the gel or soft material between two parallel plates—where the top plate can rotate back and forth. Researchers can control the speed and length of the top plate. When Valentine and his team put the diblock polymer crystals into this shear cell, they were able to cause the crystalline phase to change into the equilibrium structure within three minutes. The Minnesota team had previously found this same structural change to take almost five months sitting at room temperature without shear.

"Shear processing can help with the dynamics, the speed, and the rates of structural change, not just the final result, which is something people don't really think about," said Valentine. "They often think when you shear these materials, it's going to change the structure into something different, but that's not necessarily true."

The team was able to measure these results by employing small-angle x-ray scattering at the X-ray Science Division Chemical & Materials Science's 12-ID-B x-ray beamline at the APS, an Office of Science user facility at Argonne National Laboratory, which is essentially a mile-wide particle accelerator. The high-intensity x-ray beams from the APS allowed the research team to measure the crystal structure in real-time.

Their findings not only showed that the speed increase occurs, but also detailed how to tune the shear parameters to achieve the desired rate of crystal formation. They even found that you can prevent the change from happening entirely if the shear is at very low frequencies with very long cycles of oscillation.

"We were able to show that this shear processing step is just a very controllable way to get the structure you want and how fast you want it," said Valentine.

See: Connor S. Valentine[1], Ashish Jayaraman[2], Mahesh K. Mahanthappa[2]**, and Lynn M. Walker[1]*, "Shear-Modulated Rates of Phase Transitions in Sphere-Forming Diblock Oligomer Lyotropic Liquid Crystals," ACS Macro Lett. **10**, 538 (2021). DOI: 10.1021/acsmacrolett.1c00154
Author affiliations: [1]Carnegie Mellon University, [2]University of Minnesota
Correspondence: * lwalker@andrew.cmu.edu,
** maheshkm@umn.edu

M.K.M. and A.J. gratefully acknowledge funding from the National Science Foundation, NSF, (CHE-1807330). C.S.V. and L.M.W. gratefully acknowledge a fellowship from PPG Industries, Inc., and the Dowd Fellows Program at CMU. Preliminary SAXS analyses were performed at the Characterization Facility at the University of Minnesota, which receives partial support from NSF through the MRSEC program (DMR-2011401). This research used resources of the Advanced Photon Source, a U.S. Department of Energy (DOE) Office of Science user facility operated for the DOE Office of Science by Argonne National Laboratory under Contract No. DE-AC02-06CH11357.

Revealing Platinum's Role in Clean Fuel Conversion

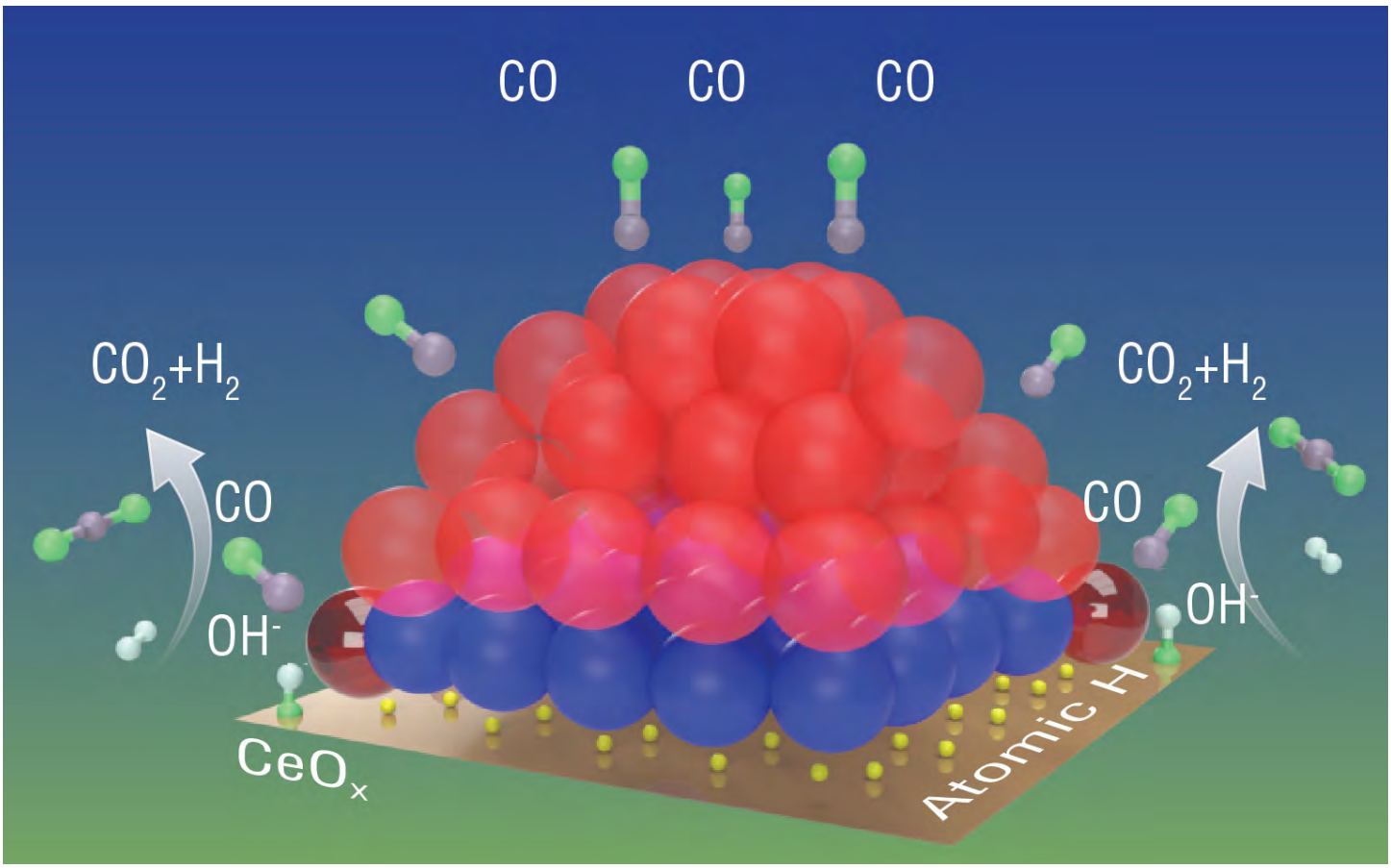

Scientists studying a water gas shift reaction catalyst made of platinum atoms (red and blue) on a cerium oxide (CeO_x) surface discovered that only some platinum atoms around the periphery of the nanoparticle (shiny dark red) get activated to take part in the reaction. These activated platinum atoms transfer oxygen from OH groups (originally from water molecules) to carbon monoxide (CO), transforming it to CO_2, leaving the H to combine with atomic hydrogen to form H_2. Understanding these dynamics may help scientists design catalysts that require fewer platinum atoms.

The original Brookhaven National Laboratory news release can be read here.

Because platinum is rare and expensive, scientists have been seeking ways to create catalysts that use less of this precious metal. Understanding exactly what the platinum does is an essential step. Using a number of U.S. Department of Energy (DOE)-funded experimental resources, including experiment facilities at Brookhaven National Laboratory and high-brightness x-rays from the APS, scientists from Stony Brook University (SBU), Brookhaven, and other collaborating institutions have uncovered dynamic, atomic-level details of how an important platinum-based catalyst works in the water gas shift reaction. This reaction transforms carbon monoxide (CO) and water (H_2O) into carbon dioxide (CO_2) and hydrogen gas (H_2), an important step in producing and purifying hydrogen for multiple applications, including use as a clean fuel in fuel-cell vehicles, and in the production of hydrocarbons.

The new study, published in the journal *Nature Communications*, identifies the atoms involved in the catalyst's active site, resolving earlier conflicting reports about how the catalyst operates. The experiments provide definitive evidence that only certain platinum atoms play an important role in the chemical conversion.

"Part of the challenge is that the catalyst itself has a complex structure," said lead author Yuanyuan Li, a research scientist at SBU's Materials Science and Chemical Engineering Department.

"The catalyst is made of platinum nanoparticles (clumps of platinum atoms) sitting on a cerium oxide (ceria) surface. Some of those platinum atoms are on the surface of the nanoparticle, some are in the core; some are at the interface with ceria, and some of those are at the perimeter--the outside edges--of that interface," Li said. "Those positions and how you put the particles on the surface may influence which atoms will interact with the support or with gas molecules, because some are exposed and some are not."

Earlier experiments had produced conflicting results about whether the reactions occur on the nanoparticles or at single isolated platinum atoms, and whether the active sites are positively or negatively charged or neutral. Details of how the ceria support interacts with the platinum to activate it for catalytic activity were also unclear.

"We wanted to address these questions," said Li. "To identify the active site and determine what is really happening at this site, it is better if we can investigate this type of catalyst at the atomic level," she noted.

The team, which included scientists from the Brookhaven Center for Functional Nanomaterials (CFN) and other institutions throughout the U.S. and in Sweden, used a range of techniques to do just that. They studied the catalyst under reaction conditions and, unexpectedly, captured a peculiar effect that occurred when the catalysts reached their active state in reaction conditions.

"The platinum atoms at the perimeter of the particles were 'dancing' in and out of focus in an electron microscopy experiment carried out by our collaborators, while the rest of the atoms were much more stable," Frenkel said. Such dynamic behavior was not observed when some of the reactants (CO or water) were removed from the stream of reacting molecules.

"We found that only the platinum atoms at the perimeter of the interface between the nanoparticles and ceria support provide the catalytic activity," Li said. "The dynamic properties at these perimeter sites allow the CO to get oxygen from the water so it can become CO_2, and the water (H_2O) loses oxygen to become hydrogen."

Now that the scientists know which platinum atoms play an active role in the catalyst, they may be able to design catalysts that contain only those active atoms.

"We might assume that all the surface platinum atoms are working, but they are not," Li said. "We don't need them all, just the active ones. This could help us make the catalyst less expensive by removing the atoms that are not involved in the reaction. We believe that this mechanism can be generalized to other catalytic systems and reactions," she added.

Electron microscopy "snapshots" at the CFN and at the National Institute of Standards and Technology revealed the dynamic nature of the perimeter platinum atoms. "In some images, the perimeter site is there, you can see it, but in some images, it is not there. This is evidence that these atoms are very dynamic, with high mobility," Li said.

Infrared (IR) spectroscopy studies in the Brookhaven Chemistry Division revealed that the appearance of the perimeter sites coincided with "oxygen vacancies"—a kind of defect in the cerium oxide surface. These studies also showed that CO tended to migrate across the platinum nanoparticle surface toward the perimeter atoms, and that hydroxy (OH) groups lingered on the ceria support near the perimeter platinum atoms.

"So it seems like the perimeter platinum atoms bring the two reactants, CO and OH (from the water molecules) together," Li said.

X-ray photoelectron spectroscopy studies in the Chemistry Division revealed that perimeter platinum atoms also became activated—changed from a nonmetallic to a metallic state that could capture oxygen atoms from the OH groups and deliver that oxygen to CO. "This really shows that these activated perimeter platinum sites enable the reaction to take place," Li said.

A final set of experiments—x-ray absorption spectroscopy studies conducted at the XSD Spectroscopy Group's 20-ID-C x-ray beamlime at the APS—showed the dynamic structural changes of the catalyst. "We see the structure is changing under reaction conditions," Li said.

Those studies also revealed an unusually long bond between the platinum atoms and the oxygen on the ceria support, suggesting that something invisible to the x-rays was occupying space between the two.

"We think there is some atomic hydrogen between the nanoparticle and the support. X-rays can't see light atoms like hydrogen. Under reaction conditions, those atomic hydrogens will recombine to form H_2," she added.

The structural features and details of how the dynamic changes are connected to reactivity will help the scientists understand the working mechanism of this particular catalyst and potentially design ones with better activity at

"Platinum's" cont'd. on page 73

Fine Tuning Single-Atom Catalysts with LCSCs

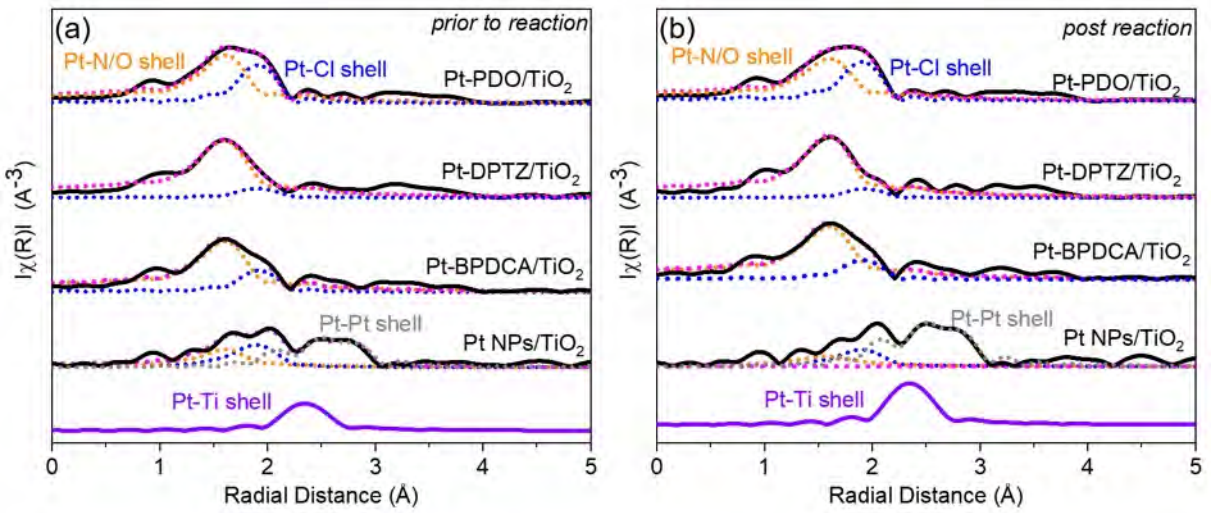

Fig. 1. Fourier transformation of k2-weighted EXAFS spectra (solid black lines) with the first shell fitting (magenta dash lines) of Pt-ligand/TiO_2 (a) before and (b) after reaction for three Pt-ligand catalysts and comparison to Pt nanoparticles (NPs). Note that the Pt-ligand LCSCs do not show Pt-Pt coordination, indicating single atom character, even after reaction.

Most of chemical and industrial manufacturing worldwide is driven by processes that involve heterogeneous catalysis, which is crucial for the large-scale production of all kinds of products and for countless other applications. This makes the quest for better, cheaper, and more versatile catalysts of enduring importance. In recent years, a new approach called single-atom catalysis (SAC) has offered fresh possibilities to increase catalyst selectivity and efficiency, but stability can be a problem. One possible solution is the use of ligand-coordinated supported catalysts (LCSCs). Researchers using the APS demonstrated that the LCSC strategy both stabilizes the structure and activity of single-atom metal centers and also allows them to be tuned and engineered for specific catalytic applications. This work was the cover subject of the journal *ChemSusChem*.

The research team examined the structure and ethylene hydrogenation reactivity of three metal-organic platinum (Pt)-ligand complexes with different coordination motifs. They characterized the structure of each by a variety of techniques, including x-ray absorption spectroscopy (XAS) at the XSD Spectroscopy Group's beamline 9-BM at the APS. In each catalyst, one of three ligands (PDO, DPTZ, or BPDCA) was coordinated to Pt atoms on a TiO_2 surface.

Extended x-ray absorption fine structure (EXAFS) measurements (Fig. 1) of the local coordination environment around the Pt centers in each of the LCSCs shows good Pt-N/O and Pt-Cl coordination without significant evidence of Pt scattering, demonstrating that most Pt on the catalyst surface is single-atom in nature without notable nanoparticle clustering. The coordination number of the Pt centers appears to be dependent on choice of ligand.

Definite differences among the three ligands were seen in the ethylene hydrogenation reaction. The highest reaction rate, lowest reaction temperature and greatest stability were shown by LCSCs made with the PDO ligand, which achieved full conversion of ethylene to ethane at 30° C. The BPDCA and DPTZ Pt-ligands required higher temperatures from 70° C to as high as 110° C. The latter two ligands also showed slower conversion rates.

The researchers attribute these differences among the three LCSC ligands to a variety of factors, including the Pt coordination number, which is lowest with the PDO ligand. This provides a greater number of active sites for Pt hydrogenation at lower temperatures, as shown by the EXAFS studies. Hydrogen dissociation is affected by temperature, and the Pt-ligands facilitate this at higher temperatures. The EXAFS experiments also show no Pt-Pt path throughout the reaction, which indicates the stability of the LCSC structures. The Pt ligands also appear to

"Fine" cont'd. on next page

"Fine" cont'd. from previous page

show no measurable changes in oxidation state or their coordination environment, also confirming their structural stability.

As a further check on the functioning of the LCSCs, the experimenters studied the Pt-TiO_2 catalyst system without supporting ligands. They found that the absence of the ligands results in greater Pt clustering and aggregation under the same conditions, which indicates that these phenomena are suppressed when the ligand is present.

Finally, the team investigated the activity of the PDO LCSCs with iridium, another metal often considered for use in the hydrogenation catalysis process. The PDO ligand formed a stable and active coordination complex with iridium on TiO_2. The hydrogenation reaction rate was notably slower with Ir than with Pt and followed a somewhat different reaction pathway, but was found to work well with no metal nanoparticle formation or clustering.

The experiments demonstrate the feasibility of ligand-supported coordinated catalysts for single-atom heterogeneous catalysis, showing their excellent stability and activity in the ethylene hydrogenation process under both ambient and reaction conditions. Of the three LCSCs tested, the Pt-PDO ligand proved the most favorable, indicating the importance of the choice of the particular ligand and its coordination with the single-atom metal centers. The work therefore suggests greater possibilities for custom-designing single-atom catalysts for specific purposes.

– Mark Wolverton

See: Xuemei Zhou[1,3], George E. Sterbinsky[2], Eman Wasim[1], Linxiao Chen[1,4], and Steven L. Tait[1]*, "Tuning Ligand-Coordinated Single Metal Atoms on TiO_2 and their Dynamic Response during Hydrogenation Catalysis," ChemSusChem **14**(18). 3825 (September 20, 2021).
DOI: 10.1002/cssc.202100208
Author affiliations: [1]Indiana University, [2]Argonne National Laboratory, [3]Sichuan University, [4]Pacific Northwest National Laboratory
Correspondence: * tait@indiana.edu

This work was supported by the U.S. Department of Energy (DOE) Office of Science-Basic Energy Sciences, Chemical Sciences program under Award Numbers DE-SC0016367 and DE-SC0021390. This research used resources of the Advanced Photon Source, a U.S. DOE Office of Science user facility operated for the DOE Office of Science by Argonne National Laboratory under Contract No. DE-AC02-06CH11357.

"Platinum's" cont'd. from page 71

lower cost. The same techniques can also be applied to studies of other catalysts.

See: Yuanyuan Li[1]*, Matthew Kottwitz[2], Joshua L. Vincent[3], Michael J. Enright[2], Zongyuan Liu[4], Lihua Zhang[4], Jiahao Huang[1], Sanjaya D. Senanayake[4], Wei-Chang D. Yang[5,6], Peter A. Crozier[3], Ralph G. Nuzzo[2,7], and Anatoly I. Frenkel[1,4], "Dynamic structure of active sites in ceria supported Pt catalysts for the water gas shift reaction," Nat. Commun. **12**, 914 (2021). DOI: 10.1038/s41467-021-21132-4
Author affiliations: [1]Stony Brook University, [2]University of Illinois Urbana-Champaign, [3]Arizona State University, [4]Brookhaven National Laboratory, [5]National Institute of Standards and Technology, [6]University of Maryland, [7]KTH Royal Institute of Technology
Correspondence: * Yuanyuan.li@stonybrook.edu

Y.L., A.I.F., and R.G.N. acknowledge support by the U.S. Department of Energy (DOE) Office of Science-Basic Energy Sciences under Grant No. DE-FG02-03ER15476. Reaction tests and DRIFTS measurements at Brookhaven National Laboratory's Chemistry Division and XAFS data analysis were made possible by the Program Development fund 21-017 to A.I.F. M.K. and R.G.N. acknowledge fellowship support from the Department of Chemistry at the University of Illinois. Work by S.D.S. and Z.L. at Brookhaven National Laboratory was supported by the U.S. DOE Office of Science-Basic Energy Sciences, Division of Chemical Sciences, Geosciences and Biosciences under contract no. DE-SC0012704. S.D.S. is partially supported by a U.S. DOE Early Career Award. This research used Hitachi2700C STEM of the Center for Functional Nanomaterials, which is a U.S. DOE Office of Science Facility at Brookhaven National Laboratory, under Contract No. DE-SC0012704. J.L.V. and P.A.C. acknowledge National Science Foundation grant CBET- 1604971 and the facilities at the National Institute of Standards and Technology at Gaithersburg, M.D., as well as those at the John M. Cowley Center for High Resolution Electron Microscopy at Arizona State University. W.D.Y. acknowledges support under the Cooperative Research Agreement between the University of Maryland and the National Institute of Standards and Technology Physical Measurement Laboratory, award 70NANB14H209, through the University of Maryland. This research used resources of the Advanced Photon Source, a U.S. DOE Office of Science user facility operated for the DOE Office of Science by Argonne National Laboratory under Contract No. DE-AC02-06CH11357.

Catalyst Technology Converts Methane Greenhouse Gas into Useful, Valuable Chemicals

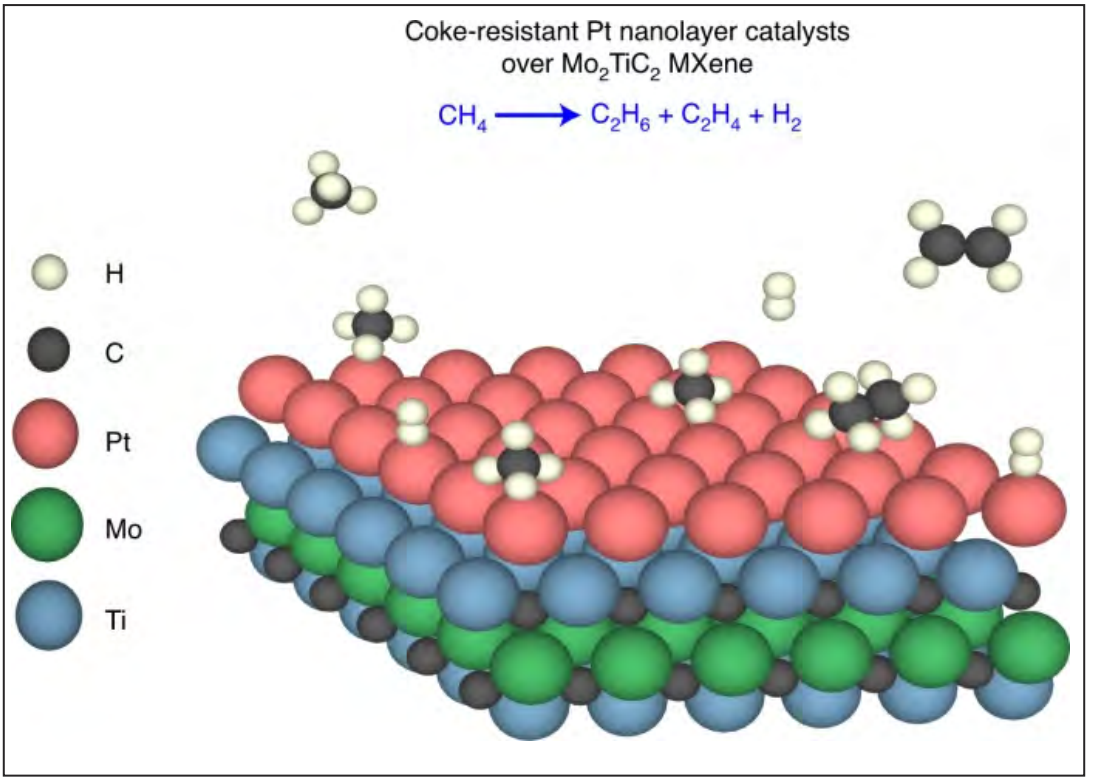

Fig. 1. Iowa State University researchers' MXene, made from carbon, molybdenum, and titanium.

The original Iowa State University press release by Mike Krapfl can be read here. Copyright ©2021 Oregon State University

Methane, which produces more warming than other greenhouse gases and is the subject of newly announced U.S. emission restrictions, is hard to break down and keep out of the atmosphere. It's not that the primary component of natural gas is chemically complex; a methane molecule is just one carbon atom and four hydrogens. But those carbon-hydrogen bonds are hard to break. Typically, that involves high temperatures and mixing the flammable gas with oxygen to produce syngas to make methanol and hydrogen to make ammonia, which is expensive and potentially explosive. Other conversion reactions aren't very efficient and also produce the most abundant of the greenhouse gases, carbon dioxide. Is there another way to use methane and keep it out of the atmosphere? One that's safe and efficient, that returns value, nd that helps fight climate change? Yue Wu and his research group at Iowa State University have been looking for ways to do all that over several years. Now, they and a group of collaborators using two U.S. Department of Energy (DOE) x-ray light sources including the APS have found and tested a catalyst technology that appears to be an answer. Their results were published in the journal *Nature Catalysis*.

"The results provided a potential solution to this long-time challenge and represented the best stability, conversion rate, and selectivity to convert methane to ethane or ethylene, two main precursors for the modern petrochemical industry," according to a project summary written by Wu, the Herbert L. Stiles Professor in Chemical Engineering at Iowa State. The Iowa State University Office of Innovation Commercialization is seeking a patent for the technology.

The catalyst consists of one or two layers of platinum, each layer just an atom thick, deposited on two-dimensional metal carbide structures called "MXenes." In this case, the structures are made from carbon, molybdenum and titanium (Fig. 1). Wu said his research group discovered the thin layers essentially allow every platinum atom

to be used as a catalyst and prevents the formation of residues that cover and deactivate the platinum. That means less platinum is required to make the catalyst.

Wu said his group started studying carbides–combinations of carbon and metals–about five years ago with support from the Office of Naval Research. The original work was to identify the electrical and thermal properties of various carbides. But the work didn't go as expected – the material's thermal conductivity was much lower than predicted.

"You can think of this as a failure," Wu said.

But the researchers discovered the MXene surfaces are very active and able to absorb many molecules. And so, with support from Wu's Stiles professorship and the Iowa State College of Engineering, Wu's research group began studying these MXenes as a potential catalyst. "We had never seen carbide so active," Wu said. "It's usually very inert. It's used, for example, for high-speed drill bits – the surface is hard and inert."

Their research included fluorescence *in situ* x-ray absorption spectroscopy measurements at the MR-CAT 10-BM bending magnet beamline at the APS, and *ex situ* x-ray absorption spectroscopy measurements carried out at beamline 2–2 of the Stanford Synchrotron Radiation Lightsource (SSRL) at the SLAC National Accelerator Laboratory.

The team started using the technology to remove hydrogen from shale gas, the natural gas found in shale rock formations. That work evolved to study other reactions involving natural gas. "Nobody tried to use these carbides for these high-volume reactions before," Wu said.

Keys to the methane-to-ethane/ethylene conversion are making the carbides pure enough and making the surfaces clean enough to support the reactions, Wu said. Get it all right, and those reactions exhibit about 7% methane conversion with about 95% selectivity toward ethane/ethylene in a continuously operating fixed-bed reactor. The products can be turned into plastics and resins, such as the common and ubiquitous polyethylene plastic.

"Remarkably, these novel catalysts run for 72 hours of continuous operation without any signs of deactivation, indicating a promising start toward technologies suitable for exploitation on the industrial scale," Wu said.

That's all very good news.

Methane emissions, after all, are such a contributor to climate change that world leaders took steps to restrict them during COP26, the United Nations summit on climate change in Glasgow, Scotland. More than 100 countries also signed a Global Methane Pledge to reduce methane emissions by 30% over the next nine years.

The researchers' new catalyst technology could advance those efforts to keep methane out of the atmosphere. Wu calls the technology "revolutionary," saying it "opens the door to reducing the emission of methane and its combustion product, CO_2, in the future."

See: Zhe Li[1], Yang Xiao[2]*, Prabudhya Roy Chowdhury[2], Zhenwei Wu[2], Tao Ma[3], Johnny Zhu Chen[2], Gang Wan[4], Tae-Hoon Kim[3‡], Dapeng Jing[3], Peilei He[1], Pratik J. Potdar[2], Lin Zhou[3], Zhenhua Zeng[2], Xiulin Ruan[2], Jeffrey T. Miller[2], Jeffrey P. Greeley[2], Yue Wu[1]**, and Arvind Varma[2‡‡], "Direct methane activation by atomically thin platinum nanolayers on two-dimensional metal carbides," Nat. Catal. **4**, 882 (2021). DOI: 10.1038/s41929-021-00686-y
Author affiliations: [1]Iowa State University, [2]Purdue University, [3]Department of Energy Ames Laboratory, [4]Stanford University ‡Present address: Chonnam National University ‡‡Deceased
Correspondence: * xiao63@purdue.edu,
** yuewu@iastate.edu

Y.W. appreciates the support from the Herbert L. Stiles Professorship and Iowa State University College of Engineering exploratory research projects. J.C.Z., Z.W. and J.T.M. were supported in part by the National Science Foundation (NSF) under Cooperative Agreement no. EEC-1647722. Y.X. and A.V. thank the R. Games Slayter Fund and the Varma Reaction Engineering Research Fund of Purdue University. Z.Z. and J.P.G. acknowledge financial support from NSF Chemical, Bioengineering, Environmental and Transport Systems Award 1804712. T.M. acknowledges the financial support of the University of Michigan College of Engineering and technical support from the Michigan Center for Materials Characterization. MR-CAT operations are supported by the U.S. Department of Energy (DOE) and the MR-CAT member institutions. Use of the Stanford Synchrotron Radiation Lightsource, SLAC National Accelerator Laboratory, is supported by the U.S. DOE Office of Science-Basic Energy Sciences under contract no. DE-AC02-76SF00515. All TEM-related work was performed using instruments in the Sensitive Instrument Facility in Ames Laboratory. Ames Laboratory is operated for the U.S. DOE by Iowa State University under contract no. DE-AC02-07CH11358. This research used resources of the Advanced Photon Source, a U.S. DOE Office of Science user facility operated for the DOE Office of Science by Argonne National Laboratory under Contract DE-AC02-06CH11357.

A Good Dose of Iron Boosts Electrocatalytic Water Oxidation

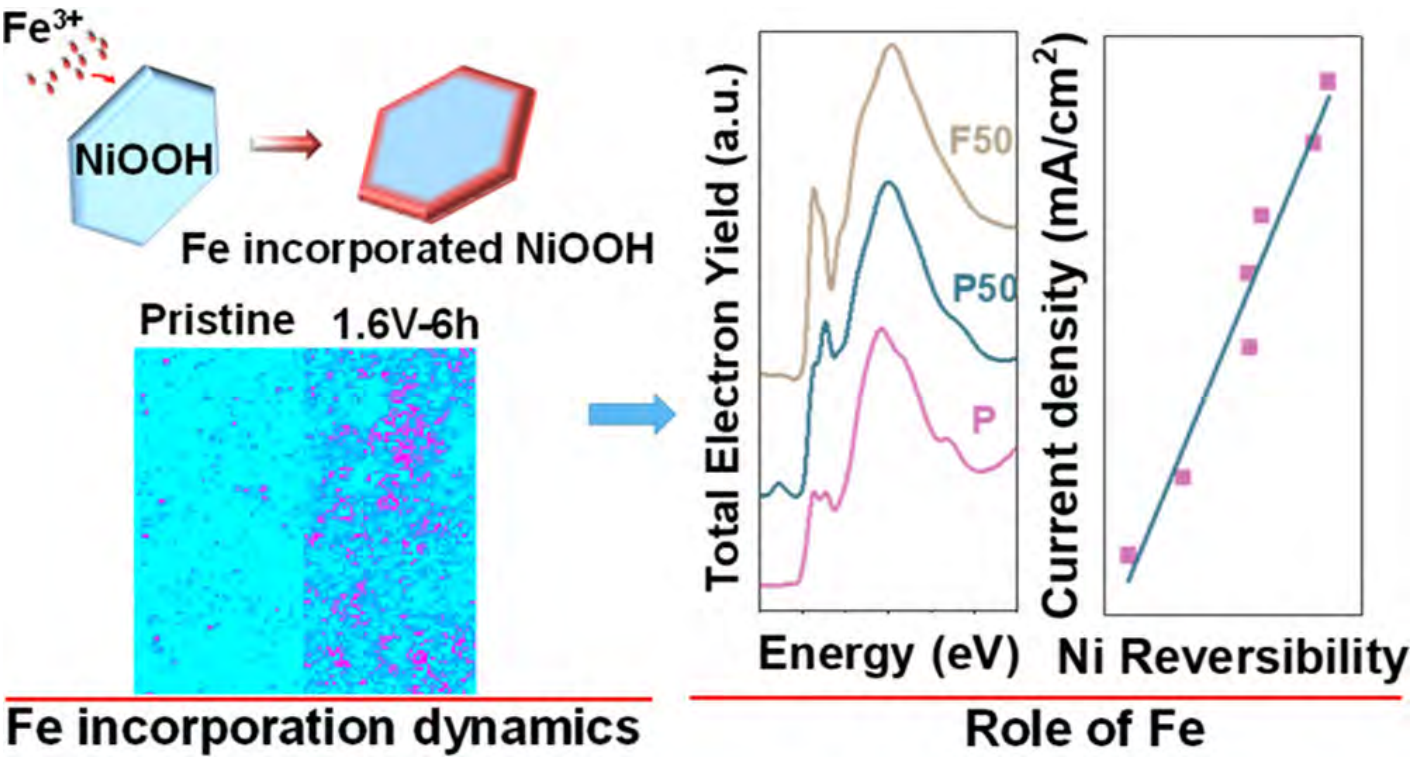

Fig. 1. Understanding how Fe in the electrolyte gets incorporated in the nickel hydroxide electrocatalyst is critical for pinpointing the roles of Fe during water oxidation. Here, the authors report that iron incorporation and oxygen evolution reaction (OER) are highly coupled, especially at high working potentials. The iron incorporation rate is much higher at OER potentials than that at the OER dormant state (low potentials). At OER potentials, iron incorporation favors electrochemically more reactive edge sites, as visualized by synchrotron x-ray fluorescence microscopy. Fe incorporation can lead to improved OER catalytic activity. From C. Kuai et al., J. Am. Chem. Soc. **143**(44), 18519 (October 2021). Copyright © 2021 American Chemical Society

One of the most important and basic processes in the continual quest for cleaner and more efficient energy is the generation of molecular oxygen from water through a catalytic process called the oxygen evolution reaction (OER). Electrocatalysis by OER is relatively slow and inefficient, however, spurring great efforts to study the OER mechanism and develop high-performance OER catalysts. One approach involves the incorporation of iron into the process, but its exact role and effect are fiercely debated. An international group of researchers used the APS and Stanford Synchrotron Radiation Lightsource (SSRL) to track iron incorporation in nickel hydroxide nanosheets and its effects on electrocatalytic performance. Their work appeared in the *Journal of the American Chemical Society*.

Nickel (Ni)-based hydroxides have been recognized for some years to be extremely promising candidates as alkaline OER catalysts. Adding to their attractiveness is the relative abundance and low cost of nickel compounds compared to catalysts based on rare precious metals. In this work, the researchers expanded on their previous studies to investigate the dynamic OER chemical environment in finer detail by following the lattice incorporation and distribution of iron (Fe) in two-dimensional Ni hydroxide nanosheets (Fig. 1) using synchrotron x-ray fluorescence microscopy (XFM) and hard x-ray absorption spec-

troscopy (XAS) at the XSD Microscopy Group's 2-ID and XSD Spectroscopy Group's 20-ID x-ray beamlines (respectively) at the APS, and soft x-ray absorption spectroscopy at the SSRL at the SLAC National Accelerator Laboratory.

The research team first conducted cyclic voltammetry (CV) studies on the nanosheets in an electrolyte solution with added Fe cations and conducted XFM studies at the APS 2-ID beamline. After 50 CV cycles, the nanosheets show definite Fe incorporation into the Ni hydroxide lattice, mostly concentrated at edge sites. The experimenters propose that this likely indicates a strong connection between Fe incorporation and the OER process, because these lattice edge sites contain more oxygen vacancies and are thus more OER reactive. Incorporation also appears to occur more actively when the sample is cycled at more reactive OER states than during dormant cycles, a conclusion confirmed with chronoamperometry (CA) measurements.

After these experiments, the x-ray studies of the nanosheets provided deeper insight into how the chemical environment at high OER potential was altered by Fe incorporation. Hard XAS measurements at the APS 20-ID beamline and soft XAS at the Stanford facility confirmed that Fe incorporation, mostly but not exclusively at the Ni edge sites, suppresses Ni oxidation and enhances Ni reducibility, with the overall effect of improving OER catalytic activity.

Electrochemical measurements of the Ni nanosheets in electrolyte with and without added Fe appears to confirm the relationship between reduced Ni and increased OER activity. The researchers hypothesize that this may be due to increased electron density between Ni and oxygen with the incorporation of Fe into the lattice, a finding confirmed with density functional theory calculations.

Along with the previous work performed by this group of researchers, these new experiments offer new and vital insight into OER electrocatalysis, demonstrating how dynamic metal dissolution and subsequent redeposition set the stage for significantly enhanced catalytic performance. With this more detailed understanding of the dynamics of the electrocatalyst-electrolyte interface, the design and tailoring of electrochemical materials becomes a practical prospect. It's possible to improve the performance of Ni-based hydroxide catalysts by tuning their electronic modulation not with expensive rare materials but with the incorporation of iron–the most common element in the Earth's crust. – Mark Wolverton

See: Chunguang Kuai[1,2,3], Cong Xi[2], Anyang Hu[3], Yan Zhang[2,4], Zhengrui Xu[3], Dennis Nordlund[4], Cheng-Jun Sun[5], Christopher A. Cadigan[6], Ryan M. Richards[6], Luxi Li[5]*, Cun-Ku Dong[2], Xi-Wen Du[2]**, Feng Lin[3]***, "Revealing the Dynamics and Roles of Iron Incorporation in Nickel Hydroxide Water Oxidation Catalysts," J. Am. Chem. Soc. **143**(44), 18519 (October 2021). DOI: 10.1021/jacs.1c07975
Author affiliations: [1]Wuhan University, [2]Tianjin University, [3]Virginia Tech, [4]SLAC National Accelerator Laboratory, [5]Argone National Laboratory, [6]Colorado School of Mines
Correspondence: * luxili@anl.gov, ** xwdu@tju.edu.cn, *** fenglin@vt.edu

This work was primarily supported by the Department of Chemistry Startup Funds and the Institute for Critical Technology and Applied Science at Virginia Tech. Use of the Stanford Synchrotron Radiation Lightsource, SLAC National Accelerator Laboratory, was supported by the U.S. Department of Energy (DOE) Office of Science-Basic Energy Sciences, under contract no. DE-AC02-76SF00515. The work at Tianjin University was supported by the Natural Science Foundation of China (grant nos. 51871160, 51671141, and 51471115). The work at Wuhan University was supported by the School of Electrical Engineering and Automation Startup Funds. This research used resources of the Advanced Photon Source, a U.S. DOE Office of Science user facility operated for the DOE Office of Science by Argonne National Laboratory under Contract No. DE-AC02-06CH11357.

Understanding Carbon-Hydrogen Bond Activation Could Improve Chemistry's Sustainability

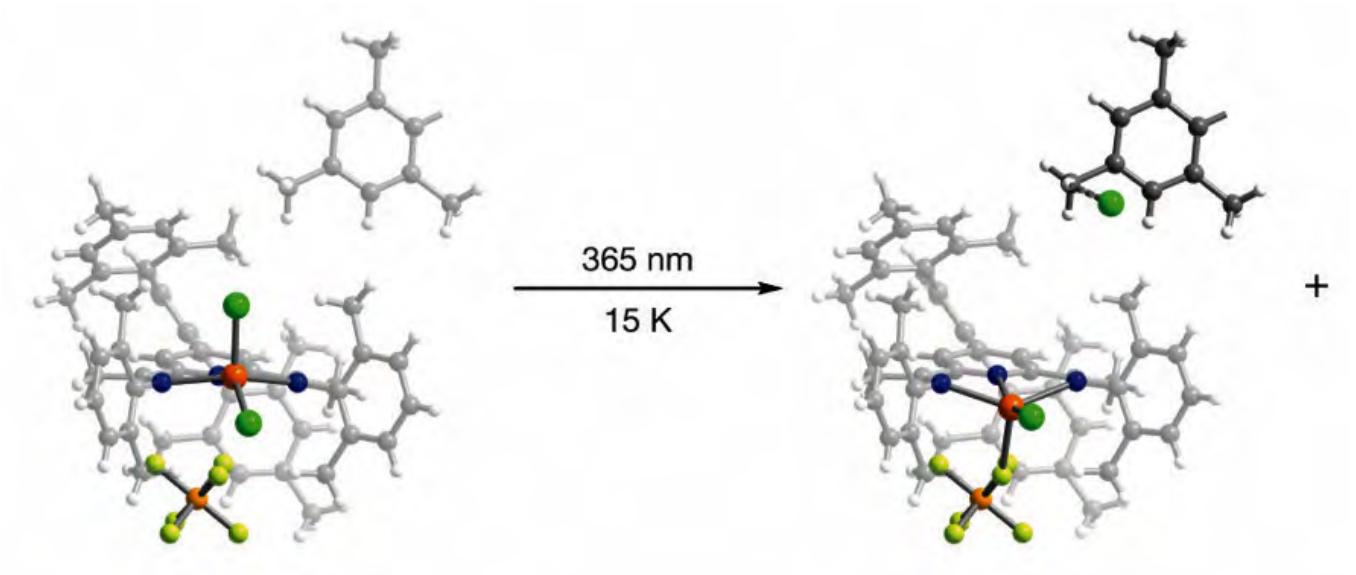

Fig. 1. The resulting molecular structure before and after photolysis cleaves the apical chlorine atom from an iron (III) chloride-pyridinediimine complex. The middle structure highlights that the apical chlorine atom activates the more distant hydrogen bond (on the methyl group depicted above the pyridinediimine complex).

To make industrial, pharmaceutical, and other common chemical processes more sustainable, chemists are turning to types of chemical reactions that require less energy and fewer precious metals. One type of reaction that fits these criteria is photoredox catalysis. In photoredox catalysis, light (such as sunlight) is used to trigger the movement of an electron from one compound to another, most often by the removal of a hydrogen atom. To be able to more efficiently apply photoredox catalysis to a variety of chemical processes, scientists need clearer insight into the intermediate reaction steps that occur when the bond between a carbon atom and a hydrogen atom is broken. Research at the APS demonstrates the synthesis of a new, metal-based photoredox catalyst that allows the team to directly observe the intermediate species during hydrogen-carbon bond cleavage, increasing society's ability to benefit from more sustainable chemical processes. These results were published in the *Journal of the American Chemical Society*.

While carbon-hydrogen bonds are ubiquitous in nature and commercial chemical processes, there are challenges in determining what occurs when a bond splits. One challenge is that the exact sequence of compounds formed during bond fission is difficult to determine because the intermediate species created in the process are unstable. Another is the challenge of designing a compound to cleave the hydrogen atom from the carbon atom.

To address the first issue, the team chose to measure the fission process using time-resolved transient absorption spectroscopy because it allows them to directly observe the intermediates. This is different from previous studies that rely on measurements from multiple techniques.

To address the second, the team designed a compound which would easily cleave hydrogen atoms from a hydrocarbon in a crystalline lattice.

To be certain that they could remove a hydrogen atom from its existing bond, the team built a specific molecular complex that leverages chlorine for two reasons: first, because chlorine radicals are very good at cleaving hydrogen atoms from their existing bonds, and second, because chlorine can be excited from its existing position in a molecular complex through photolysis.

The new molecule is an iron (III) chloride-pyridinediimine complex where the iron atom is bonded to two chlorine atoms, one of which is located above the plane of the iron-nitrogen bonds (in what is called the apical position).

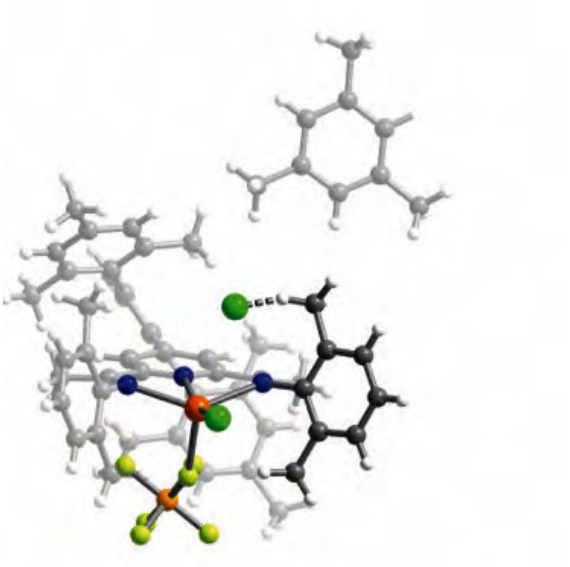

Crystallographic measurements of the complex revealed five methyl groups relatively near the apical chlorine atom, four part of the same complex and one part of an adjacent complex, giving many carbon–hydrogen bond options for the chlorine radical.

The team used photocrystallography with the ChemMatCARS 15 ID-B x-ray beamline at the APS to measure the positions of atoms in the crystalline lattice and the complex, both before and after illuminating the system (which began the fission process by photolysing the chlorine atom). The team applied molecular dynamics and density functional theory modeling to their measurements, allowing them to determine the trajectory of the relevant atoms during carbon-hydrogen bond activation. Combining the results from these techniques allowed the team to piece together the following sequence of events, whose beginning and end stages are shown in Fig. 1.

When the applied light removed the apical chlorine atom from the complex (through photoelimination), the chlorine radical interacted with a neighboring complex by sharing small amounts of electron charge (a charge-transfer complex). This then activated a carbon–hydrogen bond of either a methyl group directly adjacent to the apical chlorine atom or a methyl group on a nearby iron (III) chloride-pyridinediimine complex, which resulted in formation of a carbon-centered radical and hydrogen chloride.

Unexpectedly, the team found that activation of the more distant carbon–hydrogen bond was favored rather than the activation of one directly adjacent to the apical chlorine atom. From this the team concluded that carbon hydrogen bond activation is affected by the direction in which the chlorine radical is photo-eliminated.

By determining the sequence of events and species created during the carbon-hydrogen bond activation, the team was able to create a complete reaction profile for the process. With this greater insight into the details, the team's results make further progress toward the employment of more sustainable chemical processes in a variety of pharmaceutical and industrial applications.

– Mary Alexandra Agner

See: David Gygi[1], Miguel I. Gonzalez[1], Seung Jun Hwang[1], Kay T. Xia[1], Yangzhong Qin[1], Elizabeth J. Johnson[1], François Gygi[2], Yu-Sheng Chen[3], and Daniel G. Nocera[1]*, "Capturing the Complete Reaction Profile of a C–H Bond Activation," J. Am. Chem. Soc. **143**, 16, 6060 (April 16, 2021). DOI: 10.1021/jacs.1c02630

Author affiliations: [1]Harvard University, [2]University of California, Davis, [3]The University of Chicago
Correspondence: * dnocera@fas.harvard.edu

This research was supported by the National Science Foundation (NSF) Division of Chemistry under the Grant CHE-1855531. D.G. and E.J.J. acknowledge the NSF for Graduate Research Fellowships. M.I.G. acknowledges the Arnold and Mabel Beckman Foundation for an Arnold O. Beckman Postdoctoral Fellowship. S.J.H. acknowledges the Ludo Frevel Crystallography Scholarship. ChemMatCARS is supported by the Divisions of Chemistry and Materials Research, NSF, under Grant CHE-1834750. This research used resources of the Advanced Photon Source, a U.S. Department of Energy (DOE) Office of Science user facility operated for the DOE Office of Science by Argonne National Laboratory under contract no. DE-AC02-06CH11357.

Characterizing Countercations around a Polyoxometalate Cluster Explains its Coagulation Behavior

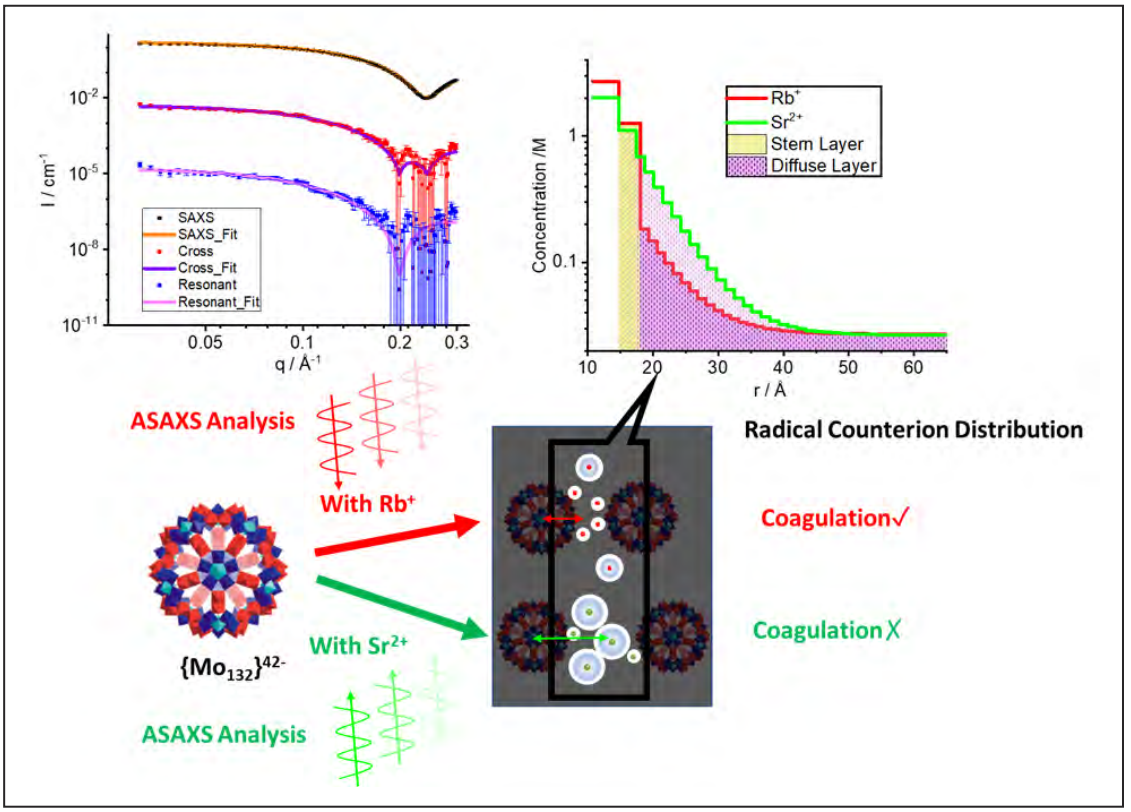

Fig. 1. Catching a rambling counterion in solution: Counterions regulate all kinds of processes in liquid solutions, and they are yet to be understood, due to their highly mobilized and diffused nature. The ASAXS studies carried out at ChemMatCARS provided a quantitative spatial distribution of counterions around charged macromolecules, which revealed the secret behind unprecedented solution behaviors of charged macromolecules with certain charge distributions.

The current pandemic has made the names of biomacromolecules like nucleic acids, antibodies, etc., common household terms. However, in order to study these biomacromolecules, scientists first need to purify them from their crude product. Salting-out is a low-cost purification technique that uses the presence of salts to precipitate biomacromolecules in solution by reducing the solubility of the macromolecules. How salt affects the solubility of the biomacromolecules is still poorly understood. One of the most famous puzzles in this field is the more than 100-year-old "Hofmeister Series," which holds that the small ions carrying the same amount of charges can still show their distinct effects on biomacromolecules. Although it is still in debate, a function of the interaction between the electrostatic and hydration effects has been proposed to explain such effects. Understanding the circumstances that allow for the domination of each type of effect requires more insight into how ions interact in solution. To illuminate the interactions, a team of scientists from The University of Akron used the APS to examine a model, measuring the quantity and spatial distribution of its surrounding small ions. Their results, published in the journal *Angewandte Chemie International Edition*, show the valency of the counterions and the charge distribution of the macromolecule directly impacts whether hydration or electrostatic effects will play a larger role.

The model chosen by the team was a molybdenum-based polyoxometalate cluster (denoted as $\{Mo_{132}\}$): a 2.5-

nanometers-diameter hollow spherical nanoparticle with a net negative charge, balanced by countercations. {{Mo_{132}} is interesting for its unusual higher solubility with divalent alkaline earth metal cations than with monovalent alkaline metal cations. It is opposite to common observations and the prediction in classical theories that the counterions with higher valency will more effectively screen the electrostatic repulsion between the macromolecules, and therefore macromolecules with higher valent counterions are easier to aggregate and eventually precipitate from solution.

Although it is known that counterions with the same valency in the Hofmeister Series have hydration-dependent interactions, electrostatic interactions dominate when it comes to the difference in valency. Therefore, classical theories cannot explain the unusual solubility behavior of the {{Mo_{132}} cluster in the presence of different valence counterions. The team hypothesized that this behavior was caused by other factors that put the effects of hydration over the difference of electrostatic interactions between the divalent strontium (Sr^{2+}) cations and monovalent rubidium (Rb^{+}) cations.

To test this hypothesis, the team characterized the distribution and quantity of the countercations around {{Mo_{132}} using anomalous small-angle x-ray scattering (ASAXS) at the ChemMatCARS 15-ID-D x-ray beamline at the APS. In solution, the counterions will form a “cloud” around the charged macromolecule, called the electrical double layer. The electrical double layer has two parts: an inner layer consisting of strongly bound ions and a diffuse one of loosely bound ions further from the core. In solution, these clusters' countercation cloud is diffused and loosely interacting in nature, so the only research technique that will directly probe the countercations is ASAXS. The team’s ASAXS results are summarized in Fig. 1. They found that, independent of the concentration of salts in the solution, most of the rubidium cations were located near the skeleton of {{Mo_{132}} or in the inner layer of its countercation cloud. Increasing the concentration of the RbCl salt increased the amount of Rb^{+} in the inner layer and eventually lead to coagulation. Larger amounts of Sr^{2+} were detected in both the inner and diffuse layers. And, unlike RbCl, increasing the concentration of the $SrCl_2$ salt did not appreciably increase the number of Sr^{2+} in the inner layer, nor did it lead to coagulation up to 1 M (compared with RbCl where coagulation occurred at approximately 15-fold less).

The team concluded that the differences in rubidium and strontium results are a function of whether the electrostatic interaction or hydration effects are stronger. The electrostatic attraction between countercation and macromolecules facilitates their association, while the hydration (layer) around countercations prevents the association. Because most of the {{Mo_{132}} charges are within its skeleton, there is a larger separation distance between its negative charge and the countercations. As the strength of the electrostatic interacts is reversely proportional to the square of the distance, the longer separation weakens the electrostatic interactions. Although Sr^{2+} has a much stronger electrostatic interaction with {{Mo_{132}} than Rb+ due to its higher valency, Sr^{2+} is also much more heavily hydrated than Rb^{+}. In this case, due to the special charge distribution of {{Mo_{132}}, the effects of the electrostatic interaction are weaker than the hydration, thus Sr^{2+} has a lower affinity to {{Mo_{132}} and stays further. The team concluded that these differences also explain why the critical coagulation concentration differs between strontium and rubidium solutions. Sr^{2+} spread further from the skeleton of {{Mo_{132}}] and, unlike Rb^{+}, cannot facilitate the short-range attraction that makes coagulation happen.

The team's results diligently show the balance between the electrostatic interaction and hydration effects, adding to our understanding of the behavior of charged macromolecules in solution and furthering the step to the solution of the long-standing puzzle of the Hoffmeister Series. – Mary Alexandra Agner

See: Jiahui Chen[1], Mrinal K. Bera[2]**, Hui Li[1], Yuqing Yang[1], Xinyu Sun[1], Jiancheng Luo[1], Jessi Baughman[1], Cheng Liu[1], Xuesi Yao[1], Steven S.C. Chuang[1], and Tianbo Liu[1]*, “Accurate Determination of the Quantity and Spatial Distribution of Counterions around a Spherical Macroion,” Angew. Chem. Int. Ed. **60**, 5833 (2021).
DOI: 10.1002/anie.202013806
Author affiliations: [1]The University of Akron, [2]The University of Chicago
Correspondence: * tliu@uakron.edu,
** mrinalkb@cars.uchicago.edu

T.L. acknowledges support by The University of Akron and the National Science Foundation (NSF, CHE1607138 and CHE1904397). ChemMatCARS is supported by the Divisions of Chemistry (CHE) and Materials Research (DMR), NSF, under grant number NSF/CHE-1834750. Use of the Advanced Photon Source, an Office of Science user facility operated for the U.S. Department of Energy (DOE) Office of Science by Argonne National Laboratory, was supported by the U.S. DOE under Contract No. DE-AC02-06CH11357.

Decker, Thurman, and Zholents of APS Receive Argonne Board of Governors Awards



L. to r.: Glenn Decker, Arista Thurman, Sasha Zholents

Alexander (Sasha) Zholents was presented with a 2021 Argonne National Laboratory Distinguished Performance Award by the UChicago Argonne, LLC, Board of Governors. Zholents is an Argonne Distinguished Fellow and a Senior Physicist in the APS Accelerator Systems Division (ASD).

Glenn Decker (APS Upgrade) was presented with a 2021 Outstanding Safety Leadership Award by the UChicago Argonne, LLC, Board of Governors.

Arista Thurman (APS Engineering Support Division) was presented with a 2021 Excellence in Diversity and Inclusion Award by the UChicago Argonne, LLC, Board of Governors.

These awards recognize distinguished performance and outstanding scientific or engineering achievement by individual members of the Argonne professional staff, technicians, and others engaged in scientific and technical activities.

Sun of ASD Named Accelerator Operations and Physics Group Leader

Yine Sun was appointed group leader of the ASD Accelerator Operations and Physics Group. Sun is a member of the Scientific Advisory Board for the International Particle Accelerator Conference and a convenor for the Snowmass 2021 Accelerator Frontier, Accelerator Technology Topical Group. Sun's honors include the ASD Appreciation Award for extraordinary effort in the planning, management, commissioning, and operation of linac interleaving; and a Fermilab Exceptional Performance Recognition Award for her work in beam phase-space manipulation in a photo-injector. She is the author or co-author on many peer reviewed publications and has an extensive list of invited talks at conferences and workshops.

Greene, NHMFL Chief Scientist and Member of the APS Scientific Advisory Committee, Named to PCAST

Laura Greene has been appointed by President Biden to serve on the President's Council of Advisors on Science and Technology (PCAST). Greene is the chief scientist at the National High Magnetic Field Laboratory located at Florida State University, the University of Florida, and Los Alamos National Laboratory; and is a member of the APS Scientific Advisory Committee. PCAST advises the president on matters involving science, technology, and innovation policy, as well as on matters involving scientific and technological information that is needed to inform public policy relating to the economy, worker empowerment, education, energy, the environment, public health, national and homeland security, racial equity, and other topics.

Ilavsky of XSD Named a Fellow of the American Crystallographic Association

Jan Ilavsky, physicist and beamline scientist with the XSD Chemical & Materials Science Group, which operates or co-operates four x-ray beamlines at the APS, has been named a Fellow of the American Crystallographic Association (ACA). Ilavsky is one of seven scientists named to the ACA Fellows class of 2021.

Kelly Named XSD Spectroscopy Group Leader

Shelly Kelly was appointed leader of the XSD Spectroscopy Group. She is an expert in x-ray absorption spectroscopy (XAS) and was a long-time user of the APS as an Argonne research physicist studying the fate and transport of contaminants in natural systems using XAS. In 2011, Kelly joined Honeywell UOP, studying catalysis systems, and served as Senior Manager R&D of the Advanced Characterization Group. Kelly is an author or co-author on over 70 peer-reviewed publications and three book chapters on XAS.

Life Sciences

Mouse Brain Imaged from the Microscopic to the Macroscopic Level

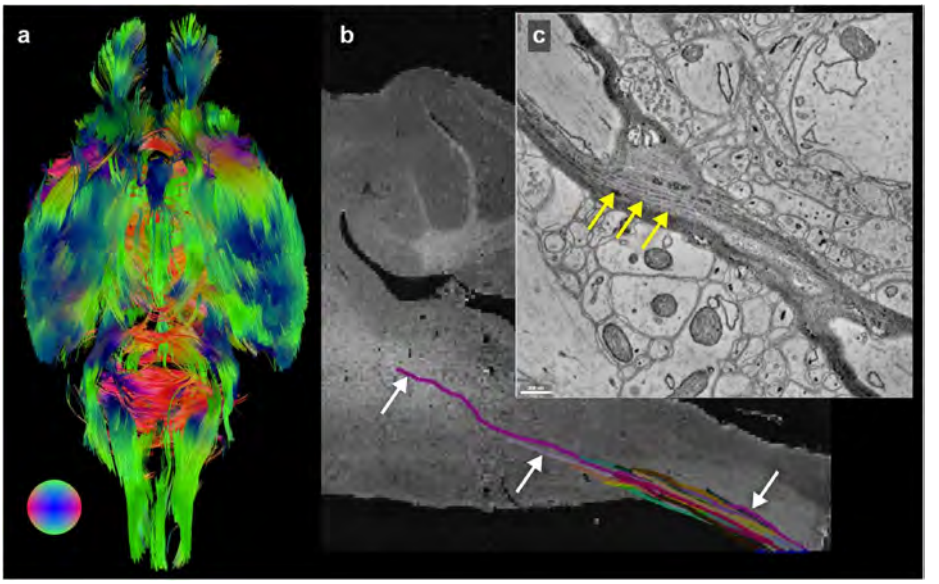

Fig. 1. By using an imaging pipeline of MRI, µCT, and EM, Foxley, Kasthuri, and their team were able to simultaneously resolve brain structures, like the white matter, at (a) macro-, (b) meso-, and (c) microscopic-scales in the same brain. Image from Foxley et al., NeuroImage **2348**, 118250 (September 2021). Copyright © 2021. Published by Elsevier Inc.

The original University of Chicago Medical Center press release by Alison Caldwell can be read here.

Researchers at the University of Chicago and Argonne have leveraged existing advanced x-ray microscopy (EM) techniques to bridge the gap between MRI (magnetic resonance imaging) and electron microscopy imaging, providing a viable pipeline for multiscale whole brain imaging within the same brain. The proof-of-concept demonstration involved using high-brightness, intense x-rays from the DOE's APS to image an entire mouse brain across five orders of magnitude of resolution, a step which researchers say will better connect existing imaging approaches and uncover new details about the structure of the brain. The advance, which was published in the journal *NeuroImage*, will allow scientists to connect biomarkers at the microscopic and macroscopic level (Fig. 1), improving the resolution of MRI imaging, and provide greater context for electron microscopy.

"Our lab is really interested in mapping brains at multiple scales to get an unbiased description of what brains look like," said senior author Narayanan "Bobby" Kasthuri, Assistant Professor of Neurobiology at the University of Chicago and a neuroscience researcher at Argonne. "When I joined the faculty here, one of the first things I learned was that Argonne had this extremely powerful x-ray microscope [the APS], and it hadn't been used for brain mapping yet, so we decided to try it out."

The "microscope" uses a type of imaging called synchrotron-based x-ray tomography, which can be likened to a "micro-CT," or micro-computerized tomography (µCT) scan. Thanks to the powerful x-rays produced by the APS the researchers were able to image the entire mouse brain—roughly one cubic centimeter—at the resolution of a micron, or 1/10,000 of a centimeter. It took roughly six hours to collect images of the entire brain, adding up to around 2 terabytes of data. This is one of the fastest approaches for whole brain imaging at this level of resolution.

Magnetic resonance imaging can quickly image the whole brain to trace neuronal tracts, but the resolution isn't sufficient to observe individual neurons or their connections. On the other end of the scale, EM can reveal the details of individual synapses, but generates an enormous amount of data, making it computationally challenging to look at pieces of brain tissue larger than a few micrometers in volume. Existing techniques for studying neuroanatomy at the micrometer resolution typically are either merely two-dimensional or use protocols that are incompatible with MRI or EM imaging, making it impossible to use the same brain tissue for imaging at all scales.

The researchers realized that their new micro-CT approach could help bridge this existing resolution gap. "There have been a lot of imaging studies where people use MRI to look at the whole brain level and then try to validate those results using EM, but there's a discontinuity in the resolutions," said article first author Sean Foxley, Research Assistant Professor at UChicago. "It's hard to say anything about the large volume of tissue you see with an MRI when you're looking at an EM dataset, and the X-ray can bridge that gap. Now we finally have something that can let us look across all levels of resolution seamlessly."

Combining their expertise in MRI and EM, Foxley, Kasthuri, and the team opted to attempt mapping a single mouse brain using these three approaches. "Why did we choose the mouse brain? Because it fits in the microscope," Kasthuri said with a laugh. "But also, the mouse is the workhorse of neuroscience; they're very useful for analyzing different experimental conditions in the brain."

After collecting and preserving the tissue, the team placed the sample in an MRI scanner to collect structural images of the entire brain. Next, it was placed on a rotating stage in the μCT scanner at the XSD Imaging Group's 32-ID x-ray beamline at the APS to collect the CT data before specific regions of interest were identified in the brainstem and cerebellum for targeting for EM.

After months of data processing and image tracing that included using μCT reconstruction algorithms at the Argonne Leadership Computing Facility's supercomputers, the researchers determined that they were able to use the structural markers identified on the MRI to localize specific neuronal subgroups in designated brain regions, and that they could trace the size and shape of individual cell bodies. They could also trace the axons of individual neurons as they traveled through the brain and could connect the information from the μCT images with what they saw at the synaptic level with the EM.

This approach will not only be helpful for imaging the brain at the μCT resolution, but also for informing MRI and EM imaging. "Imaging a 1-millimeter cube of the brain with EM, which is the equivalent to about the minimum resolution of an MRI image, produces almost a million gigabytes of data," Kasthuri said. "And that's just looking at a 1-millimeter cube! I don't know what's happening in the next cube, or the next, so I don't really have context for what I'm seeing with EM. MRI can provide some context except that scale is too big to bridge. Now this μCT gives us that needed context for our EM work."

Foxley is excited about how this approach can be used for understanding the living brain via MRI. "This technique gives us a really clear way to identify changes in the microstructure of the brain when there is a disease or injury present," he said. "So now we can start looking for biomarkers with the μCT that we can then trace back to what we see on the MRI in the living brain. The APS x-rays lets us look at things on the cellular level, so then we can ask, what changed at the cellular level that produced a global change in the MRI signal on a macroscopic level?"

The team is already using this technique to begin exploring important questions in neuroscience, looking at the brains of mice that have been genetically engineered to develop Alzheimer's disease to see if they can trace the Ab plaques seen with μCT back to measurable changes in MRI scans, especially in early stages of the disease.Because this work was done at Argonne, this resource will be open and freely accessible to other scientists around the world, making it possible for researchers to begin asking and answering questions that span the whole brain and reach down to the synaptic level.

At the moment, the UChicago team is most interested in continuing to refine the technique. "The next step is to do an entire primate brain," said Kasthuri. "The mouse brain is possible, and useful for pathological models. But what I really want to do is get an entire primate brain imaged down to the level of every neuron and every synaptic connection. And once we do that, I want to do an entire human brain."

See: Sean Foxley[1]*, Vandana Sampathkumar[1], Vincent De Andrade[2] , Scott Trinkle[1], Anastasia Sorokina[1], Katrina Norwood[1], Patrick La Riviere[1], and Narayanan Kasthuri[1], "Multimodal imaging of a single mouse brain over five orders of magnitude of resolution," NeuroImage **2348**, 118250 (September 2021). DOI: 10.1016/j.neuroimage.2021.118250
Author affiliations: [1]The University of Chicago, [2]Argonne National Laboratory
Correspondence: * foxley@uchicago.edu

N.K. and V.S. are supported from a Technical Innovation Award from the McKnight foundation, a Brain Initiative of the National Institutes of Health (NIH) (U01 MH109100), and National Science Foundation Neuro Nex grant. P.LR. is partially supported by the NIH (R01EB026300). S.T. is supported by the National Institute of Neurological Disorders and Stroke of NIH (F31NS113571). Partial funding for this work was provided by the NIH S10 Award OD025081-01, and by the previous awards NIH S10 RR021039 and P30 CA14599. Additional funding supporting this work was provided by the NIH (S10-OD025081, S10- RR021039, and P30-CA14599). This research also used resources of the Argonne Leadership Computing Facility, which is a U.S. Department of Energy (DOE) Office of Science user facility supported under Contract DE-AC02-06CH11357, and of the Advanced Photon Source, a U.S. DOE Office of Science user facility operated for the DOE Office of Science by Argonne National Laboratory under Contract No. DE-AC02-06CH11357.

Shining a Healing Light on the Brain

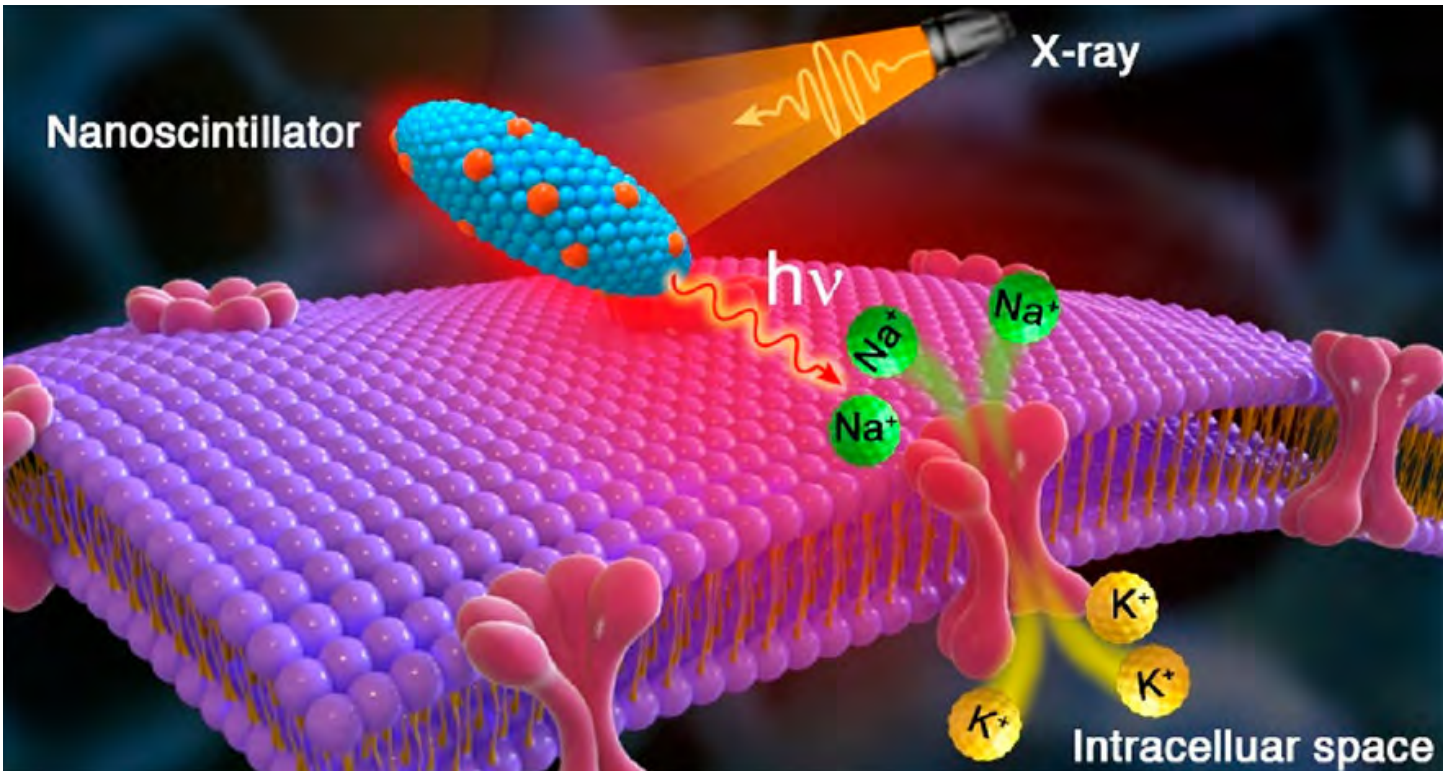

Artist's rendering shows x-rays striking radioluminescent nanoparticles in the brain, which emit red light that triggers a sodium (Na^+) and potassium (K^+) ion influx and thereby activates brain neurons. Image: Zhaowei Chen/Argonne National Laboratory.

The original Argonne press release by Joseph E.Harmon can be read here.

Many people worldwide suffer from movement-related brain disorders. Epilepsy accounts for more than 50 million; essential tremor, 40 million; and Parkinson's disease, 10 million. Relief for some brain disorder sufferers may one day be on the way in the form of a new treatment invented by researchers from Argonne and four universities. The treatment is based on breakthroughs in both optics and genetics as reported in the journal *ACS Nano*. It would be applicable to not only movement-related brain disorders, but also chronic depression and pain.

This treatment involves stimulation of neurons deep within the brain by means of injected nanoparticles that light up when exposed to x-rays (nanoscintillators) and would eliminate an invasive brain surgery currently in use.

"Our high-precision noninvasive approach could become routine with the use of a small x-ray machine, the kind commonly found in every dental office," said Elena Rozhkova, a lead author of the *ACS Nano* paper and a nanoscientist in Argonne's Center for Nanoscale Materials (CNM).

Traditional deep brain stimulation requires an invasive neurosurgical procedure for disorders when conventional drug therapy is not an option. In the traditional procedure, approved by the U.S. Food and Drug Administration, surgeons implant a calibrated pulse generator under the skin (similar to a pacemaker). They then connect it with an insulated extension cord to electrodes inserted into a specific area of the brain to stimulate the surrounding neurons and regulate abnormal impulses.

"The Spanish-American scientist José Manuel Rodríguez Delgado famously demonstrated deep brain stimulation in a bullring in the 1960s," said Vassiliy Tsytsarev, a neurobiologist from the University of Maryland and a co-author of the study. "He brought a raging bull charging at him to a standstill by sending a radio signal to an implanted electrode."

About 15 years ago, scientists introduced a revolutionary neuromodulation technology, "optogenetics," which relies on genetic modification of specific neurons in the

brain. These neurons create a light-sensitive ion channel in the brain and fire in response to external laser light. This approach, however, requires very thin fiberoptic wires implanted in the brain and suffers from the limited penetration depth of the laser light through biological tissues.

The team's alternative optogenetics approach uses nanoscintillators injected in the brain, bypassing implantable electrodes or fiberoptic wires. Instead of lasers, they substitute x-rays because of their greater ability to pass through biological tissue barriers.

"The injected nanoparticles absorb the x-ray energy and convert it into red light, which has significantly greater penetration depth than blue light," said Zhaowei Chen, former CNM postdoctoral fellow.

"Thus, the nanoparticles serve as an internal light source that makes our method work without a wire or electrode," added Rozhkova. Since the team's approach can both stimulate and quell targeted small areas, Rozhkova noted, it has other applications than brain disorders. For example, it could be applicable to heart problems and other damaged muscles.

One of the team's keys to success was the collaboration between two of the world-class facilities at Argonne: the CNM and the APS. The work at these facilities began with the synthesis and multi-tool characterization of the nanoscintillators. In particular, the x-ray excited optical luminescence of the nanoparticle samples was determined at the XSD Spectroscopy Group's 20-BM beamline at the APS. The results showed that the particles were extremely stable over months and upon repeated exposure to the high-intensity x-rays.

According to Zou Finfrock, a staff scientist at the 20-BM beamline and at the Canadian Light Source, "They kept glowing a beautiful orange-red light."

Next, Argonne sent CNM-prepared nanoscintillators to the University of Maryland for tests in mice. The team at University of Maryland performed these tests over two months with a small portable x-ray machine. The results proved that the procedure worked as planned. Mice whose brains had been genetically modified to react to red light responded to the x-ray pulses with brain waves recorded on an electroencephalogram.

Finally, the University of Maryland team sent the animal brains for characterization using x-ray fluorescence microscopy performed by Argonne scientists. This analysis was performed by Olga Antipova on the Microscopy Group's microprobe beamline (2-ID-E) at the APS, and by Zhonghou Cai of the Microscopy Group on the Hard X-ray Nanoprobe at APS beamine 26-ID, which is jointly operated by the CNM and the APS Microscopy Group.

This multi-instrument arrangement made it possible to see tiny particles residing in the complex environment of the brain tissue with a super-resolution of dozens of nanometers. It also allowed visualizing neurons near and far from the injection site on a microscale. The results proved that the nanoscintillators are chemically and biologically stable. They do not wander from the injection site or degrade.

"Sample preparation is extremely important in these types of biological analysis," said Antipova, a physicist in the XSD. Antipova was assisted by Qiaoling Jin and Xueli Liu, who prepared brain sections only a few micrometers thick with jeweler-like accuracy.

"There is an intense level of commercial interest in optogenetics for medical applications," said Rozhkova. "Although still at the proof-of-concept stage, we predict our patent-pending wireless approach with small x-ray machines should have a bright future."

See: Zhaowei Chen[1,3], Vassiliy Tsytsarev[2]**, Y. Zou Finfrock[1], Olga A. Antipova[1], Zhonghou Cai[1], Hiroyuki Arakawa[4], Fritz W. Lischka[5], Bryan M. Hooks[6], Rosemarie Wilton[1], Dongyi Wang[2], Yi Liu[2], Brandon Gaitan[2], Yang Tao[2], Yu Chen[2], Reha S. Erzurumlu[4], Huanghao Yang[3], and Elena A. Rozhkova[1]*, "Wireless Optogenetic Modulation of Cortical Neurons Enabled by Radioluminescent Nanoparticles," ACS Nano **15**, 5201 (2021). DOI: 10.1021/acsnano.0c10436

Author affiliations: [1]Argonne National Laboratory, [2]University of Maryland, [3]Fuzhou University, [4]University of Maryland School of Medicine, [5]University of the Health Sciences, [6]University of Pittsburgh

Corresponding authors: * rozhkova@anl.gov,
** tsytsarev@umaryland.edu

Histological analyses of brain sections conducted in the Erzurumlu Laboratory were supported by Grant Nos. NIH/NINDS R01NS092216 and R01NS092216S1. Work performed in part at the University of Maryland was supported by the National Science Foundation, under Grant No. CBET-1254743. Use of the Advanced Photon Source and work performed in part at the Center for Nanoscale Materials, both U.S. Department of Energy (DOE) Office of Science User Facilities, was supported by the U.S. Department of Energy, Office of Science, under Contract No. DE-AC02-06CH11357.

From Amphibians to Mammals, the Same Spark of Life

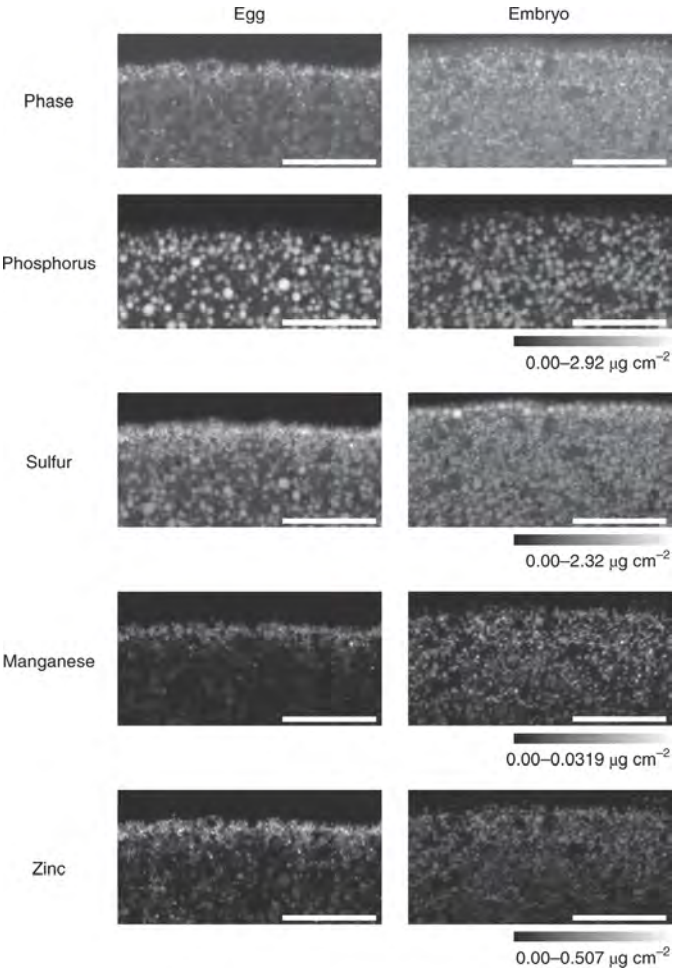

Fig. 1. X-ray fluorescence microscopy images of the animal poles of fixed *Xenopus* egg/embryo slices show that zinc and manganese are localized in small cortical compartments. Scale bars, 20 µm. Images were acquired at APS beamline 2-ID. Pixel size, 300 × 300 nanometers; slice thickness, 2 µm; scan time, 500 ms per pixel. These are representative images of slices of eggs/embryos from seven different frogs imaged over three experiments. From J.F. Seeler et al., Nat. Chem. **13**, 683 (July 2021). © 2021 Springer Nature Limited

At the very earliest moments of mammalian life—immediately after fertilization of an egg—there is metallic explosion. The newly minted embryo releases a coordinated display of zinc ions into the surrounding environment, with the goal of confounding unwanted extra sperm from attempting to enter the cell. Such polyspermy can be devastating. While scientists have observed the "zinc spark" in mice, monkeys, and humans, it hasn't been clear how far down the evolutionary line this phenomenon stretches. To help find out, researchers looked to a species of frog—*Xenopus laevis*—known for the large size and abundance of their eggs. Using the APS they performed x-ray fluorescence microscopy (XFM) on frog eggs and embryos. This and other published data suggested that frog eggs do indeed exhibit the zinc spark, but the researchers also found something surprising: a manganese spark. The findings, published in *Nature Chemistry*, point to the conservation of zinc and manganese release in vertebrates, with the overall goal of blocking polyspermy, and saving a life.

It wasn't always clear that frog eggs would exhibit the zinc spark; in fact, some studies suggested otherwise. While the zinc content in mouse eggs decreases by 20% after fertilization, mass spectroscopy studies—which can hone in on zinc concentrations in cells—showed that *Xenopus* eggs and embryos appear to have similar amounts of zinc. Inductively coupled plasma mass spectrometry (ICP-MS) studies also didn't show zinc concentration differences between *Xenopus* eggs and embryos 1 hour after fertilization. And yet, fluorescence optical microscopy clearly reveals zinc exiting cells immediately after fertilization. To explain this seeming discrepancy, the researchers in this study point to the size of the *Xenopus* eggs. Unlike mammalian eggs, *Xenopus* eggs store most of their zinc in the yolk, which wouldn't be accessible for release after fertilization. The methods that failed to observe a difference in zinc levels between eggs and embryos may not be sensitive enough to account for the relatively small release of zinc after fertilization compared to the large store of zinc in the yolk.

But why stop at zinc? The researchers used these same methods to explore the concentrations of other transition metals in *Xenopus* eggs before and after fertilization. That's when they saw a whopping 53% drop in manganese levels after fertilization, which clearly required some additional study, as such a phenomenon had not been noticed previously across the animal kingdom.

As a first step in their manganese exploration, the researchers tried to figure out where in the cell the manganese was located and with what other molecules the manganese was associating. Using XFM at the XSD Microscopy Group's 2-ID x-ray beamline at the APS, they were able to visualize metals within single cells and discovered that the manganese, along with the zinc, was compartmentalized (Fig. 1). The cellular location of these metals was further characterized using analytical electron microscopy (AEM) performed using the Argonne PicoProbe as well as AEM resources in the Argonne Center for Nanoscale Materials. In mammalian cells, the zinc that eventually leaves the cell upon fertilization is first housed within the cell in compartments called cortical granules. These organelles are found in egg cells, located around the outskirts of the cell, and are designed to be secreted from the cell. Upon fertilization, the cortical granules emerge from the cell to release zinc, promoting the hardening of the cell that thwarts polyspermy. It turns out that manganese release also blocks polyspermy.

In the end, the study established that zinc aggregates in vesicles near the surface of frog eggs, which are released after fertilization to block sperm from entering the cell. The surprising release of manganese alongside zinc demands that scientists ask the question of whether manganese plays a similar role in other vertebrates, particularly humans. Future single cell studies in other organisms, similar to those performed in these frog cells, may reveal the importance of manganese at these critical early moments of life. – Erika Gebel Berg

See: John F. Seeler[1], Ajay Sharma[1], Nestor J. Zaluzec[2], Reiner Bleher[1], Barry Lai[2], Emma G. Schultz[1], Brian M. Hoffman[1], Carole LaBonne[1]*, Teresa K. Woodruff[1,3]**, and Thomas V. O'Halloran[1,3]***, "Metal ion fluxes controlling amphibian fertilization," Nat. Chem. **13**, 683 (July 2021). DOI: 10.1038/s41557-021-00705-2
Author affiliations: [1]Northwestern University, [2]Argonne National Laboratory, [3]Michigan State University
Correspondence: * clabonne@northwestern.edu, ** tkw@msu.edu, *** ohallor8@msu.edu

This research is supported by National Institutes of Health (NIH) grants R01GM115848 (T.V.O. and T.K.W.), R01GM038784 and P41GM181350 (T.V.O.), and R01GM111097 (B.M.H.). J.F.S. was supported by The Cellular and Molecular Basis of Disease Training Program at Northwestern University (NIH T32GM008061), N.J.Z. was supported by both LDRD funding no. 2017-153-N0 and the Photon Sciences Directorate at Argonne. The Argonne PicoProbe and the Center for Nanoscale Materials (CNM) are U.S. Department of Energy (DOE) Office of Science user facilities at Argonne National Laboratory. Use of the APS and CNM was supported by the U.S. DOE Office of Science-Basic Energy Sciences, under contract no. DE-AC02-06CH11357. This work made use of the BioCryo facility of Northwestern University's NUANCE Center, which has received support from the Soft and Hybrid Nanotechnology Experimental (SHyNE) Resource (NSF ECCS-1542205), the MRSEC programme (NSF DMR-1720139) at the Materials Research Center, the International Institute for Nanotechnology (IIN) and the State of Illinois. Microscopy was performed at the Biological Imaging Facility at Northwestern University (RRID: SCR_017767), supported by the Chemistry for Life Processes Institute, the NU Office for Research and the Department of Molecular Biosciences. Elemental analysis was performed at the Northwestern University Quantitative Bio-element Imaging Center supported by the Office of the Director, NIH, via NIH grants S10OD026786 and S10OD020118.

"Dancing Molecules" Successfully Repair Severe Spinal Cord Injuries

The original "Northwestern [University] Now" article by Amanda Morris can be read here.

Northwestern University researchers have developed a new injectable therapy that harnesses "dancing molecules" to reverse paralysis and repair tissue after severe spinal cord injuries. In a new study, which included research at the APS and was published in the journal *Science*, the team administered a single injection to tissues surrounding the spinal cords of paralyzed mice. Just four weeks later, the animals regained the ability to walk.

By sending bioactive signals to trigger cells to repair and regenerate, the breakthrough therapy dramatically improved severely injured spinal cords in five key ways: (1) The severed extensions of neurons, called axons, regenerated; (2) scar tissue, which can create a physical barrier to regeneration and repair, significantly diminished; (3) myelin, the insulating layer of axons that is important in transmitting electrical signals efficiently, reformed around cells; (4) functional blood vessels formed to deliver nutrients to cells at the injury site; and (5) more motor neurons survived.

After the therapy performs its function, the materials biodegrade into nutrients for the cells within 12 weeks and then completely disappear from the body without noticeable side effects. This is the first study in which researchers controlled the collective motion of molecules through changes in chemical structure to increase a therapeutic's efficacy.

"Our research aims to find a therapy that can prevent individuals from becoming paralyzed after major trauma or disease," said Northwestern's Samuel I. Stupp, who led the study. "For decades, this has remained a major challenge for scientists because our body's central nervous system, which includes the brain and spinal cord, does not have any significant capacity to repair itself after injury or after the onset of a degenerative disease. We are going straight to the FDA to start the process of getting this new therapy approved for use in human patients, who currently have very few treatment options."

According to the National Spinal Cord Injury Statistical Center, nearly 300,000 people are currently living with a spinal cord injury in the United States. Life for these patients can be extraordinarily difficult. Less than 3% of people with complete injury ever recover basic physical functions. And approximately 30% are re-hospitalized at least once during any given year after the initial injury, costing millions of dollars in average lifetime health care costs per patient. Life expectancy for people with spinal cord injuries is significantly lower than people without spinal cord injuries and has not improved since the 1980s.

"Currently, there are no therapeutics that trigger spinal cord regeneration," said Stupp, an expert in regenerative medicine. "I wanted to make a difference on the outcomes of spinal cord injury and to tackle this problem, given the tremendous impact it could have on the lives of patients. Also, new science to address spinal cord injury could have impact on strategies for neurodegenerative diseases and stroke."

The secret behind Stupp's new breakthrough therapeutic is tuning the motion of molecules, so they can find and properly engage constantly moving cellular receptors. Injected as a liquid, the therapy immediately gels into a complex network of nanofibers that mimic the extracellular matrix of the spinal cord. By matching the matrix's structure, mimicking the motion of biological molecules and incorporating signals for receptors, the synthetic materials are able to communicate with cells.

"Receptors in neurons and other cells constantly move around," Stupp said. "The key innovation in our research, which has never been done before, is to control the collective motion of more than 100,000 molecules within our nanofibers. By making the molecules move, 'dance' or even leap temporarily out of these structures, known as supramolecular polymers, they are able to connect more effectively with receptors."

Stupp and his team found that fine-tuning the molecules' motion within the nanofiber network to make them more agile resulted in greater therapeutic efficacy in paralyzed mice. They also confirmed that formulations of their therapy with enhanced molecular motion performed better during *in vitro* tests with human cells, indicating increased bioactivity and cellular signaling.

The team employed a wide range of experimental

techniques to characterize the synthetic materials, including nuclear magnetic resonance imaging; transmission electron microscopy; cryogenic transmission electron microscopy; scanning electron microscopy; circular dichroism spectroscopy; Fourier transformed infrared spectroscopy; and synchrotron solution small-angle x-ray scattering, which was carried out at the DND-CAT x-ray beamline station 5-ID-D at the APS.

"Given that cells themselves and their receptors are in constant motion, you can imagine that molecules moving more rapidly would encounter these receptors more often," Stupp said. "If the molecules are sluggish and not as 'social,' they may never come into contact with the cells."

Once connected to the receptors, the moving molecules trigger two cascading signals, both of which are critical to spinal cord repair. One signal prompts the long tails of neurons in the spinal cord, called axons, to regenerate. Similar to electrical cables, axons send signals between the brain and the rest of the body. Severing or damaging axons can result in the loss of feeling in the body or even paralysis. Repairing axons, on the other hand, increases communication between the body and brain.

The second signal helps neurons survive after injury because it causes other cell types to proliferate, promoting the regrowth of lost blood vessels that feed neurons and critical cells for tissue repair. The therapy also induces myelin to rebuild around axons and reduces glial scarring, which acts as a physical barrier that prevents the spinal cord from healing.

"The signals used in the study mimic the natural proteins that are needed to induce the desired biological responses. However, proteins have extremely short half-lives and are expensive to produce," said Zaida Álvarez, the study's first author. "Our synthetic signals are short, modified peptides that — when bonded together by the thousands — will survive for weeks to deliver bioactivity. The end result is a therapy that is less expensive to produce and lasts much longer." A former research assistant professor in Stupp's laboratory, Álvarez is now a visiting scholar at SQI and a researcher at the Institute for Bioengineering of Catalona in Spain.

While the new therapy could be used to prevent paralysis after major trauma (automobile accidents, falls, sports accidents and gunshot wounds) as well as from diseases, Stupp believes the underlying discovery — that "supramolecular motion" is a key factor in bioactivity — can be applied to other therapies and targets.

"The central nervous system tissues we have successfully regenerated in the injured spinal cord are similar to those in the brain affected by stroke and neurodegenerative diseases, such as ALS, Parkinson's disease and Alzheimer's disease," Stupp said. "Beyond that, our fundamental discovery about controlling the motion of molecular assemblies to enhance cell signaling could be applied universally across biomedical targets."

See: Z. Álvarez[1], A. N. Kolberg-Edelbrock[1], I. R. Sasselli[1‡], J. A. Ortega[1], R. Qiu[1], Z. Syrgiannis[1], P. A. Mirau[2], F. Chen[1], S. M. Chin[1], S. Weigand[1], E. Kiskinis[1], S. I. Stupp[1*], "Bioactive scaffolds with enhanced supramolecular motion promote recovery from spinal cord injury," Science **374**, 848 (2021). DOI: 10.1126/science.abh3602

Author affiliations: [1]Northwestern University, [2]Air Force Research Laboratories ‡Present address: Center for Cooperative Research in Biomaterials

Correspondence: * s-stupp@northwestern.edu

E.K. is a Les Turner ALS Research Center Investigator and a New York Stem Cell Foundation–Robertson Investigator. The experimental work and simulations were supported by the Louis A. Simpson and Kimberly K. Querrey Center for Regenerative Nanomedicine at the Simpson Querrey Institute for BioNanotechnology (S.I.S.). Work on Nuclear magnetic resonance analysis was supported by the Air Force Research Laboratory under agreement no. FA8650-15-2-5518. Part of the biological experiments reported here was supported by the National Institute on Neurological Disorders and Stroke (NINDS) and the National Institute on Aging (NIA) R01NS104219 (E.K.), NIH/ NINDS grants R21NS107761 and R21NS107761-01A1 (E.K.), the Les Turner ALS Foundation (E.K.), and the New York Stem Cell Foundation (E.K.). We thank the Paralyzed Veterans of America (PVA) Research Foundation PVA17RF0008 (Z.A.), the National Science Foundation (A.N.K.-E. and S.M.C.), and the French Muscular Dystrophy Association (J.A.O.) for graduate and postdoctoral fellowships. Imaging work was performed at the Center for Advanced Microscopy, and CD measurements were performed at the Northwestern University Keck Biophysics facility. Both of these facilities are generously supported by NCI CCSG P30 CA060553 awarded to the Robert H. Lurie Comprehensive Cancer Center. Electron microscopy experiments were performed at the Electron Probe Instrumentation Center (EPIC) and the BioCryo facility of Northwestern University's NUANCE Center, both of which have received support from the SHyNE Resource (NSF ECCS-1542205); the MRSEC program (NSF DMR-1720139) at the Materials Research Center; the International Institute for Nanotechnology (IIN); the Keck Foundation; and the State of Illinois, through the IIN. NMR and Fourier transform infrared spectroscopy characterization in this work made use of IMSERC at Northwestern University, which has received support from the SHyNE Resource (NSF ECCS-1542205), the State of Illinois, and IIN. The DuPont- Northwestern-Dow Collaborative Access Team is supported by Northwestern University, The Dow Chemical Company, and DuPont de Nemours, Inc. This research used resources of the Advanced Photon Source, a U.S. Department of Energy (DOE) Office of Science user facility operated for the DOE Office of Science by Argonne National Laboratory under contract no. DE-AC02-06CH11357.

Measuring Cartilage Dynamics at Nanoscale

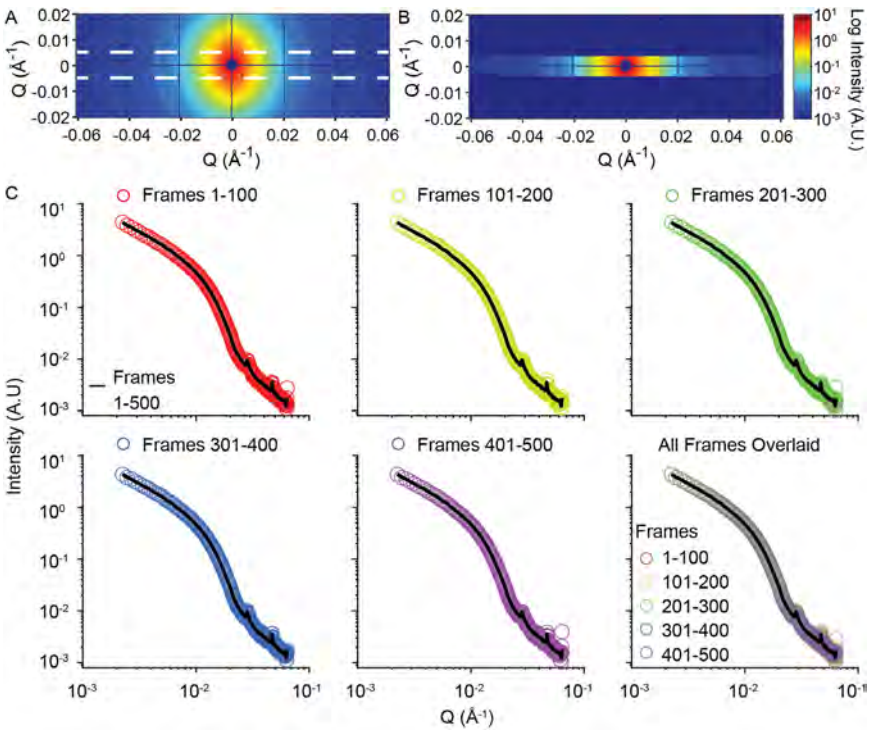

Fig. 1. A time-averaged two-dimensional small-angle x-ray scattering (SAXS) pattern was determined for a representative cartilage sample (A). The cartilage structure is anisotropic; therefore, beam scattering is also anisotropic. A horizontal mask was created to simplify data analysis and can be visualized with the white dashed lines (B). Only data between the two white dashed lines were analyzed. XPCS acquisition parameters were adjusted to reduce radiation damage to the cartilage (C). The one--dimensional SAXS was averaged in 100 frame increments and then the 100 frame increments were overlaid. The overlaid static structures remained the same, demonstrating the structural integrity of the cartilage extracellular matrix did not change during XPCS measurement collection. From B.D. Partain et al., Osteoarthr. Cartilage **29**(9), 1351 (September 2021).

Cartilage is a connective tissue made of solid and fluid components. Cartilage mechanics vary according to interactions between these components. Therefore, understanding how they interact is crucial to developing accurate models of how cartilage functions. In this study, researchers used high brightness x-rays at the APS to directly measure solid/fluid interactions in a model system comprising bovine cartilage and various fluids. The qualities of the APS x-rays and the capacity of the technique they employed (x-ray photon correlation spectroscopy or XPCS) to capture nanometer-scale dynamics enabled the researchers to study these components at microscopic-length scales and depths for the first time, providing novel insight into factors that influence the mobility of the extracellular matrix (ECM) of cartilage. Their findings suggest that smaller ECM components are more mobile than larger components; dehydration slows mobility; and ECM dynamics are faster the closer they are to the cartilage surface. Their findings, published in the journal *Osteoarthritis and Cartilage*, also show that XPCS can be used to effectively measure ECM dynamics simultaneously at the submicron scale and the nanometer scale due to the use of large area detectors. Taken together, these results advance our understanding of cartilage dynamics and demonstrate a valuable new research tool.

Biological tissues perform complex mechanical functions, but questions remain regarding how the dynamics of biosolid-biofluid interactions affect tissue mechanics. Current cartilage biomechanics models are largely based on assumptions about how the viscous fluid interacts with the solid ECM, with many models showing that small shifts in nanoscale physical structures produce major effects. Di-

rect measurements would help verify these models but capturing these interactions at the necessary nanoscale is challenging.

Small-angle x-ray photon correlation spectroscopy (SA-XPCS) can make these direct measurements at nanoscale. When a coherent x-ray beam from a light source like APS passes through a sample, the microstructure of the sample scatters the beam and generates an optical interference pattern called a "speckle" pattern on the x-ray detector. The motion of the sample microstructure creates time-dependent changes in the speckles, thereby conveying information about the sample's dynamics with nanoscale sensitivity. Prior to this study, the only application of XPCS to biological samples was performed with complex fluids and protein solutions. In this study, half-moon-shaped cartilage samples (3 mm diameter and 3 mm thickness) from three juvenile bovine femoral condyles (two rounded prominences at the end of the femur) were inserted into a specimen holder and exposed to different conditions for specific XPCS experiments at the 8-ID-I beamline operated by the XSD Dynamics & Structure Group at the APS.

First, a proof-of-concept experiment was performed showing hydration was necessary for XPCS to measure cartilage mobility. As cartilage contains multiple components of varying sizes and lengths, the researchers used XPCS to determine the lengths of components that contributed to ECM dynamics.

Cartilage has a hierarchical structure, such that the ECM composition and hydration varies at different depths into the sample. Thus, in the second experiment, the researchers assessed ECM mobility at various depths in cartilage exposed to bovine synovial fluid (the viscous liquid that bathes the cartilage in joints). XPCS was able to measure submicron- to nanometer-level fluctuations, making this the first study to show that biosolid-biofluid dynamics change with depth.The cartilage ECM is often described as having different structural zones, all of which contain collage. Therefore, in the third experiment, the researchers evaluated the effects of collagen cross-linking to selectively determine collagen's contribution to matrix dynamics. Collagen was cross-linked by soaking the cartilage samples in genipin and XPCS measurements were collected near the cartilage surface. They found that as cross-linking increases, ECM mobility decreases (Fig. 1).

Even though the surface of cartilage is in contact with synovial fluid, many experiments modeling ECM mobility use phosphate buffered saline or deionized water. In the fourth experiment, the researchers explored the effects of different fluids on ECM mobility. They exposed the cartilage samples to deionized water, phosphate buffered saline, or non-degraded bovine synovial fluid for 20 to 30 minutes, and then collected XPCS measurements near the cartilage surface. They found that ECM mobility was slowest in synovial fluid and fastest in deionized water.

In joint diseases like osteoarthritis (OA), the long hyaluronic chains in synovial fluid break down, causing a loss in synovial fluid viscosity. In the final experiment, the researchers evaluated whether a change in viscosity affected ECM mobility. They found that the less viscous the synovial fluid was, the more mobile the ECM became. This could affect the stability of the ECM at the surface of the cartilage as the disease advances.

This research is significant in a number of ways. First, the data collected at the APS can be used to expand our understanding of cartilage mobility and how it contributes to biomechanics of healthy and diseased joints. The data also help to verify the accuracy of assumption-based models, improve the design of cartilage therapies, and help scientists evaluate the effect that cartilage drugs have on the dynamics of the ECM. Finally, it shows the effectiveness of the XPCS technique in evaluating nanoscale dynamics in an opaque biological tissue and the spatial selectivity enabled by the micro-focused beam that allows for comparative studies at different regions of the sample. For these reasons, both the research itself and the XPCS that facilitated it may help scientists remediate joint diseases like osteoarthritis. – Judy Myers

See: B. D. Partain[1], Q. Zhang[1], M. Unni[1], J. Aldrich[1], C. M. Rinaldi-Ramos[1], S. Narayanan[2], and K. D. Allen[1]*, "Spatially-resolved nanometer-scale measurement of cartilage extracellular matrix mobility," Osteoarthr. Cartilage **29**(9), 1351 (September 2021). DOI: 10.1016/j.joca.2021.05.059
Author affiliations: [1]University of Florida, [2]Argonne National Laboratory
Correspondence: * kyle.allen@bme.ufl.edu

This work was supported by the National Institutes of Health/National Institute of Arthritis and Musculoskeletal and Skin Diseases. This work used resources from the Advanced Photon Source, a U.S. Department of Energy (DOE) Office of Science user facility operated for the DOE Office of Science by Argonne National Laboratory under Contract No. DE-AC02-06CH11357.

Squeezing Fast Skeletal Myosin-Binding Protein-C Reveals Its Structure and Function

On a molecular level, muscle contraction and relaxation are achieved when thick filaments containing myosin and thin filaments containing actin interact in the sarcomere—the fundamental functional unit of striated muscle. Myosin-binding protein-C (MyBP-C) is a thick-filament regulatory protein expressed in striated muscle. It has three paralogs, each encoded by a different gene: slow skeletal (sMyBP-C), fast skeletal (fMyBP-C), and cardiac (cMyBP-C). Much effort has been expended toward studying the cardiac isoform due to its role in hypertrophic cardiomyopathy, a disease caused by abnormal genes in the heart muscle, which cause the walls of the heart chamber (left ventricle) to contract harder and become thicker than normal, causing the thickened walls to become stiff, while fMyBP-C remains the least studied. However, interest in fMyBP-C is increasing because the fast skeletal isoform has been linked to congenital skeletal muscle diseases. These myopathies include distal arthrogryposis and lethal congenital contracture syndrome, which can cause devastating impairments such as muscle weakness and atrophy, and can even be incompatible with life. A team of researchers set out to better understand fMyBP-C on a molecular level. Using knockout mice, the researchers conducted a suite of experiments including x-ray diffraction (XRD), which was carried out at the APS. Insights from these experiments helped the team elucidate the structural and functional roles that fMyBP-C plays in fast skeletal muscle contraction. These findings, published in the *Proceedings of the National Academy of Sciences of the United States of America*, elevate the field's understanding of myosin-binding proteins and move forward research related to skeletal myopathies.

Human skeletal and cardiac muscle is made up of thousands of organelles called myofibrils that allow muscles to contract. As they contract, sliding occurs between the myosin-based thick and the actin-based thin filament contractile proteins, allowing the muscles to shorten. Myosin-binding protein-C (MyBP-C) governs this process. The three MyBP-C paralogs, sMyBP-C, fMyBP-C, and cMyBP-C have similar protein structures but are each encoded by different genes and have unique functional and regulatory mechanisms.

To better understand the structural, functional, and physiological roles of fMyBP-C in skeletal muscle, the researchers in this study conducted *in vitro* and *in vivo* studies on newly generated homozygous fMyBP-C knockout mice ($C2^{-/-}$). The $C2^{-/-}$ mice showed decreased grip strength and plantar flexor muscle strength and reduced peak isometric tetanic force and isotonic speed of contraction in isolated extensor digitorum longus (EDL) muscle.

Using the Bio-CAT 18-ID beamline at the APS for small-angle x-ray diffraction studies, the researchers measured the x-ray diffraction pattern of EDL muscle both at rest and during isometric contraction. The resulting data (Fig. 1) on the $C2^{-/-}$ EDL muscle showed increased mobility of myosin heads. During contraction, there was a shift of myosin heads toward actin and, at rest, the myosin heads were less ordered. The data also suggested increased spacing in the interfilament lattice spacing for $C2^{-/-}$ EDL muscle.

These findings were corroborated by experiments which examined fMyBP-C myofilament calcium sensitivity. They found that, during Ca^{2+}-activation, $C2^{-/-}$ mice EDL muscle fibers demonstrated decreased steady-state isometric force. They also observed decreased myofilament calcium sensitivity and sinusoidal stiffness. The study also showed that fMyBP-C null muscles respond weakly to mechanical overload, displaying muscle damage and disrupted inflammatory and regenerative pathways.

This study improved our understanding about how the three fMyBP-C paralogs differ in structure and function. Results from this work reveal important functional information about fast-skeletal MyBP-C in fast-twitch muscle: that fMyBP-C regulates force, power, and contractile speed. By regulating myofilament calcium sensitivity and actin–myosin interactions, fMyBP-C produces forces that meet the demands of fast-twitch skeletal muscles. These new insights increase the field's knowledge of myosin-binding proteins and will accelerate skeletal muscle disease research. – Alicia Surrao

See: Taejeong Song[1], James W. McNamara[1‡,‡‡], Weikang Ma[2], Maicon Landim-Vieira[3], Kyoung Hwan Lee[4‡‡‡], Lisa A. Martin[1], Judith A. Heiny[5], John N. Lorenz[5], Roger Craig[4], Jose Renato[3], Thomas Irving[2], and Sakthivel Sadayappan[1*],

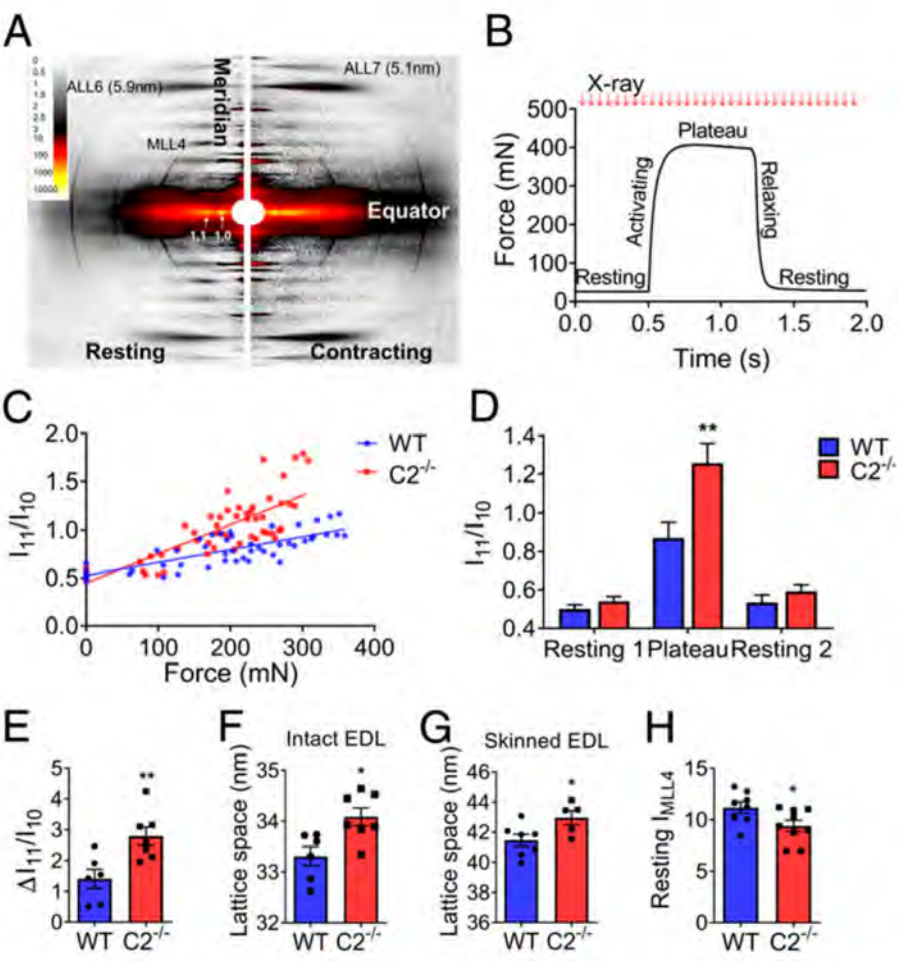

Fig. 1. Small-angle XRD data for C2$^{-/-}$ EDL fibers suggest increased myofilament lattice spacing and increased disorganization of myosin heads but smaller proportion of force-producing cross-bridges. A display of XRD patterns of EDL muscle at rest and during contraction (A). Force vs. time during maximally activated isometric tetanus (B). I11/I10 ratio as a function of force (C). Average I11/I10 during rest and contraction (D). From T. Song et al., Proc. Natl. Acad. Sci. U.S.A **118**(17), e2003596118 (2021). Copyright © 2021 National Academy of Sciences

"Fast skeletal myosin-binding protein-C regulates fast skeletal muscle contraction," Proc. Natl. Acad. Sci. U.S.A **118**(17), e2003596118 (2021). DOI: 10.1073/pnas.2003596118

Author affiliations: [1]University of Cincinnati, [2]Illinois Institute of Technology, [3]Florida State University College of Medicine, [4]University of Massachusetts Medical School, [5]University of Cincinnati College of Medicine Present addresses: ‡The Royal Children's Hospital, ‡‡The University of Melbourne, ‡‡‡ University of Massachusetts Medical School
Correspondence: * sadayasl@ucmail.uc.edu

S.S. has received support from National Institutes of Health (NIH) grants R01 HL130356, R01 HL105826, R01 AR078001, and R01 HL143490; and American Heart Association (AHA) 2019 Institutional Undergraduate Student (19UFEL34380251) and transformation (19TPA34830084) awards. T.S. (19POST34380448) and J.W.M. (17POST33630095) were supported with AHA Fellowship training grants. R.C. was supported by NIH grants P01 HL059408, R01 AR067279, and R01 HL139883. Bio-CAT is supported by grant P41 GM103622 from the National Institute of General Medical Sciences of the NIH. This research used resources of the Advanced Photon Source, a U.S. DOE Office of Science user facility operated for the DOE Office of Science by Argonne National Laboratory under contract no. DE-AC02-06CH11357.

The Unseen Complexities of Early Liquid-Liquid Phase Separation

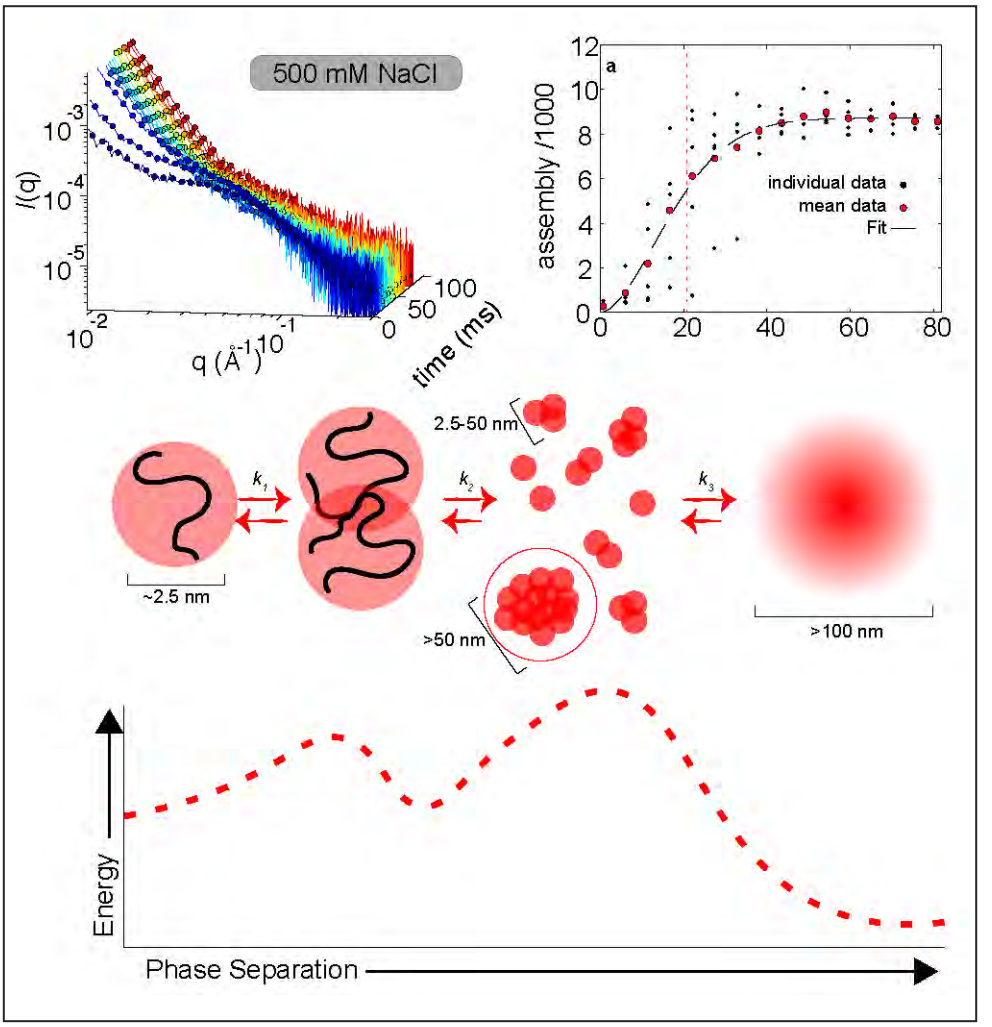

Fig. 1. TR-SAXS measurements quantify the nucleation rate in biomolecular LLPS. SAXS measurements were recorded as a function of time after initiation of LLPS (top left). The formation of critical nuclei was quantified from the SAXS profiles as a function of time (top right). These measurements revealed the two-step nucleation process shown schematically on a qualitative reaction coordinate on the bottom.

Usually, eukaryotic cells organize the functions of life by compartmentalization inside lipid membranes, but some fast processes requiring great precision happen in compartments formed through liquid-liquid phase separation (LLPS), similar to the way oil droplets will separate in a water solution. LLPS has become increasingly recognized as an important biological process not only in normal physiology but in certain pathologies, including neurodegenerative diseases such as Alzheimer's, amyotrophic lateral sclerosis, and Parkinson's. A more detailed understanding of LLPS could lead to better therapeutic approaches, but the blazingly fast microsecond-to-millisecond time scales on which LLPS happens as a solution changes from the one-phase to the two-phase regime have made characterization of the process extremely challenging. A team of researchers from a diverse range of institutions approached that challenge by using the high-brightness x-rays from the APS to capture for the first time the kinetics of how LLPS happens in a biomolecular solution. The work appeared in *Nature Communications*.

The investigators from St. Jude Children's Research Hospital, the Max Planck Institute, the Illinois Institute of

Technology, Washington University in St. Louis, and the National Institutes of Health focused on a prion-like domain called A1-LCD, the low-complexity domain of the hnRNPA1 protein, which has been implicated in neurodegenerative diseases in its mutated form. LLPS occurs when local conditions transform a single-phase solution to two phases. In the vast majority of biological systems, LLPS is initiated by a phenomenon known as nucleation. Previously, nucleation was thought to be largely dependent on perturbation of the equilibrium between the solvent and the biomolecules it contained, but the extreme time resolution achieved in this work reveals that the process is more complex than previously believed.

One factor used to facilitate A1-LCD phase separation in these experiments is the salt concentration of the solution, a parameter which can be used to control the "quench depth," defined as the degree to which the solution is perturbed into the two-phase regime. The experimenters examined this process using fluorescence correlation spectroscopy to characterize A1-LCD molecules in six samples of different salt concentrations in equilibrium. As the salt concentration of the solution is increased, interactions among protein molecules increase and they begin to form into clusters.

In studying the time-dependent process of LLPS, the research team used the technique of rapid-mixing, time-resolved small-angle x-ray scattering (TR-SAXS) at the BioCAT 18-ID-D beamline at the APS. The TR-SAXS techniques offer a detailed look into the earliest stages of the transition (Fig. 1). By combining data from two different microfluidic mixers, the investigators were able to conduct SAXS observations on a time scale from 80 microseconds to 80 milliseconds for the first time in the same experimental session. This provided key insights into the outstanding question of why the nucleation of some biomolecules can occur in fractions of a second, while others require hours to complete phase separation.

On the mesoscale, the A1-LCD phase separation seems to follow a classical homogeneous nucleation pattern. In this regime, the nucleation and assembly rate are determined by the quench depth, both slowing as quench depth decreases. Taking advantage of the power of SAXS to observe assembly also on the nanoscale, the researchers noticed that early assembly steps were unfavorable before additional monomers were added to form larger clusters. These findings indicate the presence of two distinct kinetic steps in the LLPS of A1-LCD, which introduce a time lag, noticeable for A1-LCD only with these high-precision measurements. This time lag likely contributes to the long time periods needed for phase separation in some proteins.

The work demonstrates that phase separation in some biological systems can be more complex than in simpler physical systems, which only require crossing the phase boundary. Since additional steps can occur at different timescales and conditions, equilibrium analysis is not enough to provide a full understanding of the phase separation process, and a careful kinetic analysis is necessary. Additional steps offer opportunities for cells to regulate phase separation, revealing the newly recognized biological usefulness of this process.

The small, bright beams of the APS Upgrade will make these kinds of SAXS experiments with microfluidic mixers much easier to do, with expected gains in time, resolution, and data quality. – Mark Wolverton

See: Erik W. Martin[1]*, Tyler S. Harmon[2], Jesse B. Hopkins[3], Srinivas Chakravarthy[3], J. Jeremías Incicco[4], Peter Schuck[5], Andrea Soranno[4], and Tanja Mittag[1]**, "A multi-step nucleation process determines the kinetics of prion-like domain phase separation," Nat. Commun. **12**, 4513 (2021). DOI: 10.1038/s41467-021-24727-z
Author affiliations: [1]St. Jude Children's Research Hospital, [2]The Max Planck Institute for the Physics of Complex Systems, [3]Illinois Institute of Technology, [4]Washington University in St. Louis, [5]National Institutes of Health
Correspondence: * emartin@dewpointx.com,
** tanja.mittag@stjude.org

T.M. acknowledges funding by National Institutes of Health (NIH) grant R01NS121114, the St. Jude Children's Research Hospital Research Collaborative on Membraneless Organelles in Health and Disease, and by the American Lebanese Syrian Associated Charities. This work was supported by the Intramural Research Programs of the National Institute of Biomedical Imaging and Bioengineering, NIH. This work used resources supported by grant 9 P41 GM103622 from the National Institute of General Medical Sciences of the NIH. Use of the Pilatus 3 1M detector was provided by grant 1S10OD018090-01 from NIGMS. This research used resources of the Advanced Photon Source, a U.S. Department of Energy (DOE) Office of Science user facility operated for the DOE Office of Science by Argonne National Laboratory under Contract No. DEAC02-06CH11357

Nature Uses Springs and Latches to Overcome the Limitations of Muscles

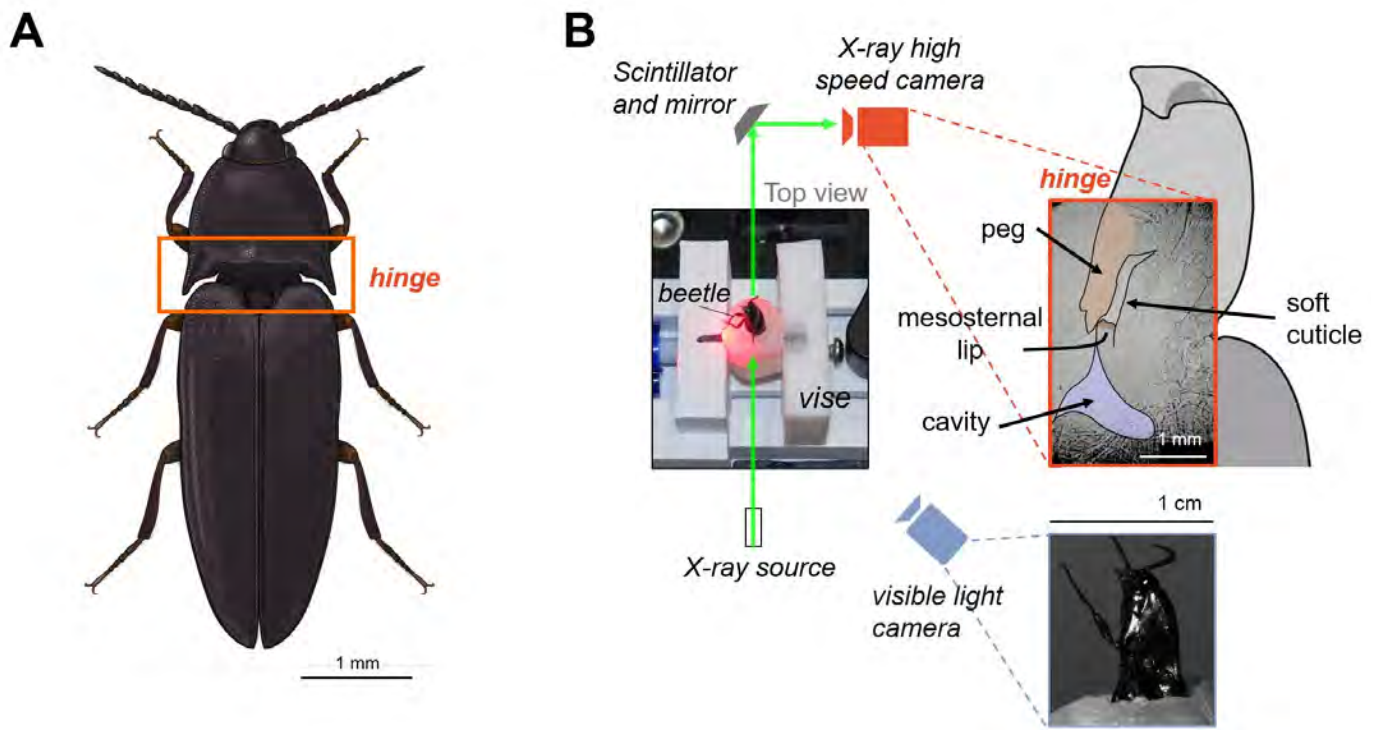

Fig. 1. High-speed synchrotron imaging analysis of click beetles. A. Click beetle hinge. B. Imaging set-up. High-speed x-ray camera shows insect's internal structures while visible light camera records beetle's movements. C. Phases of click beetles' motion: latching, loading, and energy release with timeframe in milliseconds. Image A provided by Olivia F. Boyd, Oregon State University. From O. Bolmin et al., Proc. Natl. Acad. Sci. U.S.A. **118**(5), e2014569118 (2021). Copyright © 2021 National Academy of Sciences

Some insects and plants are what are termed "power-amplified organisms." That is, they have found creative ways to slowly store elastic energy and release it quickly to create extremely fast motion that is not possible with muscle power alone. Examples of this include the trap-jaw ant that can store elastic energy in its jaw for 400 milliseconds (ms) and then close it in just 0.6 ms, 600 times faster. The Venus flytrap plant stores energy and snaps its jaw shut in about 100 ms. Amazingly fast motion for an organism without muscles! Another insect in this extreme motion category is the click beetle. This beetle stores energy in its thoracic hinge and then unbends with a click and a release of energy that causes it to jump extremely quickly. Although the kinetic aspects of the click beetle's jump have been studied, the dynamics of how the ultra-fast clicking or bending movement is generated are less well understood because it has been difficult to capture the details of the super-fast action. Now, with data generated thanks to extreme-brightness x-rays from the APS, researchers used high-speed synchrotron x-ray imaging to analyze the dynamics of the click beetle's unique spring and latch system. The work, published in the *Proceedings of the National Academy of Sciences of the United States of America*, provides tools for others interested in studying extreme motion in natural systems and also offers insights into how these systems work that may be used for the design of insect-inspired robots.

The work started with collection of four candidate click beetles from the University of Illinois Urbana-Champaign natural area and preparation of the motion capture set-up. The team of researchers from the University of Illinois at Urbana–Champaign, Virginia Tech, and Argonne National Laboratory used visible-light imaging to monitor the beetles and make sure the observed movements were clicks. High-speed synchrotron x-ray imaging at the XSD Imaging Group's 32-ID x-ray beamline at the APS allowed

for viewing and recording of the internal structures of the insect (see Fig. 1, panels A and B). Analysis of the high-speed synchrotron x-ray images allowed the researchers to identify and categorize the click beetles' motion into three phases: latching, loading, and energy release.

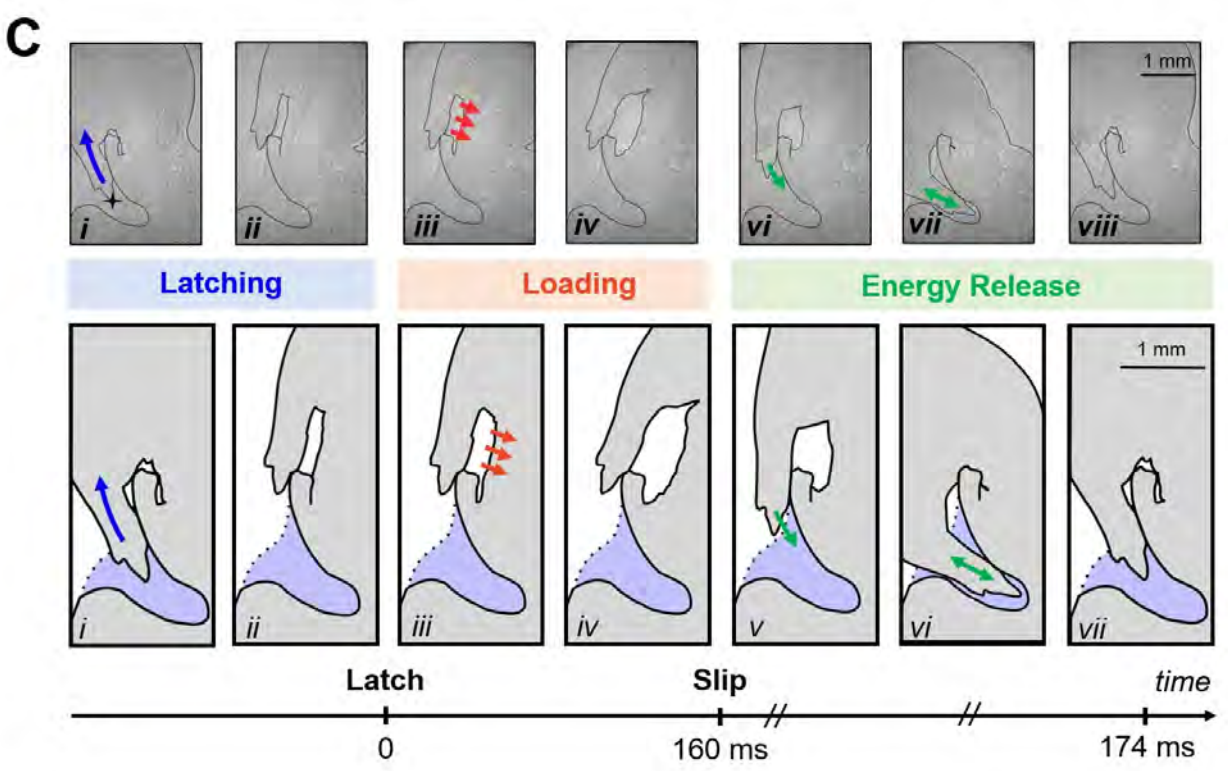

The latching phase involves the beetle rotating its head around a hinge, leaving the head angled upward compared to the back part of its body and deforming an area of soft cuticle while in this braced position (A in the figure). This position is held because the peg in the hinge (B in the figure) moves out of the cavity where it normally rests and latches onto what is called the mesosternal lip. Once latched, the beetle stays in this braced position to "load" the elastic energy in the latch. The beetles in the experiment did this for 33 ms to 243 ms.

Next, the soft cuticle displaces in less than 1 ms and the peg slips, causing rapid release of the stored energy through an elastic recoil that provides the energy for the fast-motion jump (see C in the figure). This release causes the beetle's head to move back to its normal position, and generates the click sound associated with the jump. The peg swings back into the cavity and then oscillates, very much like a spring that is tethered at one end, for a total energy release phase lasting ~10 ms.

Analysis of the kinematics of the elastic recoil in the first part of the energy release stage showed that the velocity of the release is 1.8 meters per second or 1,000 peg lengths per second with an acceleration that is 530 times the natural acceleration due to gravity. That is very fast indeed! In addition, analysis of the energy release (through the peg oscillations) as a one-degree-of-freedom system allowed the team to calculate the damping and elastic forces associated with the release. These results demonstrate how effective these power-amplified organisms are at using elastic energy storage to provide the speed and force to overcome the limitations of their muscles.

Understanding the forces governing these complex natural systems will enable the creation of insect-inspired robots capable of super-fast motion that can be used for various tasks or as research platforms to understand more about how nature achieves these amazing feats. – Sandy Field

See: Ophelia Bolmin[1], John J. Socha[2], Marianne Alleyne[1], Alison C. Dunn[1], Kamel Fezzaa[3], and Aimy A. Wissa[1], "Nonlinear elasticity and damping govern ultrafast dynamics in click beetles," Proc. Natl. Acad. Sci. U.S.A. **118**(5), e2014569118 (2021). DOI: 10.1073/pnas.2014569118
Author affiliations: [1]University of Illinois at Urbana–Champaign, [2]Virginia Tech, [3]Argonne National Laboratory
Correspondence: * obolmin2@illinois.edu,
** awissa@illinois.edu

We thank Alex L. Deriy for his help with the experimental setup at Argonne National Laboratory. This research used resources of the Advanced Photon Source, an Office of Science user facility operated for the U.S. DOE Office of Science by the Argonne National Laboratory under contract no. DE-AC02-06CH11357.

Demystifying an Important Protein Complex Pertinent to DNA Packaging and Accessibility

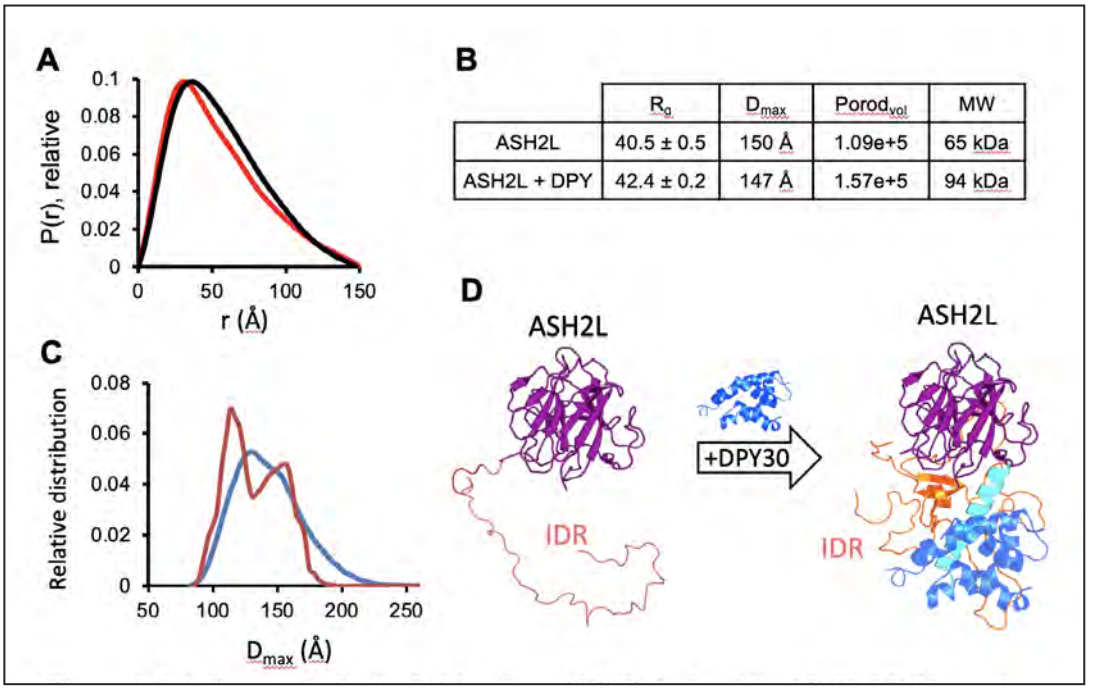

	R_g	D_{max}	$Porod_{vol}$	MW
ASH2L	40.5 ± 0.5	150 Å	1.09e+5	65 kDa
ASH2L + DPY	42.4 ± 0.2	147 Å	1.57e+5	94 kDa

Fig. 1. A. Pair distance distribution P(r) functions of ASH2L (red) and the ASH2L-DPY30 complex (black). B. Derived biophysical properties from SAXS data. Molecular weight (MW) was estimated from the Porod volume. C. Ensemble Optimized Method (EOM) analyses for ASH2L. Distribution of a pool of 10,000 structures (blue) and optimally fit ensemble (red) are plotted against D_{max}. EOM results suggest two main conformations of ASH2L are present in solution. D. Model of structural modulation of ASH2L by DPY30. Intrinsically disordered regions (IDRs, orange) in ASH2L are in extended conformation. DPY30 (blue) binding induces conformation change in ASH2L IDRs. Cyan, DPY30 interacting domain; magenta, SPRY domain.

In order for DNA to be read and converted into RNA, other proteins make modifications to densely packaged structures that make DNA accessible or inaccessible. An important set of these modifying proteins are referred to as the mixed-lineage leukemia (MLL) family of histone methyltransferases. These health-pertinent proteins are implicated in various cancers as well as distinct genetic disorders. One of these proteins, dubbed MLL1, has been reported to interact with, and be influenced by, the proteins DPY30 and ASH2L. However, details surrounding this interaction and influence are enigmatic. In recent work researchers using the APS employed a variety of sophisticated methods to shed light on this complex interaction. Specifically, they show in results published in *Nature Communications* that DPY30 binds ASH2L, which in turn leads to integration with MLL1. Broadly speaking, the rotational dynamics of MLL1 are influenced by DPY30 and ASH2L. In the same publication, the authors demonstrate that DPY30 is responsible for full MLL1 activity in embryonic stem cells. In addition to teaching us more about funda-

mental biology, these findings have far-reaching implications and the potential to be built upon to better understand human disease.

Due to the sheer amount of DNA in human cells, an intricate network of collaborative proteins must work together to densely package DNA. The basic structural units of packaged DNA are referred to as nucleosomes and the entire complex of DNA and protein is referred to as chromatin. Within nucleosomes, histone proteins serve as spools for DNA to be wound around. Since DNA is tightly compressed in a complex with proteins, it is highly restricted. In order to gain access to precious base pairs, other proteins must make modifications to chromatin to open or close it. Since the proteins making these modifications ultimately serve as guardians of the genome, their biological and clinical importance cannot be understated.

A health-pertinent group of chromatin-modifying proteins are the MLL family of histone methyltransferases. These enzymes are frequently mutated in human cancers and have been connected to the human congenital disorders Kabuki, Kleefstra, and Wiedemann-Steiner syndromes. Mutations in the gene encoding the histone methyltransferase MLL1 cause the latter-most Wiedemann-Steiner syndrome, a disorder characterized by reduced muscle tone, developmental delays, issues with feeding and digestion, and other symptoms. This syndrome is autosomal dominant, meaning that only one copy is needed to pass it along from a parent to a child. MLL1 has also been directly linked to severe human malignancies, including acute leukemia, and colon and breast cancer.

As is quite common for histone methyltransferases, various proteins–like DPY30 and ASH2L–have been reported to engage with the MLL1 complex, which in turn interacts with the nucleosome. The extent of this interaction and the degree of influence these proteins have on MLL1 remain mysterious. In novel research spearheaded by these researchers, it was discovered that both DPY30 and the intrinsically disordered regions of ASH2L operate in concern to influence MLL1. Specifically, the MLL1 complex's rotational dynamics are restricted by these proteins. Moreover, the integration of ASH2L's intrinsically disordered regions into the MLL1 complex is caused by DPY30's binding to ASH2L. The overall activity of the MLL1 complex is dramatically increased by the presence of these two partner proteins. Other members of the MLL family are also influenced by DPY30 and ASH2L.

The authors of this study additionally demonstrate that the establishment of an important histone modification, H3K4me3, is caused by DPY30 in embryonic stem cells. This impressive and comprehensive study was carried out in order to better understand the conformations of DPY30 and ASH2L. The researchers used a variety of research techniques including nuclear magnetic resonance spectroscopy; cryo-EM; and small-angle x-ray scattering (SAXS), which was carried out at the Bio-CAT 18-ID x-ray beamline at the APS.

Given the connection of MLL1 to the congenital disorder Wiedemann-Steiner syndrome and deadly human cancers, the societal importance of this work is palpable. The discoveries made by these researchers have the potential to be expanded to better understand human disease. Follow-up research is certainly justified to see if these findings can be built upon to ultimately improve human health.

– Stephen Taylor

See: Young-Tae Lee[1‡], Alex Ayoub[1], Sang-Ho Park[1], Liang Sha[2], Jing Xu[1], Fengbiao Mao[1], Wei Zheng[1], Yang Zhang[1], Uhn-Soo Cho[1], and Yali Dou[1,2*], "Mechanism for DPY30 and ASH2L intrinsically disordered regions to modulate the MLL/SET1 activity on chromatin," Nat. Commun. **12**, 2953 (2021). DOI: 10.1038/s41467-021-23268-9
Author affiliations: [1]University of Michigan, [2]University of Southern California ‡Present address: Accent Therapeutics
Correspondence: * yalidou@usc.edu

The researchers are grateful to the Rogel Cancer Center at the University of Michigan and the Norris Comprehensive Cancer Center at the University of Southern California for the research support. This work is also supported by the National Institute of General Medical Sciences grant (GM082856) to Y.D. and the National Cancer Institute grant (CA250329) to Y.D. and U.S.C. A.A. is supported in part by the MERIT fellowship from the Rackham graduate school at the University of Michigan. L.S. is supported in part by the Michigan Institute for Clinical and Health Research (MICHR) Postdoctoral Translational Scholar Program (PTSP) Fellowship. Bio-CAT is supported by grant P30 GM138395 from the National Institute of General Medical Sciences of the National Institutes of Health This research used resources of the Advanced Photon Source, a U.S. Department of Energy (DOE) Office of Science user facility operated for the DOE Office of Science by Argonne National Laboratory under Contract No. DE-AC02-06CH11357.

Chen of XSD Earned U.S. DOE Early Career Research Program Award

Si Chen, a physicist with the XSD Microscopy Group, was one of six Argonne researchers who received 2021 DOE Early Career Research Program awards. Among other projects, Chen led the development of the Bionanoprobe, a hard x-ray scanning nanoprobe with cryogenic capabilities and the first instrument of its kind in the world. With colleagues at Argonne and collaborators from other institutions, Chen has successfully applied advanced technologies to solve problems in the areas of biological, biomedical, environmental, and materials science. The DOE award will support Chen's research in developing an innovative multiscale imaging platform that combines an x-ray nanoprobe and a plasma-focused ion beam. Chen's research was selected by the DOE Basic Energy Sciences Program.

Winans of XSD Named Winner of ACS Division of Energy and Fuels 2020 R. A. Glenn Award

Randall (Randy) E. Winans was named the winner of the American Chemical Society's (ACS's) R. A. Glenn Award presented for the most innovative and interesting paper presented at each ACS national meeting in the Energy and Fuels Division. The fall 2020 Glenn Award was awarded to Winans for his paper and presentation on "Enhancing unconventional reservoir ultimate recoveries with in-situ nano-catalysts." Winans, now retired, was a Senior Chemist with the Chemical & Materials Science Group in XSD. He worked with colleagues to develop and apply methods to understand the fundamental chemistry of complex disordered systems, such as batteries, catalysts, soot, coals, heavy petroleum, and carbons. He is author or co-author on more than 290 peer-reviewed journal articles.

Rivers and Sutton of GSECARS Named Winners of 2021 APSUO Compton Award

Mark L. Rivers (left) and **Stephen R. Sutton** (right) of GSECARS received the Advanced Photon Source Users Organization (APSUO) Arthur H. Compton Award, which recognizes an important scientific or technical accomplishment at the APS. Rivers is a Research Professor in the Department of the Geophysical Sciences and Center for Advanced Radiation Sources (CARS) at The University of Chicago, and currently the Executive Director of CARS. Sutton is also a Research Professor in the Department of the Geophysical Sciences and CARS, as well as a Research Associate in the Earth Sciences Section of The Field Museum in Chicago. Together, the two have co-directed the design, construction, and operation of GSECARS, which provides users with high-pressure diffraction and spectroscopy, x-ray microprobe, x-ray absorption spectroscopy, and microtomography research techniques. Rivers and Sutton were nominated for their "sustained efforts over the past three decades [which] have ensured that a national and international community of scientists have access to some of the most advanced x-ray analytical facilities and techniques, enabling thousands of scientists to conduct cutting edge research in geochemistry, cosmochemistry, petrology, mineralogy, and mineral/rock physics for environmental, Earth, and planetary sciences.

Zhao of XSD Received 2021 Gopal K. Shenoy Award for Excellence in Beamline Science

Jiyong Zhao, a physicist in the XSD Inelastic X-ray and Nuclear Resonant Scattering Group, received the 2021 APSUO Gopal K. Shenoy Award for Excellence in Beamline Science at the APS. In the last two decades, Zhao and his colleagues have built the world's leading nuclear resonant x-ray scattering programs for high-pressure and high/low-temperature research at APS Sector 3. These programs have made several exceptionally high-impact contributions in the deep-Earth research: the spin and valence transitions in the Earth's mantle, sound velocities of iron alloys in the core, iron isotope geochemistry of the deep Earth, and high-pressure physics and materials science. The Gopal K. Shenoy Award for Excellence in Beamline Science at the Advanced Photon Source is intended to recognize beamline scientists who have made significant scientific contributions in their area of research or instrumentation development and have promoted the user community in this area.

Structural Biology

APS and IMCA-CAT Help Pfizer Create COVID-19 Antiviral Treatment

On December 22, 2021, the U.S. Food and Drug Administration (FDA) issued emergency use authorization for Paxlovid, developed by the pharmaceutical company Pfizer, for the treatment of mild-to-moderate coronavirus disease in adults and children 12 years of age and older who are at high risk for progression to severe COVID-19 disease caused by the SARS-CoV-2 virus. Paxlovid was the first oral antiviral to be authorized by the FDA for treating COVID-19. This development followed the Friday, November 05, 2021, Pfizer announcement of the results of clinical trials of Paxlovid, which showed Paxlovid to be effective.

Scientists at Pfizer created Paxlovid with the help of the ultrabright x-rays of the APS, a U.S. Department of Energy Office of Science user facility at Argonne.

"Today's news is a real game-changer in the global efforts to halt the devastation of this pandemic," said Albert Bourla, chairman and chief executive officer of Pfizer, in a company press release on November 5. "These data suggest that our oral antiviral candidate, if approved or authorized by regulatory authorities, has the potential to save patients' lives, reduce the severity of COVID-19 infections and eliminate up to nine out of 10 hospitalizations."

Work to determine the structure of the antiviral candidate was done at the Industrial Macromolecular Crystallography Association Collaborative Access Team (IMCA-CAT) beamline at the APS, operated by the Hauptman-Woodward Medical Research Institute on behalf of a collaboration of pharmaceutical companies, of which Pfizer is a member.

As a member of IMCA-CAT, Pfizer routinely conducts drug development experiments at the APS, and the process of narrowing down and zeroing in on this drug candidate was performed over many months, according to Lisa Keefe, executive director of IMCA-CAT and vice president for advancing therapeutics and principal scientist at Hauptman-Woodward Medical Research Institute. IMCA-CAT, she said, delivers quality results in a timely manner, much faster than the home laboratories of the companies themselves can do. "Access like this to a DOE facility such as the APS is vitally important for a breakthrough like Paxlovid to happen. This is an important illustration of how valuable the national laboratories are to advancing the work of U.S. industries, and that has a hugely beneficial impact on society," Keefe said. "When the results have a global impact, as in the case of treatments against COVID-19, they motivate us and inspire us."

IMCA-CAT director Lisa Keefe in the 17-ID-B research station.

Paxlovid is the first oral antiviral specifically designed to inhibit a key protease (3CL) of the SARS-CoV-2 virus. For the final phase of clinical trials, Pfizer tested the treatment on more than 1200 adults, all of whom had been diagnosed with COVID-19 no more than five days prior, and had at least one medical condition or characteristic that enhanced the risk of severe illness.

Results reported by Pfizer showed an 89% reduction in risk of COVID-19-related hospitalization or death, compared with a similar number of patients who took a placebo.

Results of the first phase of trials were published in the journal *Science*.

"This is excellent news, and we're very pleased to have played a part in the creation of this potentially life-saving antiviral treatment candidate," said Stephen Streiffer, Argonne's deputy laboratory director for science and technology and then interim director of the APS. "DOE facilities such as the APS have performed an important role in the fight against this global pandemic, from providing the foundation for vaccines to enabling more reliable data about the spread of the virus."

DOE invests in user facilities such as the APS for the benefit of the nation's scientific community, and supports biological research as part of its energy mission. This research has been critical in the fight against COVID-19. The DOE national laboratories formed the National Virtual Biotechnology Laboratory (NVBL) consortium in 2020 to combat COVID-19 using capabilities developed for their DOE mission, and that consortium helps support research into antiviral treatments such as Paxlovid.

Deconstructing the Infectious Machinery of SARS-CoV-2

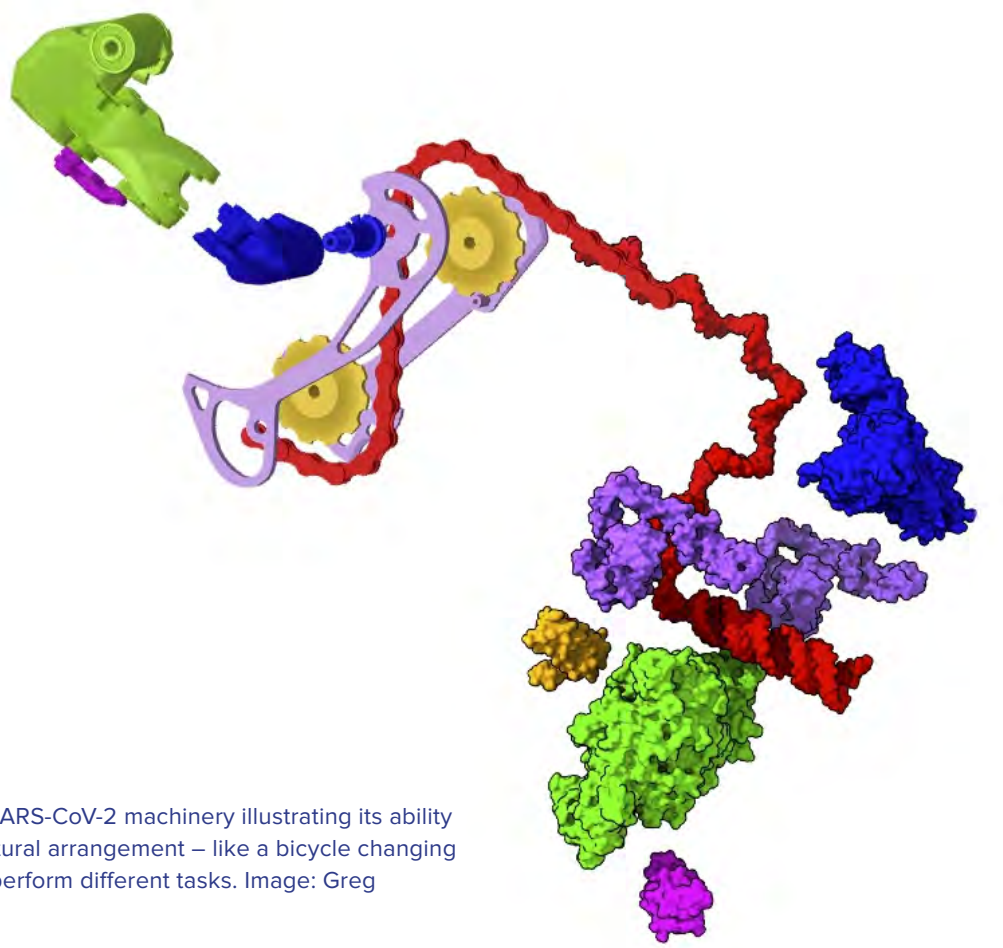

A rendering of the SARS-CoV-2 machinery illustrating its ability to rapidly shift structural arrangement – like a bicycle changing gears – in order to perform different tasks. Image: Greg Hura/Berkeley Lab

The original Lawrence Berkeley National Laboratory press release by Aliyah Kovner can be read here.

In February 2020, a trio of bio-imaging experts were sitting amiably around a dinner table at a scientific conference in Washington, D.C., when the conversation shifted to what was then a worrying viral epidemic in China. Without foreseeing the global disaster to come, they wondered aloud how they might contribute. Nearly a year and a half later, those three scientists and their many collaborators across three U.S. Department of Energy (DOE) national laboratories have published a comprehensive study in the *Biophysical Journal*, based on research at those DOE laboratories that – alongside other recent, complementary studies of coronavirus proteins and genetics – represents the first step toward developing treatments for that viral infection, now seared into the global consciousness as COVID-19. Their foundational work focused on the protein-based machine that enables the SARS-CoV-2 virus to hijack our own cells' molecular machinery in order to replicate inside our bodies.

"It has been remarked that all organisms are just a means for DNA to make copies of itself, and nowhere is this truer than in the case of a virus," said Greg Hura, a staff scientist at Lawrence Berkeley National Laboratory (Berkeley Lab) and one of the study's lead authors. "A virus's singular task is to make copies of its genetic material – unfortunately, at our expense."

Viruses and mammals, including humans, have been stuck in this battle for millions of years, he added, and over that time the viruses have evolved many tricks to get their genes copied inside us, while our bodies have evolved counter defenses. And although viruses often

"Infectious" cont'd. on page 108

Determining How Antibodies Target the Virus That Causes COVID-19

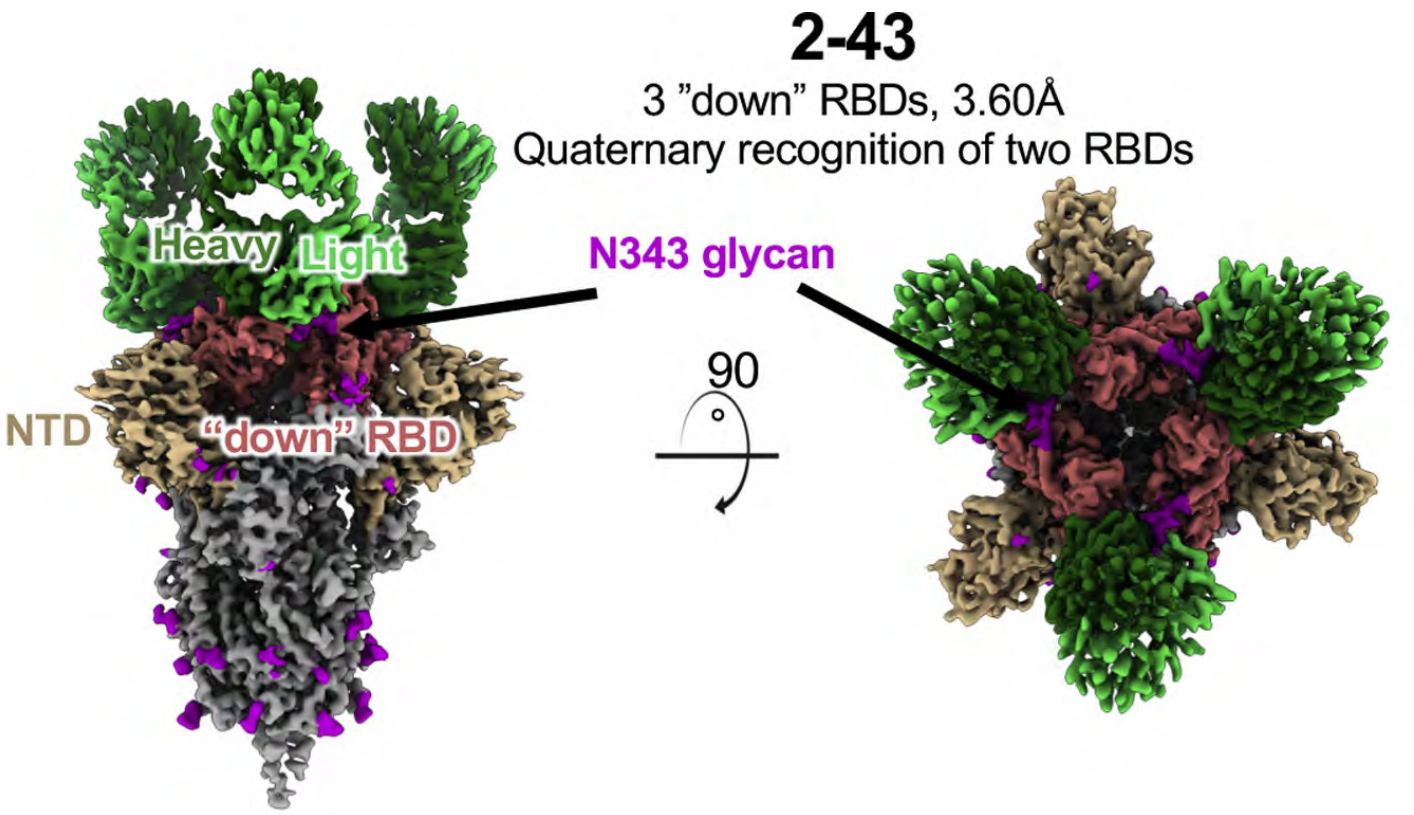

Fig. 1. Structures of three SARS-CoV-2-neutralizing VH1-2 antibodies reveal both “RBD-down” and “RBD-up” modes of spike recognition. (A) Side and top views of three 2-43 antibody Fabs bound to the prefusion SARS-COV-2 spike in the closed state. Color schemes are 2-43, green; RBD, salmon; NTD, yellow; N-linked glycans, magenta; other spike regions, gray. From M. Rapp et al., Cell Rep. **35**, 108950 (April 6, 2021). Copyright © 2021 Elsevier B.V. or its licensors or contributors.

COVID-19 has claimed millions of lives since the outbreak began in late 2019, prompting a wave of research into vaccines and therapeutics to end the pandemic. Studying the naturally occurring human antibodies created in response to SARS-CoV-2, the virus that causes COVID-19, helped researchers develop new therapies that can prevent and treat COVID-19 infections. In a study, which involved collecting x-ray diffraction data at the APS and was published in the journal *Cell Reports*, researchers discovered how different antibodies bind to the SARS-CoV-2 virus and identified clues for ways to optimize antibodies so that they are more effective at targeting the virus.

When a person is exposed to a virus or given a vaccine, their immune system reacts by combining proteins from different genes and connecting these proteins to cre-

ate a variety of antibodies that target a particular virus. These are called “neutralizing antibodies.” Researchers have isolated many different neutralizing antibodies from people who had been infected with COVID-19, and these antibodies have shown promise as a potential treatment for COVID-19 infections. If researchers learn more about how these neutralizing antibodies work, they may be able to use this information to develop more successful treatments or vaccines.

Neutralizing antibodies for the SARS-CoV-2 virus target a part of the virus called the spike protein, which helps infect host cells by interacting with angiotensin-converting enzyme 2 (ACE2) receptors on the surface of host cells. The binding between the spike protein and the ACE2 receptor allows the virus to enter the host cell. Antibodies block infection by binding to the spike protein, preventing it from being able to bind to ACE2.

A team of researchers from Columbia University, the Columbia University Vagelos College of Physicians and Surgeons, and the National Institutes of Health used various techniques to compare and contrast how different SARS-CoV-2 antibodies interact with the spike protein at a very detailed level.

First, the researchers collected information about 158 spike-specific antibodies from 10 published studies. They found that a particular class of these antibodies – those that derive from the VH1-2 antibody heavy chain gene – are especially potent. VH1-2 antibodies are known to bind to the receptor-binding domain (RBD) on the spike protein—a part of the spike protein that binds to the ACE2 receptor. The researchers concentrated their study on three different VH1-2-derived antibodies: 2-15, 2-43, and H4.

Next, the researchers used the single-particle cryo-electron microscopy (cryo-EM) technique at the National Center for Cryo-EM Access and Training and the Simons Electron Microscopy Center located at the New York Structural Biology Center, and the Columbia University Cryo-Electron Microscopy Center to create high-resolution three-dimensional reconstructions of how each antibody interacts with the spike protein. The team found differences between how the different antibodies interacted with the spike protein; While all three antibodies showed binding to the spike protein RBD, the 2-43 antibodies only bound to RBDs in a downward-facing conformation, and the H4 antibodies only bound to RBDS in an upward-facing conformation. The 2-15 antibody particles bound to a mix of upward-facing and downward-ward facing RBDs.

To get higher-resolution information about how the different antibody particles interact with the spike protein, the team used x-ray crystallography to create even more detailed three-dimensional structures of the interactions between the different antibodies and isolated spike protein fragments containing the RBD. These data were collected at the NE-CAT beamline 24-ID-C at APS. Using this technique, the researchers were able to get more accurate information about the similarities and differences between how specific parts of each antibody interface with the RBD.

Next, the researchers compared the ways six different antibodies from the VH1-2 antibody class interacted with the RBD. The team found that all six antibodies had similar interactions with the RBDs and these interactions differed from antibodies from other antibody classes. This detailed information about how VH1-2 antibodies interact with the RBD show that different humans respond similarly to SARS-CoV-2 in their derivation of highly similar antibodies, and may help explain how these antibodies are so effective at neutralizing SARS-CoV-2 and could help determine which virus variants might be effectively neutralized—or not neutralized—by this class of antibodies. Two mutations - E484K/Q and L452R - carried by variant B.1.351 (South Africa), P.1 (Brazil) or B.1.617 (India), are within the VH1-2 antibody epitopes, and ablate the binding of this class of antibodies. The enrichment of such mutations in different emerging strains, especially for E484K/Q, suggest convergent evolution of SARS-CoV-2 by selection pressure from VH1-2 class antibodies.

The researchers then wanted to see if they could improve how well VH1-2 antibodies bind to the SARS-CoV-2 virus. They inserted a targeted mutation in both the 2-43 and 2-4 antibodies. This mutation improved how tightly both antibodies bound to the spike protein, and the mu-

“Target” cont’d. on page 109

"Infectious" cont'd. from page 105

perform a long list of activities, their ability to harm us with an infection comes down to whether or not they can replicate their genetic material (either RNA or DNA, depending on the species) to make more viral particles, and use our cells to translate their genetic code into proteins.

The protein-based machine responsible for RNA replication and translation in coronaviruses – and many other viruses – is called the RNA transcription complex (RTC), and it is a truly formidable piece of biological weaponry.

To successfully duplicate viral RNA for new virus particles and produce the new particles' many proteins, the RTC must: distinguish between viral and host RNA, recognize and pair RNA bases instead of highly similar DNA bases that are also abundant in human cells, convert their RNA into mRNA (to dupe human ribosomes into translating viral proteins), interface with copy error-checking molecules, and transcribe specific sections of viral RNA to amplify certain proteins over others depending on need – while at all times trying to evade the host immune system that will recognize it as a foreign protein.

As astounding as this sounds, any newly evolved virus that is successful "must have machines that are incredibly sophisticated to overcome mechanisms we have evolved," explained Hura, who heads the Structural Biology department in Berkeley Lab's Molecular Biophysics and Integrated Bioimaging Division.

He and the other study leads–Andrzej Joachimiak of SBC-XSD at the APS and Center of Structural Genomics of Infectious Disease at the University of Chicago and Hugh M. O'Neill at Oak Ridge National Laboratory–specialize in revealing the atomic structure of proteins in order to understand how they work at the molecular level. So, the trio knew from the moment they first discussed COVID-19 at the dinner table that studying the RTC would be particularly challenging because multitasking protein machines like the RTC aren't static or rigid, as molecular diagrams or ball-and-stick models might suggest. They're flexible and have associated molecules, called nonstructural and accessory proteins (Nsps), that exist in a multitude of rapidly rearranging forms depending on the task at hand – akin to how a gear shifter on a bike quickly adapts the vehicle to changing terrain.

Each of these Nsp arrangements give insights into the protein's different activities, and they also expose different parts of the overall RTC surface, which can be examined to find places where potential drug molecules could bind and inhibit the entire machine.

So, following their serendipitous convergence in Washington, the trio hatched a plan to pool their knowledge and national lab resources in order to document the structure of as many RTC arrangements as possible, and identify how these forms interact with other viral and human molecules.

The investigation hinged on combining data collected from many advanced imaging techniques, as no approach by itself can generate complete, atomic-level blueprints of infectious proteins in their natural states. They combined small-angle x-ray scattering (SAXS), x-ray crystallography, and small-angle neutron scattering (SANS) performed at Berkeley Lab's Advanced Light Source SIBYLS beamline 12.3.1, the SBC-XSD 19-ID beamline at the APS, and Oak Ridge's High Flux Isotope Reactor and Spallation Neutron Source, respectively, on samples of biosynthetically produced RTC.

Despite the extraordinary hurdles of conducting science during shelter-in-place conditions, the collaboration was able to work continuously for more than 15 months, thanks to funding for research and facility operations support from the DOE Office of Science National Virtual Biotechnology Laboratory (NVBL). During that time, the scientists collected detailed data on the RTC's key accessory proteins and their interactions with RNA. All of their findings were uploaded into the open-access Protein Data Bank prior to the journal article's publication.

Of the many structural findings that will help with drug design, one notable discovery is that assembly of the RTC subunits is incredibly precise. Drawing on a mechanical metaphor once more, the scientists compare the assembly process to putting together a spring-based machine. You can't put a spring in place when the rest of the machine is already in position, you must compress and place the spring at a specific step of assembly or the whole device is dysfunctional. Similarly, the RTC Nsps can't move into place in any random or chaotic order; they must follow a specific order of operations.

They also identified how one of the Nsps specifically recognizes the RNA molecules it acts upon, and how it cuts long strands of copied RNA into their correct lengths.

"Having the vaccines is certainly huge. However, why are we satisfied with just this one avenue of defense?" said Hura. Added Joachimiak: "This was a survey study, and it has identified many directions we and others should pursue very deeply; to tackle this virus we will need multiple ways of blocking its proliferation."

"Combining information from different structural techniques and computation will be key to achieving this goal," said O'Neill.

Due to the similarity of RTC proteins across viral strains, the team believe that any drugs developed to block RTC activity could work for multiple viral infections in addition to all COVID-19 variants.

Reflecting back to the beginning of their research journey, the scientists marvel at the lucky timing of it all. When we started to talk, said Hura, "we had no idea that this epidemic would soon become a pandemic that would change a generation."

See: Mateusz Wilamowski[1], Michal Hammel[2], Wellington Leite[3], Qiu Zhang[3], Youngchang Kim[1,4], Kevin L. Weiss[3], Robert Jedrzejczak[1,4], Daniel J. Rosenberg[2,7], Yichong Fan[3], Jacek Wower[8], Jan C. Bierma[2], Altaf H. Sarker[2], Susan E. Tsutakawa[2], Sai Venkatesh Pingali[3], Hugh M. O'Neill[3]*, Andrzej Joachimiak[1,4]**, and Greg L. Hura[2,9]***, "Transient and stabilized complexes of Nsp7, Nsp8, and Nsp12 in SARS-CoV-2 replication," Biophys. J. **120**, (August 3, 2021). DOI: 10.1016/j.bpj.2021.06.006

Author affiliations: [1]The University of Chicago, [2]Lawrence Berkeley National Lab, [3]Oak Ridge National Laboratory, [4]Argonne National Laboratory, [7]University of California, Berkeley, [8]Auburn University, [9]University of California, Santa Cruz

Correspondence: * oneillhm@ornl.gov, ** andrzejj@anl.gov, *** glhura@lbl.gov

This research was supported by the U.S. Department of Energy (DOE) Office of Science through the National Virtual Biotechnology Laboratory, a consortium of DOE national laboratories focused on response to coronavirus disease 2019, with funding provided by the Coronavirus CARES Act. The Advanced Light Source is a DOE Office of Science user facility run under contract No. DE-AC02-05CH11231 with the SAXS SIBYLS Wilamowski, et al. Biophysical (12.3.1) beamline supported by the DOE Biological and Environmental Research Integrated Diffraction Analysis Technologies (DOE-BERIDAT) program, National Cancer Institute Structural Biology of DNA Repair (NCI-SBDR) P01 CA092584, National Institute for General Medical Sciences ALS-ENABLE (P30 GM124169) and United States-Israel Binational Science Foundation (BSF) Grant 2016070. J.W. was supported by the Hatch program of the National Institute of Food and Agriculture, U.S. Department of Agriculture. Bio-SANS is supported by Oak Ridge National Laboratory's (ORNL) Center for Structural Molecular Biology funded by the DOE-BER. EQ-SANS is supported by the Scientific User Facilities Division, DOE Basic Energy Science (DOE-BES). Neutron scattering experiments were performed using the High Flux Isotope Reactor and Spallation Neutron Source, a DOE Office of Science user facility operated by ORNL. Preliminary protein expression and purification studies were supported by the ORNL Laboratory Directed Research and Development Program. Further funding for this research was provided by the National Institute of Allergy and Infectious Diseases, National Institutes of Health, Department of Health and Human Services, under Contract HHSN272201700060C. Use of the SBC-XSD beamlines at the APS is supported by the DOE Office of Science and operated for the DOE Office of Science by Argonne National Laboratory under Contract No. DE-AC02-06CH11357. This research used resources of the Advanced Photon Source, a U.S. DOE Office of Science user facility operated for the DOE Office of Science by Argonne National Laboratory under Contract No. DE-AC02-06CH11357.

"Target" cont'd. from page 107

tated antibodies were also more effective at neutralizing SARS-CoV-2 virus exposed to host cells in a dish.

The results from this study provide more information about how antibodies bind to and neutralize the SARS-CoV-2 virus. They also provide clues for how to further optimize antibodies and vaccines against the SARS-CoV-2 virus, which may prove particularly important as new SARS-CoV-2 variants emerge. – Summer Allen

See: Micah Rapp[1], Yicheng Guo[1,2], Eswar R. Reddem[1], Jian Yu[2], Lihong Liu[2], Pengfei Wang[2], Gabriele Cerutti[1], Phinikoula Katsamba[1], Jude S. Bimela[1], Fabiana A. Bahna[1], Seetha M. Mannepalli[1], Baoshan Zhang[3], Peter D. Kwong[1,3], Yaoxing Huang[2], David D. Ho[2], Lawrence Shapiro[1,2,3]*, and Zizhang Sheng[1,2]**, "Modular basis for potent SARS-CoV-2 neutralization by a prevalent VH1-2-derived antibody class," Cell Rep. **35**, 108950 (April 6, 2021). DOI: 10.1016/j.celrep.2021.108950

Author affiliations: [1]Columbia University, [2]Columbia University Vagelos College of Physicians and Surgeons, [3]National Institutes of Health

Correspondence: * lss8@columbia.edu, ** zs2248@cumc.columbia.edu

The National Center for Cryo-EM Access and Training and the Simons Electron Microscopy Center located at the New York Structural Biology Center is supported by the National Institutes of Health (NIH) Common Fund Transformative High Resolution Cryo-Electron Microscopy program (U24 GM129539) and by grants from the Simons Foundation (SF349247) and the NY State Assembly. Data analysis was performed at the National Resource for Automated Molecular Microscopy, supported by the NIH National Institute of General Medical Sciences (GM103310). We thank D. Neau, S. Banerjee, and Igor Kourinov for help with synchrotron data collection conducted at the NE-CAT 24-ID-C beamline, which is funded by the National Institute of General Medical Sciences from the NIH (P30 GM124165). Support for this work was provided by the Intramural Research Program of the Vaccine Research Center, National Institute of Allergy and Infectious Diseases (NIAID), NIH. This study was supported by Samuel Yin, Pony Ma, Peggy, Andrew Cherng, Brii Biosciences, Jack Ma Foundation, JBP Foundation, Carol Ludwig, and Roger and David Wu. This research used resources of the APS, a U.S. Department of Energy (DOE) Office of Science user facility operated for the DOE Office of Science by Argonne National Laboratory under Contract DE-AC02-06CH11357.

The Structure of a Key Viral Enzyme Helps Identify Novel Drugs for Treatment of COVID-19

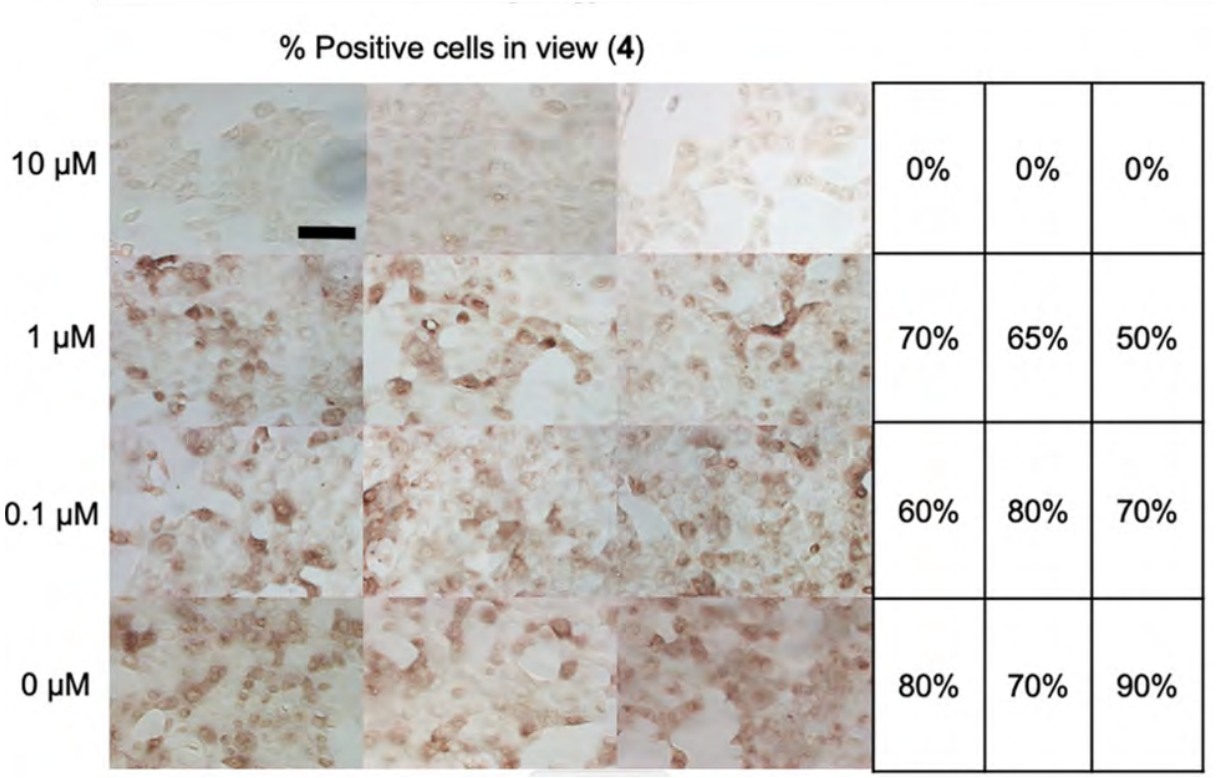

Fig. 1. Compound 4 efficacy. Three repeat experiments were done and the percentage of cells positive for the virus is reported for each experiment. 0% of cells treated with the highest concentration of 4 were positive for the virus. From Jerzy Osipiuk et al., "Structure of papain-like protease from SARS-CoV-2 and its complexes with non-covalent inhibitors," Nat. Commun. **12**, 743 (2021). © 2021 Springer Nature Limited

The globally debilitating COVID-19 pandemic is caused by severe acute respiratory syndrome coronavirus 2 (SARS-CoV-2), which is a single-stranded RNA virus that can encode for at least 29 different proteins. One of these proteins, an enzyme named PLpro, is responsible for releasing other proteins from a larger protein complex and it plays an important function in disrupting host response. A recent high-impact paper based on research at the APS and published in *Nature Communications* reports a high-resolution structure of the protein PLpro and provides *in vitro* evidence that a set of chemical compounds are capable of inhibiting the activity of this protein. Some of these compounds also demonstrate an ability to block SARS-CoV-2 from replicating in cells. Although such inhibitors will need to undergo *in vivo* testing in animal models before use in human clinical trials, the data presented in this work is shows clinical promise.

Recent studies show that the SARS-CoV-2 virus is less than 200 nanometers in diameter, contains a RNA genome, and has a lipid envelope studded with the following four structural proteins: envelope (E), membrane (M), nucleocapsid (N), and spike (S). In addition to these struc-

tural proteins, there are 15 nonstructural proteins (Nsp) and several other proteins that the SARS-CoV-2 genome encodes. One of these proteins is PLpro, a domain within Nsp3. It is an enzyme referred to as a protease. Protease enzymes cleave specific sites within proteins to produce smaller components such as individual building blocks of proteins (i.e., amino acids) or protein subunits (i.e., polypeptides). PLpro is found in all corona viruses, not just SARS-CoV-2, and cleaves a larger protein complex to liberate the three proteins Nsp1, Nsp2, and Nsp3. The protein Nsp2 has been proposed to influence the survival of infected host cells, suggesting that PLpro may be important for replication efficiency.

In a study that employed x-ray diffraction at SBC-XSD 19-ID x-ray beamline, members of SBC-XSD together with researchers from The University of Chicago who are members of the National Institutes of Health/ National Institute of Allergy and Infectious Diseases-funded Center for Structural Genomics of Infectious Diseases to generate high-quality crystal structures of PLpro and its complexes with inhibitors. The authors report that PLpro has a structure similar to the PLpro enzymes of SARS and Middle East Respiratory Syndrome (MERS) corona viruses. The structure shows fine molecular details of this enzyme that reveal how it works and how its action might be inhibited, which could potentially disrupt coronavirus replication.

Having solved this structure, the authors then tested various compounds that inhibit PLpro for their ability to affect replication efficiency in infected cells. They found that many of these compounds inhibit the activity of this enzyme *in vitro* and effectively block the replication of the SARS-CoV-2 virus in infected cells. The researchers carried out their viral replication assays at the University of Chicago Ricketts Laboratory for. Ultimately, five compounds were observed to both 1) inhibit viral replication and 2) impact cell viability. Compound 4 was especially effective, as shown in Fig. 1.

Given the severity of the COVID-19 pandemic, these data are timely and tangibly meaningful. The authors have not only solved the structure of a key viral enzyme, but have provided compelling evidence that several different compounds are capable of inhibiting this protein and combating viral replication in infected cells. If these compounds are validated in pre-clinical animal models, they will be ready for human testing and could serve as novel anti-viral medications that increase the survival of patients infected with not just SARS-CoV-2, but other coronaviruses too. — Alicia Surrao

See: Jerzy Osipiuk[1,2], Saara-Anne Azizi[1], Steve Dvorkin[1], Michael Endres[1,2], Robert Jedrzejczak[1,2], Krysten A. Jones[1], Soowon Kang[1], Rahul S. Kathayat[1], Youngchang Kim[1,2], Vladislav G. Lisnyak[1], Samantha L. Maki[1], Vlad Nicolaescu[1], Cooper A. Taylor[1], Christine Tesar[1,2], Yu-An Zhang[1], Zhiyao Zhou[1], Glenn Randall[1], Karolina Michalska[1,2], Scott A. Snyder[1]*, Bryan C. Dickinson[1]**, and Andrzej Joachimiak[1,2]***, "Structure of papain-like protease from SARS-CoV-2 and its complexes with non-covalent inhibitors," Nat. Commun. **12**, 743 (2021). DOI: 10.1038/s41467-021-21060-3
Author affiliations: [1]The University of Chicago, [2]Argonne National Laboratory
Correspondence: * sasnyder@uchicago.edu,
** dickinson@uchicago.edu, *** andrzejj@anl.gov

We thank the members of SBC-XSD at Argonne National Laboratory, especially Darren Sherrell and Alex Lavens for their help with setting beamline and data collection at beamline 19-ID. Funding for this project was provided in part by federal funds from the National Institute of Allergy and Infectious Diseases, National Institutes of Health, Department of Health and Human Services, under Contract HHSN272201700060C (to A.J.) and by the U.S. Department of Energy (DOE) Office of Science through the National Virtual Biotechnology Laboratory, a consortium of DOE national laboratories focused on response to COVID-19, with funding provided by the Coronavirus CARES Act (to A.J.). The use of SBC-XSD beamlines at the Advanced Photon Source is supported by the U.S. DOE Office of Science and operated for the DOE Office of Science by Argonne National Laboratory under Contract No. DE-AC02-06CH11357. Funding for the synthesis and biochemical studies was provided by a "BIG" Award from The University of Chicago, The University of Chicago Women's Board, the National Institutes of Health (TM GM08720, Predoctoral Training Program in Chemistry and Biology, graduate fellowship to C.A.T.), the National Institute of General Medical Sciences (R35 GM119840 to B.C.D.), and start-up funds from The University of Chicago (S.A.S.). This research used resources of the Advanced Photon Source, a U.S. DOE Office of Science user facility operated for the DOE Office of Science by Argonne National Laboratory under Contract No. DE-AC02-06CH11357. Extraordinary facility operations were supported in part by the DOE Office of Science through the National Virtual Biotechnology Laboratory, a consortium of DOE national laboratories focused on the response to COVID-19, with funding provided by the Coronavirus CARES Act.

Engineering More Powerful Antibodies against COVID-19

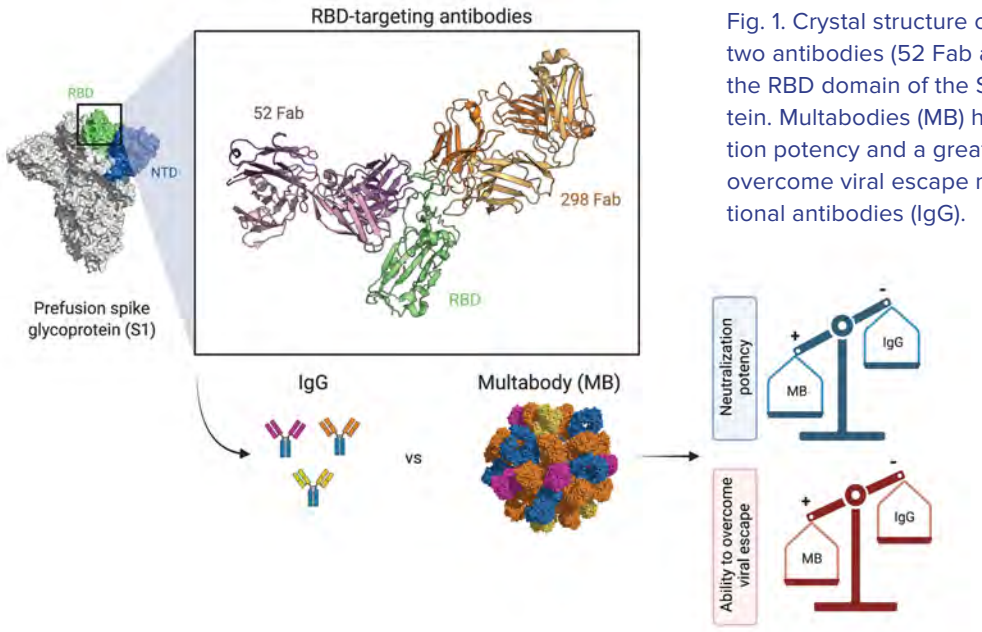

Fig. 1. Crystal structure of the Fab fragments of two antibodies (52 Fab and 298 Fab) bound to the RBD domain of the SARS-CoV-2 spike protein. Multabodies (MB) have a higher neutralization potency and a greater capacity to overcome viral escape mutations than traditional antibodies (IgG).

The COVID-19 pandemic highlights the need for new treatment options. Monoclonal antibodies—lab-produced proteins that mimic antibodies created by the immune system—can be effective treatments for viral diseases and have been used successfully to target SARS-CoV-2, the virus that causes COVID-19. However, these monoclonal antibodies have proven to be less effective against some SARS-CoV-2 variants. In a recent study, which involved collecting x-ray diffraction data at the APS and was published in *Nature Communications*, researchers developed a new "plug-and-play" antibody platform that produces exceptionally potent neutralizers of SARS-CoV-2 with the ability to overcome viral sequence variability. The results could lead to more effective therapeutics for treating COVID-19 and other viruses that threaten public health.

Monoclonal antibodies can successfully treat viral infections, including COVID-19. As RNA viruses mutate, however, these antibodies become less effective virus "neutralizers." Already, some monoclonal antibodies developed to treat COVID-19 are significantly less effective at neutralizing certain SARS-CoV-2 variants. Because there is a time cost to identifying new antibodies specific to new virus variants, researchers are looking for ways to improve the neutralizing ability and potency of existing antibodies so they can remain effective against new variants.

One way to make antibodies more potent is to increase their ability to interact with a target virus at multiple places simultaneously. This property is known as avidity. To optimize the avidity of SARS-CoV-2 antibodies, researchers developed a new method to "multimerize" several different antibodies in a single unit. They call their platform a MULTi-specific, multi-Affinity antiBODY (or Multabody for short).

To develop a Multabody, the researchers attached a human protein called apoferritin to a small antibody fragment known to target SARS-CoV-2. Because the natural state of apoferritin is a cluster of 24 protein molecules, the Multabodies are also a cluster of 24 in a spherical shape with antibody fragments sticking out. This shape allows multiple antibody fragments to interact with SARS-CoV-2 at once. The conformation was so successful at increasing avidity that the Multabody had up to ~10,000-fold greater neutralization potency against SARS-CoV-2 than the parental monoclonal antibody.

In addition to the small antibody fragment, the researchers next incorporated the portion of a human antibody known as Fc into the Multabody aiming to endow their molecules with greater human antibody-like properties. To test the effectiveness of this approach, the researchers developed a mouse version of the platform. Injection of this Multabody into mice was well tolerated, showed days of bioavailability and was distributed in the body similar to traditional antibodies.

The researchers then selected seven monoclonal anti-

bodies that, when tested in the Multabody, led to the highest neutralization potencies against SARS-CoV-2 and used structural biology techniques to determine where these antibodies interact with the receptor binding domain (RBD) of the spike protein, the part of SARS-CoV-2 that the virus uses to enter host cells. Specifically, they used macromolecular crystallography carried out at the GM/CA-XSD beamline 23-ID-D at the APS (Fig. 1)–as well as cryo-electron microscopy—to create more detailed three-dimensional images of how these antibodies interact with the spike protein.

The structural information from these experiments helped the researchers to delineate a new class of antibody-based therapy that targets an antigenic site not previously described on the receptor-binding domain (RBD) of SARS-CoV-2.

Next, the researchers tested whether the Multabodies could neutralize SARS-CoV-2 variants containing RBD mutations. Amazingly, they found that, in contrast to monoclonal antibodies, none of the mutations tested had significant effects on the neutralization potency of the corresponding Multabodies, suggesting a superior ability of the Multabodies to overcome sequence variability of SARS-CoV-2 variants.

To mitigate potential immune evasion, it is desirable to use antibody 'cocktails' — a combination of multiple antibodies that target different parts of the virus. When the research team created cocktails combining three different Multabodies against SARS-CoV-2, they found that the Multabody cocktails efficiently overcame viral sequence variability with 10 to 100-fold higher potency than the corresponding mixture of the three monoclonal antibodies. Furthermore, a single Multabody molecule that contained fragments of three different antibodies was similarly able to overcome viral mutations with exceptional potency.

Together, these results suggest that Multabodies may become a powerful treatment option for COVID-19. Moreover, the flexible "plug-and-play" Multabody platform may one day lead to next-generation antibody-based immunotherapies against other viruses, and provide solutions against other biomedical challenges where binding avidity can deliver improved health outcomes.

– Summer Allen

See: Edurne Rujas[1,2,3], Iga Kucharska[1], Yong Zi Tan[1], Samir Benlekbir[1], Hong Cui[1], Tiantian Zhao[2], Gregory A. Wasney[1], Patrick Budylowski[2], Furkan Guvenc[2], Jocelyn C. Newton[1], Taylor Sicard[1,2], Anthony Semesi[1], Krithika Muthuraman[1], Amy Nouanesengsy[1,2], Clare Burn Aschner[1], Katherine Prieto[1], Stephanie A. Bueler[1], Sawsan Youssef[4], Sindy Liao-Chan[4], Jacob Glanville[4], Natasha Christie-Holmes[2], Samira Mubareka[2,5], Scott D. Gray-Owen[2], John L. Rubinstein[1,2], Bebhinn Treanor[2], and Jean-Philippe Julien[1,2]*, "Multivalency transforms SARS-CoV-2 antibodies into ultrapotent neutralizers," Nat. Commun. **12**, 3661 (2021).
DOI: 10.1038/s41467-021-23825-2

Author affiliations: [1]The Hospital for Sick Children Research Institute, [2]University of Toronto, [3]University of the Basque Country [4]Distributed Bio, [5]Sunnybrook Health Sciences Centre
Correspondence: * jean-philippe.julien@sickkids.ca

This work was supported by Natural Sciences and Engineering Research Council of Canada discovery grant 6280100058 (J.-P.J.), by operating grant PJ4- 169662 from the Canadian Institutes of Health Research (CIHR; B.T. and J.-P.J.), by COVID-19 Research Fund C-094-2424972-JULIEN (J.-P.J.) from the Province of Ontario Ministry of Colleges and Universities, by Bill and Melinda Gates Foundation INV-023398 (J.-P.J.), and by the Hospital for Sick Children Foundation. This research was also supported by the European Union's Horizon 2020 research and innovation program under Marie Sklodowska-Curie grant 790012 (E.R.), by a Hospital for Sick Children Restracomp Postdoctoral Fellowship (I.K. and C.B.A.), by a CIHR Postdoctoral Fellowship (Y.Z.T.), by a NSERC postgraduate doctoral scholarship (T.Z.), by a Vanier Canada Graduate Scholarship (T.S.), by a CIHR Canada Graduate Scholarship—Master's Award (A.N.), by the CIFAR Azrieli Global Scholar program (J.-P.J.), by the Ontario Early Researcher Awards program (J.-P.J.), and by the Canada Research Chairs program (J.L.R., B.T., and J.-P.J.). Cryo-EM data were collected at the Toronto High Resolution High Throughput cryo-EM facility, biophysical data at the Structural & Biophysical Core facility, and biodistribution data at the CFI 3D Facility at University of Toronto, all supported by the Canada Foundation for Innovation and Ontario Research Fund. GM/CA-XSD has been funded in whole or in part with federal funds from the National Cancer Institute (ACB-12002) and the National Institute of General Medical Sciences (AGM-12006, P30GM138396). The Eiger 16M detector at GM/CA-XSD was funded by NIH grant S10 OD012289. This research used resources of the Advanced Photon Source, a U.S. Department of Energy (DOE) Office of Science user facility operated for the DOE Office of Science by Argonne National Laboratory under contract DE-AC02-06CH11357.

Escape Artist

The original Harvard Medical School article by Ekaterina Pesheva can be read here.

The vast majority of people infected with SARS-CoV-2 clear the virus, but those with compromised immunity—such as individuals receiving immune-suppressive drugs for autoimmune diseases—can become chronically infected. As a result, their weakened immune defenses continue to attack the virus without being able to eradicate it fully. This physiological tug-of-war between human host and pathogen offers a valuable opportunity to understand how SARS-CoV-2 can survive under immune pressure and adapt to it. Now, a new multi-institution study led by Harvard Medical School scientists employing data obtained at the APS offers a look into this interplay, shedding light on the ways in which compromised immunity may render SARS-CoV-2 fitter and capable of evading the immune system.

The research, published in *Cell*, shows that a mutated SARS-CoV-2 from a chronically infected immunocompromised patient is capable of evading both naturally occurring antibodies from COVID-19 survivors as well as lab-made antibodies now in clinical use for treatment of COVID-19.

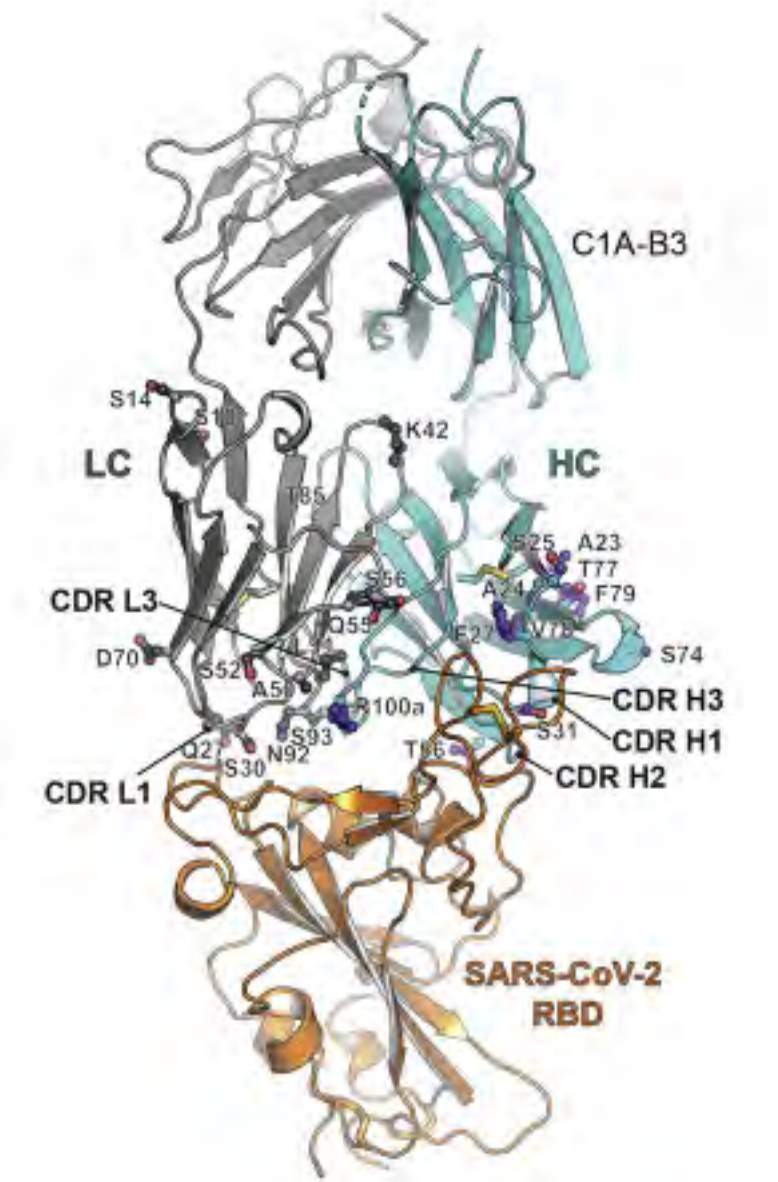

Fig. 1. Ribbon diagram of the crystal structure of the RBD complex.

The patient case was originally described December 3, 2020, as a *New England Journal of Medicine* report by scientists at Brigham and Women's Hospital a few weeks before the variants initially detected in the U.K. and South Africa were first reported to the World Health Organization. Interestingly, the patient-derived virus contained a cluster of changes on its spike protein—the current target for vaccines and antibody-based treatments—and some of these changes were later detected in viral samples in the U.K. and South Africa, where they appear to have arisen independently, the researchers said.

The newly published study, which built on the initial case report, shows something more alarming still. Some of the changes found in the patient-derived virus have not been identified yet in dominant viral variants circulating in the population at large. However, these changes have been already detected in databases of publicly available viral sequences. These mutations remain isolated, the authors of the report said, but they could be harbingers of viral mutants that may spread across the population. Crucial information for this study was derived from determination of the virus structure (Fig. 1) carried out via x-ray macromolecular x-ray diffrac-

tion at the NE-CAT 24-ID-C and 24-ID-E x-ray beamlines at the APS.

The researchers emphasize that variants initially detected in the U.K. and South Africa remain vulnerable to currently approved mRNA vaccines, which target the entire spike protein rather than just portions of it. Nonetheless, the study results could also offer a preview into a future, in which current vaccines and treatments may gradually lose their effectiveness against next-wave mutations that render the virus impervious to immune pressures.

"Our experiments demonstrated that structural changes to the viral spike protein offer workarounds that allow the virus to escape antibody neutralization," said study senior author Jonathan Abraham, assistant professor of microbiology in the Blavatnik Institute at Harvard Medical School and an infectious disease specialist at Brigham and Women's Hospital. "The concern here is that an accumulation of changes to the spike protein over time could impact the long-term effectiveness of monoclonal antibody therapies and vaccines that target the spike protein."

Although the scenario remains hypothetical for now, Abraham said, it underscores the importance of two things. First, reducing the growth and spread of mutations by curbing the virus's spread both through infection-prevention measures and through widespread vaccination. Second, the need to design next-generation vaccines and therapies that target less mutable parts of the virus.

"How the spike responded to persistent immune pressure in one person over a five-month period can teach us how the virus will mutate if it continues to spread across the globe," added Abraham, who co-leads the COVID-19 therapeutics working group of the Massachusetts Consortium on Pathogen Readiness (MassCPR). "To help stop the virus from circulating, it's critical to make sure that vaccines are rolled out in an equitable way so that everyone in every country has a chance to get immunized."

Mutations are a normal part of a virus's life cycle. They occur when a virus makes copies of itself. Many of these mutations are inconsequential, others are harmful to the virus itself and yet others may become advantageous to the microbe, allowing it to propagate more easily from host to host. This latter change allows a variant to become more transmissible. If a change on a variant confers some type of evolutionary advantage to the virus, this variant can gradually outcompete others and become dominant.

In the early months of the pandemic, the assumption—and hope—was that SARS-CoV-2 would not change too fast because, unlike most RNA viruses, it has a "proofreading" protein whose job is to prevent too many changes to the viral genome. But last fall, Abraham and colleagues became intrigued by—and then alarmed about—a patient receiving immune-suppressive treatment for an autoimmune disorder who had been infected with SARS-CoV-2. The patient had developed a chronic infection. A genomic analysis of the patient's virus showed a cluster of eight mutations on the viral spike protein, which the virus uses to enter human cells and that is the target of current antibody treatments and vaccines. Specifically, the mutations had clustered on a segment of the spike known as the receptor-binding domain (RBD), the part that antibodies latch onto to prevent SARS-CoV-2 from entering human cells.

Abraham and colleagues knew the changes were a sign that the virus had developed workarounds to the patient's immune defenses. But would these mutations allow the virus to dodge the immune assault of antibodies that were not the patient's own?

To answer the question, Abraham and colleagues created lab-made, noninfectious replicas of the patient virus that mimicked the various structural changes that had accumulated in the span of five months.

In a series of experiments, the researchers exposed the dummy virus to both antibody-rich plasma from COVID-19 survivors and to pharmaceutically made antibodies now in clinical use. The virus dodged both naturally occurring and pharmaceutical-grade antibodies.

Experiments with a monoclonal antibody drug that contains two antibodies showed the virus was entirely resistant to one of the antibodies in the cocktail and somewhat, although not fully, impervious to the other. The second antibody was four-times less potent in neutralizing the mutated virus.

"Escape Artist" cont'd. on next page

"Escape Artist" cont'd. from previous page

Not all eight mutations rendered the virus equally resistant to antibodies. Two particular mutations conferred the greatest resistance to both natural and lab-grown antibodies.

In a final experiment, the researchers created a super antibody by cobbling together proteins from naturally occurring antibodies that had evolved over time to become more attuned to and better at recognizing SARS-CoV-2 and capable of latching onto it more tightly. The process, known as antibody affinity maturation, is the principle behind vaccine booster shots used to fortify existing antibodies. One specific variant containing mutations that had occurred late in the course of the patient's infection was capable of withstanding even this super-potent antibody. But the super-potent antibody did manage to neutralize viral mutations detected at a different time in the course of the infection.

"This observation underscores two points: That the virus is smart enough to eventually evolve around even our most potent antibody therapies, but that we can also get ahead by 'cooking' new potent antibodies now, before new variants emerge," Abraham said

Taken together the findings underscore the need to further understand human antibody responses to SARS-CoV-2 and to untangle the complex interplay between virus and human host, the researchers said. Doing so would allow scientist to anticipate changes in the virus and design countermeasures around these mutations before they become widespread.

In the short term, this speaks to the greater need to design antibody-based therapies and vaccines that directly target more stable, less mutable parts of the spike protein beyond its mutation-prone RBD region.

Long-term, this means that scientists should pivot toward developing therapies that go beyond antibody immunity and include also so-called cellular immunity, which is driven by T cells—a separate branch of the immune system that is independent of antibody-based immunity.

The most immediate implication, however, Abraham said, is to stay on top of emerging mutations through aggressive genomic surveillance. This means that instead of merely detecting whether SARS-CoV-2 is present in a patient sample, the tests should also analyze the viral genome and look for mutations. The technology to do so exists and is used in several countries as a way to monitor viral behavior and track changes to the virus across the population.

"In the United States, especially, the strategy has been to test and say whether a person is infected or not infected," Abraham said. "But there's a lot more information in that sample that can be obtained to help us track whether the virus is mutating. I am encouraged by the concerted efforts across the world to monitor sequences more aggressively—doing so is critical."

"It is important for us to stay ahead of this virus as it continues to evolve," said study first author Sarah Clark, member of the Abraham lab and a fourth-year student in the Ph.D. Program in Virology at Harvard University. "My hope is that our study provides insights that allow us to continue to do that."

See: Sarah A. Clark[1], Lars E. Clark[1], Junhua Pan[1], Adrian Coscia[1], Lindsay G.A. McKay[2], Sundaresh Shankar[1], Rebecca I. Johnson[2], Vesna Brusic[1], Manish C. Choudhary[3], James Regan[3], Jonathan Z. Li[3], Anthony Griffiths[2], and Jonathan Abraham[1,3,4,5]*, "SARS-CoV-2 evolution in an immunocompromised host reveals shared neutralization escape mechanisms," Cell **184**, 2605 (May 13, 2021).
DOI: 10.1016/j.cell.2021.03.027
Author affiliations: [1]Harvard Medical School, [2]Boston University School of Medicine, [3]Brigham and Women's Hospital, [4]Broad Institute of Harvard and MIT, [5]Massachusetts Consortium on Pathogen Readiness
Correspondence: * jonathan_abraham@hms.harvard.edu

This work is based upon research conducted at the NE-CATbeamlines, which are funded by the National Institute of General Medical Sciences from the National Institutes of Health (NIH) (P30 GM124165). We thank the staff at NE-CAT for assistance with x-ray data collection. Funding was provided by the Massachusetts Consortium on Pathogen Readiness (MassCPR) and the China Evergrande Group (to J.A.). We acknowledge support for COVID-19 related structural biology research at Harvard from the Nancy Lurie Marks Family Foundation and the Massachusetts Consortium on Pathogen Readiness. The project described was also supported by the National Institute of General Medical Sciences (T32GM007753). This research used resources of the Advanced Photon Source, a U.S. Department of Energy (DOE) Office of Science user facility, operated for the DOE Office of Science by Argonne National Laboratory under Contract No. DE-AC02-06CH11357.

Novel Behavior Coordinates Construction of Cell Walls in Bacteria

Bacteria build walls around themselves as protection from the environment. Cell wall material synthesis begins in the cell; a precursor, called Lipid II, is flipped to the outside of the cell wall, where it's used to form glycan strands, which are then cross-linked. While the strands are being synthesized and transported, they are still linked to the bacterium's cell membrane. Before the strands can be cross-linked to the growing cell wall, these links must be cleaved. Up until now, the synthesizing and cross-linking steps have received a great deal of attention as targets for antibiotics, but the cleaving step remained a mystery. Using the APS, researchers have found that an enzyme outside the bacterium forms a complex with a protein spanning the bacterium's cell membrane. The complex performs two functions: it regulates the length of the strands, and it cleaves their link to the cell membrane. This newly discovered behavior provides insight into how bacteria coordinate the mechanics of cell wall growth. The finding, published is the journal *Nature Microbiology*, lays the foundation for unanticipated avenues of research in cell biology, cancer immunology, and drug discovery.

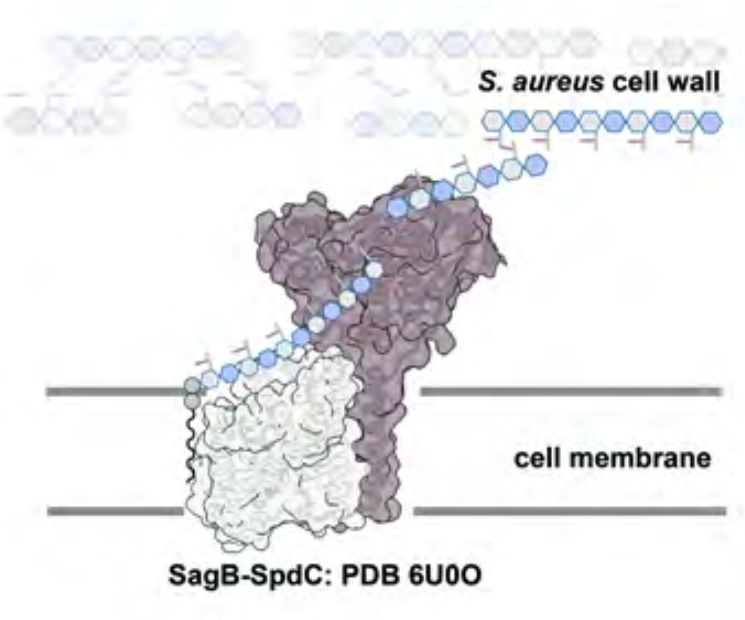

Fig. 1. Crystal structures derived from diffraction data obtained at the NE-CAT beamlines showing how the transmembrane protein SpdC positions the enzyme SagB so that its active site is precisely oriented to cleave the glycan strand.

Like other bacteria, *Staphylococcus aureus*—the toxic pathogen responsible for many skin infections, gastroenteritis, and toxic shock syndrome—synthesizes strands of peptidoglycans (PG) inside the cell, then transfers them outside the cell while they're still attached to the cell membrane. This link must be cut before the PG can be fully incorporated into the growing cell wall.

In some bacteria, like the one that causes pneumonia, the cell wall is composed of one super long strand wrapped completely around the cell. In *S. aureus*, the bacterium studied in this research, the cell walls comprise short strands, little bricks made of sugars and amino acids piled on top of each other, cross-linked by peptide bonds.

Using a variety of techniques, the researchers in this study investigated the long-standing question of how bacteria cleave the newly synthesized peptidoglycan strands from the membrane so that they can be incorporated into the cell wall. Besides answering their questions about how the strand is cleaved from the membrane, their research also revealed the mechanism by which *S. aureus* controls the length of the strands.

To begin, the researchers looked for genes that are important in cell wall assembly. They discovered that the products of genes *sagB* and *spdC* shared certain genetic and behavioral profiles, including the ability to cleave larger molecules into smaller ones. This led the researchers to conjecture that the gene products SagB and SpdC may function as a sort of cleaving complex. Through biochemical assays, they were able to show *in vitro* that their conjecture was correct.

To understand how the enzyme and the protein interacted within the complex, the researchers made crystals of SagB and SpdC in complex. Using NE-CAT beamlines 24-ID-C and 24-ID-E at the APS to collect x-ray macromolecular crystallography diffraction data, they solved the crystal structure of the complex at a resolution of 2.6 Å.

Their crystal structures showed that the transmembrane protein SpdC positions the enzyme SagB so that its active site is precisely oriented to cleave the glycan strand (Fig. 1). What's more, the SpdC provided a path extending from an entry point in the membrane straight into SagB's cleavage site. Remarkably, the length of the path cor-

"Cell Walls" cont'd. on page 119

A New Molecular Target for Therapeutic Interventions Aimed at *C. Difficile* Infection

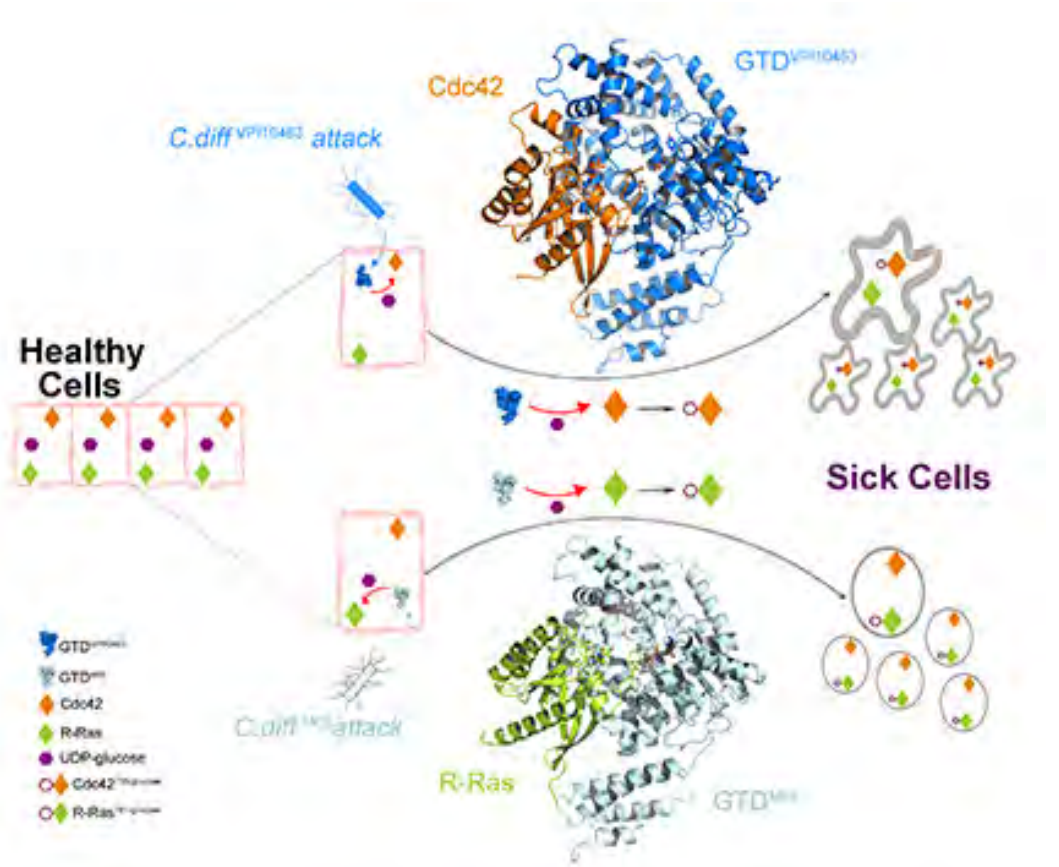

The VPI10463 and M68 represent the classic and the hypervirulent *C. difficile*, respectively. GTD-VPI preferentially modifies Rho family GTPases (Cdc42, for example) by glucosylation, while GTD-M68 more effectively modifies R-Ras. Due to their different selectivity toward Rho or Ras family GTPases, these two different TcdB variants cause two distinct types of cytopathic effects.

The original University of California, Irvine press release can be read here.© 2021 UC Regents

A University of California, Irvine (UCI)-led study suggests that the glucosyltransferase domain (GTD) is an ideal molecular target for therapeutic interventions for *Clostridioides difficile* infection (CDI). Based on their findings that established the structural basis for Toxin B recognition of the small GTPases Rho and R-Ras families, the study, which used data obtained at the APS and was published in *Science Advances,* may lead to new treatments to fight this deadly disease.

CDI is the leading cause of antibiotic-associated diarrhea and gastroenteritis-associated deaths worldwide, accounting for 500,000 cases and 29,000 deaths annually in the U.S. Classified by the Centers for Disease Control and Prevention as one of the top health threats, there is growing global concern surrounding the emerge and spread of hypervirulent *C. difficile* strains, resembling the occurrence of new virus variants in the current COVID pandemic. TcdB is one of two homologous *C. difficile* exotoxins, and TcdB alone is capable of causing the full spectrum of CDI diseases.

"We focused on the structure and function of TcdB's crucial GTD, which is the toxin's 'warhead.' The GTD is delivered by the toxin inside the host cells and causes most of the cytosolic damage to patients," said Rongsheng Jin, professor in the Department of Physiology & Biophysics at the UCI School of Medicine, and corresponding author. "We discovered molecular mechanisms by which the GTD specifically recognizes and blocks the physiological functions of the human GTPases Rho and R-Ras enzyme families that are crucial signaling molecules." To determine the structure of GTD, the team collected x-ray diffraction data at the NE-CAT beamline 24-ID-C of the APS.

The team also demonstrated how the classic form of TcdB and the hypervirulent TcdB recognize their human targets in different ways, which leads to distinct structural changes to the host cells caused by bacterial invasion.

"Once the GTD of TcdB is inside the cells, it is shielded by our cells and becomes inaccessible to passive immunotherapy. But our studies suggest that small molecule inhibitors could be developed to disarm the GTD, which will directly eliminate the root cause of disease symptoms and cellular damage," Jin said. "This new strategy can potentially be integrated with and complement other CDI treatment regiments."

See: Zheng Liu[1], Sicai Zhang[2], Peng Chen[1], Songhai Tian[2], Ji Zeng[2], Kay Perry[3], Min Dong[2], and Rongsheng Jin[1]*, "Structural basis for selective modification of Rho and Ras GTPases by Clostridioides difficile toxin B," Sci. Adv. **7**, eabi4582 (22 October 2021). DOI: 10.1126/sciadv.abi4582
Author affiliations: [1]University of California, Irvine, [2]Harvard Medical School, [3]Cornell University
Corresponding author: * r.jin@uci.edu

This work was partly supported by National Institutes of Health (NIH) grants R01AI125704, R21AI139690, and R21AI123920 to R.J.; R01NS080833 and R01AI132387 to M.D.; and R01AI139087 and R21 CA235533 to R.J. and M.D. M.D. holds the Investigator in the Pathogenesis of Infectious Disease award from the Burroughs Wellcome Fund. NE-CAT is supported by a grant from the National Institute of General Medical Sciences (P30 GM124165). This research used resources of the Advanced Photon Source, a U.S. Department of Energy (DOE) Office of Science user facility operated for the DOE Office of Science by Argonne National Laboratory under Contract No. DE-AC02-06CH11357.

"Cell Walls" cont'd. from page 117

responded to the average length of the strands to be incorporated into the cell wall.

Hydrolases like SagB are the current frontier in cell wall research. Scientists have long understood the "what" of bacterial cell wall growth. This work explains the "how." It lays the foundation for further research by this team, combining chemistry, biochemistry, genetics, and functional genomics to ultimately explain the why—a discovery that could reveal the weak points in bacterial defense systems and enable scientists to disrupt their growth.

– Judy Myers

See: Kaitlin Schaefer[1], Tristan W. Owens[2], Julia E. Page[1], Marina Santiago[1], Daniel Kahne[2], and Suzanne Walker[1]*, "Structure and reconstitution of a hydrolase complex that may release peptidoglycan from the membrane after polymerization," Nat. Microbiol. **6**, 34 (2021).
DOI: 10.1038/s41564-020-00808-5
Author affiliations: [1]Harvard Medical School [2]Harvard University
Correspondence: * suzanne_walker@hms.harvard.edu

The research was supported by grants. GM076710 and U19AI109764 to D.K. and S.W., and T32GM007753 to J.E.P. The NE-CAT beamlines are funded by the National Institute of General Medical Sciences from the National Institutes of Health (P30 GM124165). The Eiger 16M detector on 24-ID-E is funded by a NIH-ORIP HEI grant (S10OD021527). This research used resources of the Advanced Photon Source, a U.S. Department of Energy (DOE) Office of Science user facility operated for the DOE Office of Science by Argonne National Laboratory under Contract No. DE-AC02-06CH11357.

Synthesis of a Potent Antibiotic Follows an Unusual Chemical Pathway

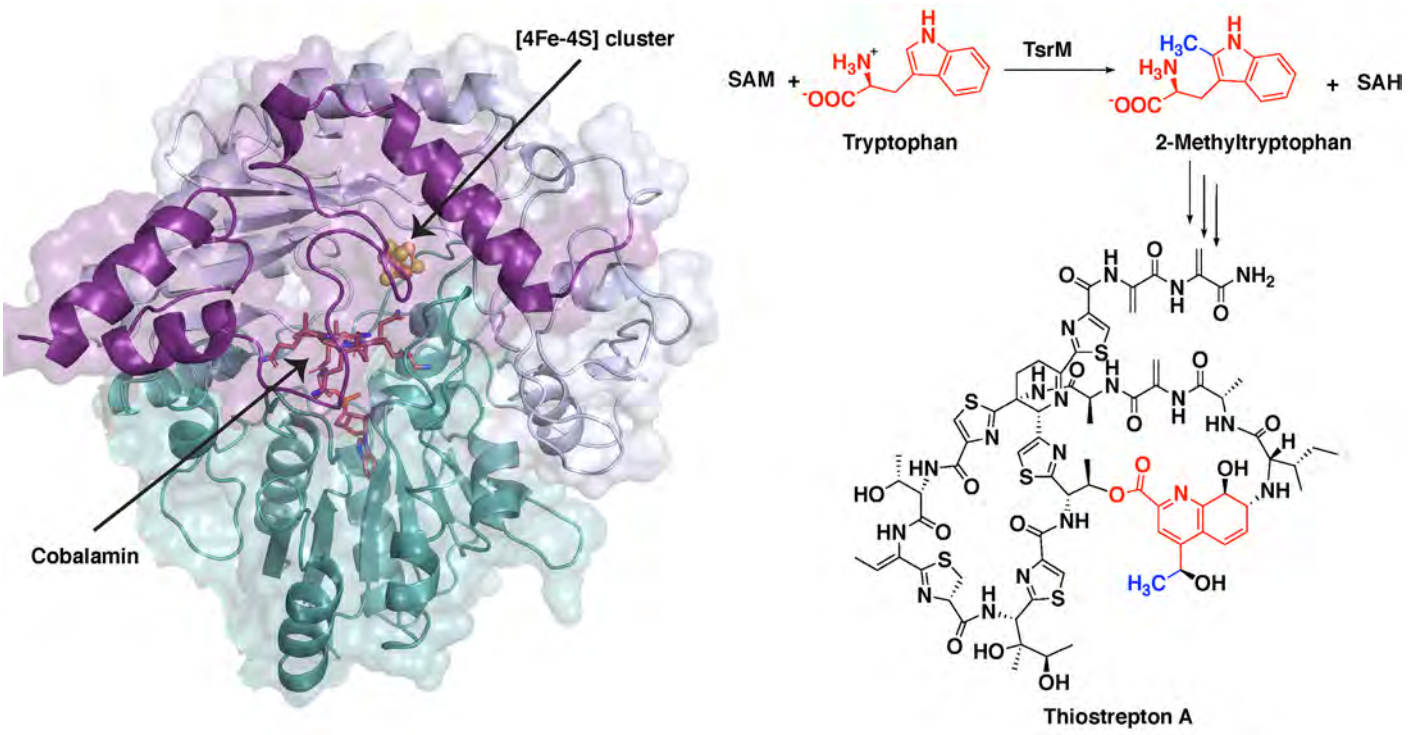

The synthesis of the potent antibiotic thiostrepton uses a radical SAM protein TsrM, whose crystal structure is shown at left while bound to an iron-sulfur cluster and cobalamin. New images of this crystal structure allowed researchers from Penn State to infer the chemical steps during the antibiotic's synthesis (right), as a methyl group moves from a molecule called S-adenosyl-L-methionine (SAM) to the cobalamin in TsrM to the substrate tryptophan. Image: Booker Lab, Penn State

The original Penn State press release by Gail McCormick, Penn State, can be read here. The Pennsylvania State University © 2021

Images of a protein involved in creating a potent antibiotic reveal the unusual first steps of the antibiotic's synthesis. The improved understanding of the chemistry behind this process is detailed in a new study led by Penn State chemists based upon research at two U.S. Department of Energy x-ray light sources, including the APS, and published in the journal *Nature Chemical Biology*. These results could allow researchers to adapt this and similar compounds for use in human medicine.

"The antibiotic thiostrepton is very potent against Gram-positive pathogens and can even target certain breast cancer cells in culture," said Squire Booker, a biochemist at Penn State and investigator with the Howard Hughes Medical Institute. "While it has been used topically in veterinary medicine, so far it has been ineffective in humans because it is poorly absorbed. We studied the first steps in thiostrepton's biosynthesis in hopes of eventually being able to hijack certain processes and make analogs of the molecule that might have better medicinal properties. Importantly, this reaction is found in the biosynthesis of numerous other antibiotics, and so the work has the potential to be far reaching."

The first step in thiostrepton's synthesis involves a process called methylation. A molecular tag called a methyl group, which is important in many biological processes, is added to a molecule of tryptophan, the reaction's substrate. One of the major systems for methylating

compounds that are not particularly reactive, like tryptophan, involves a class of enzymes called radical SAM proteins.

"Radical SAM proteins usually use an iron-sulfur cluster to cleave a molecule called S-adenosyl-L-methionine (SAM), producing a "free radical" or an unpaired electron that helps move the reaction forward," said Hayley Knox, a graduate student in chemistry at Penn State and first author of the paper. "The one exception that we know about so far is the protein involved in the biosynthesis of thiostrepton, called TsrM. We wanted to understand why TsrM doesn't do radical chemistry, so we used an imaging technique called x-ray crystallography to investigate its structure at several stages throughout its reaction." The x-ray crystallography experiments were carried out at the GM/CA-XSD and LS-CAT x-ray beamlines at the APS, and at the Berkeley Center for Structural Biology beamlines at the Advanced Light Source at Lawrence Berkeley National Laboratory

In all radical SAM proteins characterized to date, SAM binds directly to the iron-sulfur cluster, which helps to fragment the molecule to produce the free radical. However, the researchers found that the site where SAM would typically bind is blocked in TsrM.

"This is completely different from any other radical SAM protein," said Booker. "Instead, the portion of SAM that binds to the cluster associates with the tryptophan substrate and plays a key role in the reaction, in what is called substrate-assisted catalysis."

In solving the structure, the researchers from the Massachusetts Institute of Technology and the Albert Einstein College of Medicine, in addition to Pennsylvania State University, were able to infer the chemical steps during the first part of thiostrepton's biosynthesis, when tryptophan is methylated. In short, the methyl group from SAM transfers to a part of TsrM called cobalamin. Then, with the help of an additional SAM molecule, the methyl group transfers to tryptophan, regenerating free cobalamin and producing the methylated substrate, which is required for the next steps in synthesizing the antibiotic.

"Cobalamin is the strongest nucleophile in nature, which means it is highly reactive," said Knox. "But the substrate tryptophan is weakly nucleophilic, so a big question is how cobalamin could ever be displaced. We found that an arginine residue sits under the cobalamin and destabilizes the methyl-cobalamin, allowing tryptophan to displace cobalamin and become methylated."

Next the researchers plan to study other cobalamin-dependent radical SAM proteins to see if they operate in similar ways. Ultimately, they hope to find or create analogs of thiostrepton that can be used in human medicine.

"TsrM is clearly unique in terms of known cobalamin-dependent radical SAM proteins and radical SAM proteins in general," said Booker. "But there are hundreds of thousands of unique sequences of radical SAM enzymes, and we still don't know what most of them do. As we continue to study these proteins, we may be in store for many more surprises."

See: Hayley L. Knox[1], Percival Yang-Ting Chen[2‡], Anthony J. Blaszczyk[1‡‡], Arnab Mukherjee[1], Tyler L. Grove[3], Erica L. Schwalm[1‡‡‡], Bo Wang[1], Catherine L. Drennan[2*], and Squire J. Booker[1**], "Structural basis for non-radical catalysis by TsrM, a radical SAM methylase," Nat. Chem. Biol. **17**, 485 (2021). DOI: 10.1038/s41589-020-00717-y
Author affiliations: [1]Pennsylvania State University, [2]Massachusetts Institute of Technology, [3]Albert Einstein College of Medicine Present addresses: [‡]University of California, San Diego, [‡‡]Catalent Pharma Solutions, [‡‡‡]Merck & Co., Inc.
Correspondence: * cdrennan@mit.edu, ** squire@psu.edu

This work was supported by the National Institutes of Health (NIH) GM-122595 to S.J.B. and GM-126982 to C.L.D., and the Eberly Family Distinguished Chair in Science (S.J.B.). S.J.B. and C.L.D. are investigators of the Howard Hughes Medical Institute. Use of GM/CA-XSD has been funded in whole or in part with federal funds from the National Cancer Institute (ACB-12002) and the National Institute of General Medical Sciences (AGM-12006). The Eiger 16M detector at GM/CA-XSD was funded by NIH grant S10 OD012289. Use of LS-CAT was supported by the Michigan Economic Development Corporation and the Michigan Technology Tri-Corridor (grant 085P1000817). This research also used the resources of the Berkeley Center for Structural Biology supported in part by the Howard Hughes Medical Institute. The Advanced Light Source is a U.S. Department of Energy (DOE) Office of Science user facility under contract no. DE-AC02-05CH11231. The ALS-ENABLE beamlines are supported in part by the NIH, National Institute of General Medical Sciences grant P30 GM124169. This research used resources of the Advanced Photon Source, a U.S. DOE Office of Science user facility operated for the DOE Office of Science by Argonne National Laboratory under contract no. DE-AC02-06CH11357.

First Detailed Look at a Crucial Enzyme Advances Cancer Research

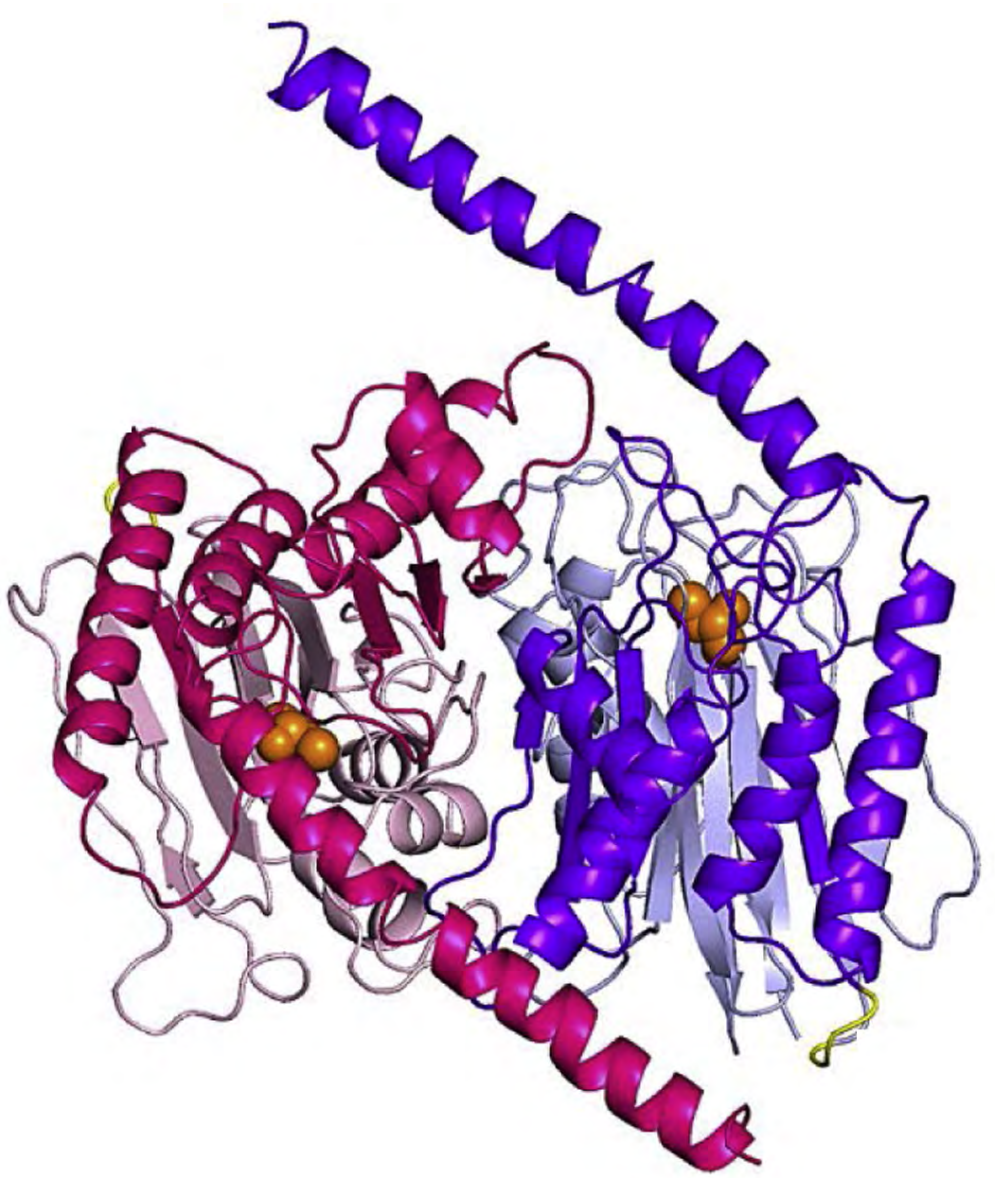

Fig. 1. Crystal structure of cp-Taspase1α41-233/β. From N. Nagaratnam et al., Structure **29**(8), 873, (5 August 2021). ©2021 Elsevier Ltd.

The Arizona State University press release by Richard Harth can be read here.

In order to develop more effective drugs against a range of cancers, researchers have been investigating the molecular structure of many disease-linked enzymes in the body. An intriguing case in point is Taspase1, a type of enzyme known as a protease. The primary duty of proteases is to break down proteins into smaller peptide snippets or single amino acids. In a new study appearing in the journal *Structure*, a collaborative team of researchers from Arizona State University, Beryllium Discovery Corp., Washington University in St. Louis, the National Institutes of Health, SRI International, and the Spanish National Research Council, describe their investigations at the APS, which reveal the structure of Taspase1 as never before.

Taspase1 appears to play a vital role in a range of physiological processes, including cell metabolism, proliferation, migration and termination. The normal functioning of Taspase1 can go awry however, leading to a range of diseases, including leukemia, colon and breast cancers, as well as glioblastoma, a particularly lethal and incurable malignancy in the brain.

Because Taspase1 dysregulation is increasingly implicated in the genesis and metastasis of various cancers, it has become an attractive candidate for drug development. But before this can happen, researchers need a highly detailed blueprint of the structure of this protease.

The study unveils, for the first time, the catalytically active 3D structure of the catalytically active Taspase1 protein, revealing a previously unexplored region that is essential for the functioning of the molecule. We developed a novel cloning strategy to generate the fully active form of Taspase1 as circularly permuted variant (cpTaspase1α41-233/β) to allow us to obtain 3D crystals, which were measured by X-ray diffraction at the GM/CA-XSD x-ray beamline 23-ID-D at the APS. The structure of cpTaspase1α41-233/β protein was solved to 3-Å resolution (Fig. 1) in the labs of Petra Fromme at Arizona State University.

Fromme, director of the Biodesign Center for Applied Structural Discovery, highlights the great importance of the work: "I am so excited that we were able to solve the first structure of the functional active enzyme, as it will have huge implications for the structure-based development on novel anti-cancer drugs."

The results of this study show that reducing the size of a critical helical region of Taspase1, limits protease activity, while eliminating the helical region deactivates Taspase1 functioning altogether. Earlier research suggested that disabling Taspase1 activity to block the progression of cancer could be achieved without harmful side effects.

"We have reported the importance of a previously unobserved long fragment of the protein in the catalytic activity of Taspase1, which can be used as an attractive target to inhibit Taspase1," said Jose Martin-Garcia, lead scientist on the project and co-corresponding author with Fromme. "The crystal structure of the active Taspase1 reported in our article will be greatly beneficial to advance the design of Taspase1 inhibitors for anti-cancer therapy."

See: Nirupa Nagaratnam[1], Silvia L. Delker[2‡], Rebecca Jernigan[1], Thomas E. Edwards[2‡], Janey Snider[3], Darren Thifault[1], Dewight Williams[1], Brent L. Nannenga[1], Mary Stofega[3], Lidia Sambucetti[3], James J. Hsieh[4], Andrew J. Flint[5], Petra Fromme[1*], and Jose M. Martin-Garcia[1,6**], "Structural insights into the function of the catalytically active human Taspase1," Structure **29**(8), 873, (5 August 2021).
DOI: 10.1016/j.str.2021.03.008
Author affiliations: [1]Arizona State University, [2]Beryllium Discovery Corp., [3]SRI International Menlo Park, [4]Washington University in St. Louis, [5]National Institutes of Health, [6]Spanish National Research Council ‡Present address: UCB Biosciences
Correspondence: * petra.fromme@asu.edu,
** jmmartin@iqfr.csic.es

This project has been funded in whole with Federal funds from the National Cancer Institute (NCI), National Institutes of Health (NIH), under Chemical Biology Consortium contract no. HHSN261200800001E. Use of LS-CAT was supported by the Michigan Economic Development Corporation and the Michigan Technology Tri-Corridor (Grant 085P1000817). The GM/CA-XSD structural biology facility at the APS has been funded by the National Cancer Institute (ACB-12002) and the National Institute of General Medical Sciences (AGM-12006, P30GM138396). This research used resources of the Advanced Photon Source, a U.S. Department of Energy DOE Office of Science user facility operated for the DOE Office of Science by Argonne National Laboratory under contract no. DE-AC02-06CH11357.

How Antibodies Bind a Molecule Linked to Cancer

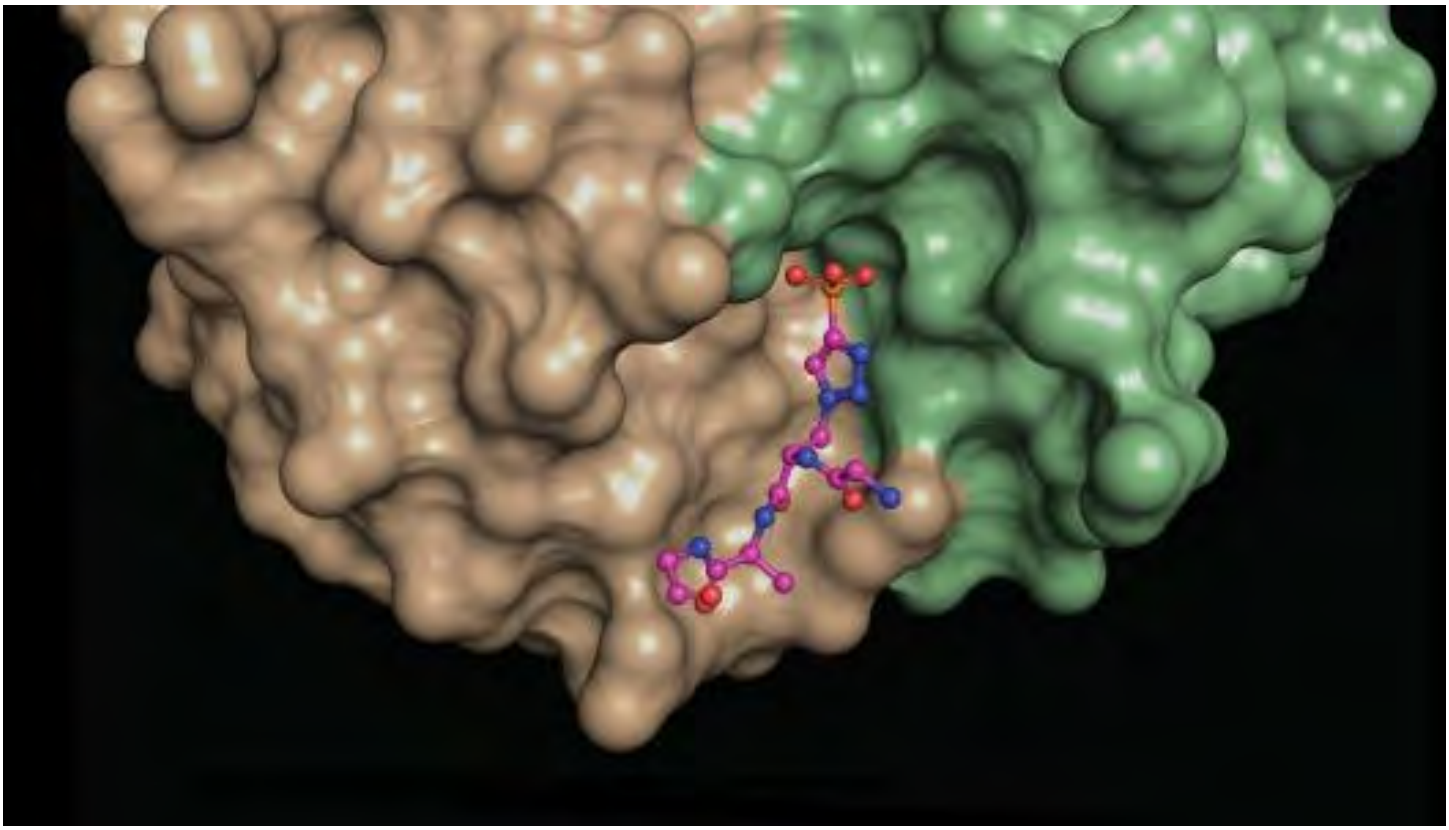

A structural snapshot of a phosphohistidine analogue (ball and stick model) nestled at the interface between different areas (green, brown) of a phosphohistidine antibody. Such structures provide insights into the molecular properties of the antibodies, which makes them useful for revealing elusive phosphohistidine-containing proteins in cells. Image: the Salk Institute.

The original Argonne news story by Joan Koka can be read here.

Scientists are harnessing hard x-rays in the fight against cancer. A team of researchers, in conjunction with the U.S. Department of Energy's (DOE) Argonne, has used ultrabright x-ray light to determine how specific types of antibodies can tell the difference between different forms of a cancer-linked molecule. These new insights will help scientists design better antibodies for potential treatments.

Tony Hunter, professor at the Salk Institute for Biological Studies, led this new research, building on years of study at his lab into amino acids, the building blocks of proteins. Hunter and his team were the first to show that adding phosphate to tyrosine, one of 20 amino acids in the human body, contributes to the progression of cancer. Their discovery not only led to the development of anti-cancer drugs, but also inspired researchers to start examining phosphate in combination with other amino acids.

Histidine, an amino acid the body uses to synthesize proteins, is the new target under study at the Hunter Lab. When phosphate is added, it forms phosphohistidine, an unstable molecule that has been linked to liver and breast cancer and neuroblastoma, a type of cancer often found in the adrenal glands.

To better understand phosphohistidine's potential role in cancer, the Hunter research team has, for the past eight years, been developing and studying antibodies that can bind to it. But to discern exactly how these antibodies work, they needed a more specialized set of tools.

The APS was one of three light source facilities the research team used to gain more insight into this problem. At the facilities, they used a technique known as x-ray crystallography to determine the crystal structures of their

antibodies bound to peptides (short amino acid sequences) containing phosphohistidine. Their work and findings were recently published in the *Proceedings of the National Academy of Sciences*.

"Our antibodies are going to be key to studying this relatively understudied process of histidine phosphorylation, and thanks to x-ray crystallography, we now know how they work," said Hunter "This means we can potentially improve them for specific purposes and even perhaps for use in the clinical arena where we see evidence that histidine phosphorylation is connected to cancer."

To make use of this technique, Hunter's team worked alongside researchers at The Scripps Research Institute and used three different DOE light sources to collect data: the GM/CA-XSD 23-ID-D beamline at the Argonne APS; beamline 12-2 at the Stanford Synchrotron Radiation Lightsource, SLAC National Accelerator Laboratory; and beamline 5.0.3 at the Advanced Light Source at Lawrence Berkeley National Laboratory. All three provide extremely intense, small x-ray beams that are particularly useful for this type of technique.

The researchers first grew crystals of their antibodies bound to phosphohistidine peptides. These were then sent to the light sources, which had capabilities that allowed the researchers to place their crystals in an x-ray beam remotely. Upon contact with the crystals, the beams scattered, creating diffraction patterns that were collected and used to determine the three-dimensional atomic structure of the antibodies combined with the phosphohistidine peptides.

"X-rays have wavelengths that are about the size of atoms, and they scatter strongly. But it's not so easy to make a lens that can recombine these rays to form an image near atomic resolution," said protein crystallographer Michael Becker of GM/CA-XSD. "So instead, researchers collect diffraction data on detectors and use mathematics, physics and chemistry in the computer to essentially calculate an image of the molecule in the crystal."

X-ray crystallography allows scientists to determine the molecular and atomic structure of these tiny crystals. By measuring these diffracted beams, scientists can reconstruct an image of the atoms and their position in the sample, as well as a host of other information.

"What crystallography did was enable us to look at atomic interactions between the antibody and the antigen, which in this case was the phosphohistidine," said Ian Wilson, a structural biology professor at The Scripps Research Institute and a co-author on the paper.

The resulting insights not only advance our understanding of phosphohistidine's potential role in cancer, but can also help other scientists looking to design better antibodies to suit their own research purposes.

"From the data, we learned how small differences in atomic interactions help the antibodies to differentiate the two different isoforms of phosphohistidine, and also how these antibodies are able to recognize different peptides which undergo histidine phosphorylation," said Rajasree Kalagiri, a Salk postdoctoral researcher and lead author of the study.

See: Rajasree Kalagiri[1], Robyn L. Stanfield[2], Jill Meisenhelder[1], James J. La Clair[1,3], Stephen R. Fuhs[1], Ian A. Wilson[2], and Tony Hunter[1], "Structural basis for differential recognition ofphosphohistidine-containing peptides by 1-pHisand 3-pHis monoclonal antibodies," Proc. Natl. Acad. Sci. U.S.A. **118**(6), e2010644118 (2021).
DOI: 10.1073/pnas.2010644118|
Author affiliations: [1]Salk Institute for Biological Studies, [2]The Scripps Research Institute, [3]University of California, San Diego
Correspondence: * hunter@salk.edu

Use of the Stanford Synchrotron Radiation Light Source, SLAC National Accelerator Laboratory, is supported by the U.S. Department of Energy (DOE) Office of Science-Basic Energy Sciences, under Contract DE-AC02-76SF00515. The Advanced Light Source is a DOE Office of Science user facility under Contract DE-AC02-05CH11231. The Pilatus detector on 5.0.1. was funded under NIH Grant S10OD021832. Funding for reagents used in this project, and salary support, was provided by NIH 5 R01 CA082683, NIH 5R01 CA194584, and NIH 1 R35 CA242443 (to T.H.); Leona M. and Harry B. Helmsley Charitable Trust Grant 2012-PG-MED002; and the Skaggs Institute for Chemical Biology at The Scripps Research Institute. The Salk Peptide Synthesis and Proteomics Cores are supported by P30 CA014195. T.H. is a Frank and Else Schilling American Cancer Society Professor and holds the Renato Dulbecco Chair in Cancer Research. I.A.W. is the Hansen Professor of Structural Biology. This research used resources of the Advanced Photon Source, a US DOE Office of Science user facility operated for the DOE Office of Science by Argonne National Laboratory under Contract DE-AC02-06CH11357.

How Malaria Evades Antibodies and How the Body Fights Back

Malaria is one of the most devastating diseases impacting human health, causing approximately half a million deaths each year. The disease is caused by infection with the intracellular parasite *Plasmodium* and is transmitted by female Anopheles mosquitoes during feeding. Of the six species of *Plasmodium, P. falciparum* is both the most lethal and responsible for most deadly cases. Some *P. falciparum* RIFINs—variant surface antigens expressed on infected red blood cells—bind to multiple inhibitory receptors, including LAIR1 and LILRB1. Researchers identified antibodies incorporating LILRB1 by screening plasma from donors from the Republic of Mali. B cell clones isolated from three of the donors showed large DNA insertions in the switch region that encodes LILRB1 extracellular domain 3 and 4 (D3D4) or D3 alone in the variable–constant (VH–CH1) elbow. By using a combination of biochemical and bioinformatic techniques, the researchers identified a large set of RIFINs that bound LILRB1 D3. Crystal and cryo-electron microscopy structures of RIFIN in complex with LILRB1 D3D4 revealed RIFIN–LILRB1 D3 interactions to be similar though distinct from those of RIFIN–LAIR1. The RIFIN–LILRB1 structures, including those obtained at the APS and published in the journal *Nature*, further revealed an unconventional triangular architecture with the inserted LILRB1 domains opening the VH–CH1 elbow. Better understanding the mechanism that leads to receptor-binding specificity of RIFINs could guide the development of malaria vaccines and therapeutic antibodies.

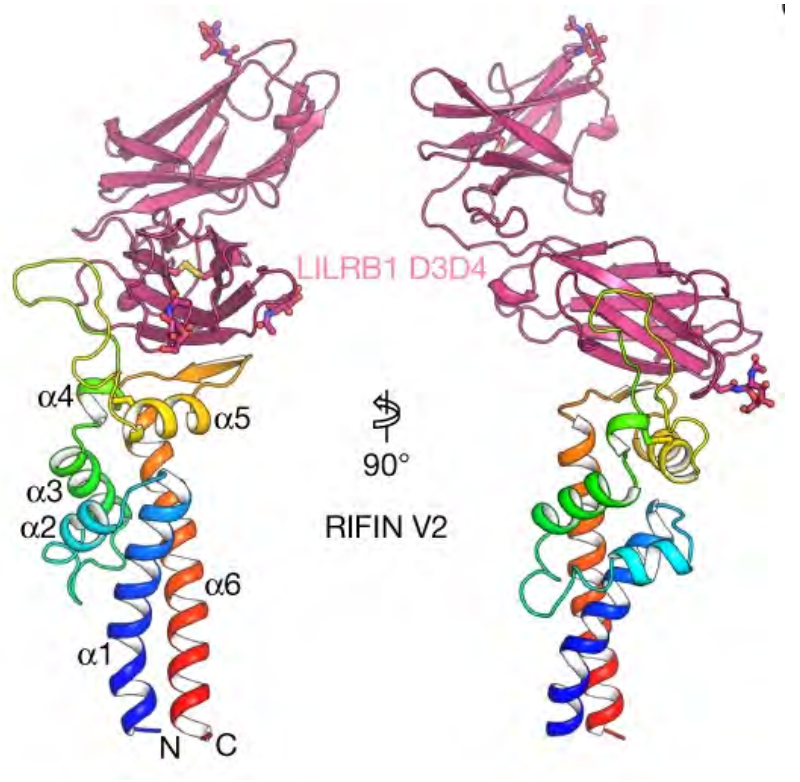

Fig. 1. Crystal structure of RIFIN V2 (PF3D7_1373400) domain in complex with LILRB1 D3D4 domains in two orthogonal cartoon views, based on data obtained at SER-CAT at the APS. RIFIN is colored in rainbow and LILRB1 is colored in red. From Y. Chen et al., Nature **592**, 639 (22 April 2021). © 2021 Springer Nature Limited

The symptoms of malaria occur as *Plasmodium* parasites replicate within blood. This nutrient-rich environment also contains much of the host's immune-defense machinery. To survive the immune response, *Plasmodium* parasites have evolved to replicate while hidden within host cells. Only a few functionally critical parasite proteins are exposed on host cell surfaces, which are grouped into large protein families, allowing a immune evasion strategy based on antigenic variation.

Repetitive interspersed families of polypeptides (RIFINs) are variable antigens expressed on infected red blood cells. They mediate formation of clusters of uninfected red blood cells surrounding a central P. falciparum-infected red blood cell that occurs in severe malaria. RIFINs bind LAIR1 and LILRB1—two inhibitory receptors found on natural killer cells, T cells, and B cells—playing a role in immune evasion by downregulating activation of these immune cells. RIFINs, therefore, may potentially be targets for protective immunity.

On the basis of their earlier discovery of LAIR1-containing antibodies in malaria-exposed individuals, researchers in the Antonio Lanzavecchia group at the Institute for Research in Biomedicine, Switzerland hypothesized that B cell clones with insertions of other inhibitory receptors recognized by *P. falciparum*, such as LILRB1, could be selected in the course of malaria infection. To test this, they screened 672 plasma samples from

a cohort of donors from Mali and identified six individuals with LILRB1-containing antibodies. From three positive donors, the researchers isolated B cell clones that produced LILRB1-containing monoclonal antibodies bound to infected erythrocytes.

Through mass spectrometry and binding assays, the researchers identified seven RIFINs that were recognized by LILRB1-containing antibodies. Antibodies containing LILRB1 D3D4 or D3 inserts bound to the seven identified RIFINs, while deletion of the inserted domains completely abolished binding, indicating a critical role for D3. These RIFINs differ from those of an earlier report that bind to LILRB1 D1D2 domains, which compete for the nature ligand binding, suggesting distinct binding mechanisms.

The researchers in the Peter Kwong group at the Vaccine Research Center, National Institutes of Health, then determined the cryo-electron microscopy structure of a RIFIN in complex with either LILRB1 D3D4 or a D3D4-containing Fab (antibody fragment) at 3.5-Å resolution. The structure revealed an unconventional triangular Fab architecture owing to the elbow insertion of LILRB1 D3D4 domains, with the VH–VL, D3D4, and CH1–CL domains composing the three apexes. In particular, the angle of the light chain elbow region was found to swing outward almost 90 degrees to accommodate the LILRB1 D3D4 insertion in the heavy chain elbow region.

Because the reconstruction of RIFIN in the LILRB1-RIFIN complex was not entirely clear, the researchers used x-ray crystallography data collected at the SER-CAT beamline 22-ID at the APS to determine the structure of the complex between the LILRB1 D3D4 domain and the RIFIN V2 domain to 2.6-Å resolution (Fig. 1). Together, the two structural papers of LILRB1–RIFIN complexes revealed that the V2 apex is the common binding site used by RIFINs to bind to different domains of the same receptor.

The results of this study provide insights into the role of RIFINs in immune evasion. The finding that phylogenetically distinct RIFINs target LILRB1 D1D2 and LILRB1 D3 provides a striking example of convergent evolution. Overall, the polygenicity and polymorphism of the RIFIN family is consistent with a strong selective pressure for evading the antibody response while developing different ways to bind to inhibitory receptors, a mechanism that can be effectively countered by receptor-based antibodies.

– Chris Palmer

See: Yiwei Chen[1,2], Kai Xu[3], Luca Piccoli[1], Mathilde Foglierini[1,4], Joshua Tan[1], Wenjie Jin[1,2], Jason Gorman[3], Yaroslav Tsybovsky[5], Baoshan Zhang[3], Boubacar Traore[6], Chiara Silacci-Fregni[1], Claudia Daubenberger[7], Peter D. Crompton[3], Roger Geiger[1], Federica Sallusto[1,2], Peter D. Kwong[3], and Antonio Lanzavecchia[1‡*], "Structural basis of malaria RIFIN binding by LILRB1-containing antibodies," Nature **592**, 639 (22 April 2021).
DOI: 10.1038/s41586-021-03378-6
Author affiliations: [1]Università della Svizzera italiana, [2]ETH Zurich, [3]National Institutes of Health, [4]Swiss Institute of Bioinformatics (SIB), [5]Frederick National Laboratory for Cancer Research, [6]University of Sciences, Techniques and Technologies of Bamako, [7]University of Basel ‡Present address: Humabs BioMed SA
Correspondence: * alanzavecchia@vir.bio

This work was partially supported by grants from the European Research Council (no. 670955 BROADimmune), the Fondation Louis-Jeantet, the Swiss Vaccine Research Institute, and the Swiss National Science Foundation (grant no. 176165). The Mali study was funded by the Division of Intramural Research, National Institute of Allergy and Infectious Diseases, National Institutes of Health (NIH). This work was supported by the Intramural Research Program of the Vaccine Research Center, National Institution of Allergy and Infectious Diseases, NIH; by the GenScript Innovation grant GS-IG-2018-003 (K.X.), and by federal funds from the Frederick National Laboratory for Cancer Research, NIH, under Contract HHSN261200800001 (Y.T.). SER-CAT is supported by its member institutions, and equipment grants (S10_RR25528, S10_RR028976 and S10_OD027000) from the NIH. Some of this work was performed at the Simons Electron Microscopy Center, and/or the National Resource for Automated Molecular Microscopy, and/or the National Center for Cryo-EM Access and Training located at the New York Structural Biology Center, supported by grants from the Simons Foundation (SF349247) and NIH National Institute of General Medical Sciences (GM103310) with additional support from NYSTAR and the New York State Assembly Majority. This research used resources of the Advanced Photon Source, a U.S. Department of Energy (DOE) Office of Science user facility operated for the DOE Office of Science by Argonne National Laboratory under Contract No. DE-AC02-06CH11357.

Shape-Shifting Ebola Virus Protein Exploits Human RNA to Change Shape

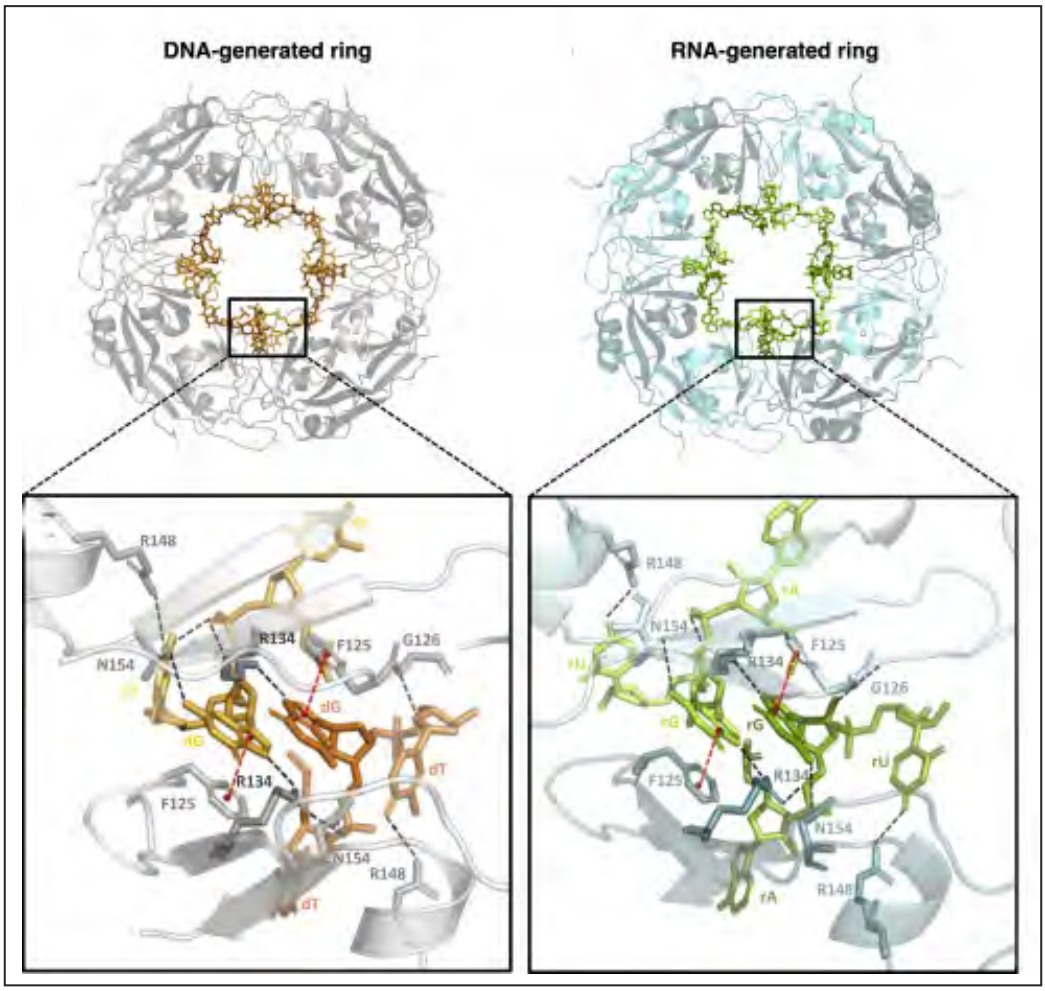

Fig. 1. Left: The crystal structure of VP40 at 1.78-Å resolution. Right: The crystal structure at 1.38-Å resolution. From S. Landeras-Bueno et al., Cell Rep. **35**, 108986, (April 13, 2021). Copyright © 2021 Elsevier Inc.

The original La Jolla Institute for Immunology press release by Madeline McCurry-Schmidt can be read here. ©2020 La Jolla Institute for Immunology. All rights reserved

The human genome contains the instructions to make tens of thousands of proteins. Each protein folds into a precise shape—and biologists are taught that defined shape dictates the protein's destined function. Tens of thousands of singular shapes drive the tens of thousands of needed functions. In a new cover story in *Cell Reports*, researchers at La Jolla Institute for Immunology, The Scripps Research Institute, and The Ohio State University using two U.S. Department of Energy x-ray light sources, including the APS, demonstrate how Ebola virus has found a different way to get things done. The virus encodes only eight proteins but requires dozens of functions in its life-cycle. The new study shows how one of Ebola virus's key proteins, VP40, uses molecular triggers in the human cell to transform itself into different tools for different jobs, presenting the possibility of new therapies to combat Ebola disease.

"We're all taught that proteins have 'a' structure," says study co-leader Erica Ollmann Saphire, president and CEO of La Jolla Institute for Immunology (LJI) and member of the LJI Center for Infectious Disease and Vaccine Research. "Ebola virus's VP40 protein, however, changes it-

self into different structures at different times, depending on the function needed."

VP40 is the protein that gives Ebola virus its distinctive string-like shape. Saphire's previous studies showed that VP40 can take on a two-molecule, butterfly-shaped "dimer" or an eight-molecule, wreath-like "octamer" form.

There are dramatic rearrangements of the protein as it transforms from one to the other. The dimer is what physically constructs new viruses that emerge and release from infected cells. The octamer functions only inside the infected cell, in a controlling role, directing other steps of the viral life cycle.

The new study shows exactly what triggers these structural changes. The researchers found that VP40 senses and relies on particular human mRNA to make the transformation from the dimer to octamer.

Saphire worked with study co-corresponding author Scripps Research Professor Kristian Andersen, to deeply sequence RNAs captured and selected by VP40 inside cells. VP40 selected particular sequences, most often found in the untranslated tails of human mRNA.

Saphire lab postdoctoral fellows Hal Wasserman and co-first author Sara Landeras Bueno, worked with purified VP40 in test tubes to get a glimpse of the dimer-to-octamer transformation in action. They tested many combinations of RNA molecules to try to trigger the transformation and found that particular human mRNA sequences rich in bases guanine and adenine were ideal for driving the same conformational change *in vitro* that they saw in high-resolution structures of VP40. The structures were obtained via macromolecular x-ray crystallography at the LRL-CAT 31-ID x-ray beamline at the APS, and the 12-2 beamline of the Stanford Synchrotron Radiation Lightsource at SLAC National Accelerator Laboratory (Fig. 1).

"We were very excited and surprised to see that the RNA that triggers this change comes from the host cell and not the virus," says Landeras Bueno. "The virus is hijacking the host cell—this is another example of a virus acting like a parasite."

Saphire says the study sheds light on the fundamentals of how information is encoded in the genome. There's the genetic code, of course, but Ebola virus also controls how VP40 is deployed during different stages of its life cycle. "It has an additional layer of programming," Saphire says.

The new study also offers further evidence that VP40 is a promising target for effective therapies. Because Ebola virus cannot spread without VP40, the virus is unlikely to acquire VP40 mutations that let it "escape" antibody therapies. This vulnerability has led the LJI team to think of VP40 as Ebola's Achilles' heel.

"VP40 fulfills an elaborate system of requirements for Ebola virus, so we don't expect it to change much," says Wasserman. "That means if we could attack VP40 specifically, the virus would be helpless."

Wasserman says the octamer's regulatory function is still slightly mysterious. The octamer is known to be essential to the Ebola virus life cycle, but more work needs to be done to understand how this VP40 structure controls Ebola virus replication.

Saphire is very interested in investigating whether other viruses—or living organisms—have proteins with the same "structural plasticity" as VP40. "I've always wanted to know if this kind of functionality is more common in biology than we think," she says.

See: Sara Landeras-Bueno[1], Hal Wasserman[1], Glenn Oliveira[2], Zachary L. VanAernum[3], Florian Busch[3], Zhe Li Salie[1], Vicki H. Wysocki[3], Kristian Andersen[2]*, and Erica Ollmann Saphire[1]**, "Cellular mRNA triggers structural transformation of Ebola virus matrix protein VP40 to its essential regulatory form," Cell Rep. **35**, 108986, (April 13, 2021). DOI: 10.1016/j.celrep.2021.108986
Author affiliations: [1]La Jolla Institute for Immunology, [2]The Scripps Research Institute, [3]The Ohio State University
Correspondence: * andersen@scripps.edu, ** erica@lji.org

The authors thank the beamline scientists at the LRL-CAT beamline and at the 12-2 beamline of the Stanford Synchrotron Radiation Lightsource. Native MS development was supported by National Institutes of Health (NIH) grant P41 GM128577 to V.H.W. Use of the Stanford Synchrotron Radiation Lightsource, SLAC National Accelerator Laboratory, is supported by the U.S. Department of Energy (DOE) Office of Science-Basic Energy Sciences under contract no. DE-AC02-76SF00515. The SSRL Structural Molecular Biology Program is supported by the DOE Office of Biological and Environmental Research, and by the NIH National Institute of General Medical Sciences (including P41 GM103393). This research used resources of the Advanced Photon Source, a U.S. DOE Office of Science user facility operated for the DOE Office of Science by Argonne National Laboratory under contract no. DE-AC02-06CH11357.

Finding New Ways to Treat Diabetes and Other Inflammatory Diseases

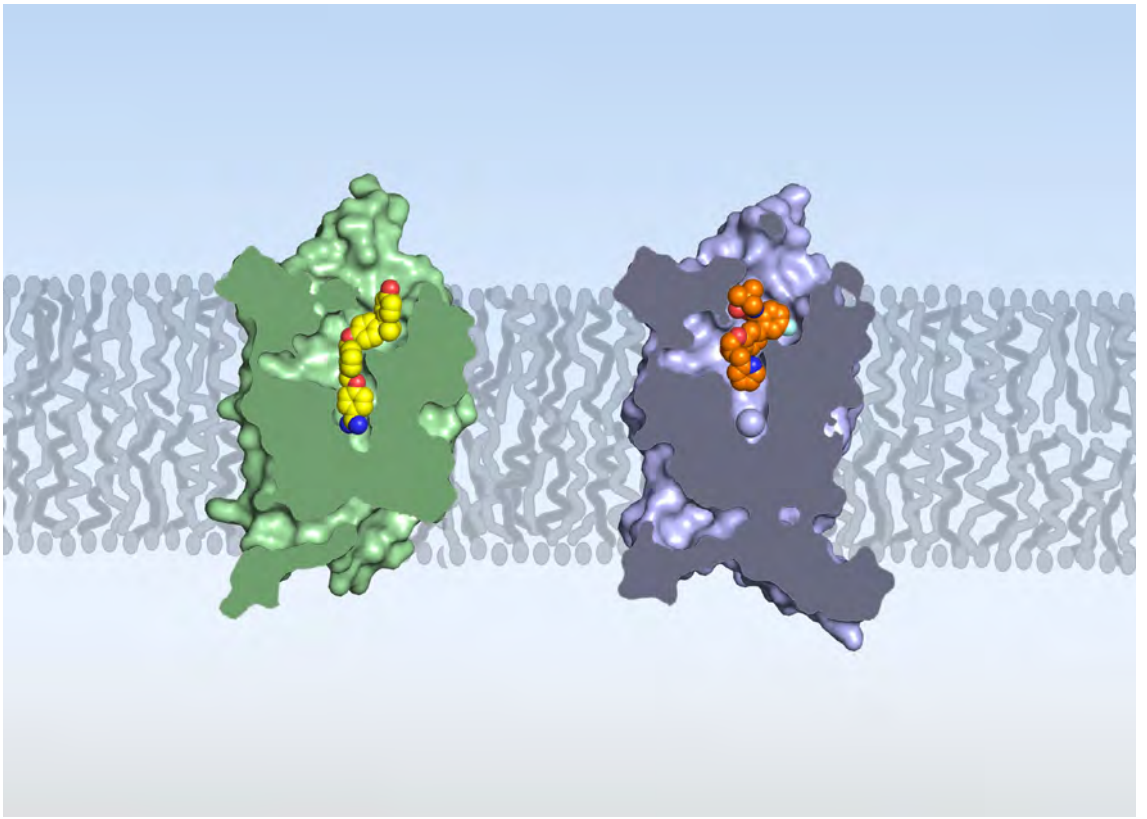

Fig. 1. The figure illustrates the difference between the guinea pig BLT1 (green) and human BLT1 (blue). Both receptors are cut in the middle to show their binding pockets with corresponding binding molecules: BIIL-260 (yellow) and MK-D-046 (orange). The receptors are shown inside a cell membrane with the extracellular side on the top and intracellular side on the bottom.

Currently, more than 460 million adults worldwide live with diabetes and its complications. That number is expected to grow to 700 million adults by 2045. Unfortunately, available treatments for type 2 diabetes, which make up approximately 90 percent of adult cases, can have serious adverse effects including gastrointestinal problems, hypoglycemia, increased cholesterol, and even heart failure. A new study carried out by a multinational, multi-institution research group, which involved collecting x-ray diffraction data at the APS, provides important insights into the structure of the human leukotriene B4 receptor 1, which is thought to play an important role in type 2 diabetes. This research, published in *Nature Communications*, could result in new treatments for diabetes as well as other inflammatory conditions like asthma, inflammatory bowel disease, rheumatoid arthritis, and cancer.

Inflammation is a key hallmark of many diseases, including diabetes. Several studies implicate a protein called the leukotriene B4 receptor 1 (BLT1), which is found in white blood cells, as being involved in inflammatory processes that cause disease. Research also suggests that blocking BLT1 activity may be a potent strategy for combating inflammatory diseases like type 2 diabetes. For example, one study found that removing BLT1 using genetic engineering prevented obese mice from developing insulin resistance, a precursor to diabetes.

Unfortunately, attempts to develop drugs that target BLT1 have been unsuccessful thus far with potential candidates showing poor efficacy and adverse side effects. One reason why these attempts have not been successful

may be that the compounds developed may not have been able to selectively bind BLT1 and block its activity.

In order to learn more about BLT1 and how it might be better targeted by candidate drugs, a multi-institution group conducted a series of experiments designed to reveal the structure of human BLT1 and to determine how various molecules interact with the receptor.

First, the researchers used macromolecular x-ray crystallography to create a detailed, three-dimensional structure of human BLT1 while it was bound to MK-D-046, a selective BLT1 blocker that was developed by Merck & Co. as a candidate GM/CA-XSD) 23-ID-B x-ray beamline at the APS.

The results showed that human BLT1 has a structure similar to many other receptors that span cell membranes and includes an internal channel pocket. The crystal structure also allowed the researchers to determine exactly how MK-D-046 "docks" within the receptor's pocket.

Using specialized software, the researchers modeled how leukotriene B4 (LTB4) likely docks with the human BLT1. LTB4 is a naturally occurring binding partner for the receptor and is thought to play a protective role in viral infections and in some forms of lung injury.

The researchers also compared the structure of human BLT1 to the previously reported structure of guinea pig BLT1, which had been the previous best model for understanding drug interaction with the human receptor (Fig. 1). They found significant differences in the receptor structures, including at sites where potential drugs would bind. This is despite the fact that the amino acid sequences of human BLT1 and guinea pig BLT1 are nearly 74% similar.

To test which differences between the human and guinea pig BLT1 are likely to be most important for drug binding, the researchers mutagenized particular amino acids within human BLT1 so they matched sites from guinea pig BLT1. They then tested how well MK-D-046 blocked the mutated human BLT1. They found that certain amino acid substitutions significantly decreased the ability of MK-D-046 to inhibit human BLT1 activity, thus gaining an understanding of which amino acids are critical for high-affinity binding of drugs to human BLT1.

Together, these results suggest that the structure of human BLT1 will be useful for designing compounds that target BLT1. By presenting a detailed structure of human BLT1, the results from this study may one day lead to the development of more effective methods for preventing and treating inflammatory diseases, including diabetes.

– Summer Allen

See: Nairie Michaelian[1], Anastasiia Sadybekov[1], Élie Besserer-Offroy[2,3], Gye Won Han[1], Harini Krishnamurthy[4], Beata A. Zamlynny[4], Xavier Fradera[4], Phieng Siliphaivan[4], Jeremy Presland[4], Kerrie B. Spencer[4], Stephen M. Soisson[4], Petr Popov[5,6], Philippe Sarret[2], Vsevolod Katritch[1], and Vadim Cherezov[1,6]*, "Structural insights on ligand recognition at the human leukotriene B4 receptor 1," Nat. Commun. **12**, 2971 (2021).
DOI: 10.1038/s41467-021-23149-1
Author affiliations: [1]University of Southern California, [2]Université de Sherbrooke, [3]University of California at Los Angeles, [4]Merck & Co., [5]Skolkovo Institute of Science and Technology, [6]Moscow Institute of Physics and Technology
Correspondence: * cherezov@usc.edu

This research was supported in parts by the National Institute of General Medical Sciences grant R35 GM127086, the GPCR Consortium, and the Canadian Institutes of Health Research (CIHR) grant FDN-148413. É.B.-O. is the recipient of research fellowships from the CIHR (MFE-164740) and the Fonds de recherche du Québec–Santé (255989) and a member of the California NanoSystem Institute. P.S. is the recipient of a Tier 1 Canada Research Chair in Neurophysiopharmacology of Chronic Pain and a member of the FRQ-S-funded Centre de recherche du CHUS. GM/CA-XSD has been funded in whole or in part with federal funds from the National Cancer Institute (ACB-12002) and the National Institute of General Medical Sciences (AGM-12006, P30GM138396). The Eiger-16M detector at GM/CA-XSD was funded by National Institutes of Health grant S10 OD012289. This research used resources of the Advanced Photon Source, a U.S. Department of Energy (DOE) Office of Science user facility operated for the DOE Office of Science by Argonne National Laboratory under Contract DE-AC02-06CH11357.

Clearing Up an Antiviral Immune System Strategy

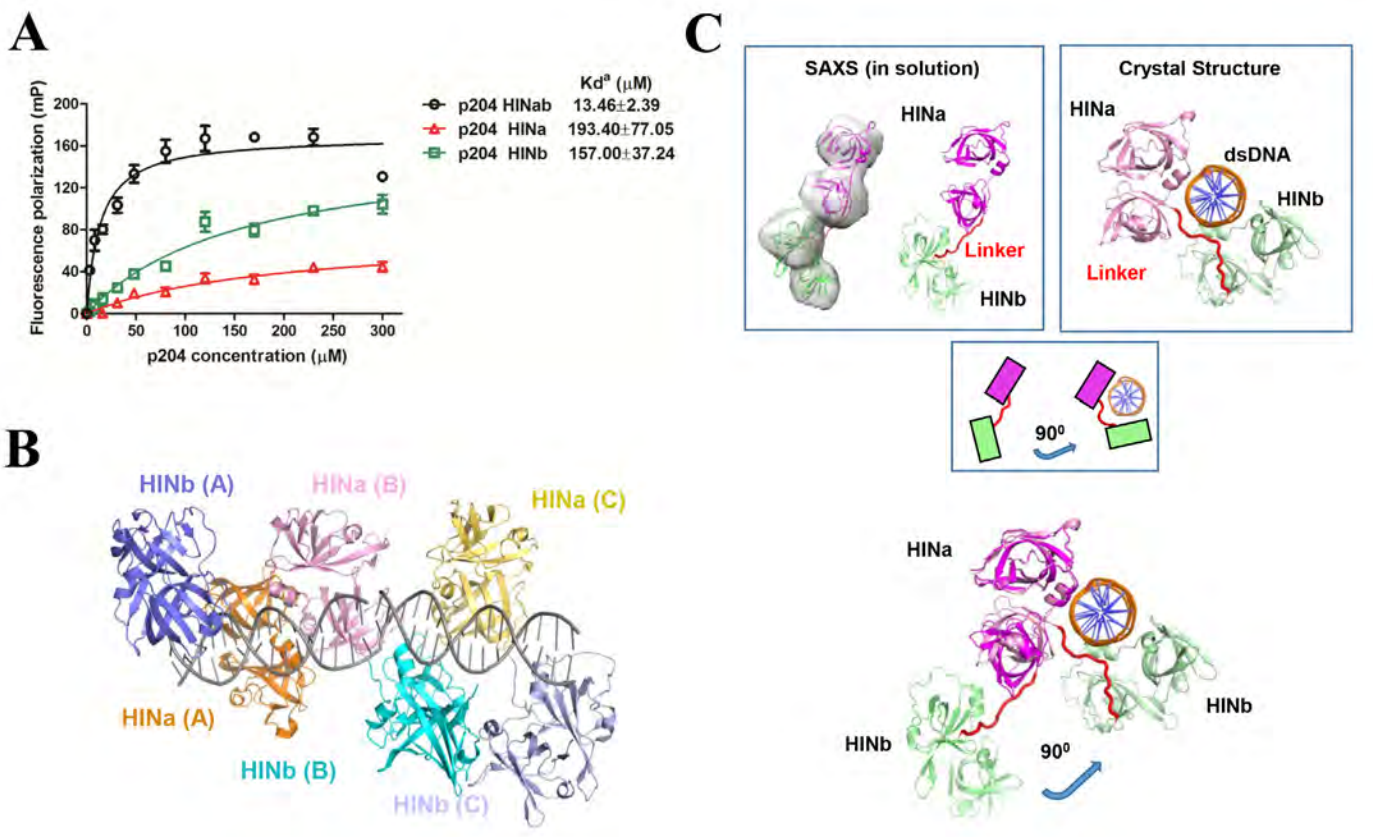

Fig. 1. A) A fluorescence polarization assay assessing binding of p204 HIN domains to double-stranded DNA. The apparent dissociation values (Kda) are shown for p204 HINab, HINa, and HINb domains. B) The overall crystal structure of the p204 HINab:DNA complex. Three p204 HINab molecules bind two copies of double-stranded DNA. Molecule A is shown in orange (HINa) and slate (HINb). Molecule B is shown in pink (HINa) and cyan (HINb). Molecule C is shown in yellow orange (HINa) and light blue (HINb). Two copies of double-stranded DNA are shown in gray. C) p204s dynamic flexible linker between HINa and HINb. (Top, left) HIN domain linker of p204 (DNA free) in solution by SAXS analysis. (Top, right) HIN domain linker in the crystal structure of the p204 HINab:DNA complex. (Middle schematic, Bottom) Conformational changes of the HIN domain linker in p204 with and without double-stranded DNA. The superposition of the SAXS model (DNA free) and crystal structure (DNA bound) of p204 shows HINb domain swings 90 degrees to bind DNA.

The immune system has devised many clever ways to thwart invading viruses and other pathogens. One approach is the deployment of protein sentinels that monitor the body for viral genetic material. Viral genomes can consist of RNA or DNA, with nucleic acid patterns that reveal their viral nature to immune system proteins. A class of immune system proteins focuses on detecting double-stranded viral DNA, in a non-sequence dependent manner. In many cases, it remains a mystery how the protein identifies the viral DNA. Researchers studying one such protein in mice called p204–a homolog of human protein interferon gamma-inducible protein 16 (IFI16)–uncovered the mechanism behind how it detects viral DNA. They used the DOE's APS at Argonne National Laboratory and National Light Synchrotron Light Source II (NSLS II) at Brookhaven National Laboratory to solve the structure of p204 in complex with viral DNA. Additionally, small-angle x-ray scattering data from the NSLS II helped the researchers figure out the size of p204 complexes. Together, the data pointed to a mechanistic model for how

p204 ensnares viral DNA and triggers a chain reaction that recruits the immune system to initiate a virus-fighting inflammatory response. The results, published in the journal *Nucleic Acids Research*, indicate that the human homolog uses a similar mechanism, offering new insight into the functioning of the innate immune system, not only providing a deeper understanding of how the innate immune system works, but having implications for cancer and other pathologies as well, as IFI16 appears to play multiple roles in human health.

The p204/IFI16 homologs are in a family of receptor proteins known as PYHIN or hematopoietic interferon-inducible nuclear (HIN)-200. PYHIN proteins are thought to be cystolic (the fluid portion of the cytoplasm exclusive of organelles and membranes) DNA sensors that can recognize both self and pathogenic DNA, with diverse downstream signaling. p204/IFI16 contains two HIN domains (HINa and HINb). How the HIN domains grab onto DNA generally is rather straightforward: positively charged residues on the HIN surface interact with the negatively-charged phosphate backbones of DNA. But the details had remained elusive; prior to this study, no one had solved the structure of both HIN domains in complex with double-stranded DNA.

Part of the reason p204/IFI16 had remained so mysterious was that it's rather unique. Unlike other members of the PYHIN family, p204/IFI16 has two HIN domains in tandem, one right after the other. One of the big lingering questions had been "why two?" There was a lack of consensus over the extent to which each domain contributes to DNA binding. So in this study, the researchers performed fluorescence polarization assays to assess the DNA-binding affinity of p204 HINa and HINb separately, and then both domains together (HINab). Indeed, binding affinity for HINab was higher than HINa or HINb, but the question remained as to why.

To answer that question, the researchers turned to x-ray crystallography. They solved the structures of double stranded DNA in complex with HINa, HINb, and HINab using x-ray diffraction data collected at the SER-CAT 22-ID x-ray beamline and GM/CA-XSD structural biology facility 23-ID beamline, both at the APS; and at beamlines X12C, X29A, and X25 of the NSLS II at Brookhaven National Laboratory (both the APS and NSLS II are Office of Science user facilities). The structure gave insight not only into how the protein binds viral DNA but also how the protein then triggers the downstream activation of immune system proteins (Fig. 1).

In addition to the two HIN domains in p204/IFI16, the protein also has an N-terminal PYD domain. Based on the structural studies and other data, the researchers developed a working model of double-stranded DNA recognition. In the absence of DNA, the researchers believe p204/IFI16 adopts an elongated structure as it hunts around for signs of pathogens. When the protein happens upon double-stranded viral DNA, the two HIN domains cooperatively bind to the DNA. Multiple p204/IFI26 proteins start binding along double-stranded DNA, with the HINa domains from separate molecules associating together, forming a complex. The PYD domains become critical at this point; the PYD domains from different molecules of p204/IFI26 interact and aggregate. This triggers the activation of STING, a mediator of cystolic DNA-induced signaling events, setting in motion a cascade of protein interactions that ultimately prompts the release of pro-inflammatory cytokines to go after the virus.

– Erika Gebel Berg

See: Xiaojiao Fan[1], Jiansheng Jiang[2], Dan Zhao[1], Feng Chen[1], Huan Ma[1], Patrick Smith[2], Leonie Unterholzner[3], Tsan Sam Xiao[4], and Tengchuan Jin[1,5]*, "Structural mechanism of DNA recognition by the p204 HIN domain," Nucleic Acids Res. **49**(5), 2959 (2021).
DOI: 10.1093/nar/gkab076
Author affiliations: [1]University of Science and Technology of China, [2]National Institutes of Health, [3]Lancaster University, [4]Case Western Reserve University, [5]CAS Center for Excellence in Molecular Cell Science
Correspondence: * jint@ustc.edu.cn

Funding was provided by the National Natural Science Fund for Young Scholars [31800639]; Strategic Priority Research Program of the Chinese Academy of Sciences [XDB29030104]; National Natural Science Foundation of China [31870731, 31971129]; Fundamental Research Funds for the Central Universities, and the 100 Talents Program of the Chinese Academy of Sciences; National Institutes of Health [R01GM127609]; intramural research program of National Institute of Allergy and Infectious Diseases. This research used resources of the Advanced Photon Source, a U.S. Department of Energy (DOE) Office of Science user facility operated for the DOE Office of Science by Argonne National Laboratory under Contract No. DE-AC02-06CH11357.

Solving the Structure of BRCA2 Protein Complex Important in DNA Repair

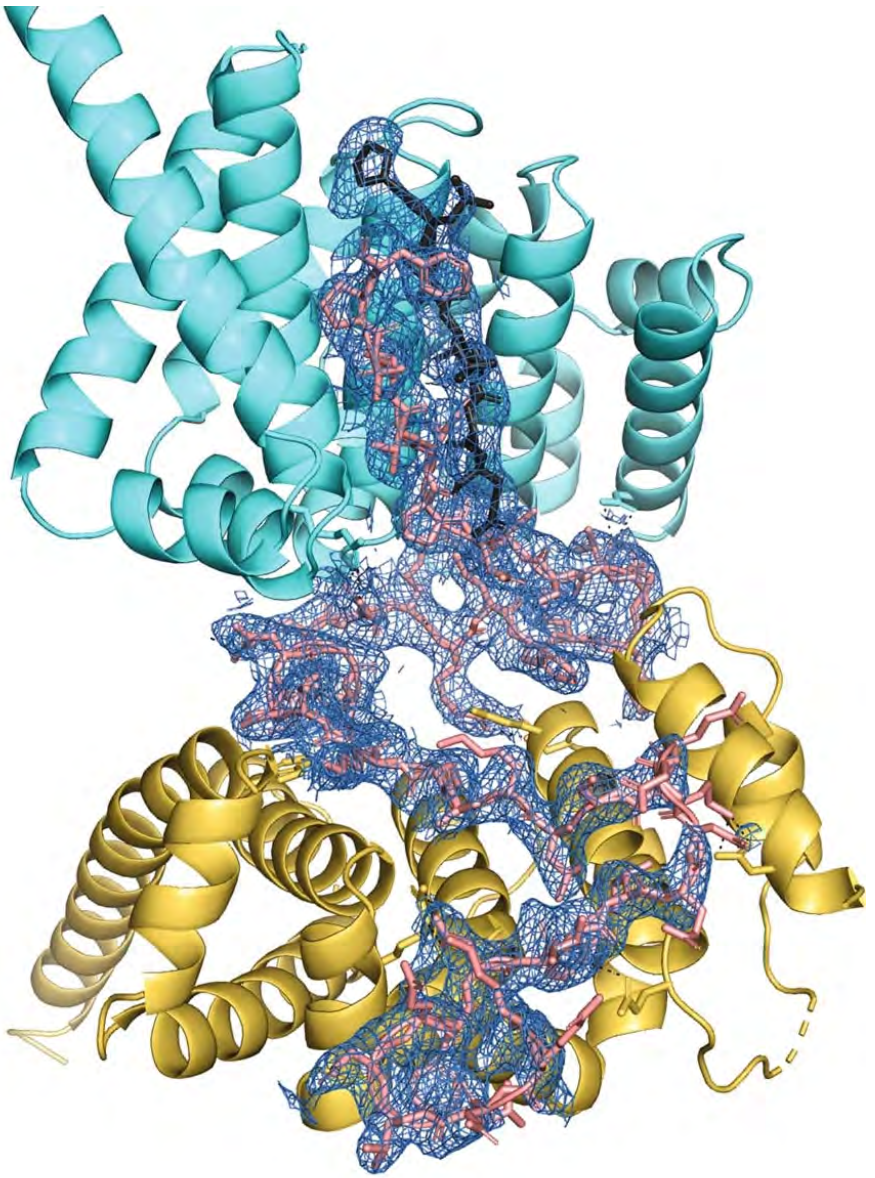

Electron density for BRCA2MBD. From D. F. Pendlebury et al., Nat. Struct. Mol. Biol. **28**, 671 (August 2021). © 2021 Springer Nature Limited

The original University of Michigan press release by Suzanne Tainter can be read here. © 2021 The Regents of the University of Michigan

The initials BRCA2 may be best known for a gene associated with many cases of breast cancer, and the protein encoded by the BRCA2 gene is critical to repairing breaks in DNA. The breakdown of this interaction is a hallmark of many cancers. University of Michigan (U-M) and University of Gothenburg scientists used the APS to determine the structure of a complex of two proteins—BRCA2 together with MEILB2—that allows repairs to happen efficiently in cells undergoing cell-splitting, called meiosis. Their results, reported in *Nature Structural and Molecular Biology*, have major implications for cancer and infertility.

"We know how the literature is rich with examples of BRCA2 mutations in cancer, but our findings now suggest that the MEILB2-binding region of BRCA2 might be a hotspot for discovering mutations related to infertility," said study author and U-M structural biologist Jayakrishnan Nandakumar, associate professor of molecular, cellular, and developmental biology.

In germ cells—the cells that give rise to sperm or eggs—DNA breaks occur in every chromosome before the cells undergo meiosis. The breaks ensure mixing of genes to create genetic diversity rather than exact copies of the parents. In meiosis, each germ cell splits twice so that each egg or sperm ends up with only one copy of each chromosome. Then when egg meets sperm, the embryo has the right number of chromosome pairs.

Before the first split occurs, the chromosomes in the germ cell pair up tightly and then each chromosome within a pair breaks and rejoins with pieces from its partner to exchange genes in a process called crossover. Then all these DNA breaks need to be rejoined quickly.

Think of a sandwich, Nandakumar explains. The "bun" is composed of four identical copies of a protein called MEILB2 on the top and bottom, with the two BRCA2 proteins between. The MEILB2 protein sandwich carries the BRCA2 protein precisely to the DNA break points.

To determine the structure of this BRCA2 complex, the researchers used x-ray crystallography at the LS-CAT 21-ID-D x-ray beamline at the APS. This helped them figure out how the BRCA2 protein is connected to the MEILB2 protein.

The first step was to grow crystals of the BRCA2 complex. After much trial and error, Devon Pendlebury, a chemical biology graduate student in the Nandakumar lab, successfully crystallized the human form of the BRCA2 complex. In a bit of good fortune, the U-M researchers were able to collect data at the Argonne National Laboratory days before all research was shut down in March 2020. From the x-ray crystallography data and additional experiments by MCDB graduate student Ritvija Agrawal, the team determined the structure of the protein complex and how the two proteins worked together. It was a somewhat unusual protein-interaction, they report.

To validate their findings, they created mutant versions of BRCA2 and MEILB2 based on their structure and showed how these mutants failed to form this complex with each other. In further validation of the MEILB2-BRCA2 complex structure, Hiroki Shibuya's research group at the University of Gothenburg in Sweden introduced equivalent mutant versions in mouse cells undergoing meiosis. Mutant BRCA2 or MEILB2 failed to get to the DNA breaks that needed to be rejoined.

"While we have known BRCA2 was necessary for DNA recombination in meiosis, we didn't know how it was able to do this critical job efficiently," Nandakumar said. "The MEILB2 that is part of this repair complex is only supposed to be present in cells that undergo meiosis but MEILB2 has also been found in several cancers. It may be that MEILB2 is very efficiently 'hijacking' the BRCA2 in cancer cells, preventing proper repair of the DNA."

Without other factors usually found in meiotic cells, the BRCA2 in these MEILB2-positive cancers might not get to the DNA breakpoints. Having a structure of this complex in hand, researchers may now find new approaches to regain BRCA2 function in MEILB2-positive cancers, Nandakumar suggests.

See: Devon F. Pendlebury[1‡], Jingjing Zhang[2], Ritvija Agrawal[1], Hiroki Shibuya[2*], and Jayakrishnan Nandakumar[1**], "Structure of a meiosis-specific complex central to BRCA2 localization at recombination sites," Nat. Struct. Mol. Biol. **28**, 671 (August 2021). DOI: /10.1038/s41594-021-00635-01038/s41594-021-00635-0

Author affiliations: [1]University of Michigan, [2]University of Gothenburg ‡Present address: University of California Irvine

Correspondence: * hiroki.shibuya@gu.se,
** jknanda@umich.edu

The authors thank J. S. Brunzelle at LS-CAT for help with x-ray diffraction data collection and initial processing. This work was supported by National Institutes of Health grants R01-AG050509 (J.N.) and R01-GM120094 (J.N.), American Cancer Society Research Scholar grant RSG-17-037-01-DMC (J.N.), an American Heart Association predoctoral fellowship award ID 830111 (R.A.), Assar Gabrielssons Foundation grant FB-20-57 (J.Z.), European Research Council grant StG-801659 (H.S.), Swedish Research Council grant 2018-03426 (H.S.), Cancerfonden grant 2018/326 (H.S.) and the Knut och Alice Wallensbergs Stiftelse KAW2019.0180 (H.S.). Use of LS-CAT was supported by the Michigan Economic Development Corporation and the Michigan Technology Tri-Corridor (Grant 085P1000817). This research used resources of the Advanced Photon Source and Center for Nanoscale Materials, both U.S. Department of Energy (DOE) Office of Science User Facilities operated for the DOE Office of Science by Argonne National Laboratory under Contract No. DE-AC0206CH11357.

How Proteins Fold: A Guided Model

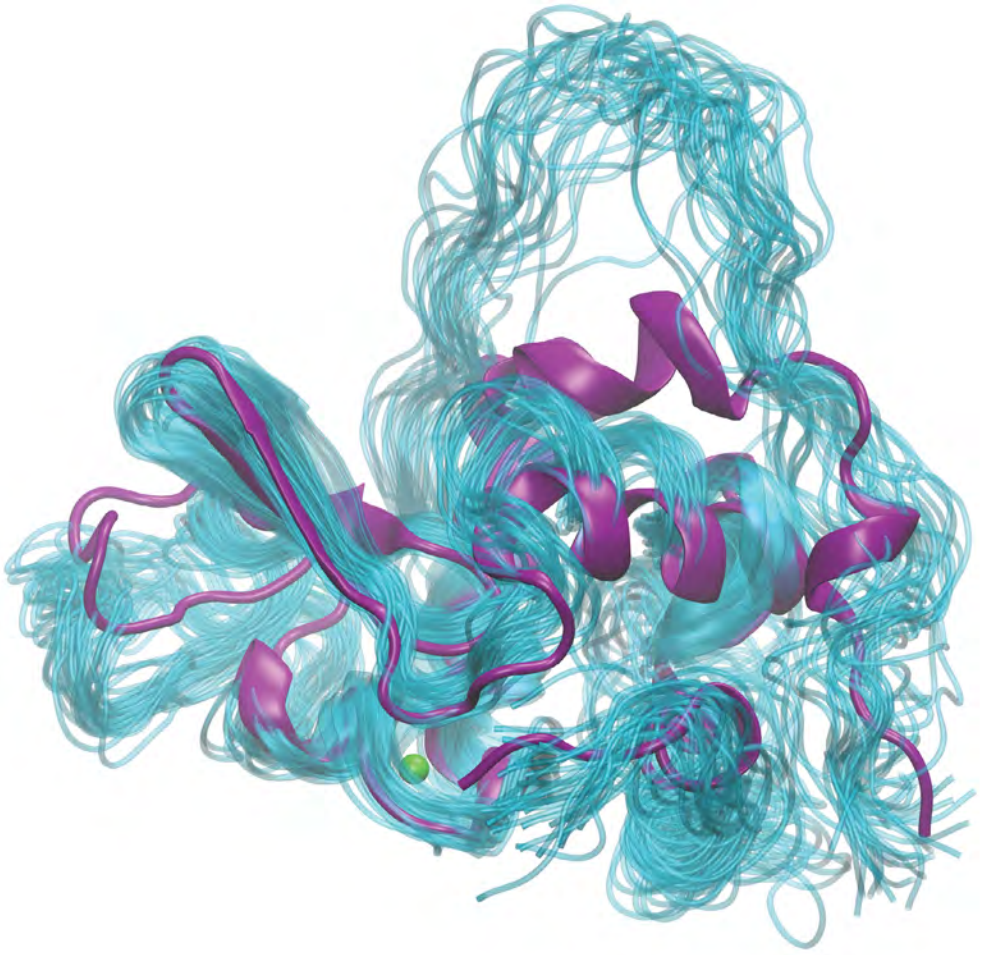

Fig. 1. Molten globule structures derived from TRXSS and MD simulation data (cyan) for folding intermediate states overlaid on the crystal structure (purple) of BLA. The bound calcium ion is shown as a green dot.

Biologists have studied the question of protein folding for a long time because understanding how proteins fold can help us to understand what goes wrong in diseases caused by misfolded proteins and can guide structure-based drug design efforts to develop new disease therapies. However, on a more basic level, scientists are also fascinated by the wonder of a process that takes an RNA message and "prints" out the correct amino acids in a linear string that then automatically folds itself, via a number of partially-folded transient states, into a complex three-dimensional structure, such as an enzyme. One model that has been extensively used for these investigations is a small protein from milk called bovine lactalbumin (BLA) for which the structure is well known, including some, but not all, details of its folding intermediates. Recently, a team using the APS reported on a new approach that has provided a way to capture more detailed information about these important folding intermediates. Their results were published in *The Journal of Chemical Physics*.

The basis for this technical advance was the development of a method for transforming the structural data signal from time-resolved x-ray solution scattering (TRXSS) experiments to a format that can be fed into molecular dynamics (MD) simulations to provide a kind of "guardrail" to guide the simulations and make sure that atomic-level data provided by the simulation agree with the secondary structure data provided by the TRXSS. The MD simulations balance the TRXSS data by filling in the details that

are inherently lost in the spatial orientation data for TRXSS compared to x-ray crystallography. For the TRXSS, the high time resolution of the synchrotron pulsed x-rays (100 picoseconds) at the BioCARS 14-ID-B beamline at the APS allowed separation of distinct conformational states of the protein.

One important aspect of this experiment was to find conditions in which the BLA protein molecules in the solution could be triggered to rapidly unfold all at once, and allow researchers from Northwestern University, The University of Chicago, and Argonne to capture the transformation process in action. This is achieved by a sudden temperature rise, called a T-jump, provided by a nanosecond infrared pulse that heats the solvent and unfolds the proteins while the researchers capture the TRXSS structural data. There is evidence that folding and unfolding travel through the same intermediates, so this method provides a way to capture the event in a controlled manner.

The first steps were to decide on the temperature for the T-jump and to calibrate the MD simulations of BLA to equilibrium conditions. After performing melting temperature experiments, the team settled on an 11.5° C T-jump performed at 60° C, 65° C, and 70° C with data recorded from 20 microseconds to 70 milliseconds after the jump. The TRXSS data captured several intermediates that fit to a kinetic model in which the protein went from a folded state to an intermediate state and then an unfolded state or from a folded state directly to one of two unfolded states. The initial molecular modeling simulations using data derived from TRXSS to steer the simulations converged on the same structures, demonstrating that the MD simulations guided by the scattering data were finding relevant conformations.

Further investigation of the unfolding process using the TRXSS data-guided MD simulations enabled the researchers to look at changes in the features of secondary structures, well-known α-helical and β-sheet structures in BLA, during the unfolding process. Interestingly, the unfolded structures retain some α-helical secondary structure that is likely to be stabilized by the presence of a bound calcium ion and a disulfide bridge in the protein. The intermediate structure was determined to represent the "molten globule" state that describes a protein that has reached a thermodynamic threshold for folding. Perhaps surprisingly though, the intermediate molten globule displayed more unstructured helices than the unfolded state. However, the intermediate state was more conformationally ordered than the unfolded state with a more compact size, consistent with it being the molten globule state.

Taken together, these data provide a confirmation that this approach of using the TRXSS data to guide MD simulations can provide atomic-level data for understanding the protein folding process. Now that this proof-of-concept experiment has been successful, the team hopes to apply their TRXSS-guided simulation method to other important protein folding questions. – Sandy Field

See: Darren J. Hsu[1], Denis Leshchev[1], Irina Kosheleva[2], Kevin L. Kohlstedt[1]*, and Lin X. Chen[1,3]**, "Unfolding bovine α-lactalbumin with T-jump: Characterizing disordered intermediates via time-resolved x-ray solution scattering and molecular dynamics simulations," J. Chem. Phys. **154**, 105101 (2021). DOI: 10.1063/5.0039194
Author affiliations: [1]Northwestern University, [2]The University of Chicago, [3]Argonne National Laboratory
Correspondence: * kkohlstedt@northwestern.edu,
** l-chen@northwestern.edu

This work was supported by the National Institutes of Health (NIH) under Contract No. R01-GM115761. D.J.H. acknowledges support from the National Institute of General Medical Sciences (NIGMS) of NIH for a training grant (Grant No. 5T32GM008382) and the U.S. Department of Energy (DOE) (Grant No. DESC0000989), Office of Science Graduate Student Research program, administered by the Oak Ridge Institute for Science and Education, managed by ORAU under Contract No. DE-SC0014664. BioCARS is supported by the NIGMS of the NIH under Grant No. R24GM111072. The time-resolved setup at BioCARS Sector 14 was funded in part through collaboration with Philip Anfinrud (NIH/National Institute of Diabetes and Digestive and Kidney Diseases). The authors would like to acknowledge Guy Macha (BioCARS) for his assistance in designing the sample holder. This research used resources of the Advanced Photon Source, a U.S. DOE Office of Science user facility operated for the DOE Office of Science by Argonne National Laboratory under Contract No. DE-AC02-06CH11357.

Understanding How Cyanobacteria Tune Photoreceptors to Sense Far-Red Light

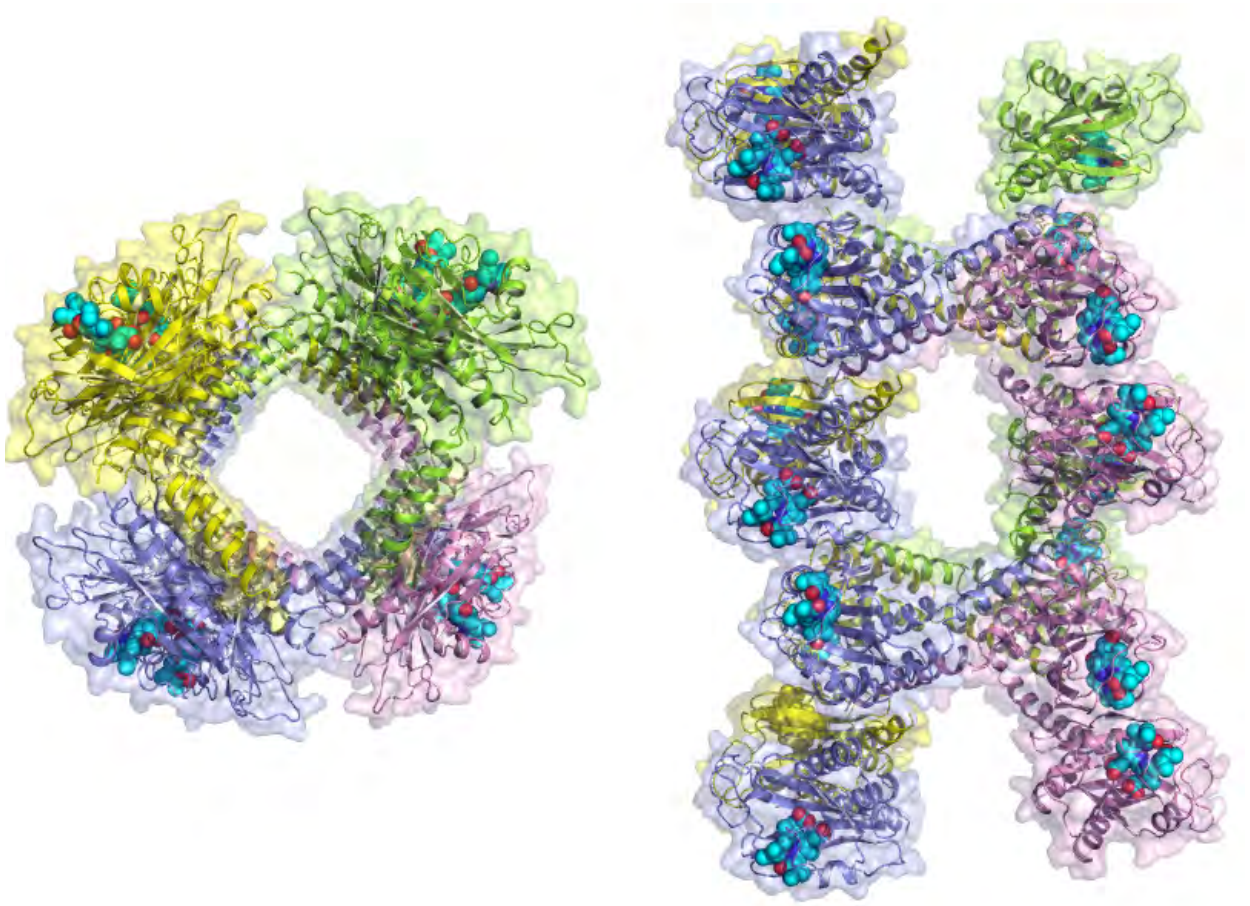

Fig. 1. Crystal structure of a far-red-light sensing CBCR from *Anabaena*. A network of protein molecules in the crystal lattice of space group P4(2)22 are shown in two orthogonal views. Left: the top view looking down the major 4-fold axis. Right: the side view highlights the helical bundles via which two adjacent protein molecules are tethered. Space-filling models in cyan mark the positions of the bilin chromophores.

Cyanobacteria are some of the oldest organisms on earth, dating back 3.5 billion years, and can be found almost everywhere on our planet. These single-cell organisms are photosynthetic and have found ways to adapt to a variety of diverse and extreme ecological niches. One way they have achieved this is by adapting and tuning their photosynthetic machinery to the light color of the environment. This process, known as complementary chromatic acclimation, is mediated by photoreceptor proteins containing light-sensing chromophores, in particular, a family of bilin-binding photoreceptors called cyanobacteriochromes (CBCRs). CBCRs were previously thought to absorb light in the shorter wavelength range of the visible spectra. However, a family of CBCRs has been recently discovered to absorb far-red light, suggesting a new mechanism of spectrum tuning. Making use of the high-brightness x-rays produced by the APS the structural basis for the far-red sensing ability has been investigated for one representative far-red absorbing CBCR (frCBCR). Due to the fact that far-red light can penetrate deep tissues in animals, mechanistic studies on frCBCRs may offer strategies for developing novel optical reagents and fluorescent probes for a variety of medical applications. These results obtained by researchers from the University of Illinois at Chicago and the University of California Davis, were published in the *Proceedings of the National Academy of Sciences of the United States of America*.

Light-sensing phytochromes from plants, fungi, and bacteria, including cyanobacteria, possess a conserved light-sensing module to perceive and relay the light signal to whatever output domain the sensor is connected to. Cyanobacteria have evolved to integrate a wide array of sensor and signaling modules to feed into a variety of bacterial metabolic processes that respond to light. This work focused on elucidating the structure of the far-red-absorbing dark state of the chromophore-binding domain of the frCBCR from *Anabaena* cylindrica, a genus of filamentous cyanobacteria that exist as plankton. This frCBCR uses a phycocyanobilin (PCB) chromophore, similar to those found in most known CBCRs, to undergo a previously unexplored far-red/orange photocycle. The team solved the crystal structure of the *Anabaena* frCBCR domain at both cryogenic and room temperature (Fig. 1). The cryogenic data were obtained at the LS-CAT 21-ID-D x-ray station at the APS. Room-temperature Laue diffraction data were obtained at the BioCARS 14-ID beamline, also at the APS.

The structural data showed that the *Anabaena* frCBCR exhibits many of the typical features of other known CBCRs including an α/β fold with a central β sheet and a chromophore pocket surrounded by several conserved aromatic residues observed in other CBCRs (Fig. 1). However, the PCB chromophore, which is covalently attached to the protein via cysteine 943, adopts a very unusual *all-Z,syn* configuration that differs from all known CBCRs and phytochromes. This unusual configuration along with the clockwise rotation of the chromophore gives rise to unique protein-chromophore interactions in the chromophore binding pocket.

In order to identify amino acids responsible for the far-red absorption properties of frCBCRs, the team performed 34 site-directed mutagenesis changes at 25 different amino acid positions that potentially affect protein-chromophore interactions. These mutational studies pointed to two hallmark residues of frCBCRs, namely leucine 944 and glutamic acid 914, positioned at the opposite faces of the chromophore. As a result of their dispositions relative to the chromophore, the side chain of Glu914 engages direct hydrogen bond interactions with the pyrrole rings A and D of the chromophore, suggesting two distinct mechanisms of spectrum tuning. Together with pH titration and chromophore swapping experiments, the team proposed that the far-red sensing ability of the *Anabaena* frCBCR comes from the additive effects of these two mechanisms.

The team hopes to answer unresolved questions regarding their proposed far-red tuning mechanism with follow-up experiments using vibrational and NMR spectroscopy and learn more about the transition between the far-red sensing dark state and the photoproducts using dynamic crystallography. – Sandy Field

See: Sepalika Bandara[1], Nathan C. Rockwell[1], Xiaoli Zeng[1], Zhong Ren[1], Cong Wang[1], Heewhan Shin[1], Shelley S. Martin[2], Marcus V. Moreno[2], J. Clark Lagarias[2]*, and Xiaojing Yang[1]**, "Crystal structure of a far-red–sensing cyanobacteriochrome reveals an atypical bilin conformation and spectral tuning mechanism," Proc. Nat. Acad. Sci. U.S.A. **118**(12), e2025094118 (2021).
DOI: 10.1073/pnas.2025094118
Author affiliations: [1]University of Illinois at Chicago, [2]University of California, Davis
Correspondence: * jclagarias@ucdavis.edu,
** xiaojing@uic.edu

We thank the staff at BioCARS and LS-CAT for support in x-ray diffraction data collection. This work is supported by grants from the U.S. Department of Energy (DOE) Office of Science-Basic Energy Sciences, under Contract E-FG02- 09ER16117 to J.C.L., and from the National Institutes of Health (NIH) under R01EY024363 to X.Y. Use of LS-CAT is supported by the Michigan Economic Development Corporation and the Michigan Technology Tri- Corridor under Grant 085P1000817. Use of BioCARS was supported by the National Institute of General Medical Sciences of the NIH under grant number P41 GM118217. This research used resources of the Advanced Photon Source; a U.S. DOE Office of Science user facility operated for the DOE Office of Science by Argonne National Laboratory under Contract DE-AC02-06CH11357.

Using Protein Structural Information to Understand the Mechanism of an Essential Enzyme for Fighting Tuberculosis

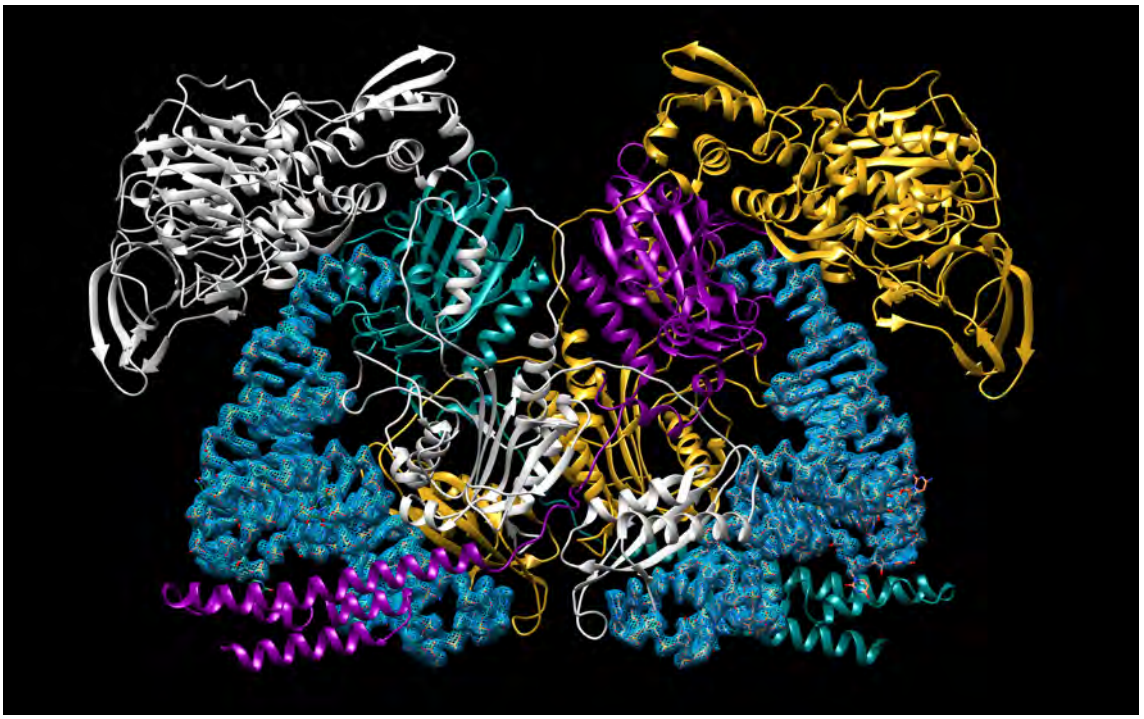

Fig. 1. Structure of the *M. tuberculosis* PheRS heterotetramer in complex with tRNA molecules.

Antibiotic resistance is a global problem that many scientists are racing to solve. Bacterial infections that were once easily controlled by penicillin or tetracycline are now impossible to treat except with our most recently developed antimicrobials. This is due to the fact that bacteria can develop, and spread/disperse, mutations that allow them to evade the effects of antibiotics. One type of bacteria that has been very successful at this is *Mycobacterium tuberculosis*, a deadly bacterium responsible for the deaths of ~1.5 million people in 2018. Multi-drug resistant and extensively drug-resistant strains of *M. tuberculosis* have become a major global problem, increasing the need for new antibiotics. This has driven researchers to seek new bacterial targets for structure-based drug design. In recent work conducted at the APS, researchers gained important insights into understanding the structure and mechanism of a critical enzyme involved in protein synthesis in M. tuberculosis. Their work, published in *Nucleic Acids Research*, will form the basis of structure-based drug design efforts aimed at exploiting the unique features of this enzyme, a method that has been successful in developing pharmaceuticals against methicillin-resistant *Staphylococcus aureus* (MRSA) and some fungal infections.

The research focuses on learning more about an essential enzyme involved in making proteins from a messenger RNA (mRNA) transcript. This is a basic function of all cells, in both bacteria and multi-cellular organisms, and involves a coordinated set of specific enzymes and special RNA molecules called transfer RNAs (tRNAs). The tRNAs show "L" shape and they recognize a 3-base sequence in the mRNA called a codon and translate it into the correct amino acid code using a matching anticodon sequence. A set of 20 critical enzymes in this process are the aminoacyl tRNA synthetases (aaRS). Each aaRS loads the specific amino acid onto correct tRNA molecule in a

two-step reaction. One important consideration is that, although aaRSs function in a very evolutionarily conserved process that all organisms carry out, these enzymes have diverged structurally enough make the ones in bacteria distinct from our own so we can target them without disrupting protein synthesis in our own cells.

The work was done as a collaboration between researchers at Argonne National Laboratory, The University of Chicago, Auburn University, and the University of Dundee (Scotland) and involved structural analysis of the *M. tuberculosis* aaRS, called MtFRS, that transfers the amino acid phenylalanine to its specific tRNA, tRNAPhe. In order to join the correct amino acid to its appropriate tRNA, the enzyme must recognize specific features of tRNAPhe that distinguish it from the tRNAs for the other 19 amino acids and then bring the phenylalanine and tRNAPhe into proximity to catalyze the ligation reaction.

Using the SBC-XSD x-ray beamline 19-ID at the APS, the team solved four structures of large complexes that capture the two steps of the MtFRS enzyme's catalytic action and tRNA recognition (Fig. 1). The initial binding of the amino acid was demonstrated by two crystal structures of MtFRS bound to M. tuberculosis tRNAPhe (MttRNAPhe) with phenylalanine and one with a non-hydrolyzable phenylalanine analog. The aminoacylation "ready" state, in which the tRNA is set to accept loading of the amino acid, was demonstrated by crystallization of MtFRS bound to MttRNAPhe with an inhibitor, the non-hydrolyzable analog of amino acid.

The structures confirmed previous work showing that MtFRS adopts a large and complex heterotetrameric structure and it binds two molecules of MttRNAPhe. In this work, the team discovered that initial recognition of the tRNAPhe is performed by one half of the heterotetramer while aminoacylation is performed by the other half. Selective recognition of the tRNA is provided by enzyme interactions with the anticodon loop and stem regions of the tRNAPhe but, surprisingly, not the unique anticodon sequence itself. Instead, MtFRS appears to recognize only the wobble base, the least important aspect of recognition between the tRNAPhe anticodon and mRNA codon sequence. These interactions are maintained in the ready state and this work reported, for the first time, the process of stabilization and ordering of the active site that brings the correct catalytic groups into the appropriate geometry for the aminoacylation reaction, confirming the proposed catalytic mechanism of MtFRS. Comparison of these structures to those of human aaRSs and those of other bacteria allowed the team to identify some unique features of MtFRS that provide a good starting point for the design of small molecule inhibitors to fight tuberculosis infection.

– Sandy Field

See: Karolina Michalska[1,2], Robert Jedrzejczak[1,2], Jacek Wower[3], Changsoo Chang[1,2], Beatriz Baragaña[4], Ian H. Gilbert[4], Barbara Forte[4], and Andrzej Joachimiak[1,2]*, "Mycobacterium tuberculosis Phe-tRNA synthetase: structural insights into tRNA recognition and aminoacylation," Nucleic Acids Res. **1**, 5351 (21 May, 2021).
DOI: 10.1093/nar/gkab272
Author affiliations: [1]The University of Chicago, [2]Argonne National Laboratory, [3]Auburn University, [4]University of Dundee
Correspondence: * andrzejj@anl.gov

The authors thank the members of SBC-XSD for their help with setting beamline and data collection at beamline 19-ID. Funding: National Institute of Allergy and Infectious Diseases, National Institutes of Health (NIH), Department of Health and Human Services [HHSN272201200026C, HHSN272201700060C, in part]; U.S. Department of Energy (DOE) Office of Science and operated for the DOE Office of Science by Argonne National Laboratory [DE-AC02-06CH11357]; J.W. was supported by the Hatch program of the National Institute of Food and Agriculture, U.S. Department of Agriculture. Funding for open access charge: NIH. SBC-XSD is operated by UChicago Argonne, LLC, for the U.S. DOE Office of Biological and Environmental Research under contract DE-AC02-06CH11357. This research used resources of the Advanced Photon Source, a U.S. DOE Office of Science user facility operated for the DOE Office of Science by Argonne National Laboratory under Contract DE-AC02-06CH11357.

Uncovering Mechanisms that Regulate Activation of the Immune System

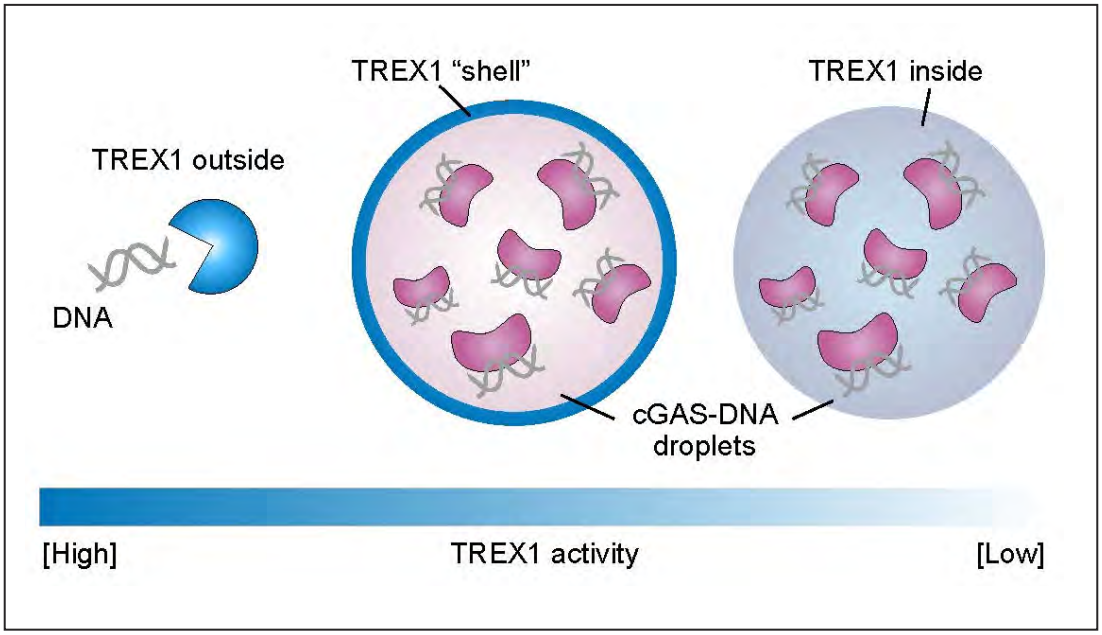

Fig. 1. cGAS phase separation inhibits TREX1-mediated DNA degradation and enhances cytosolic DNA sensing.

Inside a cell, DNA belongs in the nucleus. DNA that appears elsewhere, such as in the surrounding semi-fluid substance called the cytosol, signifies possible disease, including viral infection or cancer. When this happens, the cGAS enzyme recognizes the out-of-place DNA and signals the immune system to come to the rescue. Under normal conditions, this defense mechanism works well, but when unregulated, it can trigger either too much or too little immune reaction. One of the key players that regulates cGAS activity is TREX1, a protein that degrades DNA, thereby controlling how much immune response is generated. Too little degradation of DNA will result in overreaction of the immune system and autoimmune disease, while too much degradation will let a virus or cancer cell escape immune reaction. For example, mutated TREX1 that is unable to degrade cytosolic DNA can lead to severe conditions like Aicardi-Goutières syndrome. Using APS, researchers discovered that mutations alter the way TREX1 interacts with cGAS and DNA, upending previous models and suggesting new targets for treating cancer and autoimmune disease. The research was published in the journal *Molecular Cell*.

When cGAS recognizes DNA, the two bind together and form a liquid droplet that functions as a unique environment within the cell—a process called liquid-liquid phase separation (Fig. 1). Within the droplet, DNA activates cGAS to synthesize a small signaling molecule called cGAMP, which activates the immune system via the STING pathway. In the absence of any regulation, cGAS will synthesize cGAMP over and over, issuing an incessant alarm and overexciting the immune system. Fortunately, our bodies produce regulators—chief among them TREX1, which mediates the process by degrading the DNA.

Scientists wanted to understand why cGAS formed liquid droplets in the presence of DNA. Prior to the current research, the working model postulated that phase separation was necessary to activate cGAS and drive synthesis

of cGAMP. In the new work, the researchers used a variety of techniques, such as *in vitro* reconstitution and in cell microscopy, to disprove this model by showing that phase separation had little to no effect on the synthesis of cGAMP but was necessary for cGAS to sense DNA in the cytosol.

They also found that within the physical environment of the droplet, DNA, cGAS, and various nucleotides and metals diffuse freely in and out, but TREX1 is restricted to the droplet's exterior. Based on this finding, the researchers proposed a new model: phase separation creates a selective environment that suppresses the activity of regulators like TREX1 while protecting DNA sensing by cGAS. Their model was confirmed when they found that a genetically engineered form of TREX1 was capable of penetrating the interior of the droplet but, once inside, could not degrade the DNA it found there.

One of the most frequent causes of Aicardi-Goutières syndrome and systemic lupus erythematosus are mutations in TREX1 that impair regulation of cGAS. To investigate the connection on an atomic level, the researchers determined crystal structures of TREX1 protein with a mutation associated with disease. Using the NE-CAT beamline 24-ID-E x-ray beamline at the APS to collect x-ray diffraction data, they found that mutations change the surface electric charge of TREX1, altering its interaction with the cGAS-DNA droplet. Specifically, a single mutation significantly changed the surface charge from neutral to very positive, leading them to postulate that a positive charge may attract mutated TREX1 into the interior of the droplet, where its activity is repressed.

Finding a new point of regulation within the cGAS activation pathway affects research in many different areas: DNA replication, pathogen replication in the cytosol, phagocytosis of cancer cells, among many others. The discovery also suggests targeting cGAS phase separation or the way TREX1 interacts with the phase-separated droplet may be a new opportunity for drug discovery. Moreover, it demonstrates how mutations control TREX1 behavior in cells and result in disease. – Judy Myers

See: Wen Zhou[1,2], Lisa Mohr[3], John Maciejowski[3], and Philip J. Kranzusch[1,2,4*], "cGAS phase separation inhibits TREX1-mediated DNA degradation and enhances cytosolic DNA sensing," Mol. Cell **81**, 739 (February 18, 2021). DOI: 10.1016/j.molcel.2021.01.024

Author affiliations: [1]Harvard Medical School, [2]Dana-Farber Cancer Institute, [3]Memorial Sloan Kettering Cancer Center, [4]Parker Institute for Cancer Immunotherapy at Dana-Farber Cancer Institute

Correspondence: * philip_kranzusch@dfci.harvard.edu

This work was funded by grants to P.J.K. from the Richard and Susan Smith Family Foundation, Charles H. Hood Foundation, V Foundation, Concern Foundation, a Cancer Research Institute CLIP grant, and Parker Institute for Cancer Immunotherapy, and grants to J.M. from the National Cancer Institute (R00CA212290), the Geoffrey Beene Cancer Research Center, and a MSKCC core grant (P30-CA008748). W.Z. is supported as a Benacerraf Fellow in Immunology and through a Charles A. King Trust Postdoctoral Fellowship. This work is based upon research conducted at the NE-CAT beamlines, which are funded by the National Institute of General Medical Sciences from the National Institutes of Health (P30 GM124165). The Eiger 16M detector on the 24-ID-E beam line is funded by a NIH-ORIP HEI grant (S10OD021527). This research used resources of the Advanced Photon Source, a U.S. Department of Energy (DOE) Office of Science user facility operated for the DOE Office of Science by Argonne National Laboratory under Contract DE-AC02-06CH11357.

APS X-ray Availability and Reliability

In fiscal year 2021*, the APS x-ray source continued to function as a highly reliable delivery system for x-ray beams for research. Several factors support the overall growth in both the APS user community and the number of experiments carried out by that community. But there is a direct correlation between the number of x-ray hours available to users; the success of the APS experiment program; and the physicists, engineers, and technicians responsible for achieving and maintaining optimum x-ray source performance. Below are definitions of important measures for the delivery of x-ray beam to users (latest data shown graphically).

X-ray availability FY99-FY21

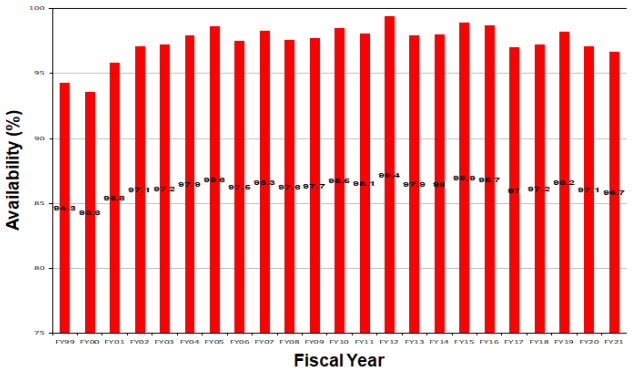

X-ray Availability: The number of hours that beam is available to users divided by the number of hours of scheduled beam delivery prior to the beginning of a run. The specific definition of available beam is that the APS main control room has granted permission to users to open shutters, and there is more than 50-mA stored beam in the storage ring.

MTBF FY99-FY21

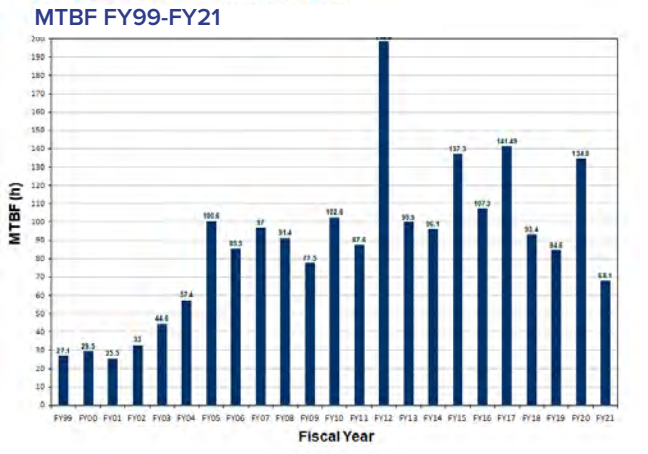

Storage Ring Reliability: A measure of the mean time between beam losses (faults, MTBF, calculated by taking the delivered beam and dividing by the total number of faults. A fault is defined as complete unavailability of beam either via beam loss or removal of shutter permit not related to weather. A fault also occurs when beam has decayed to the point where stability and orbit can no longer be considered reliable (50 mA).

* While the highlights in, and title of, this report cover calendar year 2021, data on accelerator performance and user statistics are measured on the basis of fiscal years.

Typical APS Machine Parameters

Linac

Output energy	425 MeV
Output beam charge	0.3–3 nC
Normalized emittance	5–20 mm-mrad
Frequency	2.856 GHz
Modulator pulse rep rate	30 Hz
Gun rep rate	2–26 Hz
(1-13 pulses, 33.3 ms apart every 0.5 s)	
Beam pulse length	8–15 ns
Bunch length	1–10 ps FWHM

Particle Accumulator Ring

Nominal energy	425 MeV
Circumference	30.66 m
Cycle time	0.5 s or 1 s
Fundamental radio frequency (RF1)	9.77 MHz
12th harmonic RF frequency (RF12)	117.3 MHz
RMS bunch length	0.34 ns
(after compression)	

Injector Synchrotron (Booster)

Nominal extraction energy	7.0 GeV
Injection energy	425 MeV
Circumference	368.0 m
Ramping rep rate	2 Hz or 1 Hz
Natural emittance	132 nm-rad (on momentum)
	87 nm-rad (with -0.6% offset)
Booster RMS bunch length	100 ps
Radio frequency	351.935 MHz
Momentum offset	0.6%

Storage Ring System

Nominal energy	7.0 GeV
Circumference	1104 m
Number of sectors	40
Length available for insertion device	5.0 m
Nominal circulating current, multibunch	100 mA
Natural emittance	2.5 nm-rad
RMS momentum spread	0.096%
Effective emittance	3.1 nm-rad
Vertical emittance	0.035 nm-rad
Coupling (operating)	1.4%
Revolution frequency	271.555 kHz
Radio frequency	351.935 MHz
Operating number of bunches	24 to 324
RMS bunch lengths	33 ps to 25 ps
RMS bunch length of 16 mA in hybrid mode	50 ps

Environmental, Geological, and Planetary Science

The Effects of Toxic Metalloids on Indigenous Microorganisms near an Antimony Mine

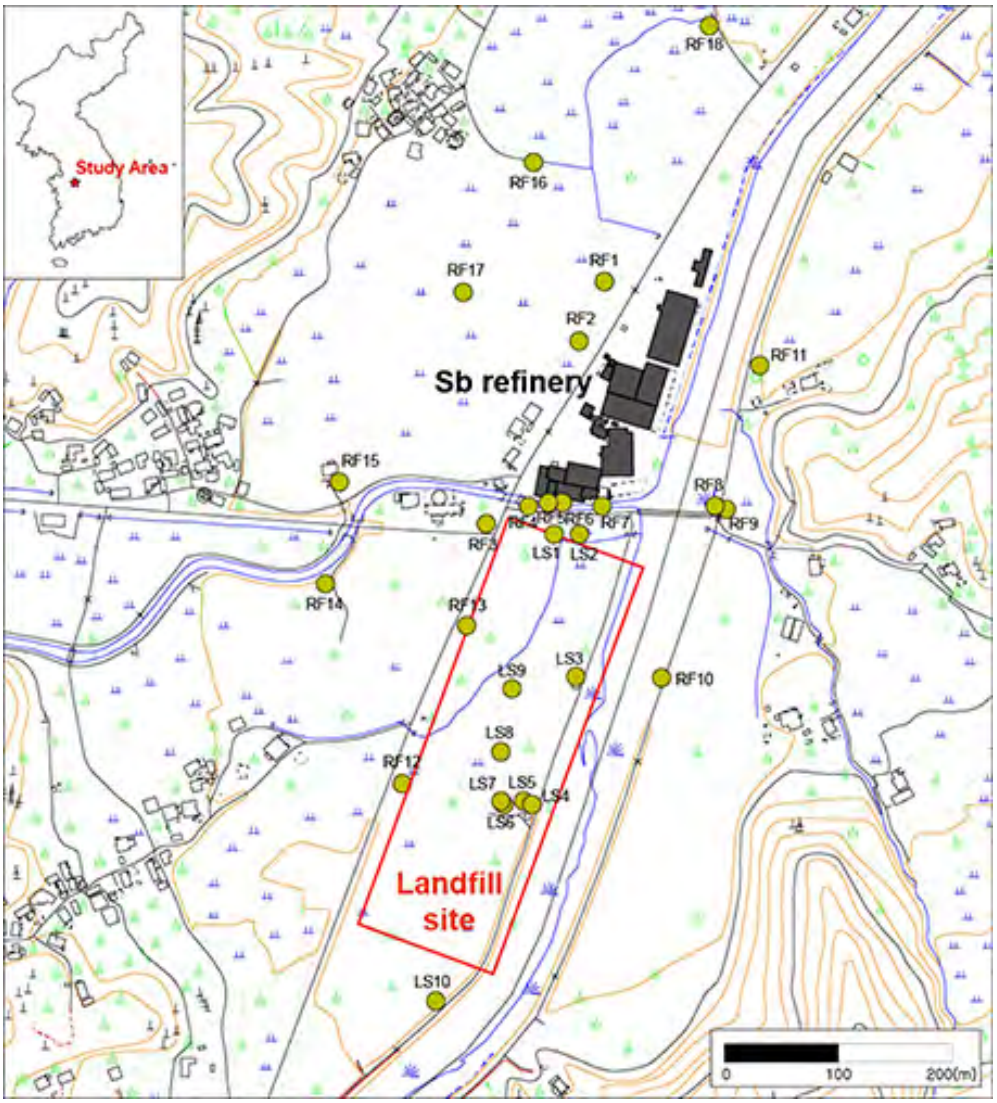

Fig. 1. Study site and sampling locations. Samples were designated as RF or LS depending on their location. (RF: soil samples near the refinery, LS: soil samples from the landfill site). From S.-C. Park et al., J. Hazard. Mater. **403**, 123625 (2021).

This study, carried out at the APS and published in the *Journal of Hazardous Materials*, determined the distribution, speciation, and deleterious effects of antimony (Sb) and other toxic contaminants on the soil and the indigenous microbial community at an antimony refinery in South Korea. Researchers can now use this information to determine new and more effective ways to clean up antimony-contaminated sites.

Antimony is a trace element in Earth's crust, water, and soils. Although Sb is toxic, its alloys are used in batteries, printing presses, and bullets. Other antimony compounds appear in flame-retardant materials, paints, enamels, glass, and pottery. To isolate Sb for use, Sb-containing compounds must undergo mining and smelting.

Waste materials from ore refining are high in Sb and other toxic co-contaminants. Sb is genotoxic and so can damage DNA. Humans exposed to high levels of Sb may develop serious metabolic disorders. Sb also has deleterious effects on indigenous microorganisms. Sb methylation by microorganisms impacts Sb transformation and is criti-

cal in its biogeochemical cycle. Despite these dangers, South Korea does not limit antimony pollution, although many other nations, including the European Union, do.

To determine the best *in situ* and *ex situ* remediation strategies, researchers must understand the element's speciation. The majority of Sb found in soils is as Sb(V), the mineral tripuhyite ($FeSbO_4$), an immobile phase with low Sb bioavailability. Oxidation is caused by both abiotic and biotic processes. Little is known about the effects of co-contaminants, such as arsenic (As) and lead (Pb), on Sb, although they appear to help control Sb bioavailability and transport. For example, Sb(III) mobility is significantly decreased by adsorption to iron (hydr)oxides or by precipitation as Sb(III) sulfide.

This study analyzed Sb and other toxic metal(loid)s near an operating Sb refinery and landfill site in South Korea (Fig. 1). In the 1980s, Sb-containing wastes were buried near the processing plant, resulting in local contamination. The site was remediated in the early 2000s by excavating and relocating the wastes. Nonetheless, there is still heavy residual contamination of Sb and the other toxic metal(oids) in the soil.

The researchers used antimony K-edge (30,491 eV) x-ray absorption near-edge spectroscopy (XANES) and extended x-ray absorption fine-structure (EXAFS) spectra collected under ambient conditions at the MR-CAT 10-BM x-ray beamline at the APS. For microbial analyses, DNA was isolated, quantified, sequenced, and compared with DNA data from Sb-oxidizing bacteria.

In sediment samples taken horizontally and vertically, at both the refinery and landfill, Sb concentrations were high relative to EU guidelines. In the topsoil near the refinery, Sb levels were high, but other toxic metal(oids) were low. Some of the Sb appeared as Sb(III) in Sb_2O_3, but most was oxidized to Sb(V). Tripuhyite is stable with low solubility and so is a sink for Sb in oxidizing and supergene environments. At greater depths, concentrations of As and Pb increased; Sb was up to 15 times higher than in the topsoil. Sb concentrations decreased with distance from the refinery in the path of the prevailing wind.

Indigenous microorganisms are affected by Sb speciation and also by co-contamination with other heavy metal(oids). Throughout the study site, microbial populations were low relative to bulk soil but seemed unaffected by Sb. The populations were lowest where levels of co-contaminants were highest. Yet, even small differences in co-contaminants greatly influenced the composition of the microbial communities.

The researchers suggest that high Sb in topsoil is due to the release of Sb-containing dust from the refinery. Higher concentrations of Sb and other toxic metal(loid)s with soil depth is likely due to impurities in the Sb2O3 starting material used in earlier (1980s) refining operations. Apparently, this material was not removed during remediation in the 2000s. – Dana Desonie

See: Soo-Chan Park[1], Maxim I. Boyanov[2,3], Kenneth M. Kemner[3], Edward J. O'Loughlin[3], and Man Jae Kwon[1]*, "Distribution and speciation of Sb and toxic metal(loid)s near an antimony refinery and their effects on indigenous microorganisms," J. Hazard. Mater. **403**, 123625 (2021). DOI: 10.1016/j.jhazmat.2020.123625
Author affiliations: [1]Korea University, [2]Bulgarian Academy of Sciences, [3]Argonne National Laboratory
Correspondence: * manjaekwon@korea.ac.kr

The authors thank the MR-CAT beamline staff for assistance during data collection. M.I.B., K.M.K., and E.J.O. were supported in part by the Wetland Hydrobiogeochemistry Scientific Focus Area (SFA) at Argonne National Laboratory funded by the Environmental System Science Program, Office of Biological and Environmental Research, Office of Science, U.S. Department of Energy (DOE), under MR-CAT operations are supported by DOE and the MR-CAT member institutions. This work was also supported by the Basic Science Research Program through the National Research Foundation of Korea (NRF) funded by the Ministry of Education (2018R1A2B6001660) and by the Korea Environmental Industry & Technology Institute (KEITI) through the Subsurface Environment Management Project, funded by Korea's Ministry of Environment (grant number 2018002440002). This research used resources of the Advanced Photon Source, a U.S. DOE Office of Science user facility operated for the DOE Office of Science by Argonne National Laboratory under Contract No. DE-AC02-06CH11357.

Reading Between the Diamonds: Expanding Deep Carbon

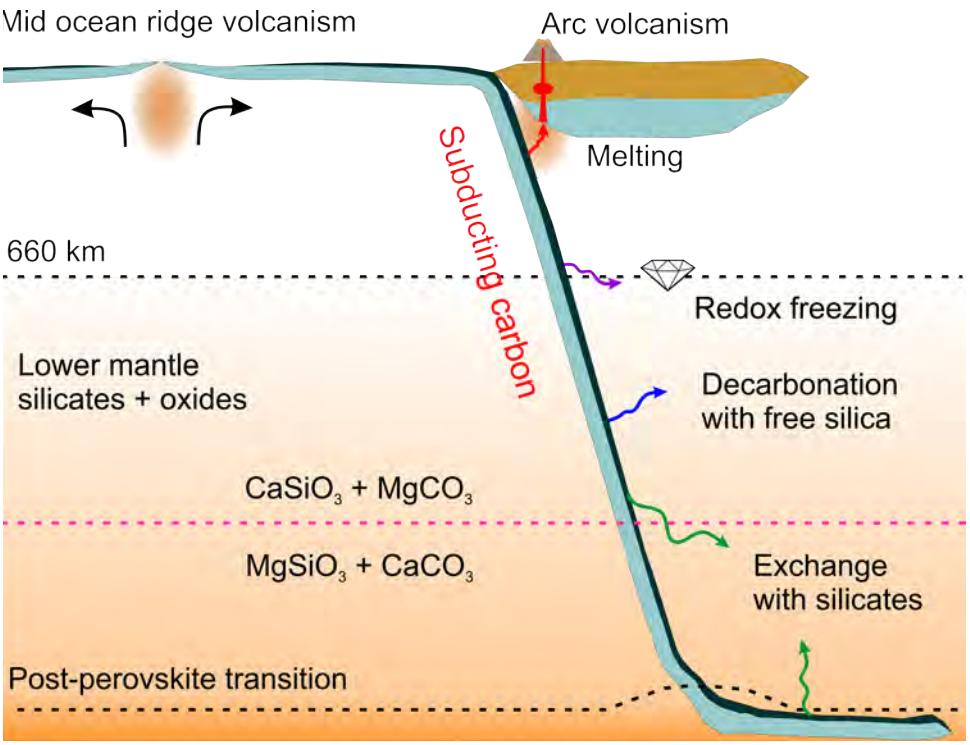

Fig. 1. Schematic illustration of the fate of carbonates in the oceanic crust (dark blue) subducted to the lower mantle. Through subduction, the carbonates may undergo melting (red arrow), redox freezing with metallic iron (purple arrow), decarbonation reaction with free silica (blue arrow), and exchange reaction with lower mantle silicates (green arrow). Based on the observation of reversal of the carbonate-silicate cation exchange reaction at conditions relevant to cold subducted slabs at mid-lower-mantle depths, $CaCO_3$ is the potential stable phase that hosts oxidized carbon in the lowermost mantle. From M. Lv et al., Nat. Commun. **12**, 1712 (2021). © 2021 Springer Nature Limited

The original Michigan State University press release can be read here. © Michigan State University

In a paper published in *Nature Communications* based on research at the APS, scientists in Susannah Dorfman's Experimental Mineralogy Lab at Michigan State University (MSU) redefined the conditions under which carbonates can exist in the Earth's lower mantle, adding to our understanding of the deep carbon cycle and the Earth's evolution.

"The circulation of carbon and minerals from the surface of the Earth through subduction to the base of the Earth's mantle has been happening for billions of years," said Dorfman, assistant professor in the MSU Department of Earth and Environmental Science (EES) in the College of Natural Science and co-author of the paper. "Our lab asks, 'how can we use experiments to predict what it looks like and to follow it chemically?'"

During subduction, surface carbonates (think limestone and coral skeletons) hitch a ride on cold slabs of rock diving under Earth's crust through tectonic motion fueled by the mantle's heat. Some carbonates melt and are spewed back into the atmosphere by volcanoes. Some travel further down and are pressed into diamonds.

But what about the carbonates that make it even deeper, toward the Earth's core-mantle boundary almost 1,800 miles below the surface? A place so deep it is impossible to recover a sample?

Dorfman's previous research showed that some carbonates could indeed escape being melted or turned into diamonds in a hot, oxygen-poor environment like the core-mantle boundary, but no one knew what form they would take in a real rock until now.

In the current study, Dorfman and co-author Mingda Lv, a fifth-year EES doctoral student, conducted highly

complex experiments to synthesize mantle rock and illuminate the fate of those deeply subducted carbonates for the first time.

"For this project, we wanted to know how carbonate would coexist with the majority of mantle silicates when subducted to the lower mantle," Lv explained. "We designed the experiments to extend the pressure and temperature conditions on these minerals to high regimes, simulating conditions at the core-mantle boundary of the Earth."

"What we were interested in is, when is carbon not diamond?" added Dorfman.

Cooking up rock under the extreme temperature and pressure conditions of Earth's lower mantle goes far beyond the ability of your kitchen's pressure cooker. Their experiments required a device made of material with the highest-pressure tolerance of any substance on Earth—diamonds. "The diamond anvil cell, even though it is something you can hold in your hand, gives us the very highest pressures in any lab without using explosions," Dorfman said. "All of what we know about what goes on in the center of planets is dependent on this device."

Dorfman and Lv assembled thin carbonate and silicate discs like a sandwich between the two diamonds of the diamond anvil cell. Then, they squeezed the discs together like a mineral panini and used powerful lasers to heat them to soaring temperatures of up to 4,500°F.

The result was something no one thought possible, a synthesized form of highly pressurized calcium carbonate rock that could exist in lower mantle conditions.

"Before this study, the idea was that you should never have calcium carbonate in the deep Earth, but only in a shallow environment where it hasn't gotten down to great depths," Dorfman said. "Our experiments show that toward the base of the mantle, the chemical reaction changes direction and swaps minerals like partners in square dancing—the magnesium and calcium swap their carbonate and silicate partners producing calcium carbonate and magnesium carbonate" (Fig. 1).

The size of their newly synthesized rock was only the width of a human hair, and the individual crystals comprising the rock were up to 1,000 times smaller. To read between the diamonds, Dorfman and Lv needed the sharpest knife and brightest light they could find.

Working at the GSECARS x-ray beamline 13-ID-D at the APS, the team reproduced high-temperature conditions found at the mantle by using a double-sided ytterbium fiber laser-heating system and then employed the extremely powerful, high-brightness APS x-rays to probe sample properties *in situ* at extreme conditions with the high-resolution angle-dispersive x-ray diffraction technique before, during, and after laser heating. Then, with the help of collaborators at the Institute of Earth Physics of Paris and the University of Michigan's Center for Materials Characterization, they used ion beams to slice the new rock into cross-sections.

Finally, using the state-of-the-art electron microscopy techniques at MSU's Center for Advanced Microscopy, they successfully characterized the elemental distribution of their recovered samples.

"Without these labs, we would never have been able to directly observe what is going on in our experiments," Lv said. "Our collaboration with these facilities is a highlight of the study."

"We know that a vast majority of the Earth's carbon isn't up in the atmosphere, it's in the interior, but our guess as to how much and where depend mostly on measurements of chemical reactions," Dorfman added. "Mingda Lv's work shows that calcium carbonate can be stable in mantle conditions and provides a new mechanism to take into account when we make models of the carbon cycle inside the Earth."

See: Mingda Lv[1]*, Susannah M. Dorfman[1]**, James Badro[2], Stephan Borensztajn[2], Eran Greenberg[3‡], and Vitali B. Prakapenka[3], "Reversal of carbonate-silicate cation exchange in cold slabs in Earth's lower mantle," Nat. Commun. **12**, 1712 (2021). DOI: 10.1038/s41467-021-21761-9
Author affiliations: [1]Michigan State University, [2]Institut de physique du globe de Paris, [3]The University of Chicago
[‡]Present address: Soreq Nuclear Research Center (NRC)
Correspondence: * lyumingd@msu.edu,
** dorfman3@msu.edu

This work was supported by new faculty startup funding from Michigan State University, the Sloan Foundation's Deep Carbon Observatory Grant G-2017-9954, and National Science Foundation (NSF) grant EAR-1751664 to S.M.D. Parts of this work were supported by IPGP multidisciplinary program PARI, and by Region Île-de-France SESAME Grant no. 12015908. GSECARS is supported by the National Science Foundation–Earth Sciences (EAR – 1634415) and Department of Energy (DOE)-GeoSciences (DE-FG02-94ER14466). This research used resources of the Advanced Photon Source, a U.S. DOE Office of Science user facility operated for the DOE Office of Science by Argonne National Laboratory under Contract No. DE-AC02-06CH11357.

Where Does Iron Go in Earth's Lower Mantle?

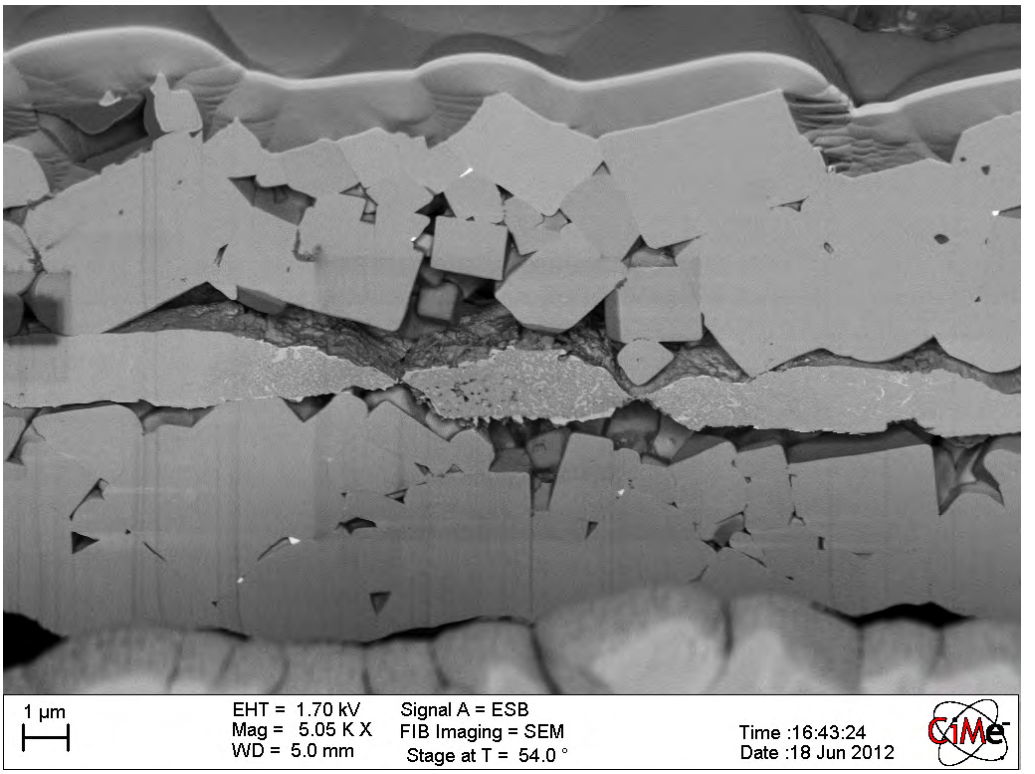

Fig. 1. In this cross-section of a sample recovered from high-pressure experiments in the laser-heated diamond anvil cell at beamline 13-ID-D of the GSECARS sector, layers of salt (recrystallized to larger cubes due to time spent in air before microscopy) and the region of the sample that was heated with the laser can be seen. The dark sections are bridgmanite and the bright sections are magnesiowüstite—the two most abundant minerals of Earth's lower mantle.

To investigate the effects of iron enrichment on the properties of dense pockets of material within Earth's lower mantle, researchers using the APS examined partitioning of iron among magnesiowüstite, bridgmanite, and post-perovskite phases synthesized from Fe^{2+}-rich olivine in laser-heated diamond anvil cells at pressure and temperature conditions spanning the entire range of the lower mantle: 33 gigapascals (GPa) to 128 GPa and 1900 K to 3000 K. The researchers characterized these assemblages with a combination of *in situ* x-ray diffraction and *ex situ* transmission electron microscopy. They found that the preference of iron for bridgmanite relative to magnesiowüstite decreases with pressure and iron enrichment and increases with temperature. Thermodynamic modeling determined that both incorporation and partitioning of iron in bridgmanite are well explained by excess volume associated with Mg-Fe exchange. Partitioning results were used to model compositions and densities of mantle phase assemblages as a function of pressure, FeO-content, and SiO_2-content. Unlike average mantle compositions, iron-rich mantle compositions were found to exhibit negative dependence of density on SiO_2-content at all mantle depths, an important finding for better understanding deep lower-mantle structures. Their results were published in the journal *Minerals*.

Earth's mantle is about 82.5% of the volume of the planet, and its behavior is responsible for the motions of tectonic plates that make earthquakes and volcanoes. The biggest challenge in studying the mantle is that it can't be seen, and samples cannot be retrieved. So, instead, geologists study it with seismographs. Seismic wave patterns reveal changes in contrast that suggest variations in squishiness and density.

Seismic observations combined with experimental measurements of mineral properties indicate the lower mantle is composed of three major mineral species: bridgmanite [$(Mg,Fe)(Si,Al)O_3$], ferropericlase [(Mg,Fe)O], and calcium silicate perovskite [$CaSiO_3$]. However, global analysis of seismic observations suggests there are two vast regions within the mantle that have different chemical composition (and that are warmer and softer) than the surrounding mantle. These regions, called large low-shear-velocity provinces (LLSVPs), and smaller ultra-low-velocity zones (ULVZs) at their bases, may have settled near the boundary between the mantle and the core like crystallized honey at the bottom of a honey jar.

These heterogeneities are thought to be enriched in iron, as measured by Fe/(Mg + Fe), or Fe#, up to 7% higher than surrounding areas, and their physical properties are thought to depend on the exact distribution of iron among the species $(Mg,Fe,Al)(Fe,Al,Si)O_3$ bridgmanite, its polymorph $(Mg,Fe,Al)(Fe,Al,Si)O_3$ post-perovskite, and (Mg,Fe)O magnesiowüstite. Partitioning of Fe between these species, or phases, is the preference of iron for oxide versus silicate.

The dependence of partitioning on bulk iron content is key to the modern composition of dense mantle heterogeneities. Previous studies of silicate-oxide iron partitioning have found that the preference of iron for bridgmanite decreases with increasing amounts of ferrous iron, but these studies have not been performed at the intense pressure and temperature conditions representative of the deep lower mantle.

To investigate iron partitioning among bridgmanite, post-perovskite, and magnesiowüstite, researchers at the Swiss Federal Institute of Technology Lausanne, Michigan State University, Université de Paris, and the University of Chicago reacted synthetic ferrous-iron-rich olivine crystals with compositions $(Mg_{0.55}Fe_{0.45})_2SiO_4$ and $(Mg_{0.28}Fe_{0.72})_2SiO_4$, dubbed Fa72 and Fa45, to form the lower mantle bridgmanite-oxide mixture in a device called a laser-heated diamond anvil cell (Fig. 1). This powerful tool for studying materials under extreme pressures and temperatures allowed the researchers to mimic conditions of the lower mantle, which range from 33 GPa to 128 GPa and 1,900 K to 3,000 K. Laser heating was performed for 15 to 60 minutes at beamline 13-ID-D of the GSECARS sector of the APS (Fig. 1) and at the Earth and Planetary Science Laboratory at Ecole polytechnique fédérale de Lausanne (EPFL).

The researchers used high-resolution synchrotron x-ray diffraction technique combined with double-sided laser heating at GSECARS beamline to confirm the identities of the high-pressure phase assemblages *in situ* at high-temperature, high-pressure conditions. They then used a combination of focused ion beam and analytical transmission electron microscopy to measure percent-level material compositions of all phases.

In all samples, magnesiowüstite composition was found to be enriched in Fe relative to the starting material, demonstrating that Fe favors the oxide over the silicate phase throughout the lower mantle. In Fa72 samples, x-ray diffraction indicated that magnesiowüstite was within 5% Fe# of pure FeO between 50 and 100 GPa. Fe-content in bridgmanite increased with pressure up to about 80 GPa, reaching a maximum Fe# of 51 in Fa72 at 82 GPa. At 128 GPa, the iron content of the silicate phase was found to be higher than that measured at lower pressures due to the higher favorability of Fe dissolution into post-perovskite relative to bridgmanite. The observations also showed no evidence of change in partitioning due to a spin transition in bridgmanite and magnesiowüstite. Finally, observed partitioning behaviors were successfully reproduced by self-consistent thermodynamic modeling with updated equation of state parameters for iron-rich bridgmanite and FeO.

These results provide important constraints on the effect of iron content on partitioning of iron and the resulting physical properties of iron-rich lower mantle heterogeneities. The researchers conclude that the dynamics of iron-rich regions over Earth's history may have resulted in silicate depletion at the base of the mantle in LLSVPs and ULVZs. – Chris Palmer

See: Susannah M. Dorfman[1,2]*, Farhang Nabiei[1], Charles-Edouard Boukaré[3], Vitali B. Prakapenka[4], Marco Cantoni[5], James Badro[1,3], and Philippe Gillet[1], "Composition and Pressure Effects on Partitioning of Ferrous Iron in Iron-Rich Lower Mantle Heterogeneities," Minerals **11**, 512 (2021). DOI: 10.3390/min11050512
Author affiliations: [1]Swiss Federal Institute of Technology Lausanne, [2]Michigan State University, [3]Université de Paris, [4]The University of Chicago, [5]Swiss Federal Institute of Technology Lausanne
Correspondence: * dorfman3@msu.edu

GSECARS is supported by the National Science Foundation–Earth Sciences (EAR-1634415) and Department of Energy (DOE)-GeoSciences (DE-FG02-94ER14466). S.M. Dorfman acknowledges the Marie Heim-Vögtlin program of the Swiss National Science Foundation (NSF) for financial support through project PMPDP2_151256 and NSF EAR-1664332. J. Badro acknowledges the financial support of the UnivEarthS Labex program at Sorbonne Paris Cité (ANR-10-LABX-0023 and ANR-11-IDEX-0005-02). J. Badro and Ch.-E. Boukaré acknowledge funding from the Swiss NSF through FNS Grants 200021_169854. Parts of this work were supported by IPGP multidisciplinary program PARI, and by Paris–IdF region SESAME Grant no. 12015908. This research used resources of the Advanced Photon Source, a U.S. DOE Office of Science user facility operated for the DOE Office of Science by Argonne National Laboratory under Contract No. DE-AC02-06CH11357.

Using Chromium Valence Systematics to Model Crystallizing Basaltic Magma Systems

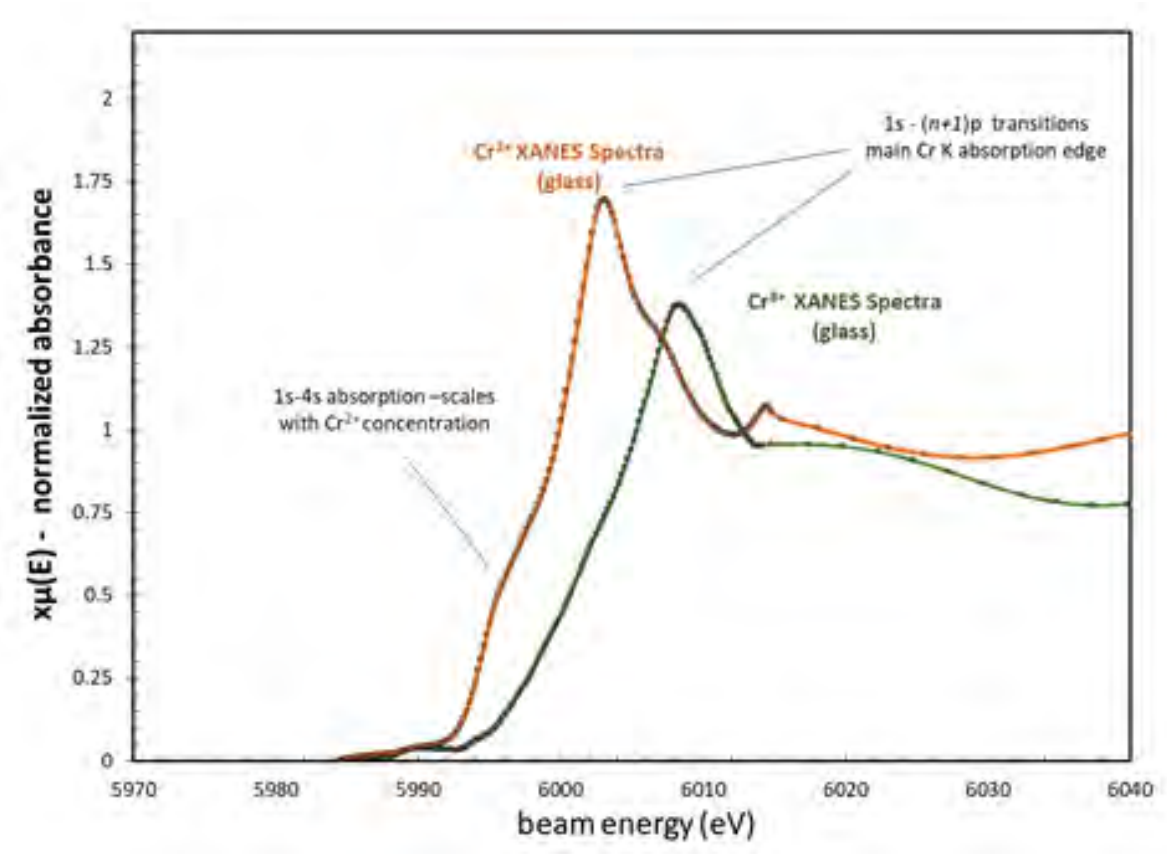

Fig. 1. XANES spectra of Cr^{2+} and Cr^{3+}-bearing glass standards showing shift in energy of the main Cr K absorption edge and appearance of the 1s-4s shoulder absorption that accompany changes in Cr valence.

Basaltic rocks represent one of the most abundant igneous rock types found on the Earth's surface and in many extraterrestrial bodies including on the Moon and on Mars. These are typically hard, dense, dark igneous rocks composed chiefly of plagioclase feldspar, pyroxene, and olivine, and often having a glassy appearance. These rocks may also preserve samples of quenched magmas and lavas as glasses in these igneous rocks. Redox studies of basaltic rocks frequently employ synchrotron spectroscopic analysis of such glasses as a means of trying to constrain the oxygen fugacity (the vapor pressure of oxygen corrected for non-ideal gas behavior) of the magmas from which these rocks formed.

For this work, the researchers developed a new technique using the Cr^{2+}/Cr^{3+} measured in olivine phenocrysts (a common very crystal that precipitates in basaltic magmas as they cool) to determine the oxygen fugacity of their basaltic parental liquid at the time of olivine crystallization. Using this model, which was tested at the APS, will provide researchers with a better understanding of magma source chemistry in terrestrial and even extraterrestrial settings. Their results were published in the journal *Geochimica et Cosmochimica Acta*.

At the Earth's mid-ocean ridges, low silica mafic are derived from the olivine-rich source rock, peridotite, in the mantle materials below the ridge. These magmas are ex-

truded onto the seafloor as lavas and quench instantly in the frigid ocean as basalt. This process typically results in the formation of a layer of glass around the basaltic rock. Such glasses can also be found trapped within magmatic phenocrysts as small samples of magma referred to as melt inclusions. The glass often reflects the chemistry of the mantle source if no minerals have crystallized to modify its composition. Geochemical analyses of the glass can reveal the exact composition of the source from which they melted, and oxygen barometers (such as x-ray absorption near edge structure [XANES]-based Fe^{3+}/Fe^{2+} measurements) have been developed to measure the oxygen fugacity ($f O_2$) of the glass. However, most magmas cool too slowly to form glasses, so making such oxygen fugacity measurements from basalts from other types of geological settings can be difficult due to their scarcity.

For this work, the authors developed a new technique for determining the oxygen fugacity from analysis of the crystalline (non-glassy) components preserved in basalt. As this primitive basaltic magma cools, the mineral olivine is the first phase to crystallize. Chromium is a minor element found in basaltic magmas and the minerals that crystallize from them, including some spinels, pyroxenes, and olivine, will incorporate the trace element. Olivine can accommodate both Cr^{2+} and Cr^{3+} equally. Synchrotron XANES measurements of the Cr valence ratio in olivine provides a high-resolution, temporally resolved record of $f O_2$ in the early magma source. Olivine is ideally suited for capturing and storing information about the Cr^{2+} and Cr^{3+} ratio of the parent liquid at the time the olivine crystallized.

The researchers' goal was to create a framework and predictive model to relate Cr^{2+} and Cr^{3+} in olivine phenocrysts to the temperature, liquid composition, and $f O_2$ of the parental melt of the olivine. This model was calibrated from a suite of laboratory experiments in which olivine and melts equilibrated at magmatic temperatures and controlled $f O_2$. Chromium K-edge XANES data from these experiments were acquired with the x-ray microprobe at the GSECARS beamline 13-ID-E at the APS. With these data, the researchers constructed a model that allows them to translate the Cr^{2+} and Cr^{3+} measured in olivine phenocrysts into geologically useful, quantitative redox information (Fig. 1). This model will help future researchers calculate magmatic $f O_2$ values from olivine phenocrysts in non-glassy basalts and extrapolate these data to infer the degree of redox heterogeneity present in the mantle peridotite source of the basalt in question.

Since the spectroscopy beamline at the APS allows for synchrotron-based XANES measurements to be made on a micrometer scale, this new technique can also reveal information on the redox changes that take place as the olivine phenocrysts grow from the melt. That is, evaluating how changes in Cr valence correlates with compositional zoning of major elements such as Fe and Mg in the phenocrysts. This method can be used as a redox chronometer, so using this as a clock that tracks the redox evolution of basaltic magmas over the course of their crystallization and degassing history. This method works for basalts from magmas that erupt, not only at mid-ocean ridges, but in other terrestrial and extraterrestrial settings.

– Dana Desonie

See: Aaron S. Bell[1]*, Zoltán Váci[2], and Antonio Lanzirotti[3], "An Experimental-XANES Investigation of Cr Valence Systematics in Basaltic Liquids and Applications to Modeling Cr^{2+}/Σ Cr Evolution in Crystallizing Basaltic Magma Systems," Geochim. Cosmochim. Acta **292**, 130 (2021). DOI: 10.1016/j.gca.2020.09.020
Author affiliations: [1]University of Colorado Boulder, [2]University of New Mexico, [3]The University of Chicago
Correspondence: * aaron.bell@colorado.edu

This work was funded by National Science Foundation EAR 1550929 awarded to A.S.B. GSECARS is supported by the National Science Foundation–Earth Sciences (EAR–1634415) and Department of Energy (DOE)-GeoSciences (DE-FG02-94ER14466). This research used resources of the Advanced Photon Source, a U.S. DOE Office of Science user facility operated for the DOE Office of Science by Argonne National Laboratory under Contract No. DE-AC02- 06CH11357.

Getting to Mercury's Core

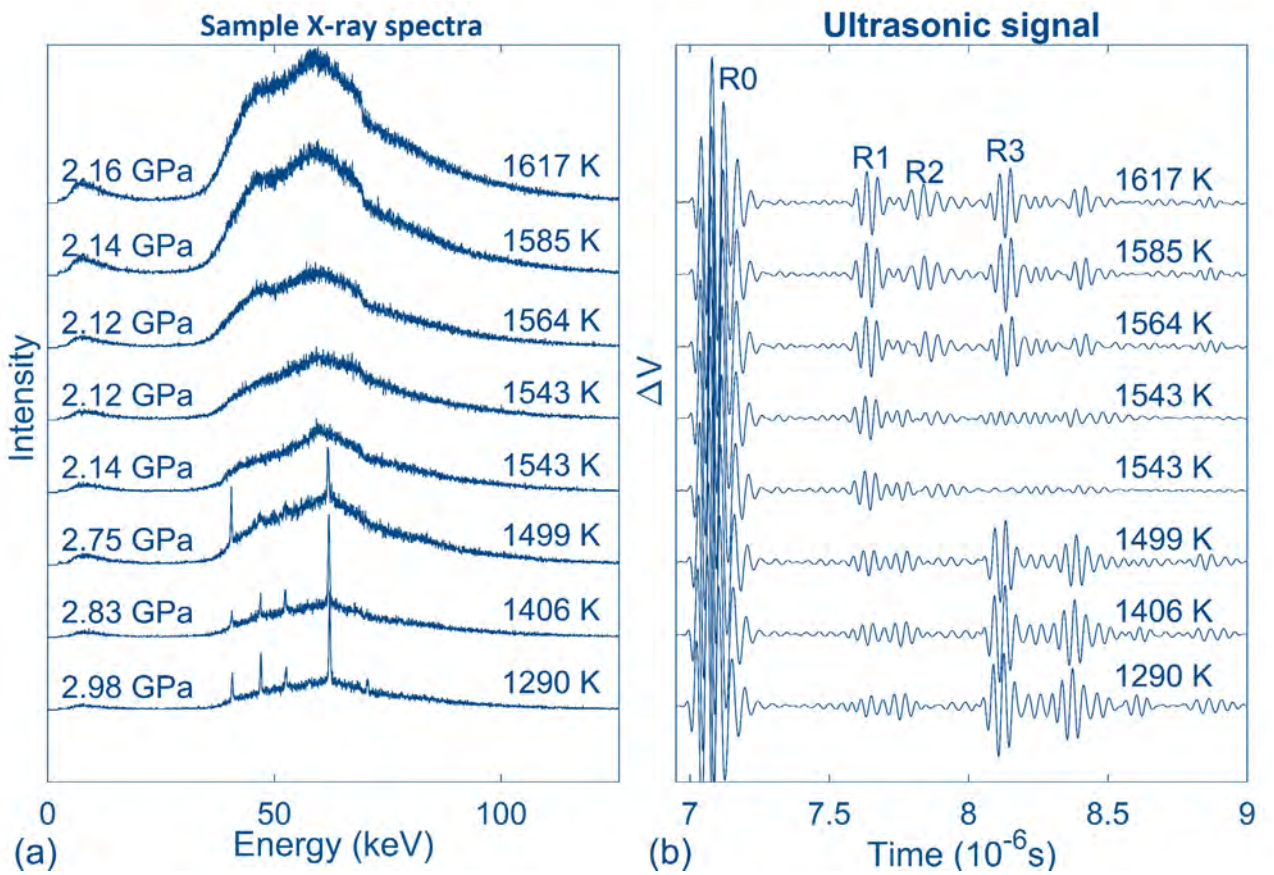

Fig. 1. Data obtained during heating the sample at high pressure. (a) X-ray spectra up at temperatures to 1599 K show crystalline sample. At 1543 K and higher temperature, the sample is (at least partially) molten. At temperatures above 1564 K, the ultrasonic (sound) signal shows the R2 signal, which is the reflection from the back side of the fully liquid sample, whereas R1 is the ultrasonic reflection at the top of the sample. The travel time of sound through the samples is determined as the time delay between R1 and R2. A radiographic image of the sample is used to determine the thickness of the sample. The sound velocity (V_P) is, then, obtained by dividing the travel time by sample thickness.

Understanding the physics and chemistry of the planet Mercury requires determining the density and composition of the planet's core at extremely high temperatures and pressures. For this work, experiments carried out at the APS and the European Synchrotron Radiation Facility (ESRF, France) revealed the properties of a liquid iron-silicon-carbon (Fe-Si-C) metal alloy at pressures up to 5.8 gigapascals (GPa) and temperatures around 2000 K. The researchers used these properties in new interior structure models with variable core compositions. Using geophysical constraints on the structure of the planet and the density of Mercury's core, the group of multi-nation, multi-institution researchers determined possible core compositions and hypothesized on the origin of Mercury's magnetic field. Their results were published in the *Journal of Geophysical Research: Planets*.

Mercury's metallic core makes up 85% of its radius, a much larger proportion than in the other rocky planets and moons in our solar system. Therefore, understanding the core is essential for understanding the planet's composition and magnetic field. Researchers use the planet's gravitational and rotational parameters to constrain the possi-

ble core compositions at the tremendous pressures and temperatures found in Mercury's interior. Mercury's core controls the distribution of elements in the planet and also hosts the dynamo that generates the magnetic field, induced by the convection of metallic liquid in the core.

Mercury's surface is low in iron but high in sulfur (S), suggesting that the core has low oxygen fugacity; it is therefore likely that silicon is the dominant light element in the planet's core, with small amounts of carbon and silicon. The magnesium-rich surface and low oxidation state of Mercury are similar to that of a rare carbonaceous chondrite, the CB chondrite, and also to a subgroup of the enstatite chondrites, the EH chondrites; both are primitive meteorites that are unmodified by the processes of melting or differentiation. Such chondrites represent the materials that were present as the rocky planets formed, and they yield many clues about the origin and age of the solar system.

For this work (Fig. 1), the researchers measured the density and P-wave velocities (V_P) of Fe-Si-C liquids at extremely high pressures (up to 5.8 GPa) and temperatures (2000 K). After the material's density was determined by x-ray absorption, density measurements of Fe-Si liquid metals [Fe-(<17 wt%) Si-(<4.5 wt%)] were performed by x-ray absorption techniques with a Paris-Edinburgh (PE) press at beamline ID-27 of the European Synchrotron Radiation Facility (France). Ultrasonic Vp measurements of Fe-Si liquid metals were performed with a PE press at the HPCAT-XSD beamline 16-BM-B of the APS. The V_P of liquid is directly related to its compressibility and is used to formulate expressions for the liquid's density up to higher pressure.

The researchers characterized the planet's internal core layers by assuming an Fe-Si-C composition for the largely liquid core. Models of Mercury's interior structure are constrained by the planet's moment of inertia, which is determined from geodetic measurements. Assuming a bulk planet composition similar to a CB-chondrite allows only low concentrations of light elements, Si and C, consistent with a large range of feasible interior structure models of Mercury. Alternatively, a bulk planet composition similar to an EH chondrite requires high concentrations of Si in Mercury's core, which are difficult to reconcile with the available geodetic measurements. The addition of such a large amount of Si strongly lowers the core's density such that the planet's mantle would need to be denser, because the core-mantle boundary is independently constrained. Therefore, the planet's moment of inertia would end up larger than the value that is inferred from geodetic measurements.

The consequences for Si, C and/or S in the liquid outer core for magnetic field generation were also briefly studied. Because C and S strongly partition into the liquid core, the growth of the inner core produces significant compositional buoyancy that helps generate convection and a dynamo. If Si is the dominant light element in the core, the compositional buoyancy is limited and convection is possibly confined to the deeper region of the liquid core and generated mainly by thermal buoyancy (a large heat flow). These consequences for the measured magnetic field need to be studied in more detail by numerical simulation of core convection. – Dana Desonie

See: J. S. Knibbe[1,2,3]*, A. Rivoldini[3], S. M. Luginbuhl[2], O. Namur[1], B. Charlier[4], M. Mezouar[5], D. Sifre[5], J. Berndt[6], Y. Kono[7], D. R. Neuville[8], W. van Westrenen[2], and T. Van Hoolst[1,3], "Mercury's Interior Structure Constrained by Density and P-Wave Velocity Measurements of Liquid Fe-Si-C Alloys," J. Geophys. Res.: Planets **126**, e2020JE006651. DOI: 10.1029/2020JE006651
Author affiliations: [1]KU Leuven, [2]VU University Amsterdam, [3]Royal Observatory of Belgium, [4]University of Liège, [5]European Synchrotron Radiation Facility, [6]Westfälische Wilhelms-Universität Münster, [7]Ehime University, [8]Université de Paris
Correspondence: * j.s.knibbe@vu.nl

The x-ray absorption measurements were performed on beamline ID-27 at the European Synchrotron Radiation Facility, Grenoble, France. HPCAT-XSD operations are supported by U.S. Departmen of Energy (DOE)-National Nuclear Securitry Administration's Office of Experimental Sciences. This project has received funding from the European Union's Horizon 2020 research and innovation program under the Marie Sklodowska-Curie grant agreement MERCURYREFINEMENT, with No 845354, awarded to J.S.K. Throughout the course of this project, J.S.K. also received funding by the KU Leuven (PDM contract) and a postdoctoral Marie Curie Seal of Excellence fellowship (12Z622ON) of the FWO-Flanders. Initial data were obtained with financial support from a Netherlands Space Office User Support Programgrant to W.v.W. and a BRAIN-be program grant (BR/143/A2/COME-IN) to T.V.H. B.C. is a Research Associate of the Belgian Fund for Scientific Research-FNRS.

Deep Water on Neptune and Uranus May Be Magnesium-Rich

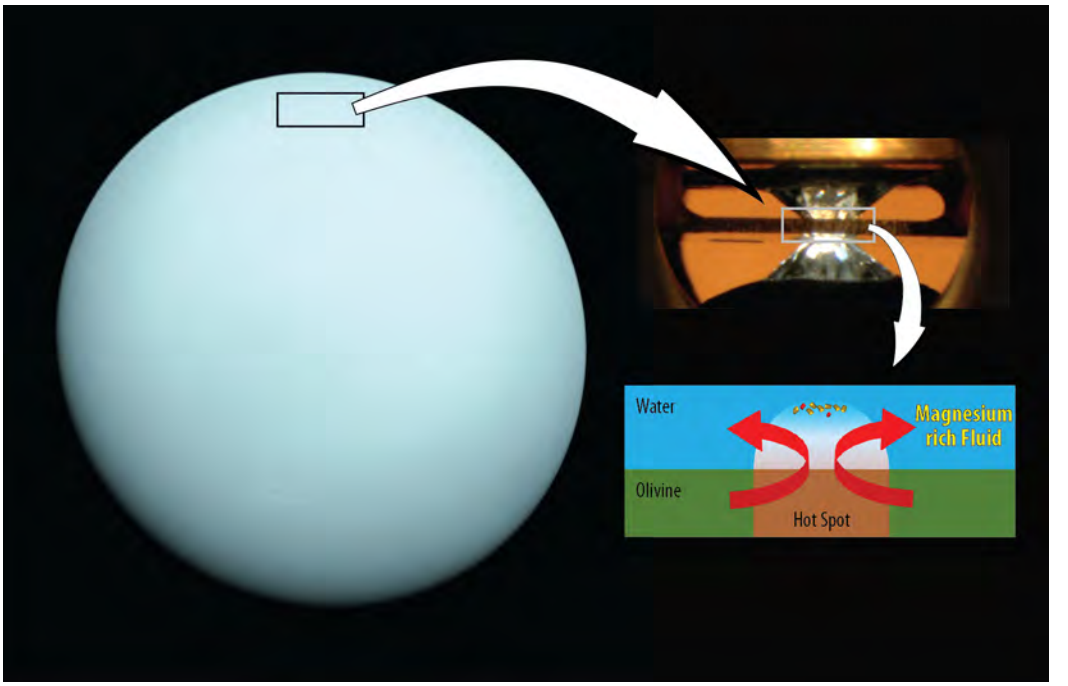

Fig. 1. A diamond-anvil (top right) and laser were used on a sample of olivine to reach the pressure-temperature conditions expected at the top of the water layer beneath the hydrogen atmosphere of Uranus (left). In this experiment, the magnesium in olivine dissolved in the water.

The original Arizona State University press release by Karin Valentine can be read here.

While scientists have amassed considerable knowledge about the rocky planets in our solar system, like Earth and Mars, much less is known about the icy water-rich planets, Neptune and Uranus. In a new study published in *Nature Astronomy*, a team of scientists recreated the temperature and pressure of the interiors of Neptune and Uranus at the APS and in so doing, have gained a greater understanding of the chemistry of these planets' deep water layers. Their findings also provide clues to the composition of oceans on water-rich exoplanets outside our solar system.

Neptune and Uranus are thought to have distinct separate layers, consisting of an atmosphere, ice or fluid, a rocky mantle and a metallic core. For this study, the research team was particularly interested in possible reaction between water and rock in the deep interiors.

"Through this study, we were seeking to extend our knowledge of the deep interior of ice giants and determine what water-rock interactions at extreme conditions might exist," said lead author Taehyun Kim, of Yonsei University in South Korea. "Ice giants and some exoplanets have very deep water layers, unlike terrestrial planets. We proposed the possibility of an atomic-scale mixing of two of the planet-building materials (water and rock) in the interiors of ice giants."

To mimic the conditions of the deep-water layers on Neptune and Uranus in the lab, the team first immersed typical rock-forming minerals, olivine and ferropericlase, in water and compressed the sample in a diamond-anvil to very high pressures. Then, to monitor the reaction between the minerals and water, they took x-ray measurements while laser heating the sample to a high tempera-

ture. High-resolution x-ray diffraction data were collected *in situ* at high-pressure and high-temperature conditions in the double-sided laser-heated diamond anvil cell (Fig. 1) at x-ray beamline 13-ID-D of the GSECARS earth sciences facility at the APS, and at the P02.2 Extreme Conditions Beamline of PETRA III at the Deutsches Elektronen-Synchrotron. In addition, infrared experiments were carried out at beamline 22-IR-1 at the National Synchrotron Light Source II using samples prepared at Yonsei University and Arizona State University.

The resulting chemical reaction led to high concentrations of magnesium in the water. Based on these findings, the team concluded that deep oceans on water-rich planets may have similar chemical concentration as the Earth's ocean but rich in magnesium.

"We found that magnesium becomes much more soluble in water at high pressures. In fact, magnesium may become as soluble in the water layers of Uranus and Neptune as salt is in Earth's ocean," said study co-author Sang-Heon Dan Shim of Arizona State University's School of Earth and Space Exploration.

These characteristics may also help solve the mystery of why Uranus' atmosphere is much colder than Neptune's, even though they are both water-rich planets. If much more magnesium exists in the Uranus' water layer below the atmosphere, it could block heat from escaping from the interior to the atmosphere.

"This magnesium-rich water may act like a thermal blanket for the interior of the planet," said Shim.

Beyond our solar system, these high-pressure and high-temperature experiments may also help scientists gain a greater understanding of sub-Neptune exoplanets, which are planets outside of our solar system with a smaller radius or a smaller mass than Neptune.

Sub-Neptune planets are the most common type of exoplanets that we know of so far, and scientists studying these planets hypothesize that many of them may have a thick water-rich layer with a rocky interior. This new study suggests that the deep oceans of these exoplanets would have fuzzy interface with underlying rocky layer due to the selective leaching of magnesium from the rocky mantle.

"In the case of Uranus, if an early dynamic process enabled a rock–water reaction during the hot phases of planetary accretion, the topmost water layer may remain rich in magnesium, possibly affecting the thermal history of the planet," said Shim.

For next steps, the team hopes to continue their high-pressure/high-temperature experiments under diverse conditions to learn more about the composition of planets. "This experiment provided us with a plan for further exploration of the unknown phenomena in ice giants," said Kim.

See: Taehyun Kim[1], Stella Chariton[2], Vitali Prakapenka[2], Anna Pakhomova[3], Hanns-Peter Liermann[3], Zhenxian Liu[4], Sergio Speziale[5], Sang-Heon Shim[6*] and Yongjae Lee[1**], "Atomic-scale mixing between MgO and H_2O in the deep interiors of water-rich planets," Nat. Astron. **5**, 815 (17 May 2021). DOI: 10.1038/s41550-021-01368-2
Author affiliations: [1]Yonsei University, [2]The University of Chicago, [3]Deutsches Elektronen Synchrotron, [4]University of Illinois at Chicago, [5]GFZ German Research Centre for Geosciences, [6]Arizona State University
Correspondence: * SHDShim@asu.edu,
** yongjaelee@yonsei.ac.kr

This work was supported by the Leader Researcher programme (NRF-2018R1A3B1052042) of the Korean Ministry of Science and ICT (MSIT). The authors also acknowledge the support by grant NRF-2019K1A3A7A09033395 of the MSIT. S.-H.S. was supported by National Science Foundation (NSF) grant EAR1338810 and National Aeronautics and Space Administration (NASA) grant 80NSSC18K0353. S.-H.S. also benefited from collaborations and information exchange within the Nexus for Exoplanet System Science (NExSS) research coordination network sponsored by NASA's Science Mission Directorate. S.S. acknowledges support by the GFZ German Research Centre for Geosciences. GSECARS is supported by the National Science Foundation–Earth Sciences (EAR–1634415) and Department of Energy (DOE)-GeoSciences (DE-FG02-94ER14466). Parts of this research were carried out at the P02.2 beamline at PETRA III, and we acknowledge Deutsches Elektronen-Synchrotron (DESY, Hamburg, Germany), a member of the Helmholtz Association HGF, for the provision of experimental facilities. We also acknowledge the scientific exchange and support of the Center for Molecular Water Science (CMWS) at DESY. This research also used beamline 22-IR-1 of the National Synchrotron Light Source II, a U.S. Department of Energy (DOE) Office of Science user facility operated for the DOE Office of Science by Brookhaven National Laboratory unational Science Foundation cooperative agreement EAR 11-57758 and CDAC (DE-FC03-03N00144). This research used resources of the Advanced Photon Source, a U.S. DOE Office of Science user facility operated for the DOE Office of Science by Argonne National Laboratory under Contract No. DE-AC02-06CH11357.

Three APS Users Received 2021 Protein Society Awards

Petra Fromme (Arizona State University) received the 2021 Christian B. Anfinsen Award, sponsored by The Protein Society (TPS). This award recognizes technological achievement or significant methodological advances in the field of protein science. Fromme, who is co-author on 20 peer-reviewed journal publications based on research at the APS, is a world leader in developing and applying novel technology for determining the structures of proteins, including the most challenging among them: membrane proteins. She has led this field by assembling a large network of collaborators spanning chemistry, physics, data science, biology, materials science, and engineering to pioneer the method of serial femtosecond crystallography, which is used to collect snapshots of molecules in action. She has made important contributions to the structural biology of large membrane protein complexes, especially those involved in light capture and energy conversion.

Janet Smith (University of Michigan) received the TPS 2021 Dorothy Crowfoot Hodgkin Award, sponsored by Genentech, which is granted in recognition of contributions in protein science that profoundly influence our understanding of biology. Smith is the scientific director of the GM/CA-XSD structural biology facility at the APS and is co-author on 60 peer reviewed journal publications based on research at the APS. She is recognized for exceptional contributions to our understanding of the biological function of proteins through knowledge of their three-dimensional structures. In major studies of natural-product biosynthetic enzymes, she demonstrated how macrolactones form, how biosynthetic assembly lines function, and how nature has adapted enzymes from primary metabolism for surprising chemical transformations such as cyclopropane formation. Her recent investigations of viral proteins and host antiviral proteins led to an understanding of how the flavivirus NS1 protein increases the virulence of dengue and Zika viruses, and how the zinc-finger antiviral protein recognizes viral RNA.

Amy Rosenzweig (Northwestern University) and Toshiya Endo (Kyoto Sangyo University) were co-recipients of the TPS 2021 Hans Neurath Award, sponsored by the Hans Neurath Foundation. This award honors individuals who have made a recent contribution of exceptional merit to basic protein research. Rosenzweig is co-author on 22 peer-reviewed journal publications based on research at the APS. She is a preeminent protein biochemist who tackles problems at the forefront of bioinorganic chemistry. Her lab studies metal-dependent methane oxidation, oxygen activation, and metal uptake and transport using structural, spectroscopic, biochemical, genetic, and bioinformatics approaches. Her contributions characterizing the membrane-bound methane monooxygenase have inspired new ways to harness the energy of methane, a potent greenhouse gas, as an alternative liquid-fuel source. Other work from Rosenzweig on copper uptake may hold therapeutic potential in Wilson's disease, a genetic disorder leading to copper overload in humans.

Haskel of XSD Selected as an American Physical Society Outstanding Referee for 2021

Daniel Haskel, an Argonne senior physicist and leader of the XSD Magnetic Materials Group, was selected as one of the 151 Outstanding Referees by the American Physical Society for 2021, who "...have demonstrated exceptional work in the assessment of manuscripts published in the *Physical Review* journals." Haskel's group supports researchers and drives advances in x-ray scattering and spectroscopy techniques and instrumentation aimed at studying frontier problems in condensed matter physics. The group currently operates four x-ray beamlines at the APS. Haskel is the only member of the Argonne scientific staff named to the 2021 list, and 1 of only 7 from DOE national laboratories. Instituted in 2008, the Outstanding Referee program annually recognizes approximately 150 out of about 78,000 referees for their invaluable work. Comparable to Fellowship in the American Physical Society and other organizations, this is a lifetime award

Nanoscience

Come Together, Right Now: Detonation Nanodiamonds' Fast Aggregation during Synthesis

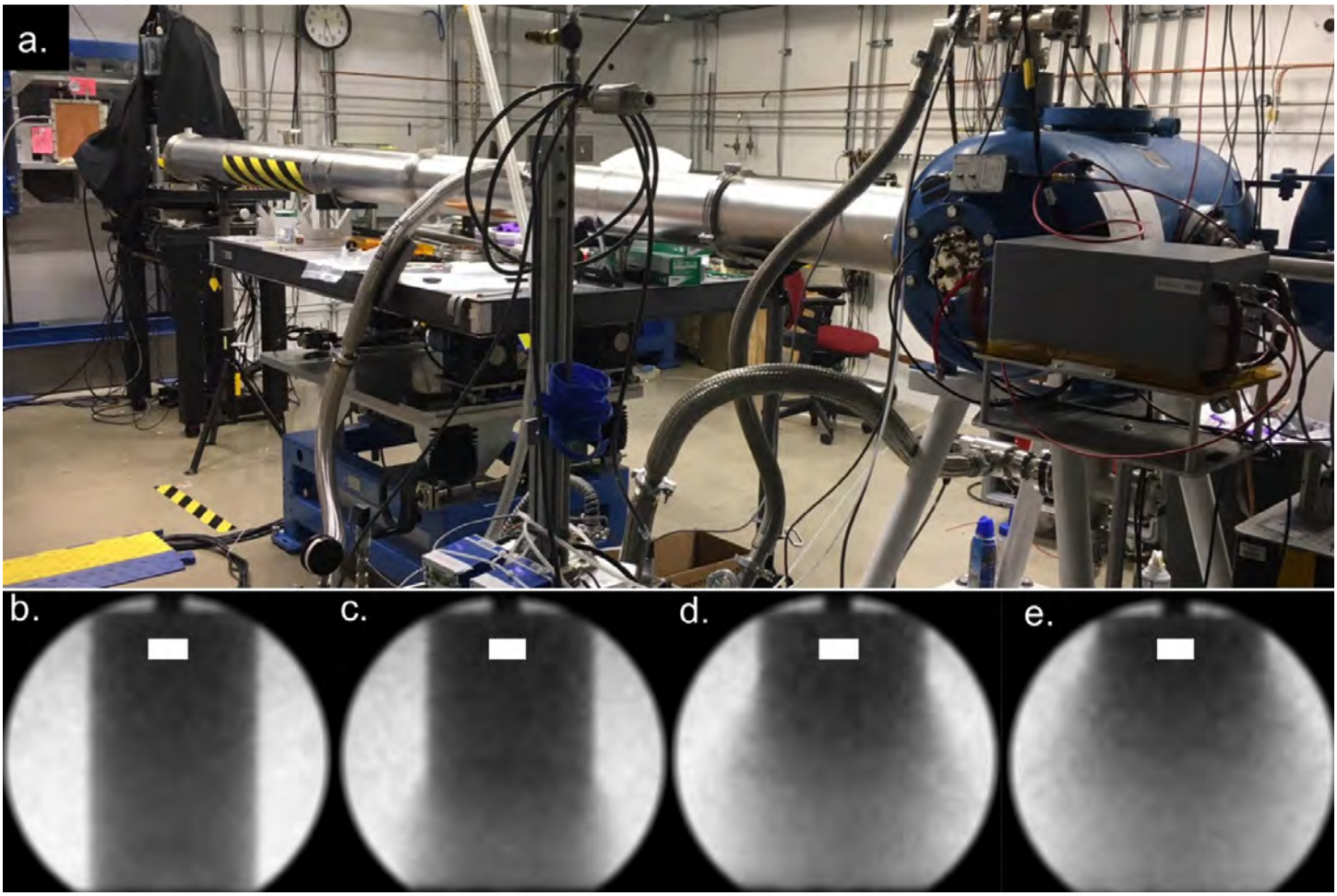

Fig. 1. (a) Photograph of the system to collect dynamic SAXS at a low q range at DCS. The detonation tank appears at the right, in blue. X-rays enter from the right. The scattered x-rays exit the tank and travel to the left to the four-camera detector system placed against the back wall of the hutch. (b–e) Time series of scatter beam images illustrating how the detonation wave moves through the x-ray beam (approximate position for small-angle scattering acquisition indicated by the enlarged white rectangle). Here the difference in time between images is 614 ns. This corresponds to four electron bunches in 24-bunch mode at the APS. From J.A. Hammons et al., J. Phys. Chem. Lett. **21**, 5286 (2021). Copyright © 2021 American Chemical Society

Nanoscale diamonds are used in a broad array of applications, including optical or quantum computing, sensors, and biomedicine. However, these materials, known as nanodiamonds, are difficult to efficiently synthesize and isolate. One way to generate nanodiamonds is through oxygen-deficient detonation of carbon-rich, explosive compounds. This method reliably produces ~4-nanometers nanodiamonds, but the resulting particles are always aggregated together and intertwined with graphitic and other unwanted phases of carbon. Techniques to separate out individual nanodiamonds, such as sonication with agents that break up and stabilize particles, can change their surfaces and adversely affect their properties. Because little is known about the aggregation kinet-

ics of detonation nanodiamonds, or even their formation or aggregation mechanisms, it's unclear whether it might be possible to implement interventions that prevent aggregation. To help elucidate the aggregation process, researchers from Washington State University and the U.S. Department of Energy's Lawrence Livermore Laboratory (LLNL) and used the APS to track nanodiamond formation and aggregation over time. Their findings–published in the *Journal of Physical Chemistry Letters*–suggest that because nanodiamond aggregation happens at nearly the same time as nanodiamond formation, aggregation may be difficult to completely prevent.

The researchers studied formation and aggregation using two explosive mixtures known to produce detonation nanodiamonds: a mixture of hexogen (RDX) and trinitrotoluene (TNT) known as comp B, and a mixture of octogen (HMX) and TNT known as octol. They also studied two explosives that produce graphitic carbon allotropes: DNTF (3,4-bis(3-nitrofurazan-4-yl)furoxan) and UFTATB (2,4,6-triamino-1,3,5-trinitrobenzene). Each of these compounds was pressed into a cylinder and detonated inside a tank while time-resolved small-angle x-ray scattering (TR-SAXS) data was collected at DCS at the APS.

Transmission electron microscopy on recovered detonation products showed that each of the four explosives produced a diverse range of carbon nanomaterials. While ribbon-like aggregates dominated the UFTATB products and distinct nano-onion structures dominated the DNTF products, the main products of comp B and octol were detonation nanodiamond aggregates.

Hierarchical scattering seen in the time-resolved small-angle scattering during detonation suggest the nanodiamonds aggregate rapidly: as early as 0.1 µs after the detonation front passes the x-ray measurement position.

Modeling experiments indicated that this phenomenon is consistent with classical diffusion-limited aggregation mechanism in colloids, suggesting that the detonation nanodiamond particles immediately attach to each other when they collide in this high-pressure, high-temperature environment. These aggregates may condense from an extended network of carbon structures, especially in the case of mixed explosives such as comp B and octol in which excess carbon is primarily supplied by only one of the components (TNT for both mixtures). Thus far, only DNTF products remain as distinct, non-aggregated spherical nanoparticles under the conditions measured to several microseconds post-detonation.

These results suggest that nanodiamond aggregation may be difficult to avoid from current detonation methods, since particle attachment occurs through irreversible chemical bonding rather than electrostatic interactions. Because the nano-onions from DNTF detonation don't tend to aggregate, it may be possible to draw inspiration from their formation mechanism to develop new ways to synthesize isolated detonation nanodiamonds.

– Christen Brownlee

See: Joshua A. Hammons[1]*, Michael H. Nielsen[1], Michael Bagge-Hansen[1], Sorin Bastea[1], Chadd May[2], William L. Shaw[1], Aiden Martin[1], Yuelin Li[2], Nicholas Sinclair[2], Lisa M. Lauderbach[1] Ralph L. Hodgin[1], Daniel A. Orlikowski[1], Laurence E. Fried[1], and Trevor M. Willey[1]**, "Submicrosecond Aggregation during Detonation Synthesis of Nanodiamond," J. Phys. Chem. Lett. **21**, 5286 (2021).
DOI: 10.1021/acs.jpclett.1c01209
Author affiliations: [1]Lawrence Livermore National Laboratory, [2]Washington State University
Correspondence: * hammons3@llnl.gov,
** willey1@llnl.gov

This work was funded in its initial stages by LLNL LDRD 14-ERD-018 and in its latter stages by the U.S. Department of Energy's (DOE's) National Nuclear Security Administration's (NNSA's) Office of Defense Nuclear Nonproliferation and Science Campaign 2 and was performed under the auspices of the U.S. DOE by Lawrence Livermore National Laboratory under contract DE-AC52-07NA27344 (LLNL-JRNL-820295). DCS is operated by Washington State University under the U.S. DOE/NNSA award no. DE-NA0003957. TEM work utilized the Molecular Foundry, a U.S. DOE user facility operated for the DOE Office of Science by Lawrence Berkeley National Laboratory under contract no. DE-AC02-05CH11231. M.H.N. acknowledges support from the Lawrence Fellowship. This research used resources of the Advanced Photon Source, a U.S. DOE Office of Science user facility operated for the DOE Office of Science by Argonne National Laboratory under contract no. DE-AC02-06CH11357.

Taking a Lesson from Kevlar® to Build Ultra-Stable Nanomaterials

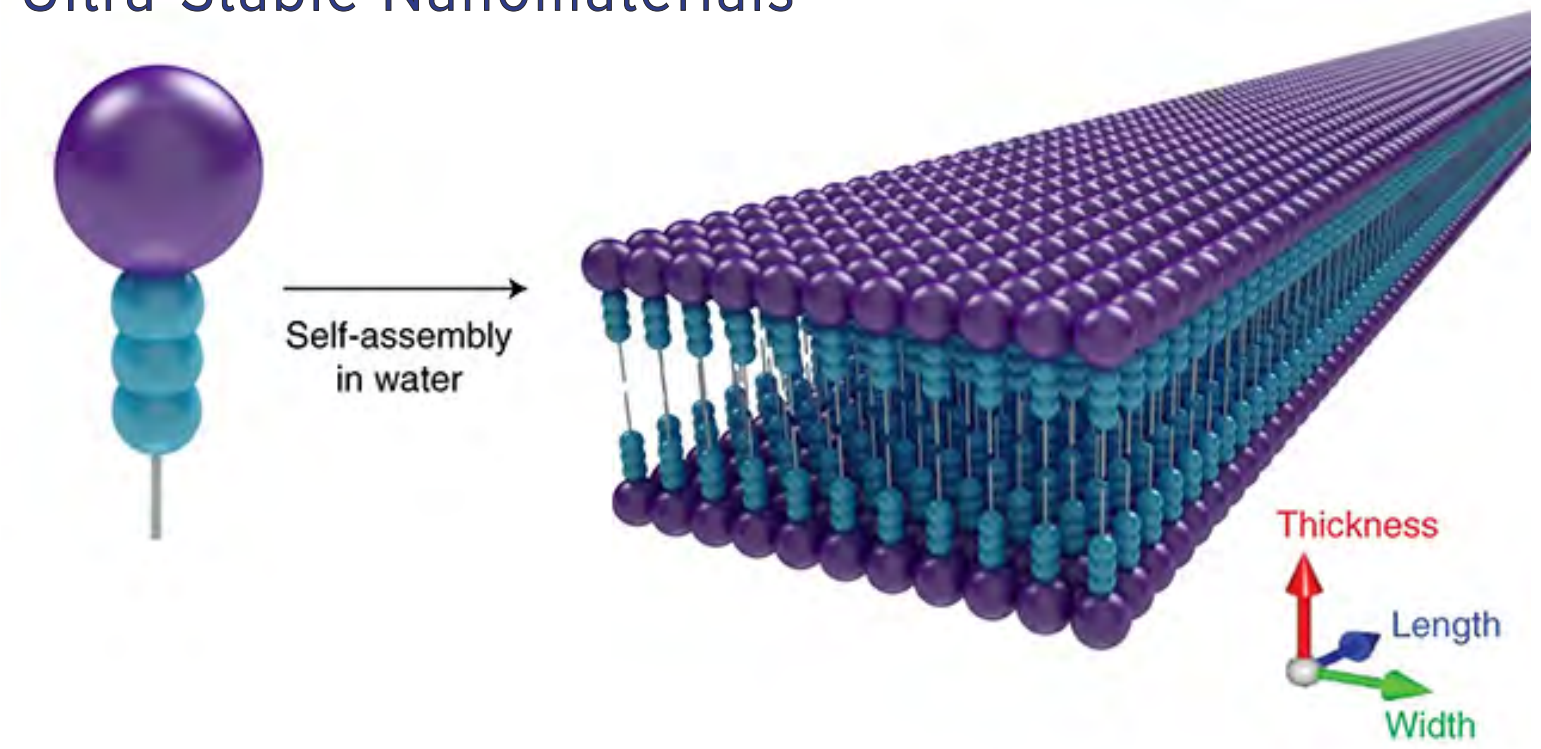

Fig. 1. Aramid amphiphiles are designed to spontaneously self-assemble in water into nanoribbons with suppressed exchange dynamics. Image: Peter Allen. From T. Christoff-Tempesta et al., Nat. Nano. **16**, 447 (April 2021). © 2021 Springer Nature Limited

Stronger than steel and flexible to boot, Kevlar® is a prized material that can withstand bullets while maintaining the flexibility to be shaped into tires or stretched into racing sails. On a molecular level, the key to Kevlar's® strength and flexibility is a collective hydrogen-bonding network formed by aromatic amides, commonly referred to as aramids. With Kevlar® as inspiration, researchers developed an lightweight but very strong heat-resistant synthetic aromatic polyamide material, or aramid, amphiphile (a chemical compound possessing both hydrophilic or water-loving, polar, and lipophilic [fat-loving] properties, that self-assembles into nanoribbons. The nanoribbons can be bundled together to create macroscale threads that can support 200 times their weight while maintaining a high degree of bendability. Synchrotron x-ray research techniques coupled to ultra-bright x-rays from the APS showed the threads to be highly organized on a molecular level, with tight regular packing, long-range hierarchical order, and extended hydrogen bonding networks. These threads could form the foundation for soft materials that conduct ions or thermal energy in electronics, optics, medicine, and architecture. These results were published in the journal *Nature Nanotechnology*.

Scientists have previously created a bunch of small amphiphilic molecules that spontaneously self-assemble in water to create ordered nanoscale structures with interesting properties. However, these structures tend to be fragile because the molecular interactions holding them together are typically weak. Furthermore, they exhibit dynamic instabilities, as the molecules within migrate, exchange, rearrange, swap, or insert with each other or other molecules in solution. Water is another problem, contributing to degradation through hydrolytic or enzymatic means. Yet many of these nanomaterials can't exist outside an aqueous environment as their structural stability stems from the hydrophobic effect.

To build a stronger nanomaterial that is stable in air, researchers in this study from the Massachusetts Institute of Technology and CNRS (France) designed a motif that incorporates aramids as a structural domain within small-molecule amphiphiles. In water, these aramid amphiphiles (Fig. 1) spontaneously form nanoribbons that have amides buried in the interior of the ribbon and charged head groups on the exterior of the ribbon. These structures boast six hydrogen bonds per molecule, pi-pi stacking,

and an overall organization that supports shorter, stronger hydrogen bonding.

One desirable trait of nanomaterials is their tunability; surface chemistries can be tweaked to fit a given application. In this study, the researchers generated aramid amphiphiles with three different head group chemistries: anionic (negatively charged), cationic (positively charged), and zwitterionic (containing both negative and positive charges). All three assembled into lamellar bilayers, according to small-angle x-ray scattering and wide-angle x-ray scattering profiles collected from an authors' lab-source machine and higher resolution profiles collected at the XSD Chemical & Materials Science Group's beamline 12-ID-B at the APS. The researchers also collected atomic force microscopy, transmission electron microscopy, and other structural data to determine that the nanoribbons range in width from 5.1 to 5.8 nanometers--depending on the headgroup–a thickness of 3.9 nanometers, and lengths up to 20 micrometers.

To assess the mechanical properties of the nanoribbons, the researchers used statistical topographical analysis of atomic force microscopy images. This provided a measure of the Young's modulus, which reports on how easy it is to stretch and deform a material, calculated to be 1.7 GPa. To assess strength, the researchers performed a statistical analysis of atomic force microscopy profiles after horn-sonication-induced scission. This approach generates microscopic bubbles which fragment the nanoribbons when they collapse; a careful analysis of the characteristic size of the resulting fragments revealed a tensile strength of 1.9 GPa.

The next step was to see if they could generate larger, macroscopic threads that could potentially be manipulated by hand and analyzed using conventional macroscale mechanical property testing methods. The researchers annealed cationic nanoribbons together in water and pulled them through a salt solution to produce gels of aligned nanoribbons, as confirmed by birefringence data. They then demonstrated the unique capacity of these nanomaterials to withstand air drying, creating a dry thread that can be handled and bent like a piece of wire. Thread diameters reached 20 micrometers and had Young's moduli ranging from 400 to 600 megapascals. These threads represent among the first strategies for creating self-assembled nanomaterials that can work outside of liquids, in the solid-state. – Erika Gebel Berg

See: Ty Christoff-Tempesta[1], Yukio Cho[1], Dae-Yoon Kim[1‡], Michela Geri[1], Guillaume Lamour[2], Andrew J. Lew[1], Xiaobing Zuo[3], William R. Lindemann[1] and Julia H. Ortony[1*], "Self-assembly of aramid amphiphiles into ultra-stable nanoribbons and aligned nanoribbon threads," Nat. Nano. **16**, 447 (April 2021). DOI: 10.1038/s41565-020-00840-w
Author affiliations: [1]Massachusetts Institute of Technology, [2]CNRS, [3]Argonne National Laboratory ‡Present address: Korea Institute of Science and Technology
Correspondence: * ortony@mit.edu

This material is based upon work supported by the National Science Foundation (NSF) under grant no. CHE-1945500. This work was supported in part by the Professor Amar G. Bose Research Grant Program, the Abdul Latif Jameel Water and Food Systems Lab, and the MIT Center for Environmental Health Sciences under National Institutes of Health Center grant P30-ES002109. D.-Y.K. acknowledges the support of the National Research Foundation of Korea's Basic Science Research Program and Chonbuk National University Fellowship Program. T.C.-T. and W.R.L. acknowledge the support of the NSF Graduate Research Fellowship Program under grant no. 1122374. T.C.-T. acknowledges the support of the Martin Family Society of Fellows for Sustainability. G.L. acknowledges support from the Université d'Evry-Paris Saclay. This work made use of the MRSEC Shared Experimental Facilities at MIT supported by the NSF under award number DMR-14-19807 and the MIT Department of Chemistry Instrumentation Facility. This work was performed in part at the Harvard University Center for Nanoscale Systems cryo-TEM facility, a member of the National Nanotechnology Coordinated Infrastructure Network, which is supported by the NSF under award no. 1541959. This research used resources of the Advanced Photon Source, a U.S. Department of Energy (DOE) Office of Science user facility operated for the DOE Office of Science by Argonne National Laboratory under Contract No. DE-AC02-06CH11357.

Revealing Fundamental Details Surrounding Nanoparticle Self-Assembly

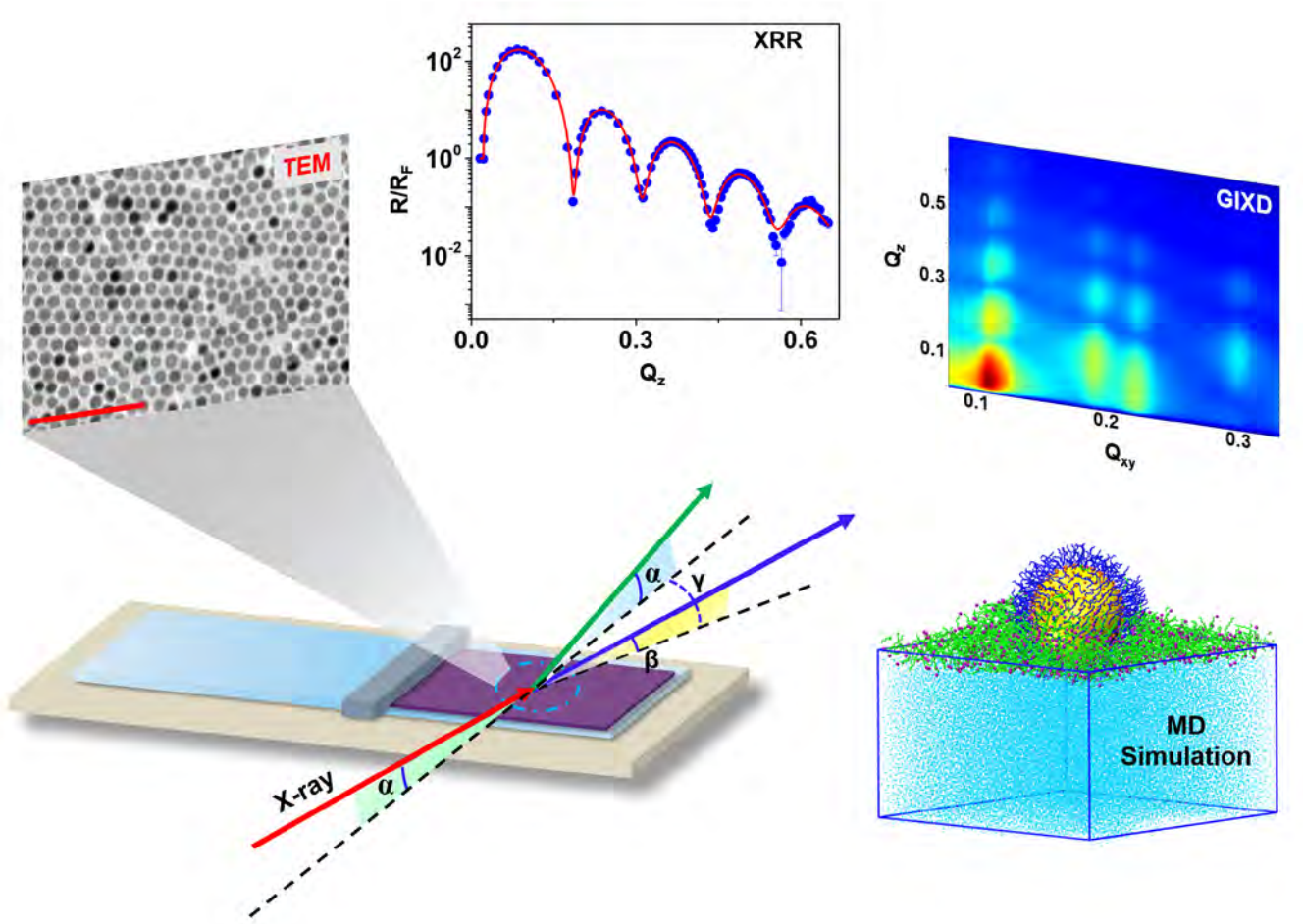

Fig. 1. Schematic of experimental geometry for *in situ* x-ray measurements of a monolayer array of nanoparticles supported on water surface. X-rays shine onto a macroscopically large water surface to reveal the nanoscale ordering of nanoparticles and ligands. X-ray reflectivity (XRR) measures the electron density profile along the interfacial depth of the entire interfacial structure, which includes the effects of both ordered and disordered regions of nanoparticles and free thiols.

Nanoparticle self-assembly is a contemporary field that shows considerable promise in various sectors, including electronics and medicine. By definition, a nanoparticle has a size in the range of 1 to 100 nanometers. Because of their small size, nanoscale particles can adopt unique properties that make them well-suited for a particular application. One potential application is the construction of liquid surfaces with tunable properties. In order for self-assembly and surface ordering to occur, ligands (ions or molecules attached to a metal atom by coordinate bonding) must be provided to coat the surface of a nanoparticle core. Presently, very little is known about how ligands organize around a core and influence self-assembly. To learn more about this exciting field, researchers investigated how sulfur-containing thiol ligands interact with monolayers of water-supported gold-core nanoparticles. Using high-brightness x-rays at the APS as well as molecular dynamics simulations, the research team found that free thiols coat the core in a near-symmetrical fashion. These results, published in the journal Nano Letters, empower our collective understanding of nanoparticle self-assembly and may significantly impact how such assemblies are prepared for important societal applications.

In contrast to their larger material counterparts, nanoparticles possess a large ratio of surface area to volume. This enables them to harness desirable physical and chemical properties, which makes them quite appealing for a variety of industries, including drug delivery, imaging, and electronics. For example, nanoparticle-based drug delivery is appealing because nanoparticles can be designed to exhibit a high stability, have a large carrying capacity, can be conducive to different routes of administration, and possess specificity for target sites. Much research is currently under way in the sub-fields of nanomedicine and nano-delivery systems to treat cancer and enhance vaccine delivery. For example, the recently FDA-approved vaccine for SARS-CoV-2 generated by Pfizer (see page 104) utilizes lipid nanoparticles.

One potential application of nanoparticles is the generation of novel liquid surfaces with tunable properties. For this to occur, ligands must be provided to coat the surface of a nanoparticle's core. This coating impacts how a nanoparticle interfaces with a liquid surface and dictates how a nanoparticle self-assembles and orders itself. Historically, most research in the field has worked on designing ligands to induce a specific type of interaction or to encourage assembly toward a certain higher-order structure. In contrast, very little work has been done to understand how ligands organize on a core and how this organization impacts nanoparticle self-assembly and interactions.

The current research has helped to overcome this gap in knowledge. The researchers chose to study thiol ligands, which are organosulfur compounds containing the chemical group R-SH, in conjunction with monolayers of gold-core nanoparticles supported by water. They employed x-ray scattering at the ChemMatCARS 15-ID x-ray beamline at the APS together with molecular dynamics simulations to investigate how these thiol ligands interact with and affect the metallic core of these nanoparticles (Fig. 1). The team discovered that free thiols thoroughly coat the gold core in a near-symmetrical fashion. Once core-ligand coverage exceeds a threshold value, the nanoparticle's core rises above the water surface. The edge-to-edge distance increases in value, which means that the nanoparticles become more spaced apart. Consequently, the total nanoparticle coverage of the liquid surface is diminished.

In summary, this work demonstrates that free thiols not only regulate ligand organization on a nanoparticle's core, but they also influence how a nanoparticle interacts with its surroundings. By filling a key knowledge gap in the field of nanoparticle self-assembly, this essential research enhances our collective ability to construct nanoparticle materials. Given the relevance of nanoparticles to medicine, electronics, and other important industries, these discoveries could be flexibly utilized to help improve various aspects of society. – Alicia Surrao

See: Pan Sun, Linsey M. Nowack, Wei Bu, Mrinal K. Bera, Sean Griesemer, Morgan Reik, Joshua Portner, Stuart A. Rice, Mark L. Schlossman, and Binhua Lin*, "Free Thiols Regulate the Interactions and Self-Assembly of Thiol-Passivated Metal Nanoparticles," Nano Lett. **21**(4), 1613 (2021). DOI: 10.1021/acs.nanolett.0c04147
Author affiliation: The University of Chicago
Correspondence: * lin@cars.uchicago.edu

This research is supported by ChemMatCARS. ChemMatCARS is funded by the Divisions of Chemistry (CHE) and Materials Research (DMR), National Science Foundation, under grant number NSF/CHE-1834750. We also acknowledge support from The University of Chicago MRSEC NSF/DMR-1420709 for B.L. and S.A.R., and NSF/DMR-2011854 for J.P. This research used resources of the Advanced Photon Source, a U.S. Department of Energy (DOE) Office of Science user facility operated for the DOE Office of Science by Argonne National Laboratory under Contract No. DE-AC02-06CH11357.

Proteins of a Feather Come Together to Create Color

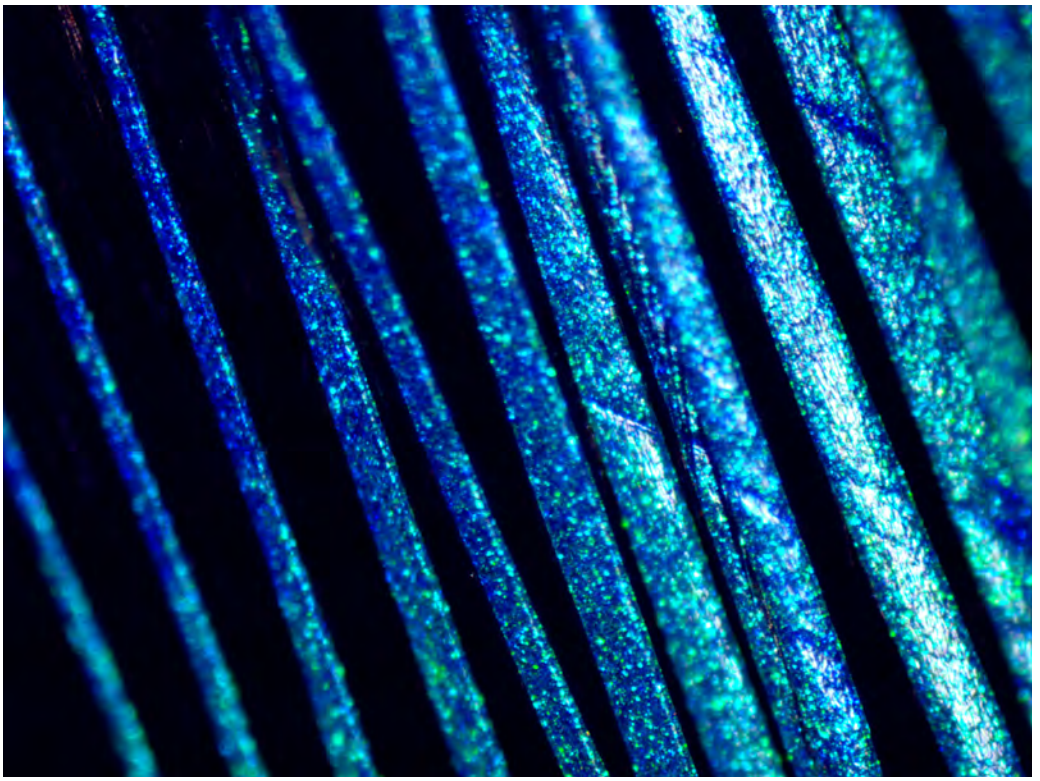

Fig. 1. The bright blue and green colors in the feather of a blue-winged leafbird, visible in a light microscope image at 4x magnification (this page), arise from the single gyroid crystal structure, seen in an SEM image (next page). Images: Vinodkumar Saranathan

Biologists would like to understand how and why birds are brightly colored. Some materials scientists, meanwhile, look to nature to find better ways to recreate such colors. A study conducted using the APS and published in the *Proceedings of the National Academy of Sciences of the United States of America* points to possible answers to both those questions. This discovery represents the first directly self-assembled single gyroid crystals known to science. The researchers say the results are not only unexpected, but also happen to be highly relevant to current challenges in the engineering of complex nanostructures for advanced applications, potentially opening new photonic technologies.

The bird in this case is the blue-winged leafbird (*Chloropsis cochinchinensis*), a brightly colored species found only in Asia. Like many animals, the color comes not from pigments, but from an ordered crystal structure in the leafbird's feathers, which is quite unusual for birds. These photonic crystals, consisting of the structural protein beta-keratin and air, are arranged in a shape known as a single gyroid and of a size scale—roughly 300 nanometers—that they interact with wavelengths of visible and ultraviolet light. The interfaces between air and protein form a repeating series of changes in refractive index, leading to the feathers' colors.

Single gyroid crystals are rare. The same researchers discovered the first one in biology in 2010 within the iridescent green scales of certain butterflies, also using the APS, and now in the feathers of only one of 10,000 bird species. The researchers say these crystals are unusual given the way birds normally grow their feather nanostructures. This process seems to resemble the way foam forms in beer, when dissolved carbon dioxide forms bubbles that push their way to the surface. In the case of the feathers, water and beta-keratin undergo phase separation to form the single gyroid, and once the water evaporates the structure of air and protein is left behind.

This is very different from the way butterflies or engi-

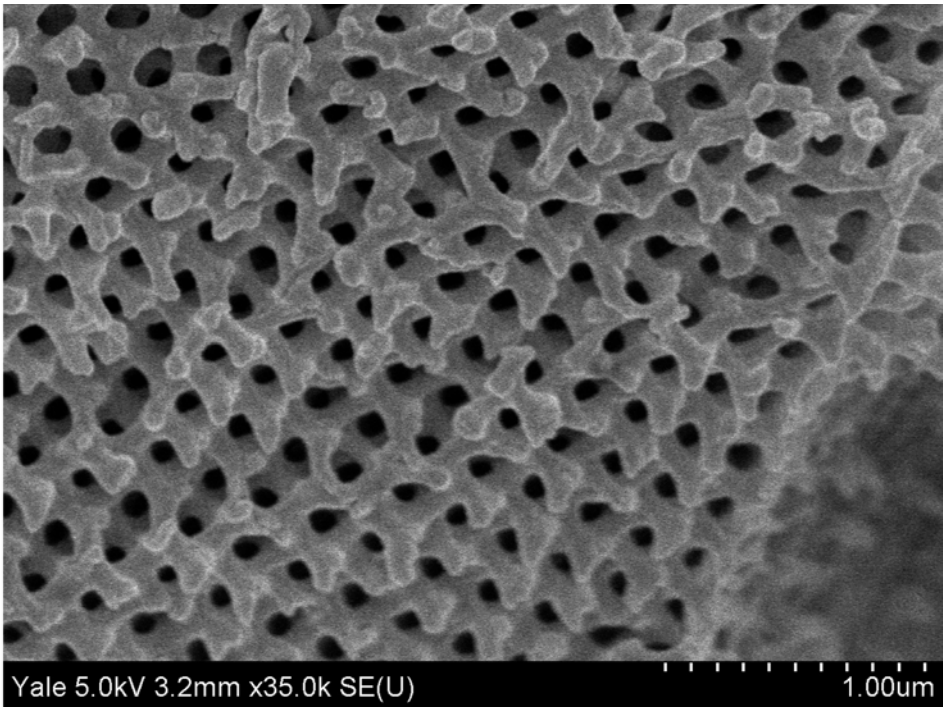

neers create single-gyroid crystals. Engineers can make larger crystals, then apply heat to shrink them to a size where they work with wavelengths of visible light, but it's difficult to do that at useful volumes, and the process can lead to defects. Taking a cue from the birds, humans might develop a process that relies on self-assembly to create the crystals. Those could then be used to improve the efficiency of photovoltaic cells, optical fibers, or catalysts.

To study the evolution of the nanostructures, the researchers compared them to nanostructures in related species of birds. They found that the ordered single gyroid structure evolved from a quasi-ordered state. The more ordered versions produce more saturated or purer hues that the birds can easily perceive. That suggests that the evolution of these structures was driven by sexual selection, where birds with more brilliant coloration were seen as more desirable mates.

To reveal the crystalline structure, the scientists performed synchrotron small-angle x-ray scattering (SAXS) at the XSD Dynamics & Structure Group's beamline 8-ID-I at the APS. They performed pinhole SAXS experiments using beams measuring either 10 x 10 µm or 15 x 15 µm, which allowed them to focus on just a small number of barb cells on the inside of the feathers. They probed cells from the feathers of 10 to 15 species of the leafbird, and from two related species, the fairy bluebird. They also imaged the feathers with a scanning electron microscope and combined the data from the studies so they could see both the short-range order and intermediate structures in the feathers. – Neil Savage

See: Vinodkumar Saranathan[1,2]*, Suresh Narayanan[3], Alec Sandy[3], Eric R. Dufresne[4], and Richard O. Prum[2], "Evolution of single gyroid photonic crystals in bird feathers," Proc. Natl. Acad. Sci. U.S.A. **118**(23), e2101357118 (2021). DOI: 10.1073/pnas.2101357118

Author affiliations: [1]National University of Singapore, [2]Yale University, [3]Argonne National Laboratory, [4]ETH Zürich

Correspondence:

* vinodkumar.saranathan@aya.yale.edu

The authors acknowledge support from a Singapore National Research Foundation Award (CRP20-2017-0004), Yale-NUS startup Grant (R-607-265-241-121), Royal Society Newton Fellowship ATRTLO0 (to V.S.), and Yale University W. R. Coe Funds (to R.O.P.). This research used resources of the Advanced Photon Source, a U.S. Department of Energy (DOE) Office of Science user facility operated for the DOE Office of Science by Argonne National Laboratory under Contract No. DE-AC02-06CH11357.

See also: "Blue Animals Are Different From All the Rest," "APS/User News" 6.22.21, *The Atlantic*, and *Quanta*.

Better-Educated Neural Networks for Nanoscale 3-D Coherent X-ray Imaging

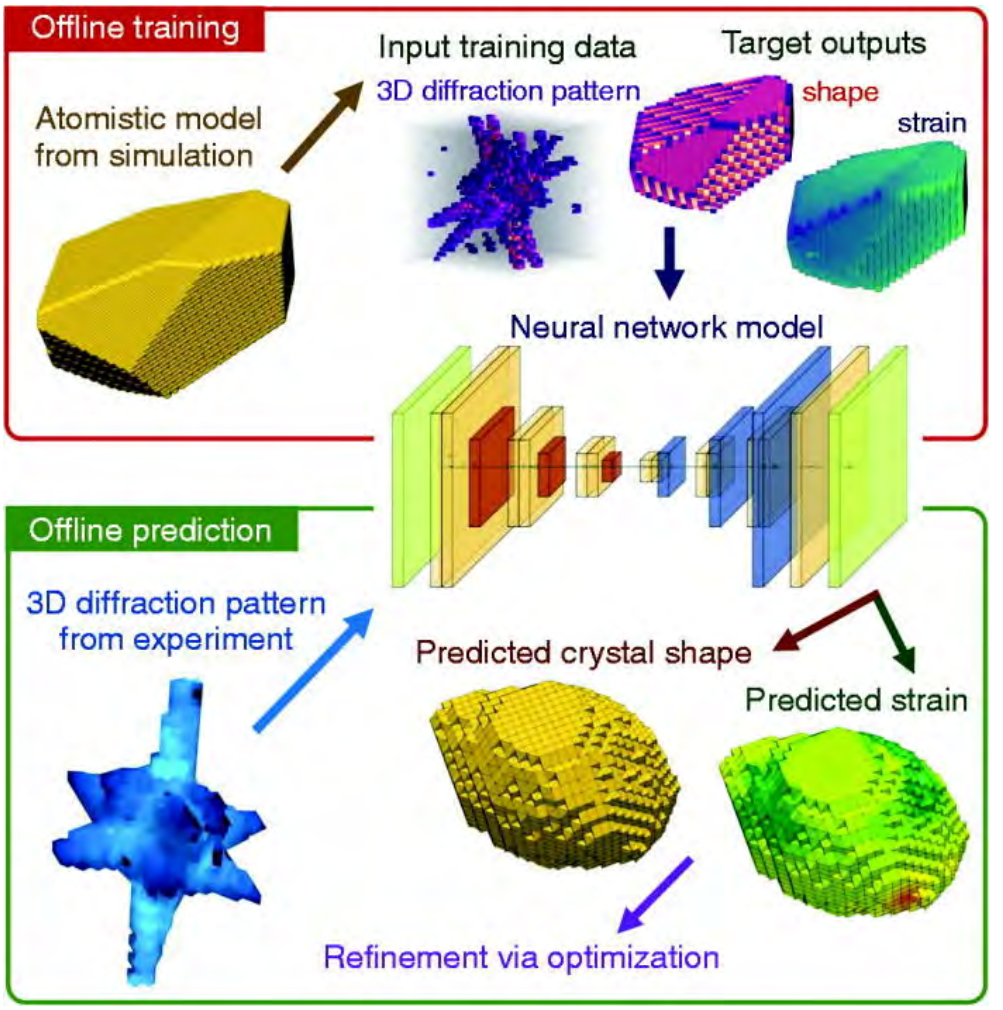

Fig. 1. Schematic of physics-aware framework for phase retrieval in 3-D coherent diffraction imaging. The main component of the framework is a neural network model (3D-CDI-NN) that is trained offline using 3-D data (simulated diffraction pattern, crystal shape, and local strain) derived from atomistic simulations that capture physics of the material. Once trained, the 3D-CDI-NN model can perform real-time prediction of crystal shape and local strain from experimentally measured diffraction pattern. The prediction can then be refined using a gradient-based optimization procedure. From H. Chan et al., Appl. Phys. Rev. **8**, 021407 (2021). ©2021 Author(s). Published under an exclusive license by AIP Publishing.

One of the inescapable realities of various imaging techniques is called the "phase problem," which simply refers to the loss of phase information inherent in the nature of imaging methods such as x-ray diffraction. Though it might be inconvenient, it can be dealt with by using various mathematical methods to retrieve the phase data from the image with inverse computation. Such methods, however, are not only time-consuming but require a great deal of computer power as they must run through multiple iterations to converge on a solution, which prevents real-time imaging. A group of researchers working at the APS has demonstrated a new approach to this perennial obstacle by using a deep-learning neural network trained and optimized for enhanced accuracy to perform fast three-dimensional (3-D) nanoscale imaging from coherent x-ray data. The work was published in *Applied Physics Review.*

Neural networks, which simulate the operation of the brain's intricate networks of nerve cells for applications

such as artificial intelligence, have been criticized because it can be difficult to adequately 'train' them for the task at hand. If the training data or methodology are insufficient, the neural network will fail to perform as desired; as the computer programmer's cliché goes, garbage in, garbage out. They may also be influenced by subtle biases in the data or may be unable to extrapolate and generalize beyond the limits of their training.

In the present work, the investigators from Argonne National Laboratory, the University of Illinois at Chicago, Stats Perform, and Northwestern University confronted this problem by using explicitly "physics-aware" training that incorporates atomistic simulation data to create diverse training sets based on the physics of the material under study (Fig. 1). The neural network predictions are then further refined in the final stage. The research team validated this 3-D convolutional encoder-decoder network (3D-CDI-NN) on 3-D coherent x-ray diffraction data of gold nanoparticles performed at the XSD Microscopy Group's 34-ID-C x-ray beamline at the APS.

The 3D-CDI-NN model begins with an offline training stage in which polyhedral shapes are created by randomly clipping an FCC crystal lattice structure, applying and relaxing various stresses in the Large-scale Atomic/Molecular Massively Parallel Simulator (LAMMPS) molecular dynamics program, and voxelizing the data into a 32 x 32 x 32 voxel grid. The grid is then entered into 3D-CDI-NN and its predictions matched with the known solutions. The 3D-CDI-NN framework is quite accurate in its predictions, even when working with under-sampled diffraction patterns.

To enhance the accuracy of 3D-CDI-NN even further, the investigators added a refinement that uses a reverse-mode automatic differentiation (AD) technique on the strain predictions and diffraction data. This proved especially effective in recovering details of structural strain within the examined crystal samples, even when not using oversampled data, as is generally done when using AD techniques.

The team demonstrated the effectiveness of the trained 3D-CDI-NN model with real-world data by imaging gold nanoparticles. Although initial predictions showed some underestimation of surface details and local strain, perhaps due to downsampling of the coherent x-ray data to the 32 x 32 x 32 size, these details were recovered after the AD refinement procedure. The 3D-CDI-NN framework was demonstrated to be ~4 times faster compared to typical iterative phase retrieval methods.

As fourth-generation synchrotron x-ray sources like the upgraded APS come online in the near future, with ever brighter and more versatile beams and capable of generating extremely large datasets, faster and more efficient phase retrieval techniques will be essential. The research team notes that machine-learning neural network approaches such as 3D-CDI-NN can be trained and improved to surpass traditional phase retrieval techniques by hundreds of times in speed while placing far lesser demands on scarce computing resources. Such automated methods can also be effectively scaled to different requirements and can even operate on datasets as they are still being collected.

Perhaps the phase problem can never be eliminated completely, but neural networks may make it easier to live with. – Mark Wolverton

See: Henry Chan[1,2]*, Youssef S.G. Nashed[3], Saugat Kandel[4], Stephan O. Hruszkewycz[1], Subramanian K.R.S. Sankaranarayanan[1,2], Ross J. Harder[1], and Mathew J. Cherukara[1]**, "Rapid 3D Nanoscale Coherent Imaging via Physics-aware Deep Learning," Appl. Phys. Rev. **8**, 021407 (2021). DOI: 10.1063/5.0031486

Author affiliations: [1]Argonne National Laboratory, [2]University of Illinois at Chicago, [3]Stats Perform, [4]Northwestern University

Correspondence: * hchan@anl.gov,
** mcherukara@anl.gov

The authors gratefully acknowledge the computing resources provided and operated by the Joint Laboratory for System Evaluation (JLSE) at Argonne. This work was performed at the Center for Nanoscale Materials and the APS, both Office of Science user facilities supported by the U.S. Department of (DOE) Office of Science-Basic Energy Sciences, under Contract No. DE-AC02- 06CH11357. This work was also supported by Argonne LDRD 2018-019-N0: A.I C.D.I: Atomistically Informed Coherent Diffraction Imaging, and by the U.S. DOE Office of Science-Basic Energy Sciences Data, Artificial Intelligence and Machine Learning at DOE Scientific User Facilities program under Award Number 34532. Development of the automatic differentiation refinement was supported by the U.S. DOE Office of Science-Basic Energy Sciences, Materials Science and Engineering Division. An award of computer time was provided by the Innovative and Novel Computational Impact on Theory and Experiment (INCITE) program.

Breaking the 10-nanometer Barrier with X-ray Nanotomography

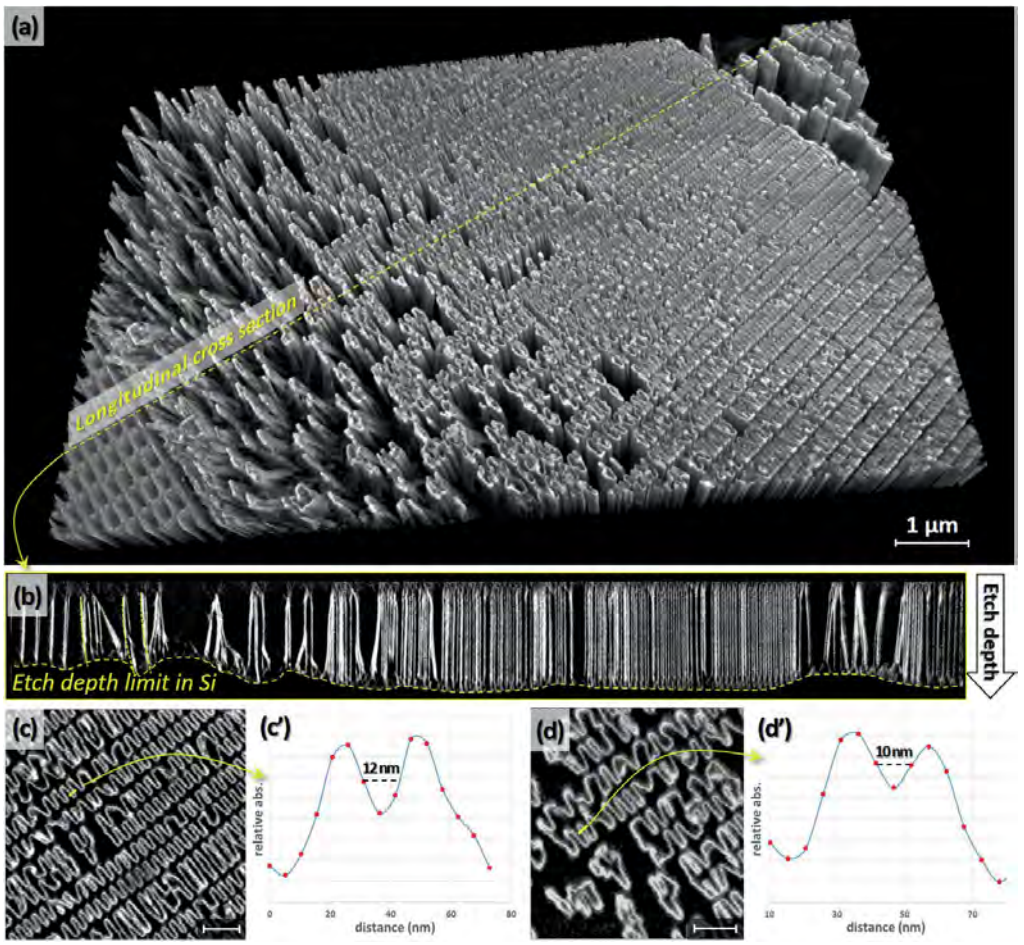

Fig. 1. Three-dimensional characterization of a defective 16-nm ΔrN FZP. a) Volume rendering with the Dragonfly ORS software of the outermost part of a 1-µm-thick FZP where most of damages are seen. b) Longitudinal cross section highlighting large variations in the etch profile, collapsed walls, and large portions of missing zones. c,d) Zoom on selected reconstructed slices showing disorganization of walls geometry. Scale bars correspond to 250 nanometers. c',d') Short profiles showing that 10-nanometers spacing between objects can be resolved. From V. De Andrade et al., Adv. Mater. **33** (21), 2008653 (May 27, 2021).

Many important things exist at very tiny scales, from neurons to the transistors on computer chips. To understand them, researchers want to be able to look at them in detail. X-ray nanotomography allows scientists to image small objects in three dimensions, but the resolution of the technique had been limited to approximately 30 nanometers, not small enough for many significant features. Now researchers using the APS have achieved nanotomography with resolution below 10 nanometers. Their results were published in the journal *Advanced Materials*.

To do that, the researchers built a transmission x-ray microscope at XSD Imaging Group's beamline 32-ID at the APS. The microscope includes a condenser to illuminate the sample with x-rays. The x-rays pass through the sample and then through a Fresnel zone plate (FZP) with an outermost zone width of 16 nanometers, which acts as an

objective lens, and then onto a detector. A rotary stage spins the sample so the x-rays strike it at different angles, necessary for computed tomography to reconstruct a three-dimensional image. The sample stack and FZP module were made extremely stiff to reduce vibrations that could blur the reconstructed images. The team confirmed that with an x-ray energy in the range of 8 kV to 9 kV, the FZP has achieved a resolution of 9.8 nanometers.

Measuring the object for a longer time to get more signal can bring the image closer to maximum theoretical resolution. Previous experiments had achieved resolution below 20 nanometers with more than 24 hours of sampling. It is impractical to tie up expensive equipment for days to acquire one dataset. In this case, the researchers achieved spatial resolution below 10 nanometers in just 85 minutes (Fig. 1).

Another problem that gets worse with long sampling times is drift. Either the sample or the optics can move, due to a change in temperature or shifts in the rotary stage, introducing blur and reducing the resolution. At these extremely small scales, even the impact of x-ray radiation can cause the sample to deform, further decreasing image quality. Along with the mechanical improvements, researchers developed algorithms to measure and compensate for those deformations, sharpening the picture [1].

To test their system, the researchers applied their techniques to examine an FZP for nanoscale defects introduced by the metal-assisted chemical etching process used in producing the optic. The etching process can go several micrometers deep and produce defects that cannot be found using a scanning electron microscope unless the FZP is cut open, thus destroying it. With nanotomography, the researchers were able to see areas where the etching pattern deviated from the intended pattern, and where thin walls had collapsed.

The team also examined thin films of titanium niobium oxide that are used as cathodes in electrochemical storage. The material was characterized with a resolution of 20 nanometers, so they could image three-dimensional voxels with 16 times larger volumes than those used for the FZP. That leads to a similar signal-to-noise ratio with a lower dose of x-rays, so the researchers were able to acquire two datasets in 10 and 20 minutes, respectively. The imaging allowed them to compare thin films created by atomic layer deposition to those created by sputtering deposition and see how the thickness of film layers differed between the two methods.

The scientists say there is still room for improvement in nanotomography. For instance, they're working on ways to build x-ray objective lenses that are even more efficient than the one they designed. The APS is undergoing an upgrade that will increase the brightness of its x-rays up to 500 times. A brighter source could increase the speed of data acquisition by at least an order of magnitude.

– Neil Savage

Reference

[1] V. Nikitin et al., "Distributed Optimization for Nonrigid Nano-Tomography," IEEE T Computational Imaging **7**, 272 (2021). DOI: 10.1109/TCI.2021.3060915

See: Vincent De Andrade[1‡]* Viktor Nikitin[1], Michael Wojcik[1], Alex Deriy[1], Sunil Bean[1], Deming Shu[1], Tim Mooney[1], Kevin Peterson[1], Prabhat Kc[1‡‡], Kenan Li[2,3], Sajid Ali[2], Kamel Fezzaa[1], Doga Gürsoy[1], Cassandra Arico[4,5,6], Saliha Ouendi[4,6], David Troadec[4,6], Patrice Simon[5,6], Francesco De Carlo[1], and Christophe Lethien[46], "Fast X-ray Nanotomography with Sub-10 nm Resolution as a Powerful Imaging Tool for Nanotechnology and Energy Storage Applications," Adv. Mater. **33** (21), 2008653 (May 27, 2021).
DOI: 10.1002/adma.202008653
Author affiliations: [1]Argonne National Laboratory, [2]Northwestern University, [3]SLAC National Accelerator Laboratory, [4]Universite Polytechnique des Hauts de France, [5]Universite Paul Sabatier, [6]Reseau sur le Stockage Electrochimique de l'Energie Present addresses: [‡]Sigray, Inc., [‡‡]The Food and Drug Administration
Correspondence: * vdeandrad@gmail.com

This research benefited from the financial support of the ANR within the MINOTORES project (ANR-16-CE24-0012-01). The French Renatech network is greatly acknowledged for the microfabrication facilities. The authors also want to thank the French network on electrochemical energy storage (RS2E) and the STORE-EX ANR project for the support. This research used resources of the Advanced Photon Source and the Center for Nanoscale Materials, U.S. Department of Energy (DOE) Office of Science user facilities operated for the DOE Office of Science by Argonne National Laboratory under Contract No. DE-AC02- 06CH11357.

Saphire Appointed President and CEO of LJI

Erica Ollmann Saphire was appointed President and CEO of La Jolla Institute for Immunology. She is co-author on 22 peer-reviewed journal articles based on her research at the APS, which has centered on the study of viruses, particularly the Ebola virus. Her research has been carried out at several APS beamlines including those operated by GM/CA-XSD, SBC-XSD, LS-CAT, and NE-CAT.

Williams Wins SER-CAT Outstanding Science Award

Scott Williams, deputy chief of the National Institute of Environmental Health Sciences Genome Integrity and Structural Biology Laboratory, received the Outstanding Science Award from SER-CAT, which operates a macomolecular x-ray crystallography facility at the APS. Williams aims to understand how DNA repair mechanisms can be used to treat diseases like cancer. He studies how the body recognizes when DNA is damaged after environmental exposures, and how it is repaired, and how mutations affect proteins that protect genome stability, in syndromes that predispose some people to cancer or neurological disease.

Kasman of XSD Selected for Next Generation of Leaders

Elina Kasman (XSD Optics Group) was selected by the Argonne Physical Sciences and Engineering (PSE) directorate to participate in the second cohort of PSE Next Generation of Leaders (NextGen Leaders). This cohort includes two focus areas: Quantum Information Science and Science Innovations for a Circular Economy. The goal of PSE NextGen Leaders is to provide leaders with the tools and skills needed to coordinate research activities across the Lab's multidisciplinary directorates and to build strategic programs. The program provides early- to mid-career staff across the Laboratory with opportunities to develop themselves and grow new strategic research directions that will result in innovations impacting future technologies and the nation. Kasman, an x-ray optics fabrication engineer, is concentrating her program development efforts on Science Innovations for a Circular Economy, first under Cynthia Jenks and now under Amanda Petford-Long, director of the Argonne Materials Science Division.

Streiffer Earns Secretary of Energy's Honor Award

Stephen Streiffer, Argonne deputy laboratory director for Science and Technology and formerly associate laboratory director for Photon Sciences and director of the APS, was among two groups of seven Argonne scientists given DOE 2020 Secretary of Energy's Honor Awards for battling the COVID-19 pandemic. Streiffer and Ilke Arslan, director of the Center for Nanoscale Materials (CNM) and the Nanoscience and Technology Division; Andrzej Joachimiak, director of the Structural Biology Center at the APS and co-director of the Center for Structural Genomics of Infectious Diseases; Charles "Chick" Macal, chief scientist for the Argonne Resilient Infrastructure Initiative; and Rick Stevens, associate laboratory director for the Computing, Environment and Life Sciences Directorate were recognized as part of the National Virtual Biotechnology Laboratory Team, which received a Secretary of Energy's Achievement Award, for its pivotal role in supporting the national response to COVID-19. The work was completed, in part, through three Argonne DOE Office of Science user facilities: the Advanced Leadership Computing Facility, the APS, and the CNM.

Godbold Uses DOE Award to Understand Green Tech at the Atomic Level

Perrin Godbold, a doctoral student in chemistry, nanomaterials, and electrocatalysis at the University of Virginia, received a DOE Science Graduate Student Research Award to work at the APS. The awardees work on research projects that are of significant importance to the Office of Science's mission and that address societal challenges at a national and international scale. The award provides Godbold wth an opportunity to learn *in situ* x-ray absorption spectroscopy and surface scattering, allowing him to gain an atomic and chemical picture of how nanocatalysts form and work. He chose his subfield because he is fascinated by nano-catalysis and its application to green energy and industry.

Novel Accelerator and X-ray Techniques and Instrumentation

Tiny, Chip-Based Device Performs Ultrafast Manipulation of X-Rays

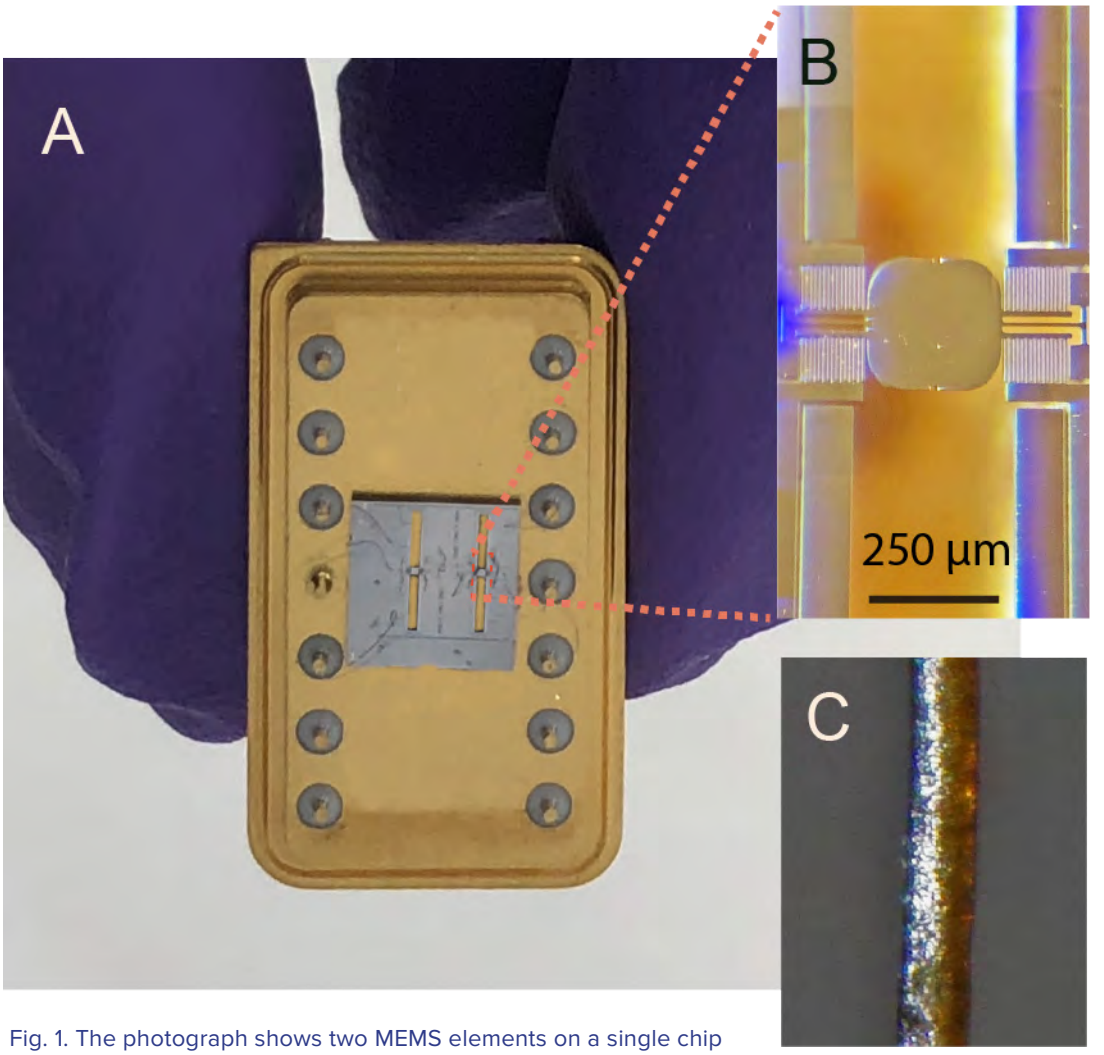

Fig. 1. The photograph shows two MEMS elements on a single chip (A), with the active elements of 250 µm × 250 µm, and the micrograph (B) highlighting the size of the diffractive element, as compared to a section of human hair (C).]

The original Optical Society press release can be read here.

Researchers from the APS and the Argonne Center for Nanoscale Materials have developed and demonstrated new x-ray optics that can be used to harness extremely fast pulses in a package that is significantly smaller and lighter than conventional devices used to manipulate x-rays. The new optics are based on microscopic chip-based devices known as microelectromechanical systems (MEMS).

"Our new ultrafast optics-on-a-chip is poised to enable x-ray research and applications that could have a broad impact on understanding fast-evolving chemical, material and biological processes," said research team leader Jin Wang from the XSD Time Resolved Research (TRR) Group at the APS. "This could aid in the development of more efficient solar cells and batteries, advanced computer storage materials and devices, and more effective drugs for fighting diseases."

In new results published in The Optical Society OSA) journal *Optics Express*, the researchers demonstrated the new x-ray optics-on-a-chip device (Fig. 1), which measures about 250 micrometers and weighs just 3 micrograms, using the TRR Group's 7-ID-C x-ray beamline at the APS. The tiny device performed 100 to 1,000 times faster than conventional x-ray optics, which that tend to be bulky.

"Although we demonstrated the device in a large x-ray synchrotron facility, when fully developed, it could be used with conventional x-ray generators found in scientific labs or hospitals," said Wang. "The same technology could also be used to develop other devices such as precise dosage delivery systems for radiation therapy or fast x-ray scanners for non-destructive diagnostics."

X-rays can be used to capture very fast processes such as chemical reactions or the quickly changing dynamics of biological molecules. However, this requires an extremely high-speed camera with a fast shutter speed. Because many materials that are opaque to light are transparent to x-rays it can be difficult to improve the speed of shutters effective for x-rays.

To solve this challenge, the researcher team turned to MEMS-based devices. "In addition to being used in many of the electronics we use daily, MEMS are also used to manipulate light for high-speed communication," said Wang. "We wanted to find out if MEMS-based photonic devices can perform similar functions for x-rays as they do with visible or infrared light."

In the new work, the researchers show that the extremely small size and weight of their MEMS-based shutter allows it to oscillate at speeds equivalent to about one million revolutions per minute (rpm). The researchers leveraged this high speed and the MEMS material's x-ray diffractive property to create an extremely fast x-ray shutter.

"The x-ray diffraction angular range is extremely small, about one-thousandth of a degree. The fast-rotating device then creates the fast x-ray shutter," said Donald Walko, a member of the research team, also from the TRR group.

Using their new x-ray optics-on-a-chip developed at the Center for Nanoscale Materials, the researchers demonstrated that it provides a stable shutter speed as fast as one nanosecond with an extremely high on/off contrast. This is used to extract single x-ray pulses from the source, even if the 352-MHz pulses were only 2.84 nanoseconds apart from each other.

"We show that our new chip-based technology can perform functions not possible with conventional large macroscopic optics," said Wang. "This can be used to create ultrafast probes for studying fast processes in novel materials."

The researchers are now working to make the devices more versatile and robust so that they can be used continuously over long periods of time. They are also integrating the peripheral systems used with the tiny chip-based MEMS devices into a deployable stand-alone instrument.

See: Pice Chen, Woong Jung, Donald A. Walko, Zhilong Li, Ya Gao, Tim Mooney, Gopal K. Shenoy, Daniel Lopez, and Jin Wang*, "Optics-on-a-chip for ultrafast manipulation of 350-MHz hard x-ray pulses," Opt. Express **29**(9), 13624 (26 April 2021). DOI: 10.1364/OE.411023
Author affiliation: Argonne National Laboratory
Correspondence: * wangj@aps.anl.gov

This research is supported by the Accelerator and Detector Research (ADR) Program of the U.S. Department of Energy (DOE) Office of Sciences-Basic Energy Sciences. The use of the CNM and APS was supported by the U.S. DOE Office of Science-Basic Energy Sciences under Contract no. DE-AC02-06CH11357. Critical technical support of a fast APD from Michael Hu of the APS is gratefully acknowledged.

A New Method for Probing Material Strength

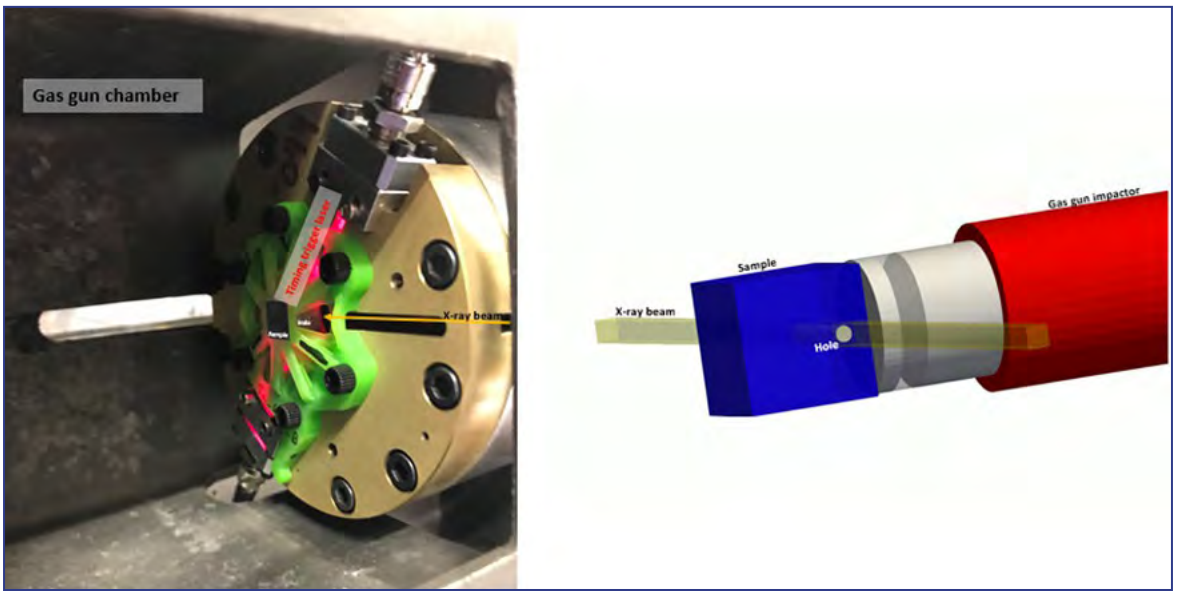

Fig. 1. Components used in the experiments at DCS alongside a schematic of the flyer plate geometry.

The original Lawrence Livermore National Laboratory article by Michael Padilla can be read here.

In an effort to better understand how materials deform under extreme conditions, researchers from the U.S. Department of Energy's (DOE's) Lawrence Livermore National Laboratory (LLNL) using the APS have developed a new experimental method for probing large-strain and high strain-rate material strength. In a paper published in *Acta Materialia*, Jonathan Lind, LLNL physicist and lead author, said results of the work aid in providing updated strength information that can be used in simulation codes.

"This study demonstrated that the method can observe differences in mechanical behavior due to the way a material was manufactured and processed prior to the experiment," Lind said. "The work provides updated strength model parameters that more reliably capture the high strain-rate, large plastic strain behavior of copper."

The researchers also observed that a material's prior processing history influences its high strain-rate behavior. With a demonstration of the efficacy of the approach, Lind and his colleagues are now planning and conducting experiments on five other materials.

Lind said the National Nuclear Security Administration (NNSA) mission needs require LLNL to understand materials under extreme conditions, including under combined large-strain and high strain-rate conditions that are challenging to access in well-controlled and diagnosed experiments. This mission is carried out through NNSA's Stockpile Stewardship Program, which utilizes materials research and physics modeling and simulation codes to accurately model nuclear weapons performance.

"Novel experiments that provide information on the behavior of materials under extreme environments allow for comparisons with existing models, comparisons across manufacturing processes, and direct observation of phenomenology not currently captured in models," he said.

Many models of large-strain mechanical response (strength) of materials have phenomenological aspects that are calibrated to the observed behavior of materials. These models are constrained in regimes where experimental data exists. Certainty/reliability/confidence in these models diminishes where models are unchecked, such as at high strain-rates and large plastic strains where data are currently lacking.

Lind and his team conducted the work by drilling a small hole into a chunk of material. Plate-impact was performed on the sample to subject it to a controlled mechanical impulse—the passage of a shock that produces

stresses in the material—while the hole is imaged over longer time scales than those in traditional one-dimensional plate impact experiments.

In the experiment setup (Fig. 1) at the DCS 35-ID beamline at the APS, high-speed parallel-beam x-ray phase contrast imaging was used to image the hole and to monitor its shape change.

"The experimental imaging data is directly compared with hydrocode simulations, and we can examine the predictions associated with various strength models," Lind said, adding that the discrepancy between experiment and calculations can be ascribed to inadequacies in the strength models and provide a path toward model modification to bring the models into better agreement.

Lind said this is a topic of ongoing investigation. "While one-dimensional experiments probing high-rate material behavior provide valuable data about material response, they are limited in the conditions that they can access," he said.

The research complements other work, such as the Rayleigh-Taylor instability strength platform that is now used at the National Ignition Facility and other facilities, to probe two-dimensional deformation conditions that can produce large strains.

"While this capability was demonstrated at the Dynamic Compression Sector, now that the concept has been demonstrated, it will be possible to field similar experiments at other facilities," Lind said. "This opens up the possibility to explore and test the behavior of other materials under these extreme conditions, enabling opportunities to collaborate with colleagues at the Department of Defense and academic institutions."

See: Jonathan Lind*, Matthew D. Nelms, Andrew K. Robinson, Mukul Kumar, and Nathan R. Barton, "Examining material constitutive response under dynamic compression and large plastic strains using *in situ* imaging of hole closure," Acta Mater. **206**, 116584 (2021).
DOI: 10.1016/j.actamat.2020.116584
Author affiliation: Lawrence Livermore National Laboratory
Correspondence: * lind9@llnl.gov

The authors thank the experimental support of the DCS staff including Paulo Rigg, Adam Schuman, Nicholas Sinclair, Yuelin Li, Pinaki Das, Drew Rickerson, and Robert Zill for their assistance in experimental operations of the imaging system and powder gun. This work is performed under the auspices of the U.S. Department of Energy (DOE) by Lawrence Livermore National Laboratory under Contract DEAC52-07NA27344, and supported in part by the Joint Department of Defense/DOE Munitions Technology Development Program (LLNL-JRNL-814062). DCS is supported by the U.S. DOE National Nuclear Security Administration, under Award No. DE-NA0 0 02442 and operated by Washington State University. This research used resources of the Advanced Photon Source, a U.S. DOE Office of Science user facility operated for the DOE Office of Science by Argonne National Laboratory under Contract No. DE-AC02-06CH11357.

APS Source Parameters

Undulator A (33 insertion devices [IDs] in 26 sectors)

Period: 3.30 cm
Length: 2.1 m in sectors 16, 21, 23, 24, 25, 34; 2.3 m in Sector 6; 2.4 m in sectors 1, 2, 5, 7, 8, 9, 10, 11, 15, 17, 18, 19, 20, 22, 26, 28, 31, 32, 33
Minimum gap: 10.5 mm
B_{max}/K_{max}: 0.892 T/2.75 (effective; at minimum gap)
Tuning range: 3.0–13.0 keV (1st harmonic)
3.0–45.0 keV (1st–5th harmonic)
On-axis brilliance at 7 keV (ph/s/mrad^2/mm^2/0.1%bw):
4.1 x 10^{19} (2.4 m), 4.0 x 10^{19} (2.3 m), 3.3 x 10^{19} (2.1 m)
Source size and divergence at 8 keV:
Σ_x: 276 μm Σ_y: 11 μm
$\Sigma_{x'}$: 12.7 μrad (2.4 m), 12.8 μrad (2.3 m), 12.9 μrad (2.1 m)
$\Sigma_{y'}$: 6.7 μrad (2.4 m), 6.8 μrad (2.3 m), 7.1 μrad (2.1 m)

2.30-cm Undulator (2 IDs in sectors 11, 14)

Period: 2.30 cm Length: 2.4 m
Minimum gap: 10.5 mm
B_{max}/K_{max}: 0.558 T/1.20 (effective; at minimum gap)
Tuning range: 11.8–20.0 keV (1st harmonic)
11.8–70.0 keV (1st-5th harmonic, non-contiguous)
On-axis brilliance at 12 keV (ph/s/mrad^2/mm^2/0.1%bw): 6.9 x 10^{19}
Source size and divergence at 12 keV:
Σ_x: 276 μm Σ_y: 11 μm
$\Sigma_{x'}$: 12.3 μrad $\Sigma_{y'}$: 5.9 μrad

2.70-cm Undulator (5 IDs in sectors 3, 12, 14, 35)

Period: 2.70 cm
Length: 2.1 m in Sector 12; 2.4 m in sectors 3, 14, and 35
Minimum gap: 10.5 mm
B_{max}/K_{max}: 0.698 T/1.76 (effective; at minimum gap)
Tuning range: 6.7–16.0 keV (1st harmonic)
6.7–60.0 keV (1st-5th harmonic, non-contiguous)
On-axis brilliance at 8.5 keV (ph/s/mrad^2/mm^2/0.1%bw):
5.7 x 10^{19} (2.4 m), 4.7 x 10^{19} (2.1 m)
Source size and divergence at 8 keV:
Σ_x: 276 μm Σ_y: 11 μm
$\Sigma_{x'}$: 12.7 μrad (2.4 m), 12.9 μrad (2.1 m)
$\Sigma_{y'}$: 6.7 μrad (2.4 m), 7.1 μrad (2.1 m)

3.00-cm Undulator (8 IDs in sectors 12, 13, 16, 21, 23, 27, 34)

Period: 3.00 cm
Length: 2.1 m in sectors 12, 13, 16, 21, 23, 34; 2.4 m in Sector 27
Minimum gap: 10.5 mm
B_{max}/K_{max}: 0.787 T/2.20 (effective; at minimum gap)
Tuning range: 4.6–14.5 keV (1st harmonic)
4.6–50.0 keV (1st-5th harmonic)
On-axis brilliance at 8 keV (ph/s/mrad^2/mm^2/0.1%bw):
4.8 x 10^{19} (2.4 m), 3.9 x 10^{19} (2.1 m)
Source size and divergence at 8 keV:
Σ_x: 276 μm Σ_y: 11 μm
$\Sigma_{x'}$: 12.7 μrad (2.4 m), 12.9 μrad (2.1 m)
$\Sigma_{y'}$: 6.7 μrad (2.4 m), 7.1 μrad (2.1 m)

3.50-cm SmCo Undulator (Sector 4)

Period: 3.50 cm Length: 2.4 m
Minimum gap: 9.75 mm
B_{max}/K_{max}: 0.918 T/3.00 (effective; at minimum gap)
Tuning range: 2.4–12.5 keV (1st harmonic)
2.4–42.0 keV (1st-5th harmonic)
On-axis brilliance at 7 keV (ph/s/mrad^2/mm^2/0.1%bw): 3.7 x 10^{19}
Source size and divergence at 8 keV:
Σ_x: 276 μm Σ_y: 11 μm
$\Sigma_{x'}$: 12.7 μrad $\Sigma_{y'}$: 6.7 μrad

3.60-cm Undulator (Sector 13)

Period: 3.60 cm
Length: 2.1 m
Minimum gap: 11.0 mm
B_{max}/K_{max}: 0.936 T/3.15 (effective; at minimum gap)
Tuning range: 2.2–11.8 keV (1st harmonic)
2.2–40.0 keV (1st-5th harmonic)
On-axis brilliance at 6.5 keV (ph/s/mrad^2/mm^2/0.1%bw): 2.8 x 10^{19}
Source size and divergence at 8 keV:
Σ_x: 276 μm Σ_y: 11 μm
$\Sigma_{x'}$: 12.9 μrad $\Sigma_{y'}$: 7.1 μrad

1.72-cm Undulator (3 IDs in sectors 30, 35)

Period: 1.72 cm
Length: 4.8 m (2 x 2.4 m) in Sector 30; 2.4 m in Sector 35
Minimum gap: 10.6 mm
B_{max}/K_{max}: 0.330 T/0.53 (effective; at minimum gap)
Tuning range: 23.7–26.3 keV (1st harmonic)
On-axis brilliance at 23.7 keV (ph/s/mrad^2/mm^2/0.1%bw):
1.0 x 10^{20} (4.8 m), 4.4 x 10^{19} (2.4 m)
Source size and divergence at 23.7 keV:
Σ_x: 276 μm Σ_y: 11 μm
$\Sigma_{x'}$: 11.6 μrad (4.8 m) 11.9 μrad (2.4 m)
$\Sigma_{y'}$: 4.3 μrad (4.8 m), 4.9 μrad (2.4 m)

1.80-cm Undulator (Sector 32)

Period: 1.80 cm
Length: 2.4 m
Minimum gap: 11.0 mm
B_{max}/K_{max}: 0.244 T/0.41 (effective; at minimum gap)
Tuning range: 23.8 - 25.3 keV (1st harmonic)
71.4 - 75.9 keV (3rd harmonic)
On-axis brilliance at 23.8 keV (ph/s/mrad^2/mm^2/0.1%bw): 2.8 x 10^{19}
Source size and divergence at 23.8 keV:
Σ_x: 276 um Σ_y: 11 um
$\Sigma_{x'}$: 11.9 urad $\Sigma_{y'}$: 4.9 urad

IEX 12.5-cm Quasi-Periodic Polarizing Undulator (Sector 29)

Period: 12.5 cm
Length: 4.8 m
Circular polarization mode:
Max. currents: horizontal coils 34.4 A, vertical coils 20.7 A
K_{max}: 2.73 (effective; at max. currents)
B_{max}: 0.27 T (peak; at max. currents)
Tuning range: 0.44–3.5 keV (1st harmonic)
On-axis brilliance at 1.8 keV (ph/s/mrad^2/mm^2/0.1%bw): 1.4 x 10^{19}
Linear horizontal polarization mode:
Max. current: vertical coils 47.6 A
K_{max}: 5.39 (effective; at max. current
B_{max}: 0.54 T (peak; at max. current)
Tuning range: 0.24–3.5 keV (1st harmonic)
0.24–11.0 keV (1st–5th harmonic)
On-axis brilliance at 2.1 keV (ph/s/mrad^2/mm^2/0.1%bw): 1.1 x 10^{19}
Linear vertical polarization mode:
Max. current: horizontal coils 50.3 A
K_{max}: 3.86 (effective; at max. current)
B_{max}: 0.37 T (peak; at max. current)
Tuning range: 0.44–3.5 keV (1st harmonic)
0.44–11.0 keV (1st–5th harmonic)
On-axis brilliance at 2.1 keV (ph/s/mrad^2/mm^2/0.1%bw): 1.1 x 10^{19}
Fast polarization switching not required
Source size and divergence at 2 keV:
Σ_x: 276 μm Σ_y: 13 μm
$\Sigma_{x'}$: 13.9 μrad $\Sigma_{y'}$: 8.8 μrad

12.8-cm Circularly Polarizing Undulator (Sector 4)

Period: 12.8 cm
Length: 2.1 m
Circular polarization mode:
Max. currents: horizontal coils 1.34 kA, vertical coils 0.40 kA
K_{max}: 2.85 (effective; at max. currents)
B_{max}: 0.30 T (peak; at max. currents)
Tuning range: 0.4–3.0 keV (1st harmonic)
On-axis brilliance at 1.8 keV (ph/s/mrad^2/mm^2/0.1%bw): 3.1 x 10^{18}
Linear horizontal polarization mode:
Max. current: vertical coils 0.40 kA
K_{max}: 2.85 (effective; at max. current)
B_{max}: 0.30 T (peak; at max. current)
Tuning range: 0.72–3.0 keV (1st harmonic)
0.72–10.0 keV (1st–5th harmonic)
On-axis brilliance at 2.1 keV (ph/s/mrad^2/mm^2/0.1%bw): 2.3 x 10^{18}
Linear vertical polarization mode:
Max. current: horizontal coils 1.60 kA
K_{max}: 3.23 (effective; at max. current)
B_{max}: 0.34 T (peak; at max. current)
Tuning range: 0.58–3.0 keV (1st harmonic)
0.58–10.0 keV (1st–5th harmonic)
On-axis brilliance at 2.1 keV (ph/s/mrad^2/mm^2/0.1%bw): 2.3 x 10^{18}
Switching frequency (limited by storage ring operation): 0–0.5 Hz
Switching rise time: 50 ms
Source size and divergence at 2 keV:
Σ_x: 276 μm Σ_y: 12 μm
$\Sigma_{x'}$: 16.7 μrad $\Sigma_{y'}$: 12.7 μrad

1.80-cm Superconducting Undulator (2 IDs in sectors 1, 6)

Period: 1.80 cm
Length: 1.1 m
Gap: 9.5 mm (fixed)
Max. current: 450 A
B_{max}/K_{max}: 0.962 T/1.61 (effective; at maximum current)
Tuning range: 11.2–24.7 keV (1st harmonic)
11.2–150.0 keV (1st-13th harmonic, non-contiguous)
On-axis brilliance at 13 keV (ph/s/mrad^2/mm^2/0.1%bw): 3.2 x 10^{19}
Source size and divergence at 13 keV:
Σ_x: 276 μm Σ_y: 11 μm
$\Sigma_{x'}$: 13.2 μrad $\Sigma_{y'}$: 7.5 μrad

3.15-cm Helical Superconducting Undulator (Sector 7)

Period: 3.15 cm
Length: 1.2 m
Coil winding diameter: 31.0 mm
Max. current: 450 A
B_{max}/K_{max}: 0.413 T/1.213 (B_x=B_y effective; at maximum current)
Tuning range: 6.0-13.0 keV (1st harmonic)
On-axis brilliance at 6.0 keV (ph/s/mrad^2/mm^2/0.1%bw): 2.2 x 10^{19}
Source size and divergence at 6 keV:
Σ_x: 276 μm Σ_y: 11 μm
$\Sigma_{x'}$: 14.7 μrad $\Sigma_{y'}$: 10.0 μrad

APS Bending Magnet

Critical energy: 19.51 keV
Energy range: 1–100 keV
On-axis brilliance at 16 keV (ph/s/mrad^2/mm^2/0.1%bw): 5.4 x 10^{15}
On-axis angular flux density at 16 keV (ph/s/mrad^2/0.1%bw): 9.6 x 10^{13}
Horizontal angular flux density at 6 keV (ph/s/mradh/0.1%bw): 1.6 x 10^{13}
Source size and divergence at the critical energy:
Σ_x: 92 μm Σ_y: 31 μm
$\Sigma_{x'}$: 6 mrad $\Sigma_{y'}$: 47 μrad

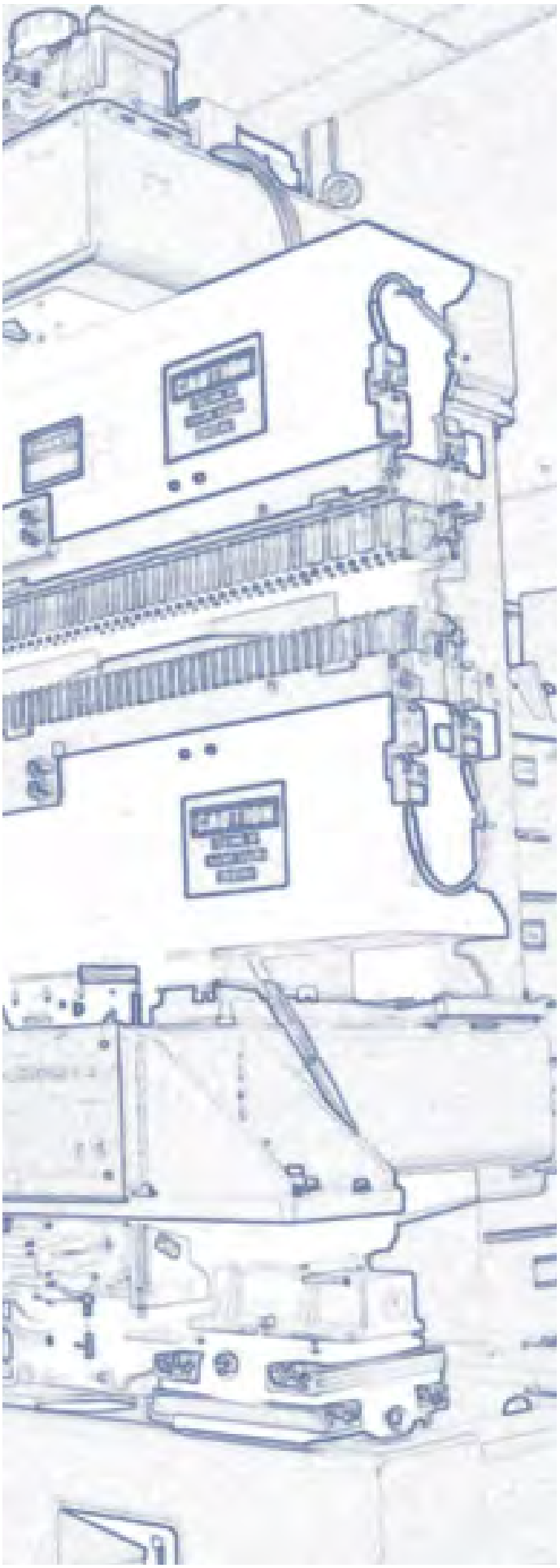

Photon Sciences Directorate Organization Chart

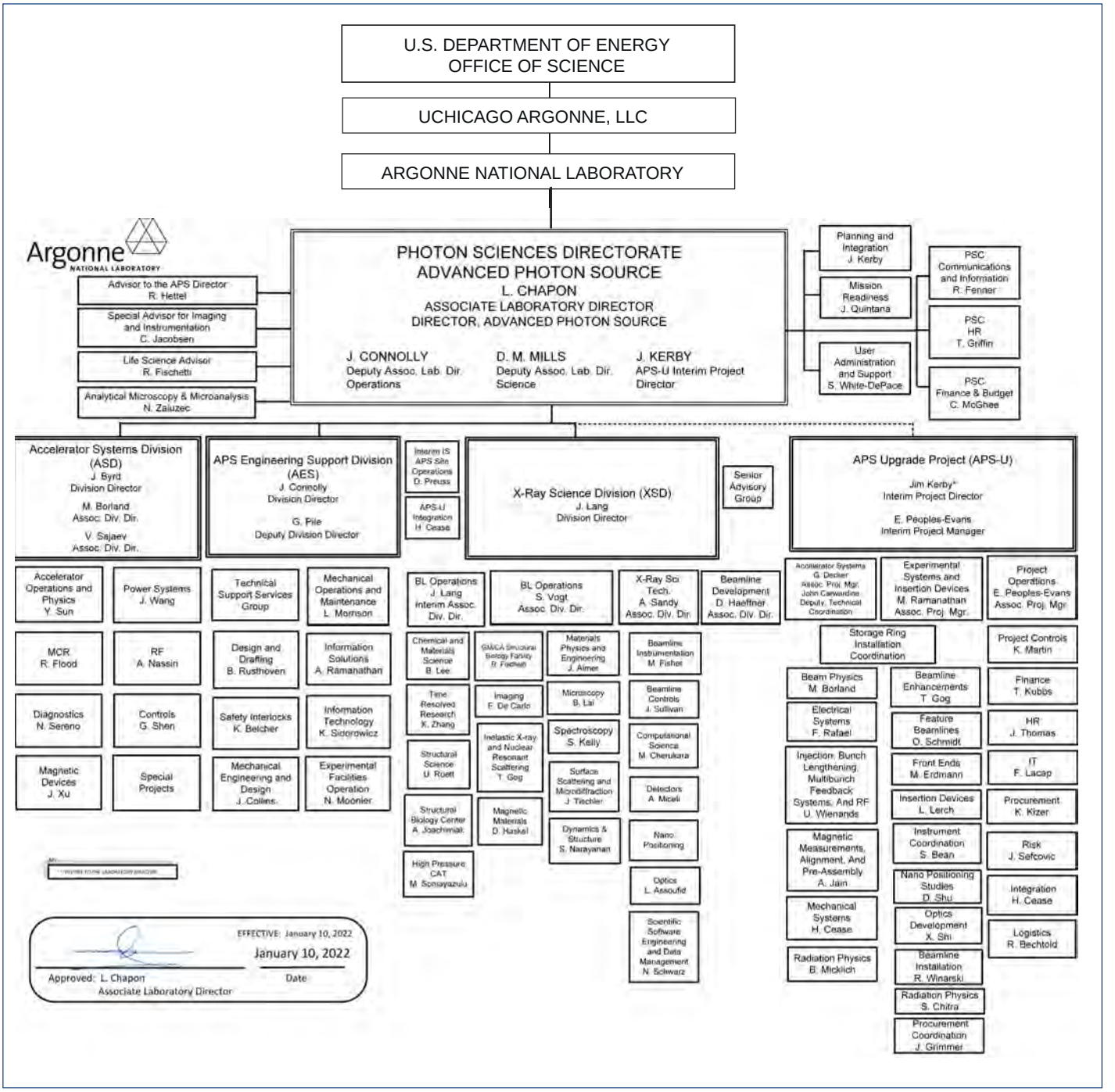

Access to Beam Time at the Advanced Photon Source

Five types of beam-time proposals are available at the APS: general user, partner or project user, collaborative access team (CAT) member, CAT staff, and APS staff. All beam time at the APS must be requested each cycle through the web-based Beam Time Request System. Each beam-time request (BTR) must be associated with one of the proposals mentioned above.

GENERAL-USER PROPOSALS AND BTRS Proposals are peer reviewed and scored by a General User Proposal Review Panel, and time is allocated on the basis of scores and feasibility. A new BTR must be submitted each cycle; each cycle, allocation is competitive. Proposals expire in two years or when the number of shifts recommended in the peer review has been utilized, whichever comes first.

PARTNER- OR PROJECT-USER PROPOSALS AND BTRS Proposals are peer reviewed by a General User Proposal Review Panel and reviewed further by a subcommittee of the APS Scientific Advisory Committee and by APS senior management. Although a new BTR must be submitted each cycle, a specific amount of beam time is guaranteed for up to three years.

CAT-MEMBER PROPOSALS from CAT members are typically much shorter and are reviewed by processes developed by individual CATs. Allocation/scheduling is determined by each CAT's management.

CAT AND APS STAFF-MEMBER PROPOSALS AND BTRS These proposals are also very short and are reviewed through processes developed by either the CAT or the APS. Each CAT/beamline determines how beam time is allocated/scheduled. Collaborative access team and/or APS staff may submit general-user proposals, in which case the rules for general-user proposals and BTRs are followed.

In addition to the above, the APS has developed an industrial measurement access mode (MAM) program to provide a way for industrial users to gain rapid access for one-time measurements to investigate specific problems. A MAM proposal expires after one visit. The APS User Information page (www.aps.anl.gov/Users-Information) provides access to comprehensive information for prospective and current APS users.

Advanced Photon Source Information

The APS produces a wide range of materials that offer insights about the APS and APS-user research.

Our Media Center provides links to:

- Argonne feature articles about the APS
- APS-related Argonne press releases
- "APS in the News" articles
- An APS chronology
- An on-line APS overview
- APS fact sheets
- APS PowerPoint decks
- Our Flickr Image Bank
- YouTube APS research videos (plus all APS videos, e.g., training, etc.)
- A 5-minute video tour of the APS, an APS drone fly-over with captions, an APS done fly-over without captions, and an Argonne drone fly-over

Our annual highlights books "APS Science," with issues dating back to 2003, feature articles on APS research and engineering highlights that are written for the interested public as well as the synchrotron x-ray, engineering, and broader scientific communities; potential facility users; and funding agencies.

An extensive collection of links to APS research highlights is continually updated with new content.

The APS brochure, "Lighting the Way to a Better Tomorrow," shows how the APS helps researchers illuminate answers to the challenges of our high-tech world, from developing new forms of energy, to sustaining our nation's technological and economic competitiveness, to pushing back against the ravages of disease.

"APS/User News" is published quarterly to provide articles about the APS Upgrade, APS staff and APS-user accomplishments, and other APS-related news.r

A list of SARS-CoV-2 publications, etc., from research at the APS is kept current with results our users contributed to the fight against the COVID-19 pandemic.

Acknowledgments

APS Science 2021 Editorial Board:

John Byrd (ANL-ASD), Laurent Chapon (ANL-PSC), John Connolly (ANL-AES/PSC), Robert Fischetti (ANL-PSC), Jim Kerby (ANL-APS-U), Jonathan Lang (ANL-XSD), Dennis Mills, (ANL-PSC), Alec Sandy (ANL-XSD), Stefan Vogt (ANL-XSD)

Reviewers:

Vukica Srajer (BioCARS); Thomas Irving (Bio-CAT); Binhau Lin (ChemMatCARS); Yogendra Gupta, Sheila Heyns, and Paulo Rigg (DCS), Denis Keane (DND-CAT); Michael Becker, Robert Fischetti, and Janet Smith (GMCA-XSD); Mark Rivers and Steve Sutton (GSECARS); Maddury (Zulu) Somayazul, Nenad Velisavljevic (HP-CAT-XSD); Lisa Keefe (IMCA-CAT); Jordi Benach, Laura Morisco (LRL-CAT); Keith Brister (LS-CAT); Carlo Segre (MR-CAT); Kay Perry (NE-CAT); Andrzej Joachimiak (SBC-XSD); John Patrick Rose, Bi-Cheng Wang (SER-CAT); Ercan Alp, Francesco De Carlo, Thomas Gog, Daniel Haskel, Shelly Kelly, Barry Lai, Byeongdu Lee, Antonino Miceli, Suresh Narayanan, Viktor Nikitin, John Okasinski, Uta Ruett, Ayman Said, Jon Tischler, Xiaoyi Zhang, Jiyong Zhao (all ANL-XSD)

Unless otherwise noted, the research highlights in this report were written by:

Mary Alexandra Agner (maryagnerbusiness@pantoum.org)
Michael Allen (michael_h_allen@hotmail.com)
Summer Allen (summer.e.allen@gmail.com)
Christen Brownlee (christenbrownlee@gmail.com)
Erika Gebel Berg (erikagebel@gmail.com)
Vic Comello (ANL-CPA; retired) (vcomello@anl.gov)
Dana Desonie (desonie@cox.net)
Sandy Field (sfield@fieldscientific.com)
Philip Koth (philkoth@comcast.net)
Kim Krieger (mskrieger@gmail.com)
Judy Myers (myers.judy@gmail.com)
Chris Palmer (crpalmer2009@gmail.com)
Neil Savage (neil@stefan.com)
Alicia Surrao (alicia@untoldcontent.com)
Stephen Taylor (stephen@untoldcontent.com)
Mark Wolverton (exetermw@earthlink.net)

Aerial photograph of the APS: John Hill (Tigerhill Studio, http://www.tigerhillstudio.com)
Publications, contracts, rights and permissions, circulation: Jessie L. Skwarek (ANL-PSC)
Editorial, project coordination, design, photography: Richard B. Fenner (ANL-PSC)

Our thanks to the corresponding authors and others who assisted in the preparation of the research highlights, to the users and APS personnel who wrote articles for the report, and our apologies to anyone inadvertently left off this list. To all: your contributions are appreciated.

Advanced Photon Source
Argonne National Laboratory
9700 S. Cass Ave.
Lemont, IL 60439 USA
www.anl.gov • www.aps.anl.gov